Chemical and Cytotoxic Studies on *Oldenlandia umbellata* Linn. and Analytical Investigation on *Carthamus tinctorius* Linn.

THESIS

Submitted in partial fulfillment

of the requirements for the degree of

DOCTOR OF PHILOSOPHY

by

Mahibalan S

ID. No. 2011PHXF020H

Under the supervision of

Prof. A. Sajeli Begum

BITS Pilani
Pilani | Dubai | Goa | Hyderabad

BIRLA INSTITUTE OF TECHNOLOGY AND SCIENCE, PILANI

2015

BIRLA INSTITUTE OF TECHNOLOGY AND SCIENCE, PILANI

CERTIFICATE

This is to certify that the thesis entitled "**Chemical and Cytotoxic Studies on** *Oldenlandia umbellata* **Linn. and Analytical Investigation on** *Carthamus tinctorius* **Linn.**" and submitted by **Mahibalan S** ID. No. **2011PHXF020H** for award of Ph. D. of the Institute embodies original work done by him under my supervision.

Signature of the supervisor :

Name in capital letters   : A. SAJELI BEGUM

Designation   : Associate Professor

Date   :

Acknowledgements

There are numerous teachers, friends, colleagues, associates and family members to thank for their support in this endeavor.

Mahibalan S

April, 2015

Abstract

ABSTRACT

In the present study we carried out chemical investigation and cytotoxic studies on *Oldenlandia umbellata* L. and its constituents along with quality evaluation and standardization of different Indian varieties of *Carthamus tinctorius*. The results were presented in two parts, part-I and part-II.

PART I

Plants have an antiquity of use in health care system and a significant number of drugs have been derived from them. Plants of *Oldenlandia* genus like *O. diffusa* and *O. corymbosa* have been extensively used in Traditional Chinese Medicine to treat cancers and declared as endangered species. A similar Indian species of *Oldenlandia* genus, *O. umbellata* was selected for the investigation with the aim if it can become a substitute for *O. diffusa*. As a first step, microscopic analysis of stem and leaves of *O. umbellata* was performed to establish distinct identification features of this species. Then, LC-PDA-ESI-MS based chemical investigation following chromatographic separation of methanolic extract (**HUM**) of *O. umbellata* and its fractions **HUM-E** and **HUM-B** were carried out which yielded twelve pure compounds.

Based on the various spectroscopic analyses of isolated compounds, the structure elucidation was carried out. A novel symmetrical coumarin dimer named as oledicoumarin (**1**), together with eleven known compounds, pheophorbide A methyl ester (**2**), cedrelopsin (**3**), ursolic acid (**4**), 1,2-dimethoxy-3-hydroxy-9,10-anthracenedione (**5**), 1,3-dimethoxy-2-hydroxy anthraquinone (**6**), hedyotiscone B (**7**), asperulosidic acid (**8**), deacetyl asperuloside (**9**), feretoside (**10**), scandoside (**11**) and 6α-hydroxygeniposide (**12**) were determined. Compounds **2** and **3** are reported for the first time from *O. umbellata* and as well Rubiaceae

plants. Also, this is the second scientific report of isolation of compound **7** from natural sources. The occurrence of compounds **8**-**12** in *O. umbellata* is also explored for the first time through the present investigation.

The study further explored the cytotoxic effect of methanolic extract (**HUM**) of *O. umbellata* and its fractions **HUM-E** and **HUM-B** against lung (A549), breast (MDA-MB-231) and colon (HT-29) cancer cell lines using MTT assay. Results displayed significant cytotoxic effect with IC_{50} values of 25.7, 67.7 and 69.3 μg/mL, against HT-29, A549 and MDA-MB-231 cells, respectively. The assay further revealed significant inhibition of growth of A549 cells (IC_{50}: 3.6-7.2 μg/mL) by compounds **2**-**6**. Similarly, compounds **2**, **4**, **5** and **6** demonstrated cytotoxic effect against MDA-MB-231 cells with the IC_{50} values of 3.6-9.1 μg/mL. Cytotoxicity against HT-29 cells was exhibited only by compounds **2**, **4** and **8** with IC_{50} values of 1.7-6.1 μg/mL. Interestingly none of the compounds were found to be toxic on human normal cells (HEK 293) except compound **8.** The difference in the inhibitory effect of ether fraction and n-butanol fraction proved that less polar constituents are accountable and imperative for cytotoxic effect.

As an outcome, diverse phytochemicals along with a novel compound, oledicoumarin (**1**), were isolated and characterized from *O. umbellata*. The active principles responsible for the cytotoxicity of **HUM-E** fraction against tested cell lines were also rationalized. Similarly the poor inhibitory property of **HUM-B** was also validated. The current report delivered some evidence supporting *O. umbellata* as one of the interesting species opening the possibility of its use as a substitute for *O. diffusa*.

1

2

3

4

5: R_1 = Me; R_2 = H
6: R_1 = H; R_2 = Me

7

8: R_1 = H; R_2 = alpha-OH; R_3 = COMe
10: R_1 = Me; R_2 = beta-OH; R_3 = H
11: R_1 = H; R_2 = beta-OH; R_3 = H
12: R_1 = Me; R_2 = alpha-OH; R_3 = H

9
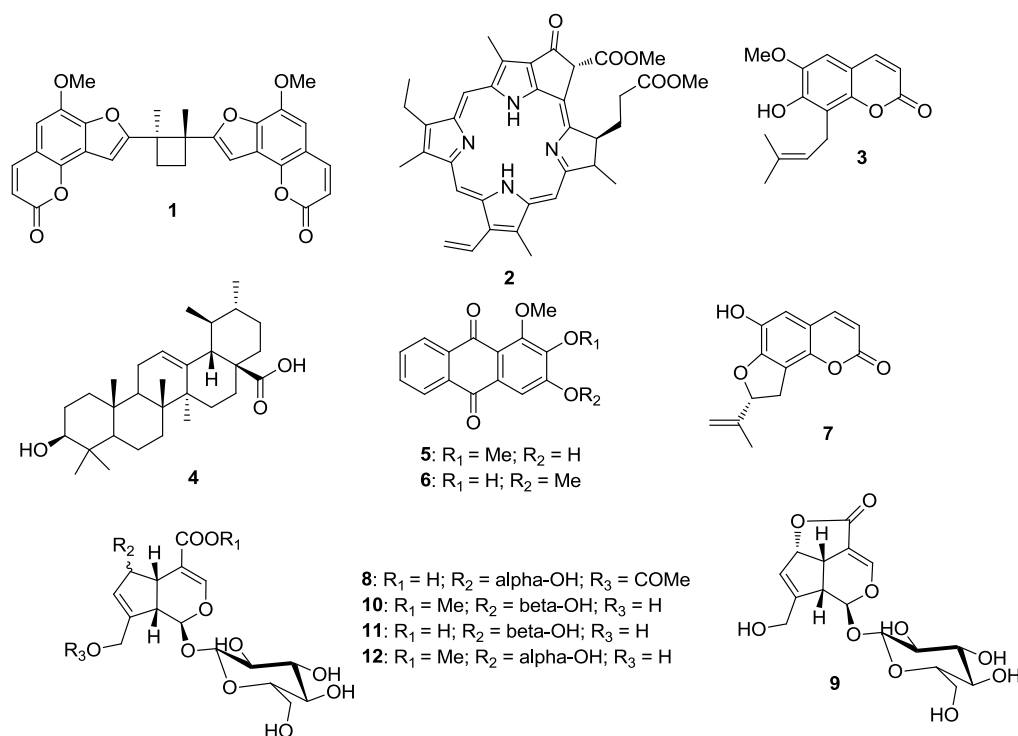
PART II

Safflower is one of the humanity's oldest plants. The decoction of safflower petals have been used as herbal tea in the treatment of various diseases like cancer, cardiovascular diseases and rheumatoid arthritis irrespective of different varieties, an attempt was made to study the safety of consumption of safflower petals and quantify bioactive flavonoids. Four widely cultivated Indian varieties of safflower, NARI-NH-01, NARI-06, TSF-1 and APRR3 were selected for the study. Quality control studies performed as per WHO, suggested that all of them were safe to consume. However, extensive examination on heavy metals content raised the safety concern with NARI-NH-01, NARI-06 and TSF-1, where the level of cadmium was more than the standard acceptable limits. The systematic quality evaluation of the decoction of APRR3 variety was found to be suitable for the consumption and recommended to be safe. Also, it was found to possess higher amount of bioactive flavonoids like rutin, quercetin and kaempferol than other varieties. Thus, the study explored that spiny APRR3 petals comprising more of anti-oxidative flavonoids and complying heavy metals test is safe for human consumption.

Table of Contents

List of Figures

List of Abbreviations / Symbols

List of abbreviations used

1D NMR	: One-dimensional nuclear magnetic spectrometry
2,4'-DDD	: (2,4'-Dichlorodiphenyl)dichloroethane
2,4'-DDE	: 2-(2-Chlorophenyl)-2-(4-chlorophenyl)-1,1-dichloroethene
2,4'-DDT	: 2,4'-Dichlorodiphenyltrichloroethane
2D NMR	: Two-dimensional nuclear magnetic spectrometry
4,4'-DDE	: 1,1-Dichloro-2,2-bis(4-chlorophenyl)ethene
4,4'-DDT	: 4,4'-Dichlorodiphenyltrichloroethane
AAS	: Atomic absorption spectrophotometer
AbE	: Abaxial epidermis
AdE	: Adaxial epidermis
AdS	: Adaxial side
AIDS	: Acquired Immune Deficiency Syndrome
ALI	: acute lung injury
amu	: atomic mass unit
Ang II	: angiotensin-II
APCI	: Atmospheric pressure chemical ionization
AR	: Analytical reagent
AYUSH	: Ayurveda, Yoga and Naturopathy, Unani, Siddha and Homoeopathy
BA	: bioavailability
Bcl	: B-cell lymphoma
Bdl	: Below detection limit
BHA	: butylated hydroxy anisole
CC	: Column chromatography

CD$_3$OD	: Deuterated methanol
CDCl$_3$	: Deuterated chloroform
CMR	: Carbon nuclear magnetic spectrometer
Co	: Cortex
COSY	: Correlation spectroscopy
Cu	: Cuticle
CVS	: Cardio vascular system
d	: doublet
dd	: double doublet
DBE	: Double bond equivalence
DEPT	: Distortionless enhancement by polarization transfer
DMSO	: Dimethyl sulfoxide
DOU	: Degree of unsaturation
DPPH	: 2,2-diphenyl-1-picrylhydrazyl
DRA	: Diffuse reflectance accessory
E	: Epidermis
EC$_{50}$	: Effective concentration 50%
ECD	: Electron capture detector
ERK	: extracellular signal regulated kinase
ESI	: Electrospray ionization
EtOAc	: ethyl acetate
FBS	: Fetal bovine serum
FC	: Flash chromatography
FT-IR	: Fourier transform infrared
GC	: Gas chromatography
GP	: ground parenchyma
GT	: Ground tissue

HCH	: Hexachlorocyclohexane
HIV	: The Human Immunodeficiency Virus
HMBC	: Heteronuclear multiple bond correlation
HMs	: Herbal medicines
HPTLC	: High Performance Thin Layer Chromatography
HR-FABMS	: High resolution fast-atom bombardment mass spectrometry
HSYA	: hydroxy safflor yellow A
HUM	: methanolic extract of *Oldenlandia umbellata*
HUM-B	: n-Butanol fraction of HUM
HUM-E	: Ether fraction of HUM
HVG	: Hydride Vapor Generator
Hz	: Hertz
i.d	: internal diameter
IC$_{50}$	: Inhibitory concentration 50%
IFN	: Interferon
IL	: Interleukin
JNK	: cJun N-terminal kinase
La	: Lamina
LC	: Liquid chromatography
Linn.	: Linnaeus
LM	: Leaf margin
LPS	: lipid polysaccharide
m	: multiplet
Me	: Methyl
Me$_4$Si	: Tetramethylsilane
MeCN	: Acetonitrile
MeOH	: methanol

min	: minutes
m. p.	: melting point
MR	: Midrib
MS	: Mass spectrometry
MTT	: 3-(4,5-dimethylthiazole-2-yl)-2,5-diphenyltetrazolium bromide
MW	: Molecular weight
n-BuOH	: n-Butanol
NF-κB	: nuclear factor kappa-light-chain-enhancer of activated B cells
NMR	: Nuclear magnetic resonance spectrometer
NOE	: Nuclear overhauser effect
NSF	: The national science foundation
ODS	: Octadecylsilane
OG	: Outer growths
OMe	: Methoxy
p	: para
PBS	: Phosphate buffer saline
PDA	: Photodiode array
PDGF	: Platelet derived growth factor
PFPD	: Phosphorus mode flame photometric detector
Ph	: Phloem
p-HPLC	: preparative-High performance liquid chromatography
Pi	: Pith
PM	: Palisade mesophyll
PMR	: Proton nuclear magnetic spectrometer
ppm	: parts per million
PSA	: primary and secondary amine

p-TLC	: preparative-Thin layer chromatography
PX	: Primary xylem
QuEChERS	: Quick, Easy, Cheap, Effective, Rugged and Safe
R_f	: retardation factor
Ri	: Ridge
RP-HPLC	: Revere phase high performance liquid chromatography
rpm	: rotation per minute
RPMI	: Roswell Park Memorial Institute
R_t	: Retention time
RT	: Room temperature
s	: singlet
sec	: second
SEM	: Standard error mean
SERT	: serotonin transporter
SiO_2	: Silicon dioxide
SM	: Spongy mesophyll
Sp	: Spine
SPh	: Secondary phloem
St	: Style
str	: stretching
SY	: safflor yellow
TBA	: tertiary butyl alcohol
TFA	: Trifluoroacetic acid
TLC	: Thin layered chromatography
TNF	: Tumor Necrosis Factor
TOL	: Toll like receptor
US	: United States

USA	: United States of America
UV	: Ultraviolet
Ve	: Vessel
VS	: Vascular strand
VSMC	: Vascular smooth muscle cells
WHO	: World Health Organization
X	: Xylem
XF	: Xylem fibres

List of symbols used

%	: percent
g	: gram
cm	: centimeter
mm	: millimeter
$	: US dollar
™	: Trademark
®	: Registered
m	: meter
mg	: milligram
kg	: kilogram
β	: beta
α	: alpha
δ	: delta
mL	: milliliter
μM	: micromole
μm	: micrometer
MHz	: megahertz
δ	: Chemical shift, δ scale (in NMR)

˚C   : Celsius

L   : Liter

μL   : microliter

kV   : kilo voltage

m/z   : mass-to-charge ratio

h   : hour

nm   : nanometer

W   : Watt

λ_{max} : wavelength of maximum absorption

ν_{max} : wavenumber of maximum absorption

Chapter 1
Introduction

1. INTRODUCTION

Nature has always been the source of structurally diverse and complex molecules. The great interest on the natural product research is not only because they possess structural diversity but they possess highly selective and specific biological effects too. Natural drugs form the basis of traditional system of treatment, especially the plants and their derived products. Several new chemical entities have been discovered based on the ethno-medicinal uses of the plants. The best examples are anti-malarial drugs, particularly artemisinin and quinine which were isolated from *Artemisia annua* and *Cinchona* species, respectively that were used by indigenous people to treat fever.

Cragg and Newman (2013) reported that, of the 1073 new chemical entities approved from 1981-2000, 64% were of natural product derived substances or nature inspired small molecules. Of 1073 small molecules, 69% of antiinfectives, 59% of anticancer agents were naturally derived or inspired molecules. Similarly, out of 317 drugs approved from 2000 to 2013, natural products derived drugs were accounted for 17% (54 drugs). At the end of 2013 there were 100 natural product derived molecules that were undergoing clinical trials. Of these 100 molecules, majority were in oncology segment (38 molecules), followed by anti-infectives (26 molecules) and cardiovascular drugs (19 molecules) (Butler et al., 2014). Despite the intensive investigations on plants, it is estimated that out of 3,00,000 species of higher plants only 6% were systematically studied for their pharmacologic effects and only 15% were subjected for phytochemical evaluations.

Selectivity of a medicinal plant material is very crucial to attain the prescribed ethno-medicinal uses. Consumption of medicinal herbs in the form of tea is becoming a common practice in many countries, however much importance is not given to the selectivity of

particular species or variety and their chemical constituents. Identity of crude herbal drugs can be well established through their pharmacognostical and phytochemical characterization. This in turn helps in ensuring the purity and quality of crude drug sample. Several herbs are in general use, without any surefire assertion for quality and identity, raising ambiguity on recommended medical cure. In view of these facts, the present study was aimed at carrying chemical and analytical investigation on two different medicinally important plants, *Oldenlandia umbellata* and *Carthamus tinctorius*. The results of the investigations are incorporated in the thesis as part I and part II.

1.1 *Oldenlandia* genus

The genus *Oldenlandia* L., that belongs to Rubiaceae family is also referred as *Hedyotis* L. It consists of approximately 500-600 species, which has made this as one of the largest genus in Rubiaceae family (Wikstrom et al., 2013). The scientific community centered their attention on *Oldenlandia* plants as they are explored for the presence of structurally diversified compounds like alkaloids (Peng et al., 1997; Phuong et al., 1998), flavonoids (Tuyen et al., 2010), saponins (Konishi et al., 1998), coumarins (Chen et al., 2006), anthraquinones (Liu et al., 2012; Purushothaman et al., 1968) and iridoids (Yongyong and Jiabo, 2008).

The traditional uses of plants of *Oldenlandia* genus against various diseases cancer (Lin et al 2010, Niu and Meng, 2013), inflammation (Lin et al., 2002, Joseph et al., 2010) and gastric ulcers (Joseph et al., 2010) have made them as medicinally important for many centuries. Fewer species of *Oldenlandia*, have shown remarkable anticancer effect. For instance, *O. diffusa* is used clinically as an anticancer herb owing to negligible side effects at a dose of 30–60 g/day and included in about 15% of Chinese anticancer herbal formula (Shao et al. 2011). *O. corymbosa* is an another interesting species exhibiting significant anticancer

2

activity on human leukemia cells K562 and human breast carcinoma dependent hormone cells MCF-7 (Sivaprakasam et al., 2014). Although, *Oldenlandia* genus is well known, yet the potential benefits of many of the species are unexplored. *Oldenlandia umbellata* L. is one such plant. Despite, its wide distribution in tropical and sub-tropical regions of the world, there were very few scientific results available on its constituents and biological properties (Hema et al., 2007; Purushothaman et al. 1968).

1.2 *Oldenlandia umbellata L.*

O. umbellata (Rubiaceae), commonly known as Indian madder or Chay root, occurs in India, Indonesia, Myanmar, Sri Lanka, Burma and Vietnam. It bears the following vernacular names: Turbuli (Bengali); Cheri-vello (Telugu); Chay, Sayawer, Imberul (Tamil). The plant is a small bush or herb found on sandy soils, chiefly near the sea-coast. It is an annual or perennial, diffusely branched, to 40 cm tall; stems 4-angled perhaps becoming terete, ribbed, scaberulous. Leaves opposite but often crowded and appearing verticillate, sessile; blade drying papery, linear to narrowly lanceolate, adaxially punctuate and glabrescent, abaxially scaberulous along midrib, base acute, margins flat to revolute, apex acute; secondary veins indistinct; stipules fused to petioles, glabrescent, truncate to rounded . Inflorescence terminal and sometimes in upper most axils, congested-cymose to congested-umbelliform, several flowered scaberulous, pedunculate; peduncles 1-2 cm; bracts stipuliform; pedicles 0.5-1.2 mm. Flowers distylous, shortly pedicellate. Calyx apparently glabrous; hypanthium portion subglobose to ovoid, limb lobed essentially to base; lobes lanceolate to triangular, ciliate. Corolla white, tubular, outside glabrous, inside sparsely pubescent (Figure 1.1). Seeds several, blackish brown (Tao and Taylor 2011). The roots are usually about 10-12 inches long, somewhat straight and stiff, tough and wiry and with few or no lateral fibres. The aqueous hot extract of root gives merely a pale yellow extract, but it

turns to blood red color when treated with alkali. The coloring matters reside chiefly, if not entirely in the bark of the root.

Figure 1.1 Aerial parts of *Oldenlandia umbellata* L.

The overall identity and limits of lineage was not understood or delineated. Despite of having long history as dye producing and medicinally important herb, *O. umbellata* often be misidentified, as they bear similar morphological features with *Oldenlandia tenelliflora* (Chen et al., 2010), *O. auricularia* and *O. pinifolia* (Tao and Taylor 2011) (Table 1). Due to the lack of availability of scientific data, identification of *O. umbellata* became more complicated. Identification of correct species is the first and foremost step to ensure safety and efficacy of herbal medicines. Hence, the authenticity of the plant was done based on macro and micro analysis.

Table 1 Comparison of macroscopical features of *O. umbellata*, *O. pinifolia*, *O. auricularia* and *O. tenelliflora* (Tao and Taylor 2011)

	O. umbellata	*O. pinifolia*	*O. auricularia*	*O. tenelliflora*
Habit	Annual or perennial herbs	Annual or perennial herbs	Perennial herbs	Annual or perennial herb
Leaves	Opposite, but often crowded and appearing verticilate; sessile, linear-narrowly lanceolate; margin: flat-revolute; apex: acute	Sessile or subsessile, linear-narrowly spatulate, adaxially glaborous to densely scaberulous, margin: markedly revolute atleast when dry, apex: acute	Subsessile-petiolate, densely strigillose-pilosulous, ovate-lanceolate, adaxially glabrous along midrib, base: acute-obtuse apex: acute or acuminate,	Sessile or subsessile, linear, linear-lanceolate, adaxially glabrous or scaberulous near margins, apex: acute or acuminate
Inflorescence	Terminal and sometimes in uppermost axils, 3-10 flowered, scaberulous, pedicle-very short, bracts: stipuliform, corolla: white, tubular, outside glabrous	Terminal and, 3-10 flowered, sessile subtended by 1 or 2 pairs of somewhat reduced leaves, bracts: lanceolate-setose, corolla: white sometimes flushed with pink, tubular-funnelform	Axillary, glomerulate to congested-cymose, 2-7 flowered, sessile, bracts: lanceolate-stipuliform, corolla: white, tubular or tubular-funnelform	Axillary, 1-3 flowered in each axil, sessile-subsessile, bracts: acicular-lanceolate, corolla: white, funnelform

1.3 Cancer and plant derived drugs

Cancer is one of the leading causes of death worldwide. Approximately 14 million new cases and 8.2 million cancer related deaths occurred in 2012. It is estimated that the number of new cases may increase from 14 million in 2012 to 22 million in next 2 decades. Among all, lung cancer is the leading cause of cancer deaths (1.59 million deaths), followed by liver (7,45,000 deaths), stomach (7,23,000 deaths), colorectal (6,94,000 deaths), breast (5,21,000 deaths) and oesophageal cancer (4,00,000 deaths). Every year more than 60% of the new cases and 70% of world's cancer deaths occur in low and middle income countries (Stewart and Wild 2014). Cancers are treated by one or more modalities such as chemotherapy, and/or surgery and/or radiotherapy. The common side effects associated with these cancer treatments are severe pain, fatigue, bleeding, hair loss, reduction in blood cells, fertility problems and memory changes. Chemotherapy is a type of treatment that encompasses the use of drugs to cure or comparatively prolong the life of cancer patient. Though the existing drugs are effectively killing the cancer cells but they do kill fast growing normal cells too, causing severe side effects. Hence there is always a demand for the development of both effective and safer drugs to combat cancer.

It is worth to note that over 60% of currently used anticancer agents are derived natural sources, including plants, marine organisms and micro-organisms (Cragg et al., 2005; Newman et al., 2003). Many exciting anticancer agents were derived from plant source. Paclitaxel is one such drug, whose annual sale is over $ 1 billion. The other important plant derived anticancer agents are belotecan, irinotecan and topotecan all of them were derived from camptothecin, obtained from a Chinese plant called *Camptotheca acuminata* (Cragg and Newman 2013). A few plant derived anticancer agents in clinical use are given in Figure 1.2. These are primarily used in combination with other cancer treatments of variety of cancers, including leukemias, lymphomas, advanced testicular cancer, breast and lung cancers and

Vincristine; R = CHO
Vinblastine; R= CH₃

Homoharringtonine

Flavopiridol

Camptothecin

Topotecan

Elliptinium

Taxol

Docetaxel

Podophyllotoxin

Etoposide

Teniposide
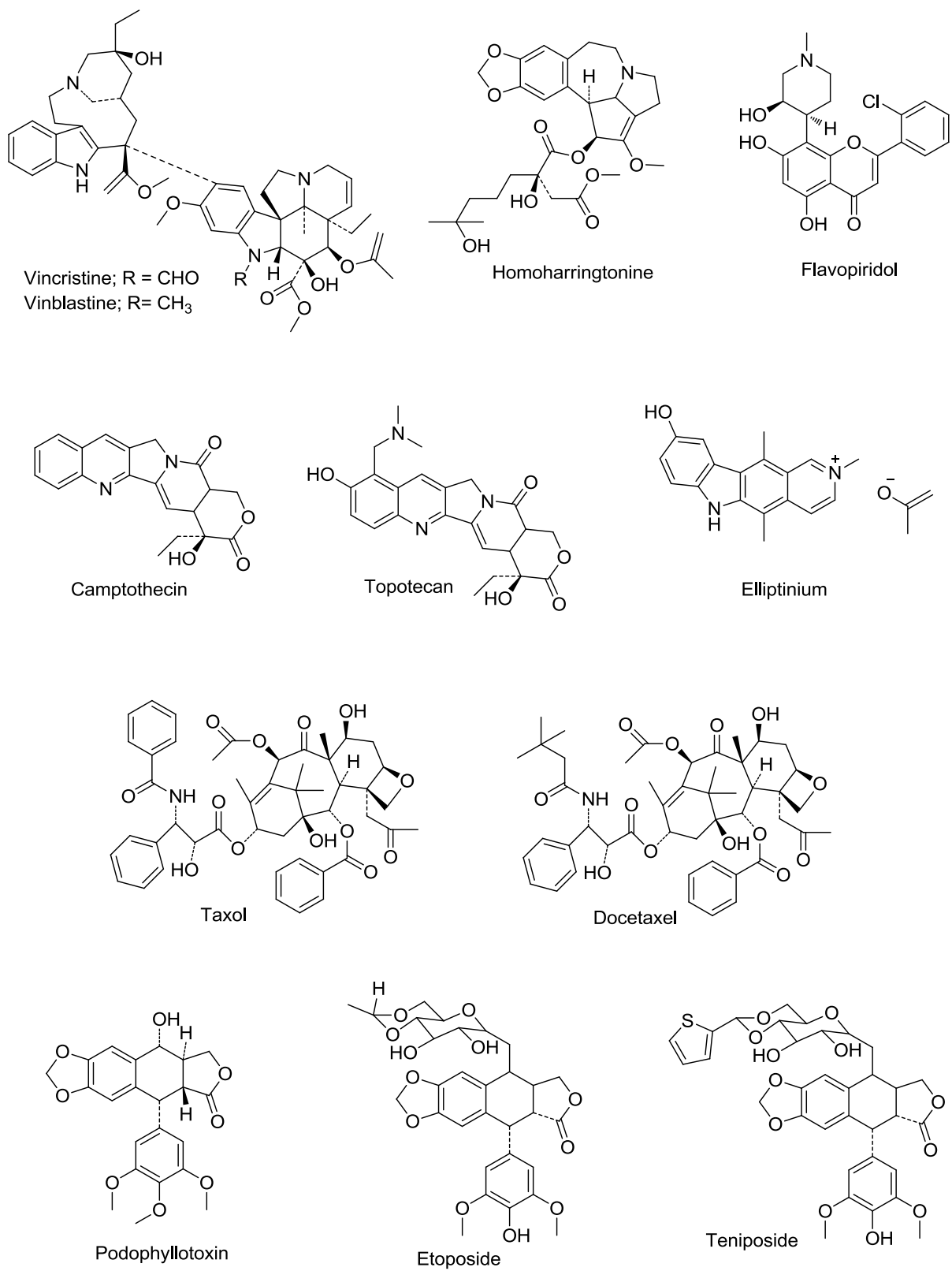
Figure 1.2 Plant derived anticancer agents in clinical use

7

Kaposi's sarcoma (Cragg and Newman 2005). In view of this, the investigation was extended to identify the cytotoxic lead molecules from *Oldenlandia umbellata*. The genus *Oldenlandia* includes several potential anticancer species like *O. diffusa, O. biflora*, etc. However, research on *O. umbellata* in the direction of discovering cytotoxic molecules were so far not carried out.

1.4 *Carthamus tinctorius* L.

Until today, there are two botanicals being approved by FDA. The first botanical was Veregen™ (Polyphenon® E ointment; Shaman Pharmaceuticals) approved in October 2006. It is a defined mixture of catechins extracted from green tea leaves used to treat genital warts. The second one was Crofelemer (Fulyzaq®, SP-303; Napo Pharmaceuticals) contains the purified form of proanthocyanidins oligomer obtained from the red bark latex of *Croton lechleri*. This was approved in December 2012 to relieve symptoms of diarrhea in HIV/AIDS patients taking antiretroviral therapy (Butler et al., 2014). As consequences, many drug makers have shown up their interests in establishing the standardized extract with proved efficacy and safety (Brevoort 1995; Blumenthal 1999). According to National Medicinal Plants Board (NMPB) India, the domestic trade of AYUSH industry is over Rs. 80 to 90 billion and around Rs. 10 billion worth of Indian medicinal products is being exported. Similar kind of trend happened globally as well. The global herbal trade at the current scenario is ~ US $ 120 billion and it is expected to go up to ~ US $7 trillion by 2050.

Globally about 2 million flora and fauna have been scientifically named on this date. India has richest flora of the world contributing 6% with about 45,000 plant species and many are endemic plants. Among that 3,000 species are officially documented for medicinal values and over 8,000 species are in folklore use. Safflower (*Carthamus tinctorius* L.) belongs to family Compositae is one of humanity's oldest crops, cultivated mainly for the production of

colorants and edible oils (Zhang and Nishiyama 2014). This was also known as false saffron, bastard saffron, dyer's saffron, as it is used as a low cost substitute for saffron (Weiss 1983). This is an ideal plant for rain-shed area as its root system elongates to 2-3 m in soils with adequate depth to get water and nutrients (Zargari, 1988). Argentina, Australia, China, Germany, Ethiopia, India, Mexico, USA are the major cultivars of safflower (Dajue and Mundel 1996).

Safflower is a highly branched, annual herbaceous plant with numerous long spines on the leaves and bracts (Figure 1.3). It grows 30-150 cm height and each stem ends in globular flower capitulum, enclosed by spiny bracts. Flowers are generally brilliant yellow, orange or red in colour. The typically white achenes, are smooth and four-sided, with a thick pericarp. Leaf size varies from 2.5-5 cm wide and 10-15 cm long. Leaves are ovate to obovate around the inflorescence (Dajue and Mundel 1996).

Safflower is used in India and Africa for purgative and antidote effects (Weiss 1971). Tea made from leaves is used to prevent abortion and infertility by women in Afghanistan and India (Weiss 1983). In China, it is grown exclusively for its flowers, which are used in treatment of many illnesses such as menstrual problems, cardiovascular disease, pain and swelling associated with trauma. Generally safflower has a bitter taste, but the Institute of Botany of the Chinese Academy of Sciences in Beijing developed a non-bitter, sweet smelling tea enriched with amino acids, minerals and vitamins. The main active ingredients in safflower are safflor yellow, carthamin, rutin, kaempferol and quercetin which are water soluble (Weiss 1971).

Figure 1.3 Spiny and non-spiny varieties of safflower petals

Over 150 formulations ranging from cosmetics to medicinal preparations contain safflower as a part of it. For instance, safflor yellow aqueous injection is extensively used in clinics to treat various cardio vascular diseases. Chinese medicinal granules containing 10-15 parts of safflower is used to treat rheumatoid arthritis. The curative ratio was reported as 95% with no recurrence and no adverse effects (Luo 2004). Decoction of safflower (5-7%) along with other herbals has been used in Chinese medicinal preparation to treat postmenopausal osteoporosis. Interestingly, no side effects were observed and less cost, high cure rate, herbal-herbal compatibility was also observed (Cong and Cong 2014).

Although, safflower finds its use everywhere like in clinical, food and chemicals, cosmetics and nutraceuticals industries; there were no systematic studies performed on the quality of safflower petals to ensure its safety and efficacy. As India is one of the largest cultivators of safflower, apparently there is a lot of hope for India to play a global leader in this matter provided that, the quality, safety and efficacy is meeting the global standards. Keeping this in thought, the present study was aimed to establish the quality control parameters and standardization of four varieties of *C. tinctorius* which will boost consumer's acceptability.

10

Chapter 2
Literature Review

2. LITERATURE REVIEW

PART I

2.1 Phytochemical reports on *Oldenlandia umbellata* L.

For several years roots are used as a source of chay-root dye for imparting red color to calico, wool, and silk fabrics (Yoganarasimhan 2000). The first investigation on constituents of *O. umbellata* had begun a way long back in 1893 by Perkin and Hummel (1893). Perkin and his team member extensively worked to unlock the structure of color producing constituents in the roots of *O. umbellata*. The results showed that compounds, purpurin, purpuroxanthin-carboxylic acids, alizarin, mono and dimethylanthragallol ether and metahydroxyanthraquinone were responsible to produce colors. The chemical formula of the isolated compounds was established based on detailed chemical methods and by comparing the melting point analysis. The second investigation on phytoconstituents of *O. umbellata* was taken up by Purushothaman and his team members (1968). The presence of 1,2,3-trimethoxyanthraquinone, 1,3-dimethoxy-2-hydroxyanthraquinone and its monoacetate, 1,2-dimethoxy-3-hydroxyanthraquinone and its monoacetate, 1,3-dimethoxy-2-*O*-glycoside and alizarin-1-methyl ether was established and the compounds were identified by mixed melting point and derivative spectroscopic techniques. Further studies were conducted to find the feasibility of using these compounds as pH indicator. The results had shown that compounds, 1,2,3-trimethoxyanthraquinone, 1,3-dimethoxy-2-hydroxyanthraquinone, 1,2-dimethoxyanthraquinone, 1-methoxy-2-hydroxyanthraquinone and 1,2-dihydroxyanthraquinone could be used as pH indicator in various titrations (Ramamoorthy et., 2009). Hema and co-workers (2007) identified the presence of triterpenoids (ursolic acid) and flavonoids (kaempferol-3-*O*-rutinoside) in the whole plant.

11

2.2 Pharmacological reports on *Oldenlandia umbellata* L.

In Indian System of Medicines, leaves and roots are used as an expectorant, given in asthma, bronchitis and consumption. A decoction of the leaves is used as a wash for poisonous bites (Rekha et al., 2006; Yoganarasimhan 2000). Despite, their wide distribution and extensive clinical use, there were very limited amount of scientific data available on *O. umbellata*. The crude methanolic extract of *O. umbellata* at 250 and 500 mg/kg, had shown significant hepatoprotective and antioxidant effect against CCl_4 induced rat model (Malaya et al., 2007). Similarly, the in-vitro studies carried out with aqueous extract have explored the anthelmintic effect of *O. umbellata* (De et al., 2014). Antitussive activity on mice was explored by Hema et al., (2007) wherein the ethanolic extract of the plant at 500 mg/kg body weight showed significant activity when compared with control group. Further investigations on this plant have demonstrated the antibacterial (Rekha et al., 2006), anti-inflammatory and antipyretic effects of *O. umbellata* (Padhy and Endale 2014).

PART II

2.3 Phytochemical reports on *Carthamus tinctorius* L.

Chemical investigations on *Carthamus tinctorius* L. (safflower) explored the presence of over 200 compounds. It was found to have completely diversified structures like flavonoids (Lee et al., 2002), coumarins, quinochalcones, alkaloids (Takii et al., 2003), lignans, fatty acids (Zhang et al., 1997), triterpene alcohols (Akihisa et al., 1996), serotonin derivatives (Koyama et al., 2006), steroids and polysaccharides (Zhou et al., 2009) (Table 2).

Several marker compounds have been established to study the quality of different varieties of safflower. The following compounds have been successfully quantified by HPLC/IR: Hydroxysafflor yellow A (HYSA) (Jiang et al., 2011; Yao et al., 2010; Fan et al.,

2009; Ye et al., 2007; Guo et al., 2006), kaempferol-3-*O*-rutinoside, safflomin A and B, bidenoside C (Li et al., 2014a), rosmarinic acid, salvia acid B, lithospermic acid (Liu et al., 2013), p-coumaric acid (Wang et al., 2011), safflomin A (Yao et al., 2010), Puerarin (Li et al., 2008), 6-hydroxy kaempferol 3,6-di-O-β-glucoside-7-O-β-glucuronide, 6-hydroxykaempferol 3,6,7-tri-O-β-glucoside, 6-hydroxykaempferol 3,6-di-O-β-glucoside, 6-hydroxyapigenin 6-O-glucoside-7-O-glucuronide, anhydrosafflor yellow B and kaempferol-3-O-β-rutinoside, guanosine and syringin (Fan et al., 2009), 6-hydroxykaempferol-3-O-glycoside (Liu et al., 2001) rutin, quercetin and kaempferol (Yu and Xu 1997).

Table 2 List of compounds reported from *C. tinctorius*

S. No.	Compounds	References
1	Isolumichrome, (2S)-4',5,6,7-tetrahydroxyflavanone 6-O-β-D-glucopyranoside, neocarthamin, kaempferol, Kaempferol 3-O-β-D-glucoside, kaempferol 3-O-β-D-rutinoside, 6-hydroxykaempferol, 6-hydroxykaempferol 3-O-β-D-glucoside, quercetin, p-hydroxybenzoic zcid, p-hydroxycinnamic acid, uracil, adenine, β-sitosterol	Olaleye et al., 2014
2	Kaempferol 3-O-rutinoside, kaempferol 3-O-glucoside	Wang et al., 2014
3	Hydroxy safflor yellow B and C, safflomin C, saffloquinoside C, 2(R)-4',5-dihydroxyl-6,7-di-O- β-D-glucopyranosyl flavanone	Yue et al., 2014a
4	Saffloflavonesides A and B	He et al., 2014a
5	A new flavanone glucoside	Liu et al., 2014

6	Luteolin, Cinaroside, 5-O-methylluteolin, azaleatin and Safloroside I	Kurkin and Kharisova., 2014
7	(2E,8E)-12R-tetradecadiene-4,6-diyne-1,12,14-triol, (8Z)-decaene-4,6-diyn-1-O-b-Dglucopyranoside, (8E)-decaene-4,6-diyn-1-O-b-D-glucopyranoside, (2S)-4',5,6,7-tetrahydroxy-flavanone 6-O-b-Dglucoside, p-hydroxybenzoic acid, 3-hydroxy-4-methoxybenzoic acid, dihydrophaseic acid Me ester-3-O-b-D-glucoside, dihydrophaseic acid Me ester, 4-hydroxybenzaldehyde, N,N'-dicoumaroyl-putrescine, 4-(4'-hydroxyphenyl) but-3-en-2-one and 4-hydroxyacetophenone	He et al., 2014b
8	p-coumaric acid	Wang et al., 2011
9	Safflomin A	Yao et al., 2010
10	Puerarin	Li et al., 2008
11	6-hydroxykaempferol 3,6-di-O-β-glucoside-7-O-β-glucuronide; 6-hydroxykaempferol 3,6,7-tri-O-β-glucoside; 6-hydroxy kaempferol 3,6-di-O-β-glucoside; 6-hydroxyapigenin 6-O-glucoside-7-O-glucuronide; anhydrosafflor yellow B and kaempferol-3-O-β-rutinoside, guanosine and syringing	Fan et al., 2009
12	6-hydroxylkaempferol-3-O-glycoside	Liu et al., 2001
13	Adenosine, rutin and quercetin	Sun et al., 2003
14	Rutin, quercetin and kaempferol	Yu and Xu 1997
15	N-[2-(5-hydroxy-1H-indol-3-yl)ethyl]-p-ferulamide; N-[2-(5-	Zhang et al.,

	hydroxy-1H-indol-3-yl)ethyl]-p-coumaramide; N-,N-[2,2'-(5,5-dihydroxy-4,4'-bi-1H-indol-3,3'-yl)diethyl]-di-p-coumaramide; N-[[3'[2-(p-coumaramido)ethyl]-5, 5'-dihydroxy-4,4'-bi-1H-indol-3-yl]ethyl]ferulamide; N,N'-[2,2'-(5,5'-dihydroxy-4,4'-1H-indol-3,3'-yl)diferulamide, N-[2[5-(beta-D-glucosyloxy)-1H-indol-3-yl-ethyl]-p-coumatamide and N-[2-[5-(beta-D-glucosyloxy)-1H-indol-3-yl]-ethyl]ferumaramide	1997
16	Serotomide (trans-N-caffeoylserotonin) and safflomide (trans-N-caffeoyltryptamine)	Park 2008
17	N(1), N(5)-(Z)-N(10)-(E)-tri-p-coumaroylspermidine	Zhao et al., 2010
18	Heliaol, α-amyrin, β-amyrin, lupeol, cycloartenol, 24-methylenecycloartanol, tirucalla-7,24-dienol and dammaradienol	Akihisa et al., 1996
19	Safflomin A and B	Onodera et al., 1981
20	Carthamidin, isocarthamidin, kaempferol, 6-Hydroxykaempferol	Jin et al., 2008
21	Hydroxysafflor yellow A, safflor yellow A, safflamin A and C	Jiang et al., 2005
22	Carthamin	Obara and Onodera 1979
23	Carthamoside A1 and A2	Zhou et al., 2006
24	Tinctormine	Meselhy et al., 1992; Meselhy et al., 1993

25	Quercetin-7-O-(6"-O-acetyl)- β-D-glucopyranoside, luteolin, quercetin, quercetin-7-O-β-D-glucopyranoside, acacetin-7-O-β-D-glucuronide and apigenin-6-C- β-D-glucopyranosyl-8-C- β-D-glucopyranoside	Lee et al., 2002
26	Hydroxysafflor yellow A , safflomin C	Onodera et al., 1989; Meselhy et al., 1993
27	Nicotiflorin	Huang et al., 2007
28	Hexatriacontane-6,8-diol; triacontane-7,9-diol; triacontane-7,9-diol acetal; octacosane-7,9-diol; dotriacontane-7,9-diol; tetratriacontane-7,9-diol; hexatriacontane-7,9-diol; nonacosane-8,10-diol; nonacosane-8,10-diol acetal; heptacosane-8,10-diol; hentriacontane-8,10-diol; tritriacontane-8,10-diol; pentatriacontane-8,10-diol	Akihisa et al., 1997
29	*cis-trans* isomers of coumaroylspermidine	Li et al., 2013
30	Saffloquinoside C; (-)-4-hydroxybenzoic acid-4-O-[6'-O-(2'-methylbutyryl)-β-D-glucopyranoside]	Jiang et al., 2013
31	Saffloquinoside A; saffloquinoside B	Jiang et al., 2010
32	Palmitic acid; 1-O-hexadecanolenin; trans-3-tridecene-5,7,9,11-tetrayne-1,2-diol; trans-trans-3,11-tridecadiene-5,7,9-triyne-1,2-diol; coumaric acid; daucosterol; apigenin; kaempferol	Liu et al., 2005
33	4-Hydroxybenzaldehyde; E-1-(4'-hydroxyphenyl)-but-1-en-3-one; 3-formylindole; 2-acetyl-5-hydroxymethylfuran; p-hydroxycinnamic acid; (6R,7E,9R)-9-hydroxy-4,7-megastigmandien-3-one; 4-hydroxyacetophenone; 5-(hydroxymethyl)-2-furaldehyde; 4-hydroxybenzoic acid;	Li et al., 2012

	stigmasterol-3-O-β-D-glucopyranoside; daucosterol; β-sitosterol	
34	Isosafflomin C; safflomin C, rutin, quercetin, kaempferol and its glycosides, hydroxysafflor yellow A	Chen et al., 2014
35	Cartorimine	Yin et al., 2000
36	Precarthamin; anhydroussafflor yellow B; cartarmin; methylsafflomin C; methylisosafflomin C	Yue et al., 2013
37	Carthamus yellow	Chen et al., 2013a
38	Carthamosides B1-B3; methyl-3-(4-O-β-D-glucopyranosyl-3-methoxyphenyl)propionate; ethylsyringin; methylsyringin	Zhou et al., 2008a
39	3β-O-[β-D-xylopyranosyl(1→3)-O-β-D-galactopyranosyl]-lup-12-ene-28 oic acid-28-O-α-L-rhamnopyranosyl ester	Yadava and Chakravarti 2008
40	(2R)-4',5-dihydroxyl-6,7-di-O-β-D-glucopyranosyl flavanone; methyl-3-(4-O-β-D-glucopyranosylphenyl) propionate; (2S)-4',5-dihydroxyl-6,7-di-O-β-D-glucopyranosyl flavanone; 6-hydroxykaempferol-3,6-di-O-β-D-glucopyranoside; 4-O-β-D-glucosyl-trans-p-coumaric acid; 4-O-β-D-glucosyl-cis-p-coumaric acid	Zhou et al., 2008b
41	Acacetin 7-O-β-D-apiofuranosyl-(1'''→6''); acacetin 7-O-α-L-rhamnopyranoside; acacetin	Ahmed et al., 2000

2.4 Pharmacological reports of safflower

2.4.1 Preclinical studies

Safflower has been extensively studied and used across the world. Its effectiveness against various diseases has been unambiguously proved by multiple preclinical and clinical evaluations. The traditional claim of safflower in curing the cardio vascular diseases including arteriosclerosis and restenosis following coronary intervention has been evaluated. Results showed that HSYA, one of the main constituent of safflower, significantly inhibit the platelet-derived growth factor (PDGF)-BB-stimulated vascular smooth muscle cells (VSMC) proliferation. In addition to that, HSYA also suppress the PDGF-BB induced production of nitrous oxide and cyclic guanosine monophosphate and activation of Akt signalling (Song et al., 2014). Further HSYA protects against cerebral ischemia-reperfusion injury by anti-apoptotic effect through PI3K/Akt/GSK3β pathway in rat (Chen et al., 2013b).

A traditional Chinese herbal formulation of *C. tinctorius* along with a few other herbals have found to increase the efficiency to 93.9% in the treatment of chronic pulmonary heart disease when it was administered with western medicine (Zhang 2014). It was also observed that HSYA alleviates the total cholesterol level without affecting beta-lipoproteins, triglycerides or liver function (Wengxuan et al., 1987). Further study on safflower yellow, have had completely inhibited aggregation of rabbit platelets and prevented experimental thrombosis in rats at the dose of 220 mg/mL (Qingliang et al., 1988). To improve the bioavailability (BA) of HSYA, Ma and co-workers (2015) conducted an in-vivo study with other excipients. It was found that the relative BA was increased to 476% when HSYA formed a complex with sodium caprate and chitosan.

In addition to that the safety and combined effect of HSYA with edaravone injection against acute cerebral infarction was analysed. The reports of meta-analysis showed that the

combined injection was safe and much more effective than the edaravone injection alone and it also improved the neuronal function and clinical symptoms (Yang et al., 2013). Similar study was conducted with HSYA injection and safflower decoction (5-7%) along with other herbals that has been used in Chinese medicinal preparation to treat postmenopausal osteoporosis. Interestingly, no side effects observed and less cost, high cure rate, herbal-herbal compatibility was seen (Cong and Cong, 2014). Audomkasok et al., (2014) evaluated the antihaemolytic activity of safflower. Experimentally, haemolysis was induced by *Plasmodium berghei* in mice. The study demonstrated that aqueous extract of safflower exhibit antihaemolysis in dose dependent manner and also suggested that this plant may act as potential source to treat malaria.

Safflower is well known for the treatment of inflammation and pain associated with trauma. This was scientifically validated on macrophage cells as well as on yeast α-glucosidase (Liao et al., 2014). Yadava and Chakravarti (2008) explored the compounds responsible for anti-inflammatory effects and that was identified as 3β-O-[β-D-xylopyranosyl(1 → 3)-O-β-D-galactopyranosyl]-lup-12-ene-28-oic acid-28-O-α-L-rhamnopyranosyl ester. Pain alleviating effect was also validated (Zhengliang et al., 1984). In a study conducted by Zhao et al., (2010) the inhibition effect of ethyl acetate extract (HE) of safflower on serotonin (5HT) uptake was explored. The study suggested that HE potentially inhibits the 5HT uptake and further evaluation led to the identification of a new bio-active coumaroylspermidine analog (CX). Primary screening demonstrated that CX had a selective antagonist activity on serotonin transporter (SERT) with the IC_{50} of $0.564 \pm 0.15 \, \mu M$.

HSYA demonstrated wide spectrum of biological effects. Its effect on lipid polysaccharide (LPS)-induced acute lung injury (ALI) showed that HSYA down-regulate the inflammatory cytokines such as tumor necrosis factor (TNF)-α, interleukin (IL)-1β, IL-6 and interferon (IFN)-β in serum. It was also noticed that HSYA prevent the activations of

mitogen activated protein kinases including p38, cJun N-terminal kinase (JNK) and extracellular signal regulated kinase (ERK). The report concluded that HSYA decreases the inflammation response in LPS induced ALI via inhibition of TLR 4-dependent signalling pathways (Liu et al., 2014a). The mechanism of antitumor effect of HSYA was established on MCF-7 cell line. It was identified that HSYA induce apoptosis through up-regulation of Bax and p53, down-regulation of Bcl-2 and cyclin D1, release of cytochrome c from the mitochondria to the cytosol, disruption of the mitochondrial transmembrane potential ($\Delta\psi_m$) and activation of caspase-3. Similarly it also inhibits the NF-κB/p65 pathway. Hence the study concluded that HSYA induce apoptosis via mitochondrial pathway in MCF-7 cells (Li et al., 2014b). Neuroprotective effect of HSYA on cerebral ischemic injury model suggested that sublingular vein injection of HSYA at a dose of 6.0 mg/kg was comparable with nimodipine at a dose of 2.0 mg/kg (Zhu et al., 2003).

In a recent study conducted by Liu et al., (2014b) indicated the reverse effect of safflor yellow (SY) on vascular remodelling. The proliferation and migration rates of angiotensin-II (Ang II) treated rat aortic adventitial fibroblasts were higher than untreated groups and increases in the expression of p-ERK1/2, AP-1, collagen I and III. This was down regulated after treatment with SY. The study was concluded that SY exhibits anti-proliferative, and pro-apoptotic activities through the Ang II/ERK/AP-1 signalling pathways (Liu et al., 2014b). Kaempferol 3-O-rutinoside and kaempferol 3-O-glucoside, obtained from safflower was evaluated for hepatoprotective effect on CCl_4 induced liver toxicity in mice. It was observed that both the compounds had increased the level of total protein and prevented the CCl_4 induced increase level of serum alkaline phosphatase, hepatic malondialdehyde and serum aspartate aminotransferase at a dose of 200 mg/kg and 400 mg/kg (Wang et al., 2014).

2.4.2 Safflower in clinical use

Traditional Chinese medicines use safflower for thousands of years to treat various ailments. It was reported that, 56 of 77 women who had been infertile for 1.5-10 years became pregnant when received safflower (Wenyu 1986). According to Yaling, labour induction was more effective when allopathic medicine is used with safflower rather than alone (Yaling 1985). In addition to that decoction of safflower have successfully exerted in the treatment of cerebral embolism (Zuolin 1992).

Clinical studies proved that, consumption of safflower preparations improve the treatment of leukaemia (Youan 1988), jaundice and viral hepatitis, migraine headaches (Guimiao and Yili 1985) and goitre (Shulin 1992). Prescription containing safflower extract have been very effective in the treatment of thorax rheumatism and its wine is recommended for 62 types of rheumatism (Yukun 1988, Honghai 1985, Yue and Luqiu 1990). More than 80% of patients who have been suffered with chronic and atrophic gastritis were found to be cured or improved when administered with 50-120 doses of safflower florets (Hang et al., 1985; Shang et al., 1989; Lianen 1992)

The common side effect occur during the treatment of schizophrenia has been effectively managed by injecting safflower medicines. Injection of safflower-bugleweed (*Lycopus lucidus*) in the early stages of treatment of epidemic haemorrhagic fever prevented the further development of disease (Guimiao and Yili 1985). Preparations of safflower florets are prescribed to regulate urethra function, improve chronic nephritis (Weiss 1983) and to treat haematuria associated with calculi (Guimiao and Yili 1985).

2.4.2.1 *Effect on joints and muscles*

Single or double doses of safflower along with millet wine helps wrenched joints and muscle injuries to heal within a week (Guimiao and Yili 1985; Jianxin 1989). Steaming and wrapping a towel that was soaked in safflower tea extract is recommended for wrist tenosynovitis (Zhangquan 1985). Chronic suppurative osteomyelitis and cervical spondylosis were effectively treated by safflower extracts in combination with other herbs (Sai 1992).

2.4.2.2 *Effect on skin and lungs*

Safflower produced many beneficial effects in the treatment of various skin related diseases like erythema nodosum (Zaihe 1989), polymorphic erythema, acne rosacea, urticaria, psoriasis, pruritis (Guimiao and Yili 1985). Similar effects were found in the treatment of acute laryngitis and pharyngitis. More than 50% of patients recovered from the disease, when they were sprayed the mixture of safflower and Japanese honeysuckle in water on throat. Likely, they did not experience any side effects (Shengyun 1985). Reports were further explored the use of safflower in the treatment of respiratory diseases including pertussis and bronchitis (Guimiao and Yili 1985).

2.4.2.3 *Effect on CVS*

Zuozuo et al., (2000) studied the antimyocardial effect of SY on the canine model. The group observed that at the lower dose level (5 mg/kg) it inhibited the heart rate whereas at higher dose (40 mg/kg) it weakened. It was also identified that the SY exhibited anti-myocardial effect by elevating the activity of erythrocuprein in the cardiac muscle and blood plasma (Yongna 2005). Extract of safflower found to reduce blood cholesterol level in patients associated with coronary disease after undergoing 6 weeks treatment (Guimiao and Yili 1985).

2.4.2.4 *Effect on brain*

Shuqun et al., (1995) discovered that safflower extract can work against the inhibition of $Ca2^+$/CaM-Pk II, an indicator enzyme of cerebral ischemia. The activity of $Ca2^+$/CaM-Pk II was increased 5.8 fold higher in safflower treated group than control. The study also concluded that cerebral ischemia induces excess of $Ca2^+$ which in turn causes brain injury. This can be prevented by safflower extract as it acts as $Ca2^+$ antagonism (Shuqun et al, 1995).

2.4.2.5 *Effect on free radicals*

At the optimum level, free radicals and radicals derived, play a crucial role in the physiological function such as regulation of vascular tone, production of erythropoietin and signal transduction in various physiological conditions. At the same time excess and/or sustained increase will result in the pathogenesis of cancer, neurodegenerative diseases, rheumatoid arthritis, ischemia, diabetes mellitus, atherosclerosis and other diseases (Droge, 2002). Zhang et al., (1997) studied the free radical scavenging effect of serotonin derivatives obtained from safflower oil cake. The study revealed that serotonin derivatives were strongly scavenging the radical ions than α-tocopherol and butylated hydroxy anisole (BHA) a widely used natural antioxidant and synthetic antioxidant respectively in 2,2-diphenyl-1-picrylhydrazyl (DPPH) model. Anti-oxidative potential of 8 flavonoids was evaluated against 2-deoxyribose degradation and rat liver microsomal lipid peroxidation induced by hydroxyl radicals generated via a Fenton-type reaction. Among those luteolin, quercetin and its acetyl glycosides has exhibited strong antioxidative properties on both the models (Lee et al., 2002). Olaleye et al., (2014) investigated the DPPH free radical scavenging activity of ethyl acetate extract and 14 compounds isolated from safflower. Results showed that ethyl acetate extract and compounds kaempferol, quercetin, p-hydroxycinnamic acid has strong radical scavenging activity on TLC-DPPH method. Yue et al., (2014b) observed showed that water

extract exhibit significance scavenging of DPPH and ABTS radicals. Further investigations led to the identification of 6-hydroxykaempferol glycosides and quinochalcone C-glycosides as the contributors for scavenging effects.

2.4.2.6 *Antiallergic effect*

Antiallergic effect of safflower was screened using RBL-2H3 cell membrane chromatography coupled with HPLC-MS. It was identified that, HSYA was responsible for observed activity. The results showed that HSYA could alleviate the immunoglobulin E induced release of allergic cytokines without affecting the normal cells at the dose of 50 μM (Han et al., 2014).

Chapter 3
Objectives and Plan of Work

3. OBJECTIVES AND PLAN OF WORK

The objectives of the proposed work include,

PART-I

Microscopic analysis, LC-MS based isolation of chemical constituents and their characterization followed by the identification of cytotoxic lead molecules from *Oldenlandia umbellata*.

PART -II

Comparative pharmacognostic evaluation and standardization through High Performance Thin Layer Chromatographic (HPTLC) analysis of *Carthamus tinctorius* (Safflower) petals of different Indian cultivars.

PLAN OF WORK

PART I

- Collection and authentication of *Oldenlandia umbellata*.

- Microscopic analysis of aerial parts of *O. umbellata*.

- Study of secondary metabolic profile of *O. umbellata* by LC-MS analysis

- Isolation and purification of chemical constituents of *O. umbellata*

- Structure elucidation of isolated constituents

- In-vitro cytotoxic studies of mother extract, fractions and characterized compounds

PART II

- Quantitative pharmacognostic studies of four Indian varieties of safflower petals as per WHO guidelines

25

- Microscopic analysis of selected varieties of safflower petals

- Determination of heavy metals and pesticide residues in selected varieties of safflower petals

- Standardization of safflower decoction through quantification of flavonoids using HPTLC analysis.

Chapter 4
Materials and Methods

4. MATERIALS AND METHODS

PART I

4.1 Collection of plant material

The aerial parts of *O. umbellata* were collected from Virudunagar District, Tamilnadu, India during December-January and authenticated by Prof. P. Jayaraman, Director, Plant Anatomy Research Centre, Chennai, India (PARC/2014/2092). A voucher specimen (HU/2012/12-1) was deposited at Department of Pharmacy, BITS-Pilani Hyderabad Campus, Telangana State, India.

4.2 General experimental procedures

All chemicals, solvents and reagents used were of analytical and molecular biology grade. Solvents used in HPLC analysis were of HPLC grade obtained from Merck Specialities Private Ltd., Mumbai, India. 3-(4,5-dimethylthiazole-2-yl)-2,5-diphenyltetrazolium bromide (MTT) assay: MTT (Sigma-Aldrich, Bangalore, India), PBS, RPMI medium and FBS (Gibco BRL, CA, USA). 5-Fluorouracil was procured Sigma-Aldrich, Bangalore, India. Cell viability: Multi-well plate reader (Spectra Max® M4, Molecular Devices, USA). Lyophilization (Coolsafe™, Scanvac). Column chromatography (CC): silica gel (60-120 μm, 100-200 μm and 230-400 μm); Merck Specialities Private Ltd., Mumbai, India. Flash Chromatography: YMC, Japan. Preparative (LC-8A) and analytical (LC-20AD) HPLC: Shimadzu, Japan, equipped with UV and PDA detector respectively. LCMS analysis: LCMS-2020 (Shimadzu, Japan, using ESI interface). UV-Visible (V-650), FT-IR spectroscopy (FT/IR-4200): Jasco Analytical Instruments, USA. Diaion resin (Sorbent Technologies, Norcross GA, USA and Kitton enterprises, Mumbai, India). Rotary evaporation: Buchi Rotavapor R-210 (Switzerland). ^{1}H- and ^{13}C-NMR spectra: Bruker *DRX-*

500 spectrometer (500 and 125 MHz for ^{1}H and ^{13}C, respectively) in CDCl$_3$ or CD$_3$OD solution.; δ in ppm relative to Me$_4$Si as internal standard, *J* in Hz.

4.3 Microscopic analysis of *O. umbellata*

4.3.1 *Preparation of specimens*

Care was taken to select healthy plants and normal organs. The required samples of different organs were cut and removed from the plant and fixed in Formalin:acetic acid:70% ethyl alcohol (5:5:90 v/v/v). After 24 hrs of fixing, the specimens were dehydrated with graded series of tertiary-butyl alcohol (TBA) as per the schedule given by Sass (1940). Infiltration of the specimens was carried out by gradual addition of paraffin wax (mp. 58 – 60 ˚C) until TBA solution attained super saturation. The specimens were cast into paraffin blocks.

4.3.2 *Sectioning*

The paraffin embedded specimens were sectioned with the help of Rotary Microtome. The thickness of the sections was 10-12 μm. Dewaxing of the sections was performed by customary procedure (Johansen 1940). The sections were stained with Toluidine blue O, as per the method published by O'Brien et al. (1964). Since Toluidine blue O is a polychromatic stain, the staining results were remarkably good; and some cytochemical reactions were also obtained. The dye rendered pink colour to the cellulose walls, blue to the lignified cells, dark green to suberin, violet to the mucilage, blue to the protein bodies etc.

4.3.3 *Photomicrographs*

Microscopic descriptions of tissues are supplemented with micrographs wherever necessary. Photographs of different magnifications were taken with Nikon Lab Photo 2

Microscopic Unit. For normal observations bright field was used. For the study of crystals and lignified cells, polarized light was employed. Since these structures have birefringent property, under polarized light they appear bright against dark background. Descriptive terms of the anatomical features are as given in the standard Anatomy book (Esau, 1964).

4.4 Extraction and fractionation of *O. umbellata*

Dried and ground aerial parts of *O. umbellata* (5.0 kg) were extracted using MeOH under heating at 45–50 °C. The methanolic extract was evaporated under reduced pressure to a dry residue, **HUM** (442 g). Around 440 g was suspended in water and subjected to solvent-solvent partition using 3×1.5 L of diethyl ether, and butanol. The diethyl ether and butanol soluble fractions were evaporated under vacuum and lyophilized to obtain dry residues, **HUM-E** (102 g) and **HUM-B** (108 g), respectively. These residues were stored at -20 °C for further studies.

4.5 LC-PDA-ESI-MS analysis of HUM-E and HUM-B

Fingerprinting of **HUM-E** and **HUM-B** was carried out using Shimadzu LCMS-2020. HPLC was performed on LC20AD liquid chromatography, consisting of an HPLC binary pump, an autosampler, a column oven and PDA detector. Separation was performed on Shim-pack XR-ODS column (100 × 3.0 mm, 3 μm, Shimadzu, Japan) and the column temperature was set at 40 °C. Under optimized conditions mobile phase consisted of A (0.4% v/v formic acid in aqueous phase) and pump B (MeCN). LC-ESI-MS fingerprinting of **HUM-E** was developed by a gradient elution of 2-95% B at 0-45 min, and then maintained at 95% for 5 min, 95-2% B at 5 min and maintained at 2% for 5 min. The flow rate was kept at 0.3 mL/min and the sample volume injected was set at 5 μL. In the same way, fingerprinting of **HUM-B** was developed with slight modifications in the method. All MS detection was conducted on a Shimadzu LCMS-2020 single quadrupole equipped with electrospray

ionization (ESI) interface. The MS analysis was performed in positive and negative scan mode under the following operation parameters: the dry gas temperature was set at 350 ˚C, the interface voltage was 4.5 kV and the flow rate of nebulising and drying gas was fixed at 1.5 L/min and 15 L/min respectively. Full scan data acquisition and dependent scan event data acquisition were performed from *m/z* 100 to 700.

4.6 Isolation of constituents of HUM-E

About 96 g of **HUM-E** was chromatographed on silica gel (#60-120, 750 g, n-hexane) with solvents of increasing polarity (hexane-toluene, toluene-EtOAc and EtOAc-MeOH). The fractions eluated with toluene-EtOAc (50:50) (51 g) were re-chromatographed on silica gel CC (#100-200, 600 g, n-hexane) and eluated with increasing concentration of EtOAc in toluene. Based on the TLC pattern, the fractions eluated with toluene-EtOAc (70:30) were combined and evaporated to give the residue (12.6 g), which was then divided into part A (5.6 g) and part B (7.0 g).

Repeated chromatography of Part A on silica gel followed by Diaion HP-20, eluting with MeOH yielded fractions enriched with compound **HU-1** (3.5 mg). Subsequent purification by preparative TLC (developed with CHCl$_3$-MeOH (20:1), R$_f$ 0.38) gave **HU-1** (1.5 mg) as amorphous solid.

Part B of the residue was rinsed with hexane and the insoluble residue was treated with EtOAc. The EtOAc soluble portion (2 g) was chromatographed on silica gel (# 100-200, 50 g, n-hexane) with hexane-EtOAc. Elution with hexane-EtOAc (90:10) afforded compound **HU-5** (31 mg), compound **HU-4** (26 mg) and two slightly impure compounds. Further elution with hexane-EtOAc (88:12) yielded compound **HU-3** (10 mg) and elution with hexane-EtOAc (75:25) furnished compound **HU-2** (6 mg). The above impure fraction was subjected for flash chromatography over silica gel (#230-400, 12g, n-hexane) using n-

hexane-EtOAc (80:20) to afford compound **HU-6** (5.3 mg). The above impure fraction HU-**7**Ex was purified by preparative RP-HPLC (Luna, 250×21.2 mm, C_{18} (2), 5 μm, 100 A$^{\circ}$, 4 mL/min) using a step gradients MeCN in H_2O to afford compound **HU-7** (1.9 mg).

4.7 Isolation of constituents of HUM-B

About 105 g of n-butanol fraction obtained from crude methanolic extract of *O. umbellata* was chromatographed on HP-20 Diaion resin column (# 250 μm, 600 g, H_2O) and eluated with step wise gradient of MeOH in H_2O. Fractions 1-12 obtained from eluate of H_2O (100%) were pooled and lyophilized. The concentrated fractions were treated with MeOH. The MeOH soluble portion (23 g) was chromatographed over silica gel (# 100-200, 150 g, $CHCl_3$) using $CHCl_3$ and MeOH to yield two major fractions, A (90:10) and B (80:20).

Fraction A was separated into two parts (AI & AII) based on their TLC profile. Fraction AI (7.5 g) was subjected for preparative RP-HPLC (Luna 5 μm, C_{18} (2), 100 A$^{\circ}$, 250 $\times$ 21.2 mm, 10 mL/min) using step wise gradient elution of MeCN in H_2O (0.05% TFA). Fractions collected between 18-24 min (MeCN 68-79%) yielded a mixture of compounds (2 g). This was further purified by flash chromatography on silica gel (# 230-400, 12 g, EtOAc) using gradient elution of MeOH in EtOAc. Two major fractions (AIa and AIb) were collected at 8% and 15% of MeOH, respectively. Fraction AIa (700 mg) was further refined by preparative RP-HPLC (Luna 5 μm, C_{18} (2), 100 A$^{\circ}$, 250 $\times$ 21.2 mm, 5 mL/min) using a gradient elution of MeOH in H_2O to afford **HU-8** (4.0 mg), **HU-9** (6.0 mg) and **HU-10** (4.7 mg) collected at 25 min, 30 min and 33 min, respectively. Fraction AIb (200 mg) was further purified by preparative RP-HPLC using same elution process of AIa to afford **HU-11** (4.1 mg).

Fraction B, (2.62 g) was subjected to series of flash chromatography (SiO_2, # 230-400, 12 g, $CHCl_3$) with step gradients of MeOH in $CHCl_3$. Eluates of $CHCl_3$:MeOH (20:80)

was further purified by preparative TLC (Silica gel GF$_{254}$, CHCl$_3$: MeOH (8:2), R$_f$: 0.39) to afford **HU-12** (2.2 mg). The homogeneity of isolated compounds was determined by analytical RP-HPLC.

HU-1 (1): Amorphous solid (CHCl$_3$); $[\alpha]_D^{25}$ = 0 (c = 0.07, CHCl$_3$); UV (MeOH) λ_{max} (log ε) 260 (4.28), 307 (3.82) nm; IR (CHCl$_3$): ν_{max} 1722, 1581, 1400, 1330 cm^{-1}; ^{1}H NMR (CDCl$_3$, 500 MHz) δ 7.77 (1H, d, J = 9.5 Hz, H-4), 6.93 (1H, s, H-1'), 6.77 (1H, s, H-5), 6.40 (1H, d, J = 9.5 Hz, H-3), 4.10 (3H, s, -OMe), 2.86 (1H, m, H-4b'), 2.06 (1H, m, H-4a'), 1.39 (3H, s, H-5'); ^{13}C NMR (CDCl$_3$, 125 MHz) δ 164.1 (C-2'), 161.2 (C-2), 146.7 (C-7), 144.5 (C-4), 142.8 (C-6), 142.7 (C-8a), 119.7 (C-8), 114.3 (C-3), 113.5 (C-4a), 103.8 (C-5), 100.4 (C-1'), 56.8 (-OCH$_3$), 45.6 (C-3'), 27.1 (C-4'), 23.0 (C-5'); HR-FAB-MS m/z 513.1469 [M+H]$^+$ (calcd for C$_{30}$H$_{25}$O$_8$, 513.1450).

HU-2 (2): Dark green crystals (CHCl$_3$); m.p. 225-227 ˚C; UV (MeOH) λ_{max} 256, 293, 326, 373, 403, 510, 664 nm; IR (KBr): ν_{max} 3394, 1732, 1696 cm^{-1}; ^{1}H NMR (CDCl$_3$, 500 MHz) δ 9.50 (1H, s, H-16), 9.35 (1H, s, H-11), 8.55 (1H, s, H-6), 7.93 (1H, m, J = 11.5, 17.5 Hz, H-27), 6.25 (1H, s, H-21), 6.29 (1H, d, H-28b), 6. 18 (1H, d, H-28b), 4.45 (1H, m, H-4), 4.19 (1H, m, H-3), 3.88 (3H, s, H-34), 3.63 (3H, m, H-3), 4.45 (1H, m, H-4), 3.57 (2H, s, H-30), 3.39 (3H, s, H-26), 3.20 (3H, s, H-29), 2.52 (2H, m, H-1), 2.20 (2H, m, H-2), 1.70 (3H, m, H-25), 1.56 (3H, m, H-31); ^{13}C NMR (CDCl$_3$, 125 MHz) δ 189.6 (C-20), 173.3 (C-35), 172.2 (C-5), 169.6 (C-33), 161.2 (C-23), 155.7 (C-12), 151.0 (C-15), 149.7 (C-24), 145.2 (C-14), 142.1 (C-7), 137.9 (C-17), 136.3 (C-10), 136.2 (C-9), 131.9 (C-8), 129.1 (C-18), 129.0 (C-19), 122.8 (C-28), 105.2 (C-22), 104.4 (C-16), 97.5 (C-11), 93.1 (C-6), 64.7 (C-21), 52.8 (C-34), 51.6 (C-36), 51.1 (C-3), 50.1 (C-4), 31.0 (C-1), 29.9 (C-2), 23.1 (C-25), 19.4 (C-30), 17.4 (C-31), 12.1 (C-32), 12.1 (C-26), 11.2 (C-29); ESI-MS m/z 607.30.

HU-3 (3): Yellow amorphous powder (CHCl$_3$); m.p. 172-175 ˚C; UV (MeOH) λ$_{max}$ 280, 319 nm; IR (KBr): ν$_{max}$ 3300, 1663, 1590, 1493 cm^{-1}; ^{1}H NMR (CDCl$_3$, 500 MHz) δ 7.57 (1H, d, *J* = 9.5 Hz, H-4), 6.72 (1H, s, H-5), 6.25 (1H, d, *J* = 9.5 Hz, H-3), 6.20 (1H, s, OH), 5.29 (1H, t, H- 2'), 3.94 (3H, s, -OMe), 3.57 (2H, d, H-1'), 1.85 (3H, s, H-4'), 1.68 (3H, s, H-5'); ^{13}C NMR (CDCl$_3$, 125 MHz) δ 161.6 (C-2), 148.4 (C-9), 147.4 (C-7), 143.7 (C-4), 143.7 (C-6), 133.2 (C-3'), 120.7 (C-2'), 116.2 (C-8), 113.1 (C-3), 111.2 (C-10), 105.1 (C-5), 56.3 (-OCH$_3$), 25.8 (C-4'), 22.2 (C-1'), 18.0 (C-5'); ESI-MS *m/z* 259.25 [M-H]$^-$.

HU-4 (4): White amorphous powder (CHCl$_3$); m.p. 275-278 ˚C; UV (CDCl$_3$) λ$_{max}$ 262, 324 nm; IR (KBr): ν$_{max}$ 3436, 1692, 1457 cm^{-1}; ^{1}H NMR (CDCl$_3$, 500 MHz) δ 11.95 (1H, s, -COOH), δ 5.24 (1H, s, H-12), 3.38 (1H, br s, -OH), 3.20 (1H, t, H-3), 2.02-1.54 (m), 1.49 (3H, s), 1.45 (3H, s), 1.27 (3H, s), 1.03 (3H, s), 2.19 (1H, d, *J* = 11.5 Hz), 0.90 (3H, d), 0.78 (3H, d); ^{13}C NMR (CDCl$_3$, 125 MHz) δ 180.6 (C-28), 138.1 (C-13), 125.4 (C-12), 78.8 (C-3), 55.1 (C-5), 52.7 (C-18), 47.7 (C-9), 47.5 (C-17), 42.0 (C-14), 41.6 (C-19), 41.1 (C-20), 41.1 (C-4), 39.4 (C-1), 39.1(C-8), 38.5(C-22), 38.3 (C-10); ESI-MS *m/z* 455.40 [M-H]$^-$.

HU-5 (5): Yellow needles (CHCl$_3$); m.p. 227-230 ˚C; UV (MeOH) λ$_{max}$ 241, 252, 278, 313, 358, 478 nm; IR (KBr): ν$_{max}$ 3312, 1663, 1573 cm^{-1}; ^{1}H NMR (CDCl$_3$, 500 MHz) δ 8.23-8.27 (2H, m, H-5 & H-8), 7.76-7.78 (2H, m, H-6 and H-7), 7.72 (1H, s, H-4), 6.38 (1H, s, OH), 4.09 (3H, s, -OMe), 4.04 (3H, s, -OMe); ^{13}C NMR (CDCl$_3$, 125 MHz) δ 182.5 (C-10), 181.6 (C-9), 154.0 (C-3), 153.8 (C-1), 145.5 (C-2), 135.0 (C-12), 134.1 (C-11), 133.3 (C-6), 132.6 (C-7), 131.6 (C-14), 127.1 (C-8), 126.7 (C-5), 120.9 (C-13), 110.4 (C-4), 61.7 (C-1-OCH$_3$), 61.6 (C-2-OCH$_3$); APCI-MS *m/z* 283.25 [M-H]$^-$.

HU-6 (6): Yellow amorphous powder (CHCl$_3$); m.p. 215-217 ˚C; UV (MeOH) λ$_{max}$ 240, 253, 279, 365 nm; IR (KBr): ν$_{max}$ 3300, 1670, 1590, 1560 cm^{-1}; ^{1}H NMR (CDCl$_3$, 500 MHz) δ 8.18-8.30 (2H, m, H-5 & H-8), 7.71-7.79 (2H, m, H-6 & H-7), 7.62 (1H, s, H-4),

3.07 (1H, s, OH), 4.04 (3H, s, -OMe), 4.0 (3H, s, -OMe); ^{13}C NMR (CDCl$_3$, 125 MHz) δ

182.5 (C-10), 181.7 (C-9), 151.5 (C-3), 147.4 (C-1), 144.9 (C-2), 134.7 (C-14), 133.9 (C-7),

133.3 (C-6), 132.7 (C-12), 127.7 (C-11), 127.0 (C-8), 126.7 (C-5), 120.8 (C-13), 106.3 (C-4),

61.8 (C-1-OMe), 56.6 (C-3-OMe); APCI-MS m/z 283.25 [M-H]$^-$.

HU-7 (7): Yellow amorphous solid (CHCl$_3$); $[\alpha]_D^{25}$ = -15.6 (c = 0.20, CH$_3$OH); UV

(MeOH) λ$_{max}$ 230, 272, 347 nm; ^{1}H NMR (CDCl$_3$, 500 MHz) δ 7.78 (1H, d, J = 9.5 Hz, H-4),

6.87 (1H, s, H-5), 6.18 (1H, d, H-3), 5.45 (1H, t, J = 18.7 Hz, H-8), 5.14 (1H, t, J = 1.5 Hz,

H-2'a), 4.96 (1H, d, J = 1.5 Hz, H- 2'b), 3.56 (1H, dd, J = 15.9, 7.8 Hz, H-9a), 3.17 (1H, dd, J

= 15.9, 7.8 Hz, H-9), 1.78 (3H, s, -Me); ^{13}C NMR (CDCl$_3$, 125 MHz) δ 163.7 (C-2), 153.6

(C-6a), 144.9 (C-6), 146.3 (C-9b), 146.3 (C-4), 140.5 (C-3'), 115.5 (C-9a), 114.6 (C-4a),

114.5 (C-3), 113.0 (C-4'), 112.6 (C-5), 89.4 (C-2'), 32.8 (C-1'), 17.0 (C-5'); ESI-MS m/z

245.05 [M+H]$^+$.

HU-8 (8): White amorphous solid (MeOH); m.p. 129-132 ˚C; $[\alpha]_D^{25}$ = +7.46 (c =

0.85, MeOH); UV (MeOH) λ$_{max}$ 238 nm; ^{1}H NMR (CD$_3$OD, 500 MHz) δ 7.63 (1H, s, H-3),

6.01 (1H, br s, H-7), 5.05 (1H, d, H-1), 4.93 (1H, m, H-6), 4.85 (1H, m, H-1'), 3.86 (2H, dd, J

= 1.8, 12.1 Hz, H- 10), 3.60 (1H, m, H-6'), 3.23-3.39 (m, H-2'-5'), 3.01 (1H, m, H-5), 2.62

(1H, m, H-9), 2.08 (3H, s, -OMe); ^{13}C NMR (CD$_3$OD, 125 MHz) δ 172.6 (C-11), 170.4

(CH$_3$<u>C</u>O), 155.2 (C-3), 146.0 (C-8), 131.9 (C-7), 108.7 (C-4), 101.2 (C-1), 100.6 (C-1'), 78.6

(C-3'), 77.9 (C-5'), 75.4 (C-6), 75.0 (C-2'), 71.6 (C-4'), 63.8 (C-10), 63.0 (C-6'), 46.3 (C-9),

42.6 (C-5), 20.7 (<u>C</u>H$_3$CO); ESI-MS m/z 431.20 [M-H]$^-$.

HU-9 (9): White amorphous solid (MeOH); m.p. 129-132 ˚C; UV (MeOH) λ$_{max}$ 234.5

nm; ^{1}H NMR (CD$_3$OD, 500 MHz) δ 7.28 (1H, d, J = 2.1 Hz, H-3), 5.94 (1H, d, J = 1.4 Hz,

H-7), 5.63 (1H, s, H-1), 5.56 (1H, m, H-6), 4.67 (1H, d, H-1'), 4.18 (2H, t, J = 2.4 Hz, H- 10),

3.89-3.92 (1H, dd, J = 2.1, 2.2 Hz, H-6'b), 3.64-3.67 (1H, m, H-6'a) 3.31-3.38 (m, H-2'-5'),

3.15-3.20 (2H, m, H-5 and H-9); ^{13}C NMR (CD$_3$OD, 125 MHz) δ 171.5 (C-11), 148.9 (C-3), 148.4 (C-8), 124.3 (C-7), 105.1 (C-4), 98.5 (C-1), 91.9 (C-1'), 85.3 (C-6), 77.0 (C-3'), 76.5 (C-5'), 73.3 (C-2'), 70.2 (C-4'), 61.4 (C-6'), 58.7 (C-10), 43.6 (C-9), 36.1(C-5); ESI-MS *m/z* 371.20 [M-H]$^-$.

HU-10 (10): White amorphous solid (MeOH); m.p. 130-133 ˚C; UV (MeOH) λ$_{max}$ 240 nm; ^{1}H NMR (CD$_3$OD, 500 MHz) δ 7.50 (1H, d, *J* = 1.0 Hz, H-3), 5.79 (1H, d, *J* = 1.2 Hz, H-7), 5.18 (1H, d, = 6.3 Hz, H-1), 4.65 (1H, d, *J* = 2.2 Hz, H-1'), 4.53 (1H, br t, *J* = 2.5 Hz, H-6), 4.31 (1H, d, *J* = 15.3, H- 10b), 4.16 (1H, d, *J* = 15.3, H-10a), 3.8 (1H, dd, H-6'a) 3.61 (1H, dd, H-6'b), 3.75 (3H, s, -COOC<u>H</u>$_3$), 3.18-3.36 (m, H-2'-H-5'), 3.00 (1H, dd, *J* = 6.5 Hz, H-9), 2.98 (1H, dd, *J* = 7.7, 4.6 Hz, H-5); ^{13}C NMR (CD$_3$OD, 125 MHz) δ 170.3 (C-11), 153.9 (C-3), 147.5 (C-8), 130.1 (C-7), 110.8 (C-4), 100.3 (C-1'), 98.3 (C-1), 82.3 (C-6), 78.4 (C-3'), 77.9 (C-5'), 74.8 (C-2'), 71.5 (C-4'), 62.7 (C-6'), 61.0 (C-10), 52.1(-OMe), 47.1(C-9), 45.6 (C-5); ESI-MS *m/z* 427.10 [M+Na]$^+$, 403.20 [M-H]$^-$.

HU-11 (11): White amorphous solid (MeOH); m.p. 142-144 ˚C; UV (MeOH) λ$_{max}$ 240 nm; ^{1}H NMR (CD$_3$OD, 500 MHz) δ 7.44 (1H, s, H-3), 5.82 (1H, s, H-7), 5.0 (1H, d, *J* = 7.7 Hz, H-1), 4.69 (1H, d, *J* = 7.9 Hz, H-1'), 4.56 (1H, br s, H-6), 4.34 (1H, d, *J* = 15.3 Hz, H-10b), 4.16 (1H, d, *J* = 15.3 Hz, H-10a), 3.83 (1H, m, H-6'b) 3.61 (1H, m, H-6'a), 3.19-3.39 (m, H-2'-H-5'), 2.92 (1H, m, H-9), 2.88 (1H, m, H-5); ESI-MS *m/z* 389.20 [M-H]$^-$.

HU-12 (12): White amorphous solid (MeOH); m.p. 131-134 ˚C; UV (MeOH) λ$_{max}$ 235.5 nm; ^{1}H NMR (CD$_3$OD, 500 MHz) δ 7.65 (1H, d, *J* = 1.1 Hz, H-3), 6.01 (1H, s, H-7), 5.04 (1H, d, *J* = 9.0 Hz, H-1), 4.72 (1H, d, *J* = 7.9 Hz, H-1'), 4.46 (1H, d, *J* = 1.4 Hz, H- 10b), 4.22 (1H, d, *J* = 15.7 Hz, H-10a), 3.85 (1H, d, *J* = 10.4 Hz, H-6'b) 3.74 (3H, s, -OMe), 3.66 (1H, m, H-6'a), 3.22-3.32 (m, H-2'-H-5'), 3.01 (1H, m, H-9), 2.56 (1H, m, H-5); ESI-MS *m/z* 403.15 [M-H]$^-$, 427.19 [M+Na]$^+$.

4.8 Cytotoxic studies of HUM, HUM-E, HUM-B and isolated compounds

In-vitro cytotoxic effect of **HUM**, **HUM-E**, **HUM-B** and isolated compounds (**HU-2** to **HU-6** and **HU-8** to **HU-10**) was carried out on a panel of three human tumor cell lines (A549, MDA-MB-231 and HT-29) and one normal cell line (HEK-293) using 3-(4,5-dimethylthiazol-2-yl)-2,5-diphenyltetrazolium bromide (MTT) method. All cell lines were procured from National Centre for Cell Science (Pune, India). Briefly, a limited number of human tumor or normal cells (5000/well) were seeded in to a 96-well microplate and became attached to the bottom of the well overnight. The primary stock solution was prepared in DMSO. This was further diluted with fresh medium to get 25, 50, 100 and 200 μg/mL wherein the concentration of DMSO was 0.01%. On the second day of the procedure, 50 μL of each concentration was added to the respective well. After an incubation period of 72 h, the living cells were assayed by the addition of 15 μL of 5 mg/mL MTT solution. After 4 h incubation at 37 °C, the medium was removed and the precipitated formazan was dissolved in 150 μL of DMSO. Finally, the reduced MTT was assayed at 545 nm, using a microplate reader. Untreated cells were taken as the negative control, and 5-Fluorouracil was used as a positive standard. All concentrations of the tested compounds were assayed in triplicates and the IC_{50} value of each compound was calculated by GraphPad Prism 5.0 (GraphPad Software; San Diego, CA, USA).

PART II

4.9 Collection of safflower petals

Safflower petals of two spiny varieties [TSF-1 and Sagaramutyalu (APRR3)], a non-spiny hybrid [NARI-NH-01] and a non-spiny variety [NARI-06] were collected from farmer's cultivation land near Ranga Reddy District, Telangana State, India and preserved at -20°C till the completion of work.

4.10 General experimental procedures

The solvents used were of HPLC grade and other reagents were of AR grade. Saponin R was procured from Loba Chemie Pvt. Ltd., Mumbai, India. All standard pesticides were procured from Dr. Ehrensortfer GmbH (Augsburg, Germany). Until unless specified, all the chemicals and reagents were purchased from Sigma-Aldrich Chemicals Pvt. Ltd., Bangalore, India. High purity water was obtained from Milli-Q water system (Millipore, Billerica, MA, USA) and the resistivity was 18.2 MΩ at 25 ˚C. Heavy metals analysis was done using Perkin Elmer-AA Analyst 700 Atomic Absorption Spectrophotometer (AAS) with flame and mercury hydride system. Pesticide residue was determined using Shimadzu GC-2010 Capillary Gas Chromatograph with electron capture detector (ECD) and phosphorus mode flame photometric detector (PFPD). HPTLC analysis was performed using CAMAG, Auto sampler IV, TLC Scanner III system operated by WIN CATS software (V 143 CAMAG).

4.11 Preparation of decoction of safflower petals

Around 500 gm of each variety of safflower petals were boiled with water (3 × 600 mL) for 30 min and the decoction was filtered through muslin cloth. The filtrate was concentrated under reduced pressure and lyophilized. This was subjected for quality control studies wherever it was necessary.

4.12 Quantitative pharmacognostic studies as per WHO guidelines

Systematic quality control studies were performed according to WHO guidelines (1998).

4.12.1 Determination of ash values

4.12.1.1 *Total ash*

Accurately weighed 3g of air dried powdered material was taken in a pre-weighed silica crucible and ignited gradually to 500˚C. Ignition was done until to get the constant weight. Weight of crucible was noted and content of total ash was calculated.

4.12.1.2 *Acid-insoluble ash*

To the total ash, 25 mL of (~70 g/L) HCl was added, covered with watch-glass and boiled for 5 min. Watch-glass was rinsed with 5 mL of water and added to crucible. This was filtered through ashless filter-paper and washed with hot water until the filtrate was neutral. The filter-paper alongside ash was transferred to crucible. This was dried in a hot-air oven and ignited until to get the constant weight. Crucible was cooled in a desiccator and its weight was noted down without delay. Content of acid-insoluble ash was calculated.

4.12.1.3 *Water soluble ash*

To the crucible containing total ash, 25 mL of water was added and boiled for 5 min. It was filtered through ashless filter-paper and washed with hot water. Filter-paper along with content was ignited at 425 ˚C for 15 min. The weight of water soluble ash was calculated from subtracting water insoluble ash from total ash.

4.12.2 Extractable matter

4.12.2.1 *Hot extraction*

Accurately weighed 4.0 g of plant material was taken in a glass-stoppered flask and 100 mL of water was added to this. The weight of the flask was noted down and allowed to stand for 1 h at room temperature. After 1 h flask was attached with reflex condenser and

boiled for 1 h; cooled and weighed. The weight was readjusted to initial weight with water. Contents were mixed well and filtered rapidly. 25 mL of the filtrate was transferred in a pre-weighed dish and dried at 150 ˚C for 6 h; cooled in desiccator and weighed.

4.12.2.2 *Cold extraction*

Accurately weighed 4.0 g of plant material was taken in a glass-stoppered and 100 mL of water was added to this. The flask was macerated for 6 h with frequent shaking, allowed to stand for 18 h and filtered around 25 mL of the filtrate was transferred in a pre-weighed dish and dried at 150 ˚C for 6 h. Later, dish was cooled in desiccator and weighed.

4.12.3 Bitterness value

4.12.3.1 *Preparation of stock solution of quinine hydrochloride*

Accurately weighed 0.1 g of quinine hydrochloride was dissolved in sufficient drinking water to produce 100 mL. Further, 5 mL of this solution was diluted to 500 mL with safe drinking water, which made up the concentration to 0.01 mg/mL. From this nine serial dilutions were made as shown in Table 4.1 for initial test.

4.12.3.2 *Stock solution of the plant extracts*

1 mg/mL of stock solution was prepared in safe drinking water. Serial dilutions were made as per Table 4.2.

4.12.3.3 *Method*

After rinsing the mouth with safe drinking water, tube no. 1 was swirled in mouth for 30 sec. If the bitter sensation was not felt in the mouth, then the solution was spitted out and waited for 1 min to ascertain the delayed response. And then rinse the mouth with safe drinking water thoroughly before testing the next higher concentration. This was continued

until to find the threshold bitter concentration. After finding the threshold of standard solution, the same steps were followed to determine the threshold of plant material. The total bitterness value was calculated from the following formula.

$$\frac{2000 \times c}{a \times b}$$

where, a = the concentration of the stock solution (St) (mg/mL)

b = the volume of St (mL) in the tube with the threshold bitter concentration

c = the quantity of quinine hydrochloride (mg) in the tube with the threshold bitter concentration

The bitterness value was expressed in units equivalent to the bitterness of the solution containing 1g of quinine hydrochloride in 2000 mL.

Table 4.1 Bitterness value: Serial dilution for standard sample

	Tube no.								
	1	2	3	4	5	6	7	8	9
Sq (mL)	4.2	4.4	4.6	4.8	5.0	5.2	5.4	5.6	5.8
Safe drinking water (mL)	5.8	5.6	5.4	5.2	5.0	4.8	4.6	4.4	4.2
Quinine HCl in 10 mL of soln. (mg)	0.042	0.044	0.046	0.048	0.05	0.052	0.054	0.056	0.058

Sq: stock solution of quinine hydrochloride

Table 4.2 Bitterness value: Serial dilutions for test samples

	Tube no.									
	1	2	3	4	5	6	7	8	9	10
St (mL)	1.0	2.0	3.0	4.0	5.0	6.0	7.0	8.0	9.0	10.0
Safe drinking water (mL)	9.0	8.0	7.0	6.0	5.0	4.0	3.0	2.0	1.0	0.0

St: Stock solutions of plant extract

4.12.4 Determination of haemolytic activity

4.12.4.1 *Preparation of erythrocyte suspension*

Erythrocyte suspension was prepared by mixing 1 part of sodium citrate (36.5 g/L) with 10 parts of freshly collected blood from a healthy ox and shaken immediately. This was stored at 2-4 °C. 1 mL of citrated blood was taken in a 50 mL volumetric flask containing sufficient amount of phosphate buffer pH 7.4 and the final volume was made with buffer. This diluted blood solution (2%) was stored at cool temperature and used for further analysis.

4.12.4.2 *Preparation of reference solution*

Accurately weighed 10 mg of saponin was transferred in to a volumetric flask and added sufficient quantity of phosphate buffer pH 7.4 to make up the volume to 100 mL.

4.12.4.3 *Preparation of test solution*

Accurately weighed 10 mg of safflower extract was transferred in to a volumetric flask and added sufficient quantity of phosphate buffer pH 7.4 to make up the volume to 100 mL.

4.12.4.4 *Method*

Four serial dilutions of safflower extract was prepared with phosphate buffer pH 7.4 and blood suspension (2%) as shown in Table 4.3. Then the tubes were inverted gently to mix well without forming foam. It was again shaken well after 30 min and allowed to stand for 6 h at room temperature. Then the tubes were examined for haemolysis, indicated by a clear, red solution without any deposit of erythrocytes. The haemolytic activity of the extract was calculated by the following formula

$$1000 \times \frac{a}{b}$$

Where, 1000 = the defined haemolytic activity of saponin R in relation to ox blood

a = quantity of saponin R that produces total haemolysis (g)

b = quantity of plant material that produces total haemolysis (g)

Table 4.3 Haemolytic activity: serial dilution

	Tube no.			
	1	2	3	4
Plant material extract (mL)	0.10	0.20	0.50	1.0
Phosphate buffer pH 7.4 (mL)	0.90	0.80	0.50	-
Blood suspension (2%) mL	1.0	1.0	1.0	1.0

4.12.5 Determination of tannins

Accurately weighed 3.0 g of petals powder was transferred into a conical flask. To that 150 mL of water was added and heated over water bath for 30 min. The flask was cooled and contents were transferred to a 250 mL volumetric flask and volume was made with water. This was allowed to settle down the solid matters and filtered discarding first 50 mL of the filtrate. The total amount of material extractable into water was calculated by evaporating 50

ml of filtrate at 105 ˚C for 4 h. The weight of the residue was noted (T1). The amount of material not bound to hide powder that was extractable into water was determined by mixing 80.0 mL of filtrate with 6.0 g of hide powder and shaken well for 60 min. This was further filtered and 50 mL of filtrate was evaporated to dryness at 105 ˚C for 4 h and weighed (T2). Further to determine the solubility of the hide powder, 6.0 g of hide powder was treated with 80.0 mL of water and shaken well for 60 min. This was filtered and 50 mL of filtrate was evaporated to dryness at 105 ˚C for 4 h and weighed (T0). Then the content of tannin was calculated by following formula.

$$\frac{[T1 - (T2 - T0)] \times 500}{w}$$

Where, w=the weight of the plant material (g)

4.12.6 Determination of swelling index

Accurately weighed 1.0 g of powder was taken in a 25 mL glass-stoppered measuring cylinder. To this 25 mL of water was added and shaken thoroughly every 10 min for 1 h and allowed to stand at room temperature for 3 h. Later the volume occupied by the plant material was measured. The mean value of 3 determinations was calculated.

4.12.7 Determination of foaming index

Accurately weighed 1.0 g of plant material was taken in a 500 mL conical flask containing 100 mL of boiling water. Moderate boiling was maintained for 30 min. The flask was cooled and filtered. The filtrate was transferred in to 100 mL volumetric flask and volume was made up with water. The decoction was poured in to 10 stoppered test tubes in successive portions of 1 mL, 2 mL, 3 mL etc up to 10 mL, and the volume was adjusted with water to 10 mL in each tube. Tubes were stoppered and shaken in lengthwise motion for 15

sec, two shakes/sec. Tubes were allowed to stand for 15 min and height of the foam was measured. Foaming index was calculated using the following formula

$$\frac{1000}{a}$$

where, a = the volume in ml of the decoction used for preparing the dilution in the tube where foaming to a height of 1 cm is observed.

4.13 Microscopic analysis of *C. tinctorius* flowers

Fresh safflower petals removed from the plant were fixed in formalin:acetic acid:70% ethyl alcohol (5:5:90 v/v/v). After 24 h of fixing, the specimen was dehydrated with graded series of tertiary butyl alcohol (TBA) as per established procedure (Sass 1940). Infiltration of the specimens was carried by gradual addition of paraffin wax (m.p. 58 - 60 °C) until TBA solution attained super saturation. The specimens were cast into paraffin blocks. The paraffin embedded specimens were sectioned with the help of Rotary Microtome. The thickness of the sections was 10-12 μm. De-waxing of the sections was by customary procedure (Johansen 1940). The sections were stained with Toluidine blue as per the method published by O'Brien et al., (1964). Microscopic descriptions of tissues are supplemented with micrographs wherever necessary. Photographs of different magnifications were taken with Nikon Lab Photo 2 Microscopic Unit. For normal observations bright field was used.

4.14 Determination of heavy metals using AAS

Samples were extracted using microwave digestion system. In brief, 0.5 g of safflower decoction was treated with 7 mL of HNO_3 and 1 mL of H_2O_2. Then this mixture was subjected to microwaves up to 1000 W at 200 °C for 10 min. When the extract reached to room temperature, the solution was transferred to 50 mL volumetric flask and volume was made with Milli-Q-water.

44

The extracted samples were analyzed on Atomic Absorption Spectrophotometer (AAS) attached with auto-sampler for the presence of heavy metals. Arsenic and mercury was analysed using Hydride Vapour Generator Mode (HVG). The respective hallow cathode lamps were used to produce specific wavelength. Initially the standards of different concentrations were aspirated into an air-acetylene flame to construct calibration curve. However, mercury was analysed in the absence of flame, argon gas was used as carrier gas in the analysis of arsenic and mercury. The concentration of different heavy metals was determined from standard linear curve.

4.15 Determination of pesticide residues

Pesticides were analysed based on QuEChERS method (Lehotay 2007). In brief, 15 g of homogenised petals were weighed into a 50 mL centrifuge tube to which 30 mL of acetonitrile containing 1% acetic acid was added and the tube was shaken and centrifuged at 15000 rpm for 3 min. Then the content was mixed with 3.0 g of sodium chloride and centrifuged for 3 min at 3000 rpm. Organic layer was separated and 16 mL of organic layer was treated with 9.0 g of anhydrous sodium sulphate to remove the moisture content. Then the solution was filtered and 6 mL of filtrate was mixed with a mixture of 0.4 g of primary and secondary amine (PSA) sorbent and 1.2 g anhydrous magnesium sulphate. This was vortexed for 30 sec and centrifuged at 3000 rpm for 5 min. The solution was filtered through 0.22 μm and injected into gas chromatography. The separation was performed on Zebron multi residue 1 capillary column (30 m x 0.25 mm, i.d. 0.20 mm) at a nitrogen flow rate of 1 mL min^{-1} in a constant flow mode, using an oven temperature program for 60 min for organochlorine and organophosphataes and 90 min for synthetic pyrethroids from 150 to 280 °C at a rate of 10 °C/min. The injection inlet was set at 260 °C, detector was set at 330 °C and makeup at 50 mL/min. Injection volume of 1 μL was used with split ratio of 5.0. Standard work solutions were prepared at a concentration of 0.1 μg/mL. The standard

mixture and all concentrated sample fraction were injected into GC-ECD/PFPD to determine the peak area recovered in each fraction.

4.16 Quantification of flavonoids by HPTLC

Quantification of three individual flavonoids was performed by HPTLC on 10×10 cm HPTLC plates pre-coated with silica gel 60 F_{254} (Merck, Darmstadt, Germany) and the plates were washed using methanol before use. The sample and standard solutions were applied as bands of 6 mm wide and 10 mm apart using Automatic TLC Sampler 4 applicator (Muttenz, Switzerland) fitted with a 25 μL Hamilton syringe supplied with Nitrogen flow. A constant application of 6 μL/sec was used. A saturated mixture of toluene: ethyl acetate: methanol: formic acid (3:1:1:0.1 v/v/v/v) was used as mobile phase and chromatography was performed using 10 mL of mobile phase in a 10×10 cm twin trough glass chamber by linear ascending development with a chromatographic run length of 8.5 cm. The optimized chamber saturation time for mobile phase was 20 min at room temperature. Subsequent to the development, the plates were dried in a current of air with the help of a dryer in wooden chamber with adequate ventilation. Densitometric scanning was done with Camag TLC scanner III in the absorbance-reflectance mode at 350 nm with a slit dimension of 5.0 mm x 0.45 mm and a scanning speed of 20 mm/sec. The instrument was operated by WIN CATS software (V 143 CAMAG) resident in the system. The source of radiation utilized was deuterium lamp emitting a continuous UV spectrum between 200 and 400 nm and the concentrations of the compound chromatographed were determined from the intensity of diffusely reflected light.

Chapter 5
Results and Discussion

5. RESULTS AND DISCUSSION

PART I

5.1 Microscopic analysis of *O. umbellata*

5.1.1 *Leaf*

The leaf was 2.25 mm wide and slightly bent upward along the midrib (Figure 5.1.1.1). It was dorsiventral with planoconvex prominent midrib and thick lamina. The adaxial epidermis was very thick; the cells were vertically oblong and thin walled; the cuticle was fairly prominent. The adaxial epidermal cells were 100 μm thick (in vertical plane) and 80 μm wide (in horizontal plane). The abaxial epidermal layer was thin and the cells were narrow and cylindrical (Figure 5.1.1.2 and 5.1.1.3).

The midrib was 400 μm thick and the abaxial part was 330 μm wide. It was flat on the adaxial side and consisted of thick and wide, squarish epidermal cells. The abaxial part of the midrib included three layer of large, angular, thin walled compact ground parenchyma cells. The palisade layer of the lamina was horizontally transcurrent in between the adaxial epidermis and the vascular strand of the midrib (Figure 5.1.1.2). The vascular strand of the midrib was small and top-shaped. It consisted of four or five vertical chains of xylem elements. Phloem was found occurring in this layer along the lower end of the xylem strand (Figure 5.1.1.3).

The lamina part of the leaf was 250 μm thick. It consisted of large, dilated adaxial epidermal cells and thin and narrow abaxial epidermal cells. The palisade cells were cylindrical and they occurred in single horizontal row; the spongy parenchyma cells were spherical and lobed with wide air-chambers (Figure 5.1.1.3).
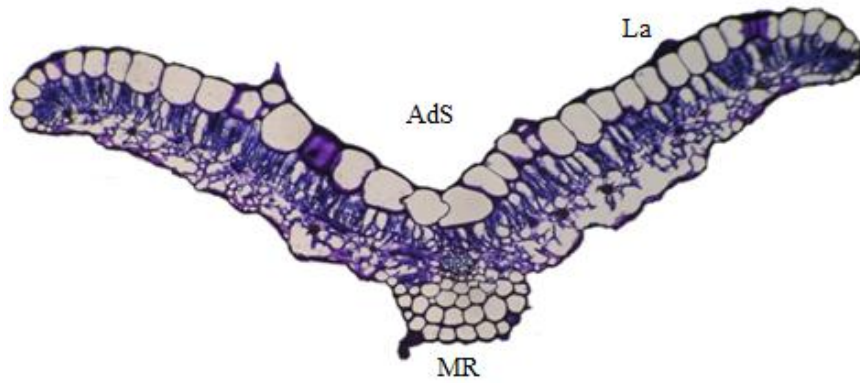
Figure 5.1.1.1 T. S. of *O. umbellata* leaf through midrib (4X)
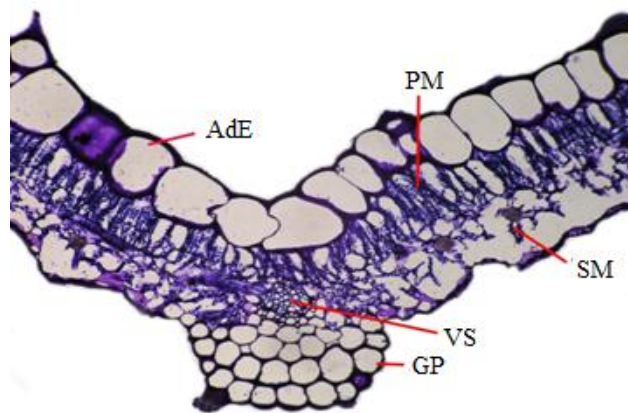
Figure 5.1.1.2 T. S. of *O. umbellata* midrib enlarged (16X)
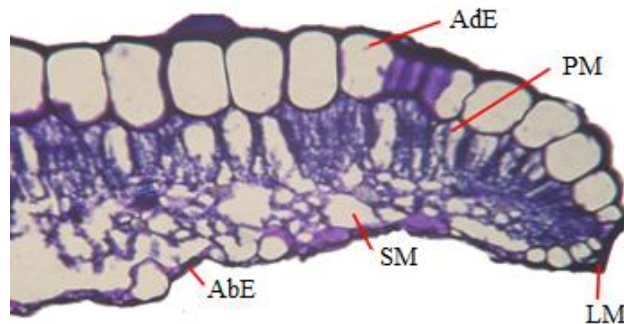
Figure 5.1.1.3 T. S. of *O. umbellata* leaf margin (40X)

(AdE: Adaxial Epidermis; AdS: Adaxial Side; AbE: Abaxial Epidermis; GP: Ground Parenchyma; La: Lamina; LM: Leaf Margin; MR: Midrib; PM: Palisade Mesophyll; SM: Spongy Mesophyll; VS: Vascular Strand)

The marginal part of the lamina was blunthy conical and slightly bent down. The structure of the margin was basically similar to that of the lamina. The leaf margin was 170 μm thick. Calcium oxalate druses are sparsely distributed in the mesophyll cells. The druses were 30 μm in diameter.

5.1.2 *Stem*

The stem was circular in cross section. It was 1.15 cm thick. The stem consisted of epidermis, cortex, hollow vascular cylinder and wide pith (Figure 5.1.2.1). The epidermal layer was thick comprising squarish wide and thick epidermal cells. The cuticle was very prominent. The epidermal cells were 50 μm thick. The cortical zone was narrow and included six layers of elliptical thin walled, compact parenchyma cells. The vascular cylinder consisted of outer continuous cylinder of secondary phloem ensheathing thick hollow cylinder of xylem elements.
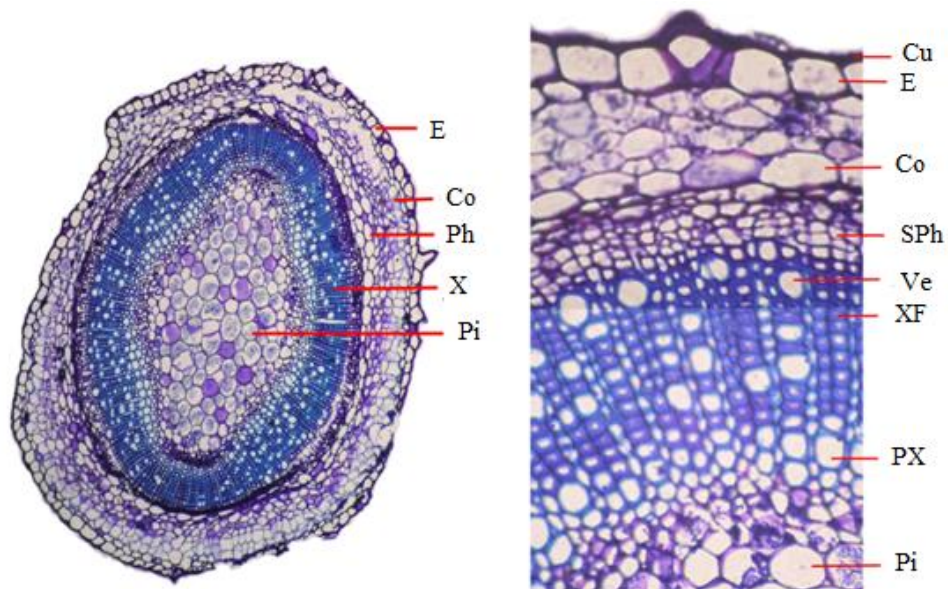
Figure 5.1.2.1 (L. side) T. S. of *O. umbellata* stem entire view (4X); (R. side) A portion of stem (40X)

(Cu: Cuticle; Co: Cortex; E: Epidermis; Pi: Pith; Ph: Phloem; PX: Primary Xylem; SPh: Secondary Phloem; Ve: Vessel; X: Xylem: XF: Xylem Fibres)

The secondary phloem included three or four layers of sieve elements and parenchyma cells. The phloem elements occurred in fairly regular compact radial lines. Xylem cylinder consisted of inner layer of primary xylem elements, outer thick secondary xylem elements. The primary xylem elements were in compact radial lines with 2-3 primary xylem elements. Secondary xylem included fairly dense solitary, circular or angular narrow thick walled vessels and compact parallel lines of thick walled lignified xylem fibres. Secondary xylem rays were narrow and straight with fairly thick lignified walls. The pith cells were circular, homogeneous, thin walled and compact. The vessels were up to 20 μm in diameter.

5.2 Extraction and fractionation of *O. umbellata*

The extraction and fractionation of aerial parts of *O. umbellata* was carried out as given in the flow chart.

Plant material (5.0 Kg)

i. Extracted using MeOH; RT; 48 h

ii. Filtered; Evaporated

HUM (440.0 g)

i. Suspended in H_2O

ii. Partition separation - diethyl ether

Organic layer

Evaporated

HUM-E (102.0 g)

Scheme-I

Aqueous layer

Treated with n-BuOH

Organic layer

Evaporated

HUM-B (108.0 g)

Scheme-II

Aqueous layer

Discarded
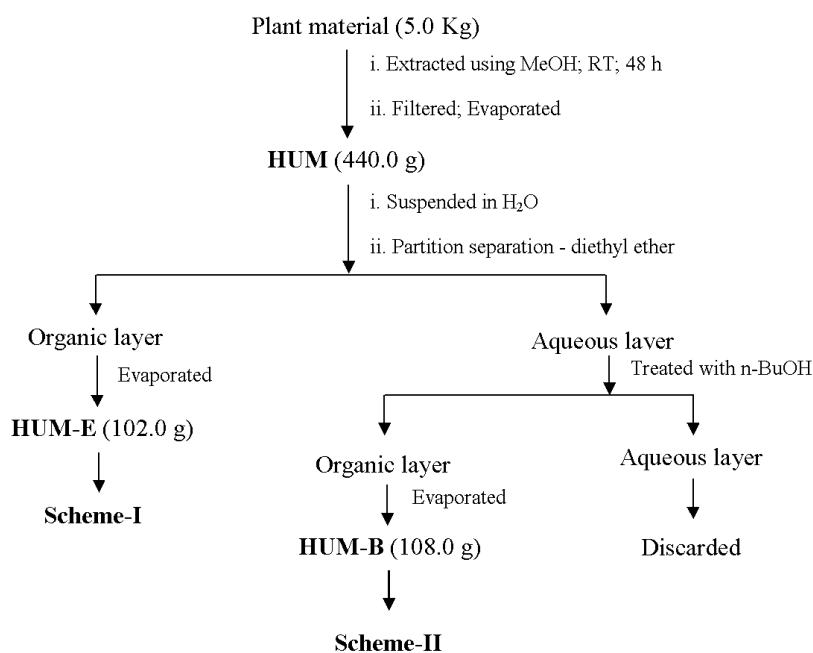
5.3 LC-PDA-ESI-MS analysis of HUM-E and HUM-B

LC-PDA-ESI-MS analysis explored the presence of 18 major compounds in **HUM-E** (Figure 5.3.1) and 9 compounds in **HUM-B** (Figure 5.3.2). Attempts were made to isolate and characterize them.
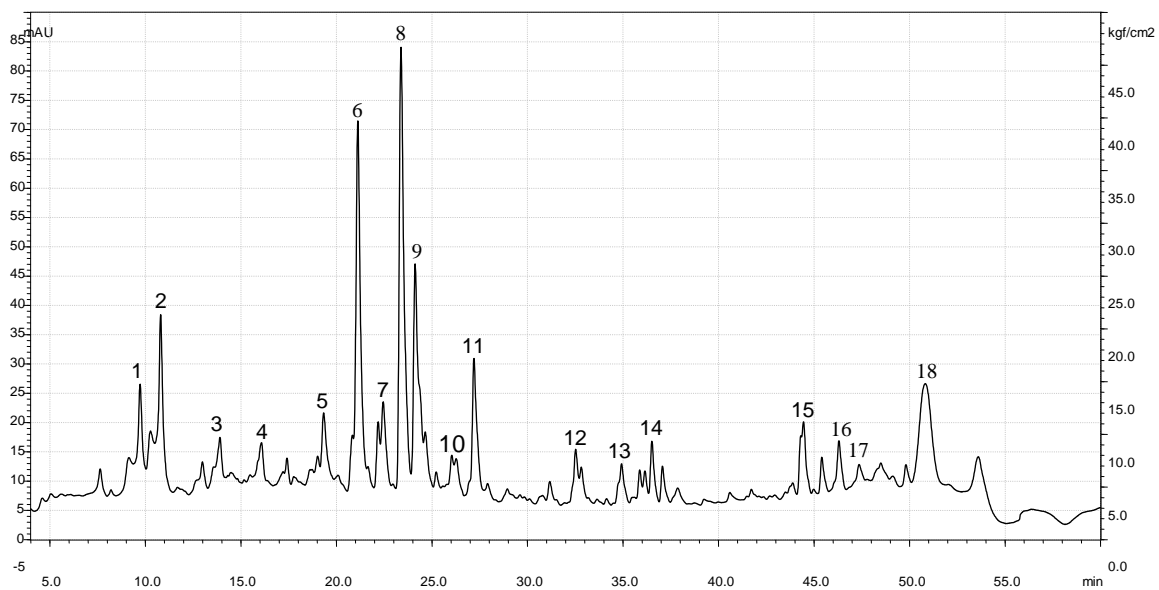
Figure 5.3.1 LC-PDA chromatogram of HUM-E
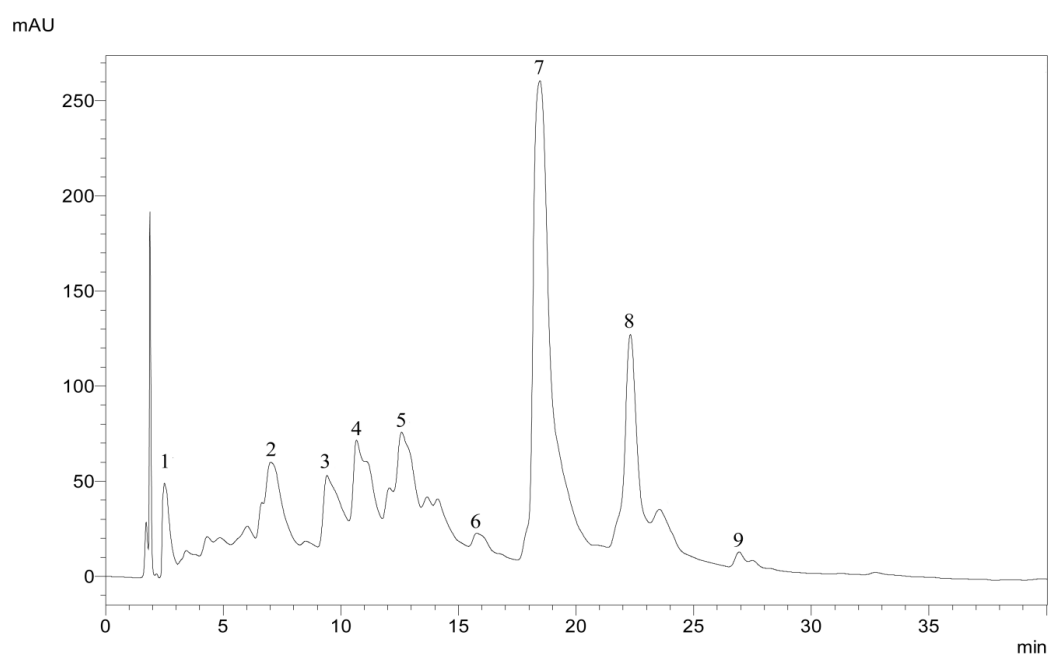
Figure 5.3.2 LC-PDA chromatogram of HUM-B

51

5.4 Isolation and characterization of chemical constituents of HUM-E

Chromatographic purification of **HUM-E** resulted in the isolation and characterization of seven compounds. The isolation procedure is outlined in Scheme I.

Scheme I

HUM-E (96.0 g)

CC; SiO$_2$; Elution with step gradient

Toluene: EtOAc
eluate (50:50)

CC.; SiO$_2$; Toluene-EtOAc

Toluene: EtOAc
eluate (70:30)

Divided into two

Part-A

i. Diaion HP-20; MeOH

ii. p-TLC; (CHCl$_3$: MeOH (20:01)); R$_f$: 0.38

HU 1

Part-B

CC; SiO$_2$; Hexane → EtOAc

Hexane: EtOAc
eluate (75:25)

Hexane: EtOAc
eluate (88:12)

Hexane: EtOAc
eluate (90:10)

HU 2

HU 3

HU 4
HU 5

Mixture of
compounds

CC; SiO$_2$; Hexane → EtOAc elute
(80:20)

HU 6

HU-7 impure

p-HPLC; C$_{18}$: H$_2$O → MeCN

HU 7

The structure of purified compounds was identified based on various spectral analyses like UV-Visible, FT-IR, 1D- and 2D-NMR and Mass spectroscopy.

5.4.1 Characterization of HU-1

HU-1 was obtained as amorphous solid. The homogeneity of the compound was determined by TLC studies using different solvent systems and the purity was assessed by RP-HPLC (R_t 19.425 min) on C_{18} column using step gradient elution of MeCN in H_2O under PDA detection (Figure 5.4.1.1). The molecular formula of **HU-1** was determined to be $C_{30}H_{24}O_8$ through ESI-MS analysis (Figure 5.4.1.2) ([M+H]$^+$ at m/z 513.40) and HR-FABMS analysis, which showed [M+H]$^+$ at m/z 513.1469.
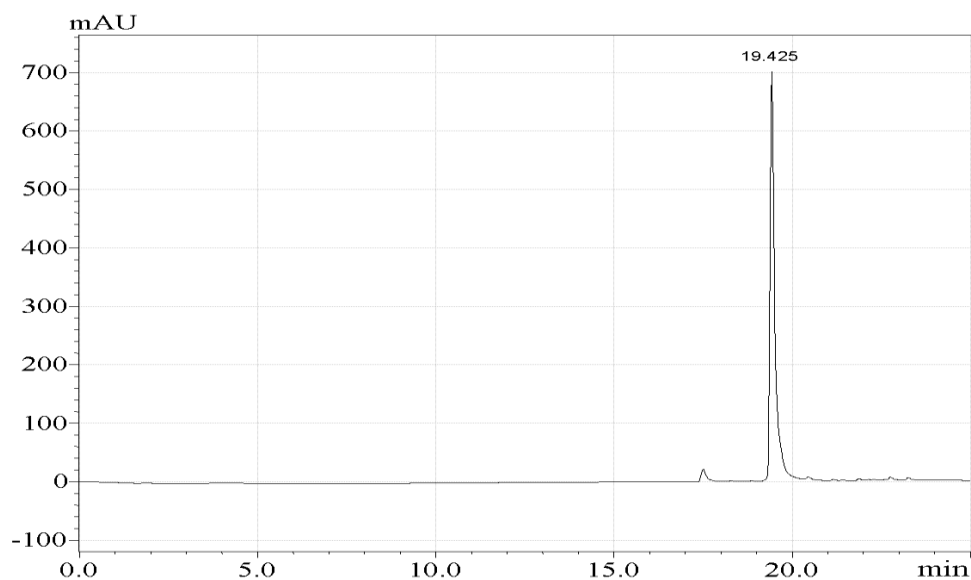
Figure 5.4.1.1 RP-HPLC chromatogram of HU-1 detected at λ_{max} 280 nm

The UV spectrum of **HU-1** showed absorption bands at λ_{max} 243, 263, 275 and 351 nm, characteristic of a tri-substituted coumarin moiety (Figure 5.4.1.3). The IR spectrum of **HU-1** revealed the presence of carbonyl (1722 cm^{-1}) and aromatic (1581 cm^{-1}) groups. The 500 MHz proton NMR and 125 MHz carbon NMR spectra were measured by dissolving HU-1 in CDCl$_3$ (Figure 5.4.1.4 and 5.4.1.5).
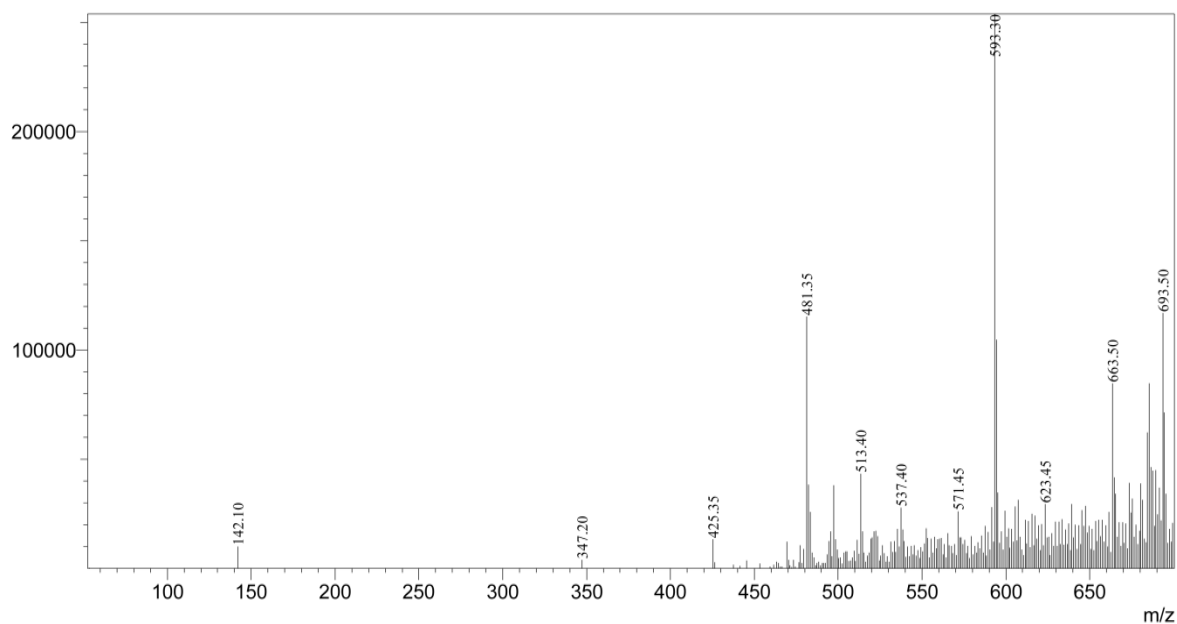
Figure 5.4.1.2 ESI-mass spectrum of HU-1
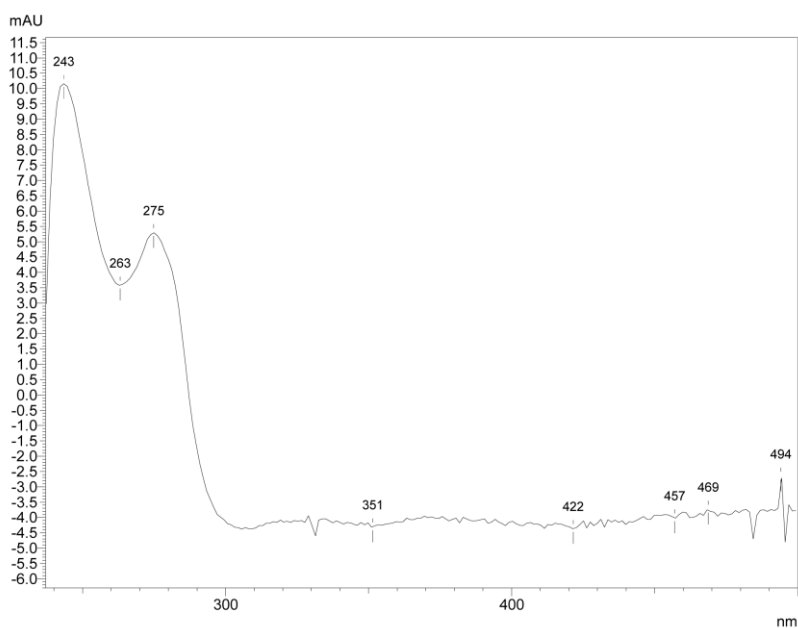
Figure 5.4.1.3 UV-Visible spectrum of HU-1

The ^{1}H NMR spectrum clearly displayed the signals for two mutually coupled doublets (J = 9.5 Hz) at δ_H 6.40 and 7.77 ppm for olefenic protons of coumarin along with the characteristic H-5 proton signal (δ_H 6.77) of a tri-substituted coumarin nucleus. The spectrum also showed the presence of one more aromatic proton singlet at δ_H 6.93 ppm. Further the up

field region of the spectrum unveiled the presence of a methyl singlet at δ_H 1.39 ppm and methoxyl singlet at δ_H 4.10 ppm along with two methylene proton multiplets at δ_H 2.86 and 2.06 ppm (Table 5.4.1.1).

Table 5.4.1.1 ^{1}H NMR data of HU-1

δ_H (ppm)	Integral proton count	Splitting pattern (J Hz)	Probable assignment
1.39	3H	singlet	-C<u>H</u>₃
2.06	1H	multiplet	-C<u>H</u>aHb-
2.86	1H	multiplet	-CHa<u>H</u>b-
4.10	3H	singlet	-OC<u>H</u>₃
6.40	1H	doublet (9.5)	α-coumaroyl-<u>H</u>
6.77	1H	singlet	Ar-<u>H</u>
6.93	1H	singlet	Ar-<u>H</u>
7.77	1H	doublet (9.5)	β-coumaroyl-<u>H</u>

The ^{13}C NMR evidenced characteristic signals of coumarin nucleus along with methoxyl carbon (δ_C 56.8 ppm), methyl carbon (δ_C 23.0 ppm), olefinic carbon (δ_C 100.4 ppm), methylene carbon (δ_C 27.1 ppm) and two quarternary carbon (δ_C 164.1, 45.7 ppm), accounting for fifteen different carbons of **HU-1**. Analysis of CMR and PMR surprisingly showed signals for exactly half of the number of hydrogens and carbon predicted through HR-FABMS. i.e. only 12 protons and 15 carbons of total 24 and 30 were found in the NMR spectra. The puzzling appearance of exactly half the number of expected NMR signals deciphered that **HU-1**, should be a symmetrical dimer.

The double bond equivalence (DBE) calculated for $C_{30}H_{24}O_8$ of **HU-1** was found to be 19. Attempts to account 19 degrees of unsaturation (DOU) in **HU-1** revealed that 14 DOU

were originating from two coumarin molecules and the remaining five were to be settled. The number of oxygens forming two coumarins and two methoxyls accounted for six and there were remaining two oxygens in **HU-1**, yet to be bonded. In view of these facts and also considering the signals existing in the CMR and PMR spectrum of **HU-1**, in addition to coumarin and methoxyls, two furan rings could be framed forming two furanocoumarin nuclei, which satisfied the total number of oxygens and DBE of 18. Interpretation of the HMBC correlations led to the unambiguous assignment of the 6-methoxy-furocoumarin (Figure 5.4.1.6a and 5.4.1.6b) as part structure for **HU-1**. The possibility of linear furanocoumarin was ruled out from the correlations found in NOE spectrum (Figure 5.4.1.7a and 5.4.1.7b).

YF1656/HU–21, in CDCl3, 1H, 500 MHz, ti 16, 2013/6/1
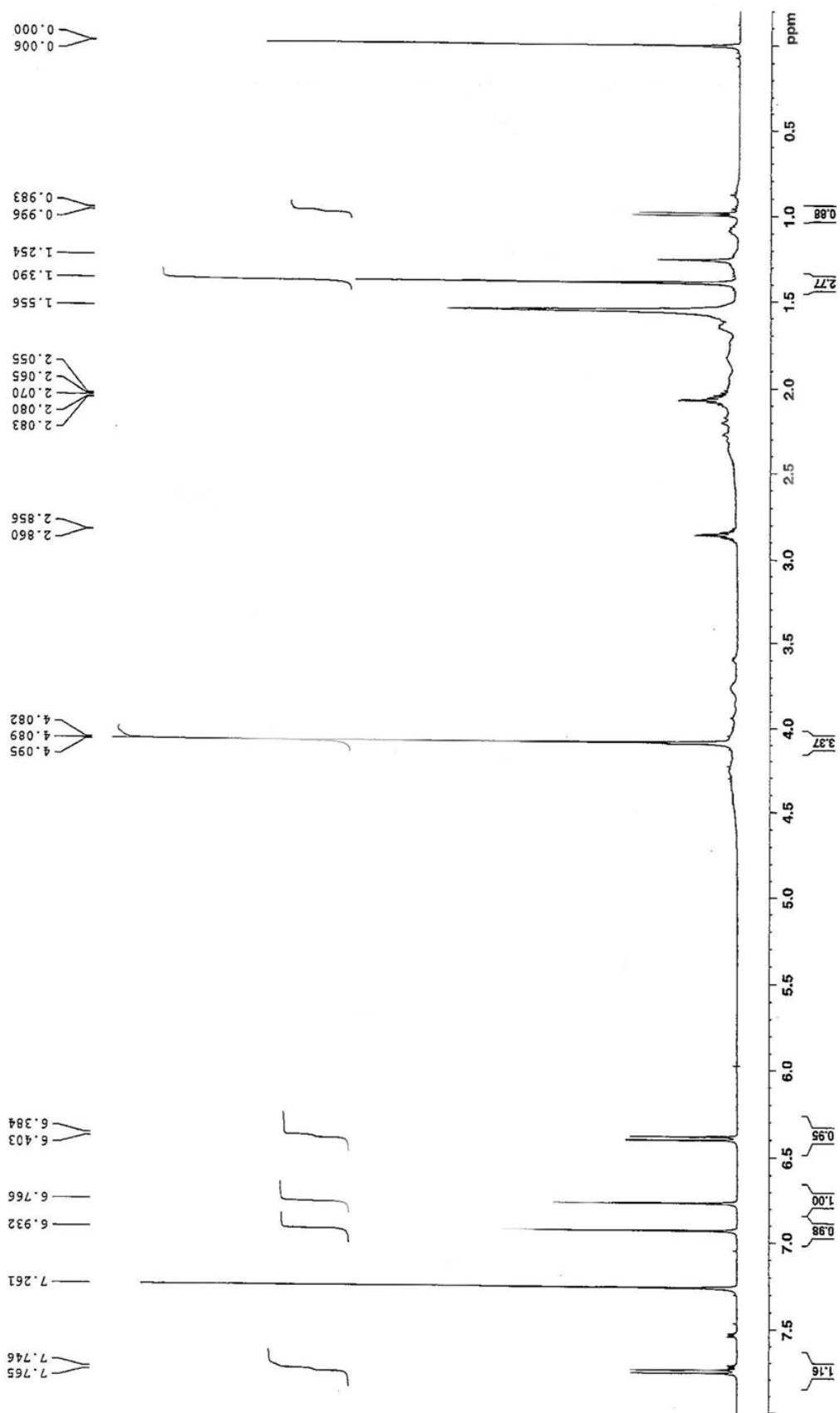
Figure 5.4.1.4 ^{1}H NMR spectrum of HU-1

57

YF1664/HU–21, in CDCl3, 13C, 125 MHz, ti 2600, 2013/6/3

19.15
22.99
27.07
45.64
56.75
76.74
77.00
77.25
100.39
103.79
113.49
114.29
119.68
142.73
142.80
144.45
146.68
161.18
164.07
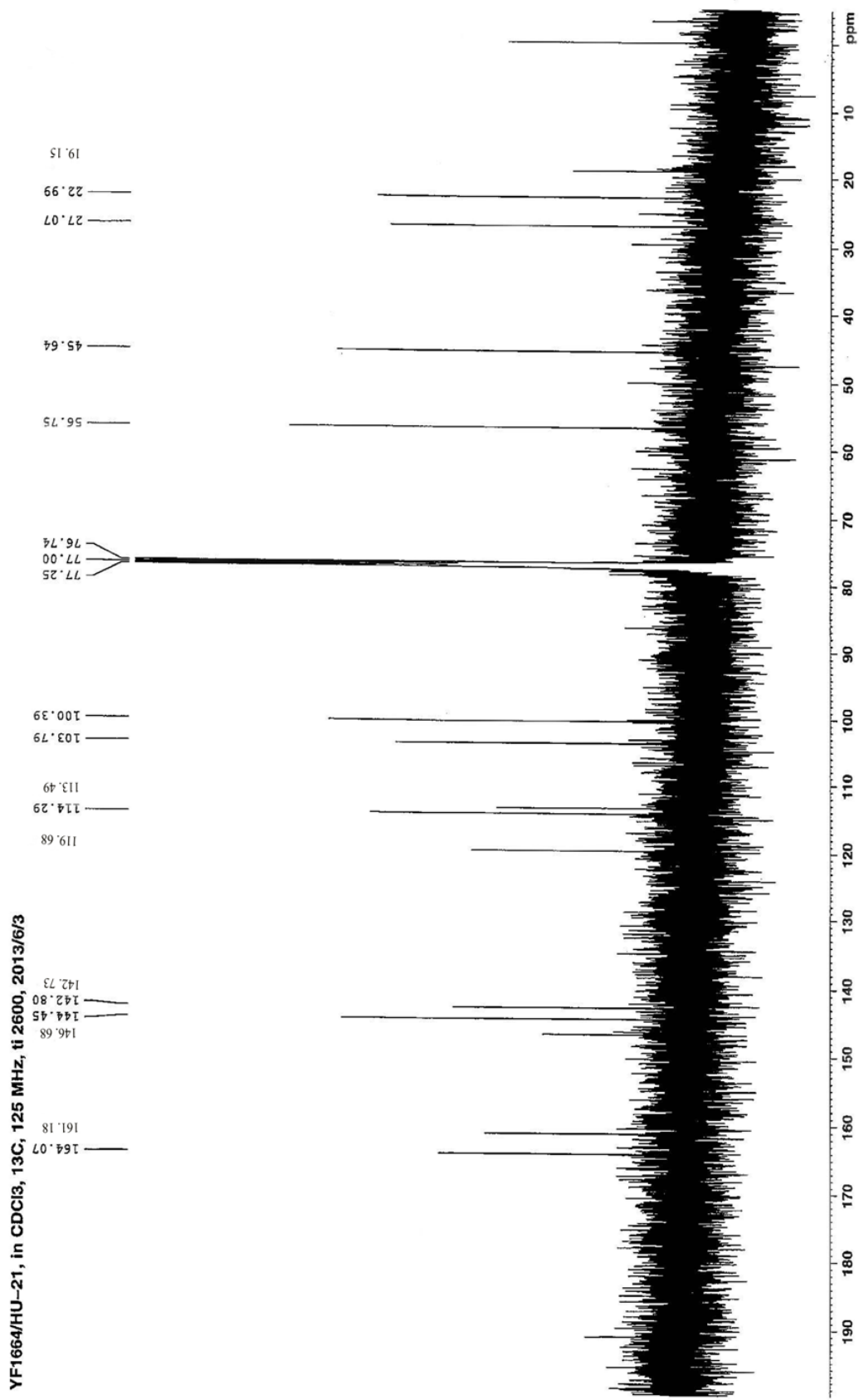
Figure 5.4.1.5 ^{13}C NMR spectrum of HU-1

58

Also, the presence of NOE correlations between H-4 (δ_H 7.75 ppm) and H-5 (δ_H 6.77 ppm) and between H-5 and methoxy methyl (δ_H 4.09 ppm) further supported the angular type furanocoumarin substructure. Thus **HU-1** was predicted to be an angular furanocoumarin derivative.

The two symmetrical halves of the **HU-1** were derived to be A and B as shown below.
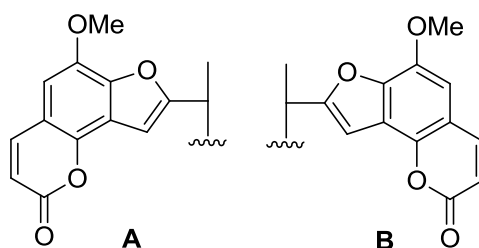
Further analysis of HMBC correlations and requirement of one more unsaturation in the molecule necessitated to make a cyclobutane ring by connecting the quaternary carbon to the other quaternary carbon (head-to-head dimeric structure) or to the methylene carbon. The head-to-head dimeric structure was assigned for **HU-1**, because the coupling pattern of C-4' methylene protons were not AA' type i.e. different. Thus the structure of **HU-1** was unambiguously assigned and the key HMBC correlations are explained in Figure 5.4.1.5. Table 5.4.1.2 presents the assigned δ_C and δ_H values of **HU-1**.
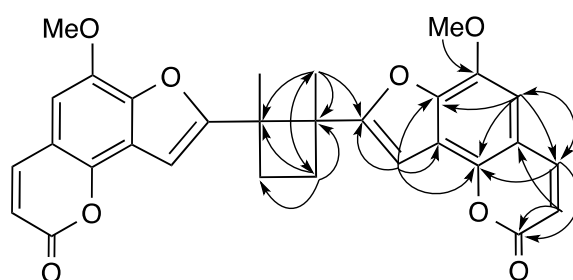
Figure 5.4.1.6a Key HMBC correlations for HU-1 (H→C)
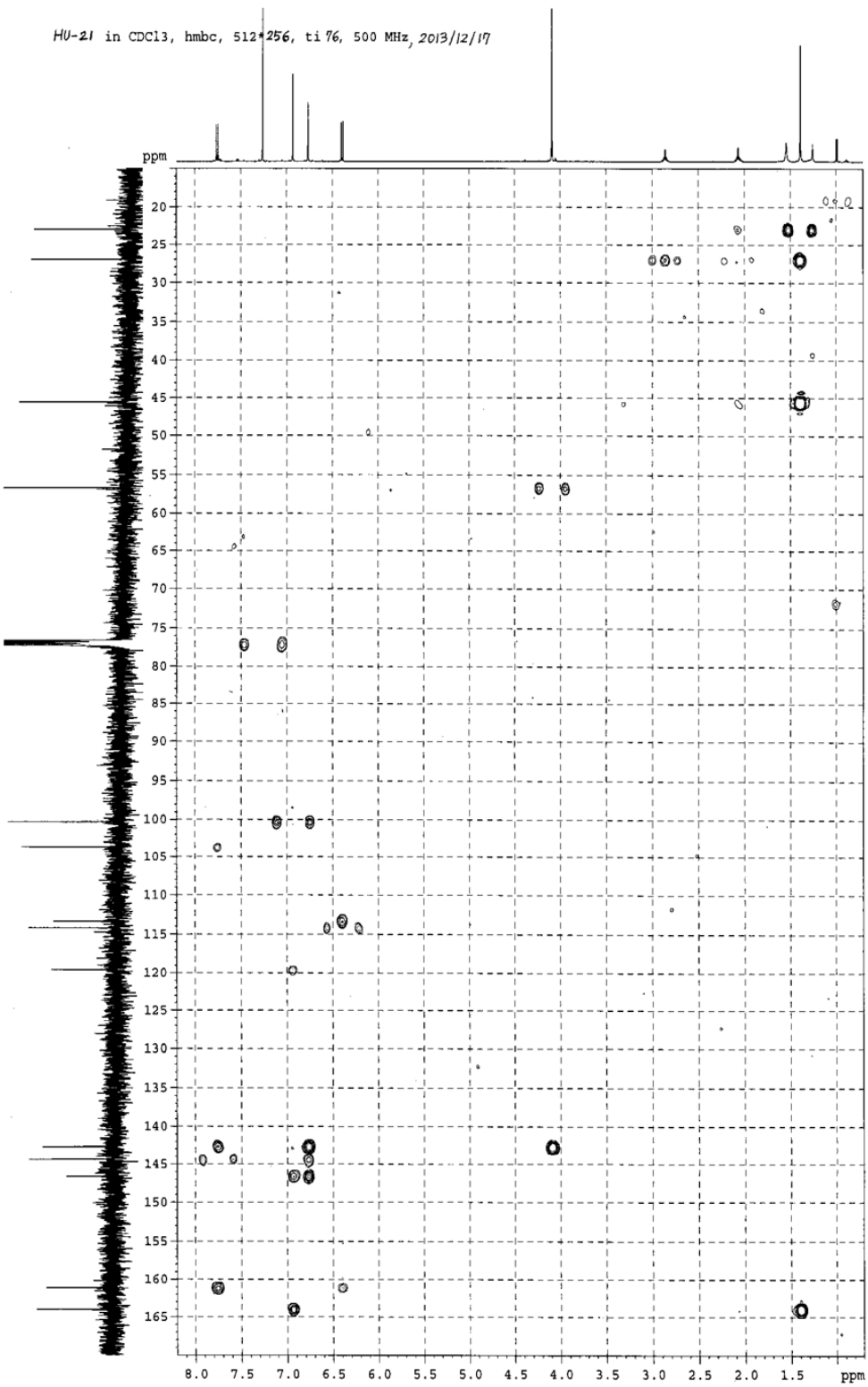
Figure 5.4.1.6b HMBC spectrum of HU-1

Table 5.4.1.2 ^{13}C and ^{1}H NMR data of HU-1

C. position	δ_C (ppm)	δ_H (ppm)
2	161.2	-
3	114.3	6.40
4	144.5	7.77
4a	113.5	-
5	103.8	6.77
6	142.8[a]	-
7	146.7	-
8	119.7	-
8a	142.7[a]	-
1'	100.4	6.93
2'	164.1	-
3'	45.6	-
4'	27.1	2.86
	-	2.06
5'	23.0	1.39
-OMe	56.8	4.10

[a] Exchangeable
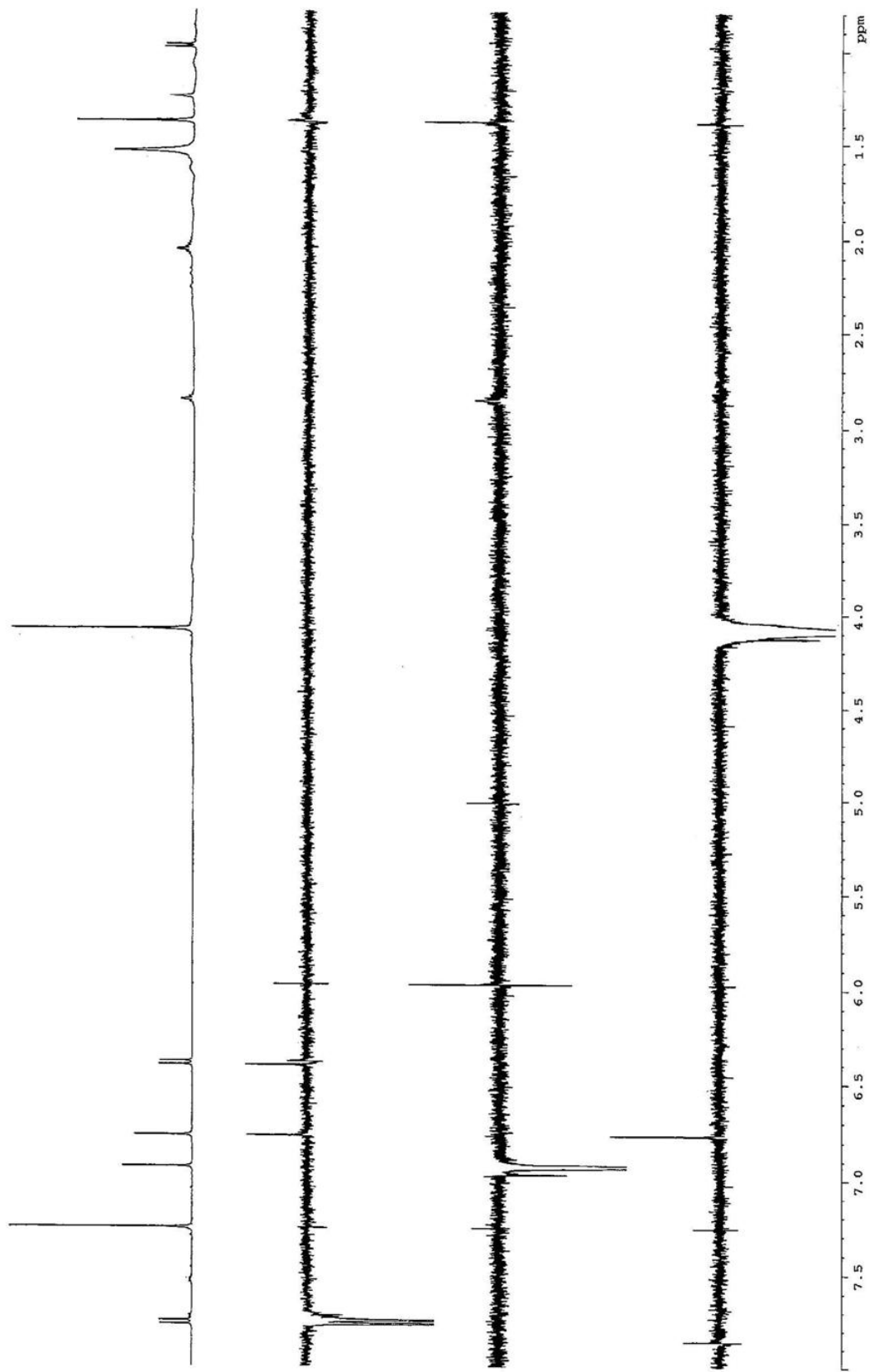
Figure 5.4.1.7a NOE spectrum of HU-1
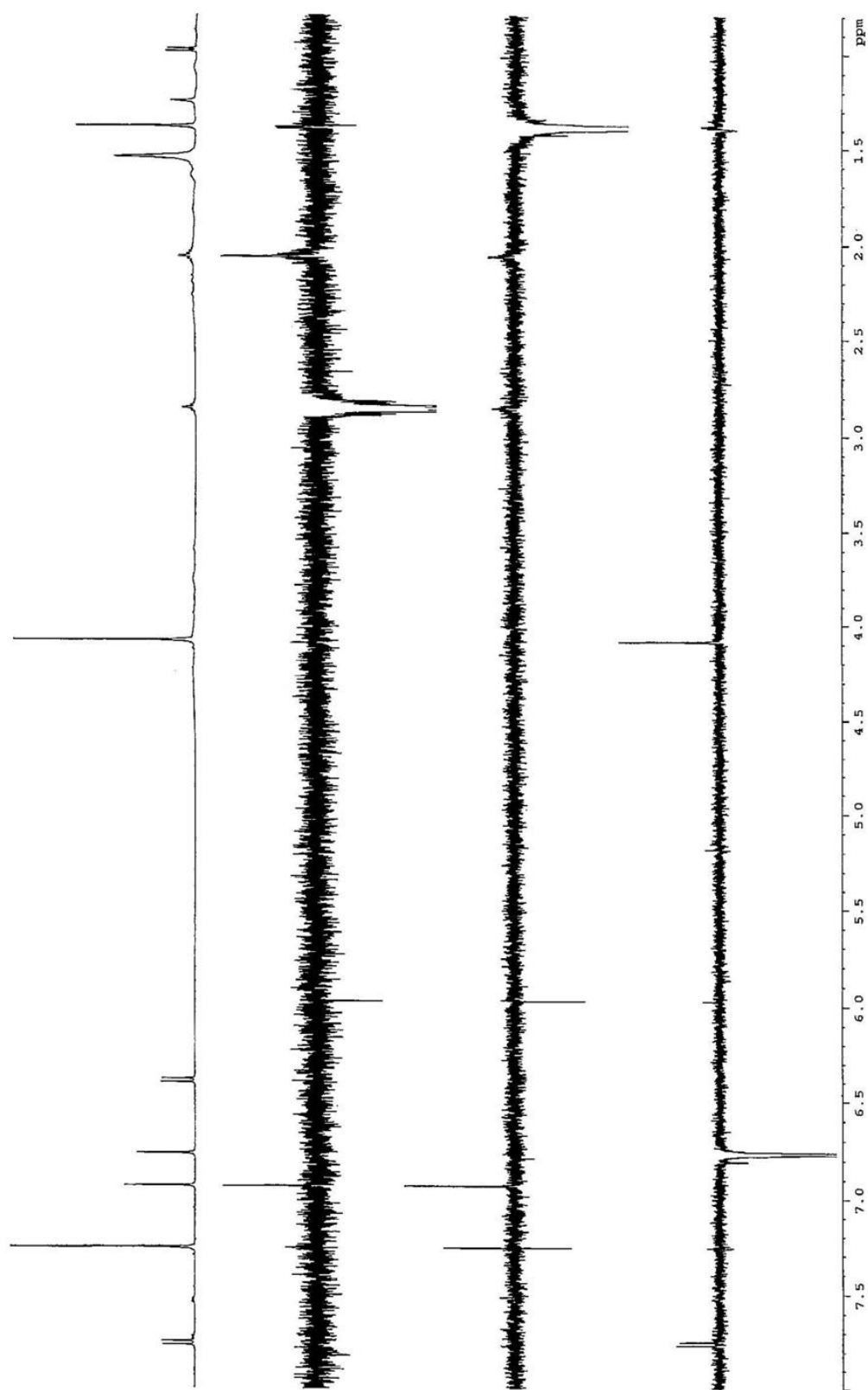
Figure 5.4.1.7b NOE spectrum of HU-1

Then, we were left with determining the configuration at both C-3 and C-3', which was done by comparing with literature data. A related dimer having cyclobutane, ligulacephalin was identified in the literature. The close similarity of the ^{13}C shifts of C-2', C-3', C-4' and C-5' (δ_C 164.1, 45.7, 27.1 and 23.0 ppm, respectively, in CDCl$_3$) of **HU-1** with the respective signals of ligulacephalin A (δ_C 163.4, 46.8, 27.9 and 23.5 ppm in CD$_3$OD) provided the evidence that **HU-1** has the same relative stereochemistry (*S,S/R,R* configuration) as ligulacephalin A (Toyoda et al., 2005). Finally the structure of **HU-1** was determined as (**1**).
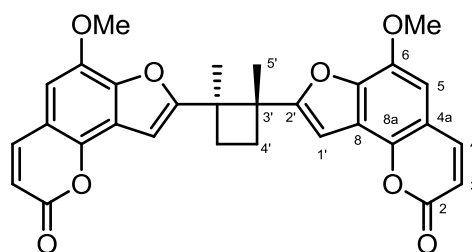
HU-1 (1)

This symmetrical dicoumarin was trivially named as Oledicoumarin and this was found to be a completely novel molecule which was confirmed through Scifinder search. Isolation and structure elucidation of Oledicoumarin is an important outcome of the present chemical investigation.

5.4.2 Characterization of HU-2

HU-2 was obtained as dark green crystals, showing m.p. of 225-227 ˚C. The homogenous nature of the compound was assessed through TLC studies using different solvent systems [n-Hexane:EtOAc (7:3)]. The purity was determined by RP-HPLC (R_t 49.48 min) on C_{18} column using MeCN and H_2O (Figure 5.4.2.1). The UV-Visible spectrum of **HU-2**, exhibited absorption bands at 256, 293, 326, 373, 403, 510 and 664 nm indicating a highly conjugated system of molecule (Figure 5.4.2.2) typical for porphyrin type compounds (Rho et al., 2003).
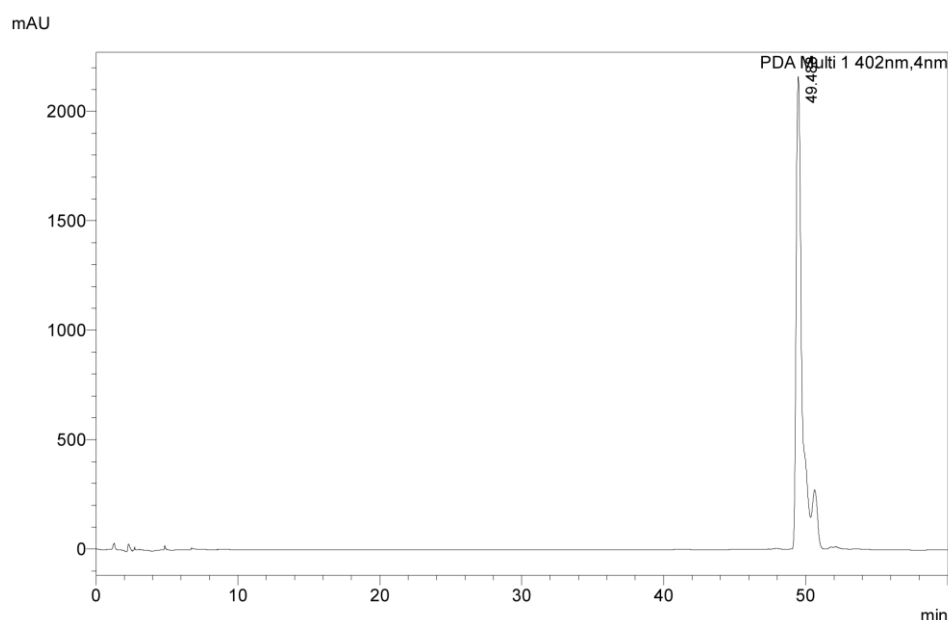
Figure 5.4.2.1 RP-HPLC chromatogram of HU-2 detected at λ_{max} 402 nm

The IR spectrum (Figure 5.4.2.3) measured using DRA technique disclosed the presence of N-H (N-H str at 3394 cm^{-1}), ester carbonyl (C=O str at 1732 cm^{-1}) and keto carbonyl (C=O at 1696 cm^{-1}) groups. The molecular weight of **HU-2** was found as 606 from the [M+H]$^+$ peak which appeared at *m/z* 607.30 in its ESI-MS spectrum (Figure 5.4.2.4). The even mass number indicated the even number of nitrogen atoms, substantiating the presence of four pyrrole rings of porphyrin A.
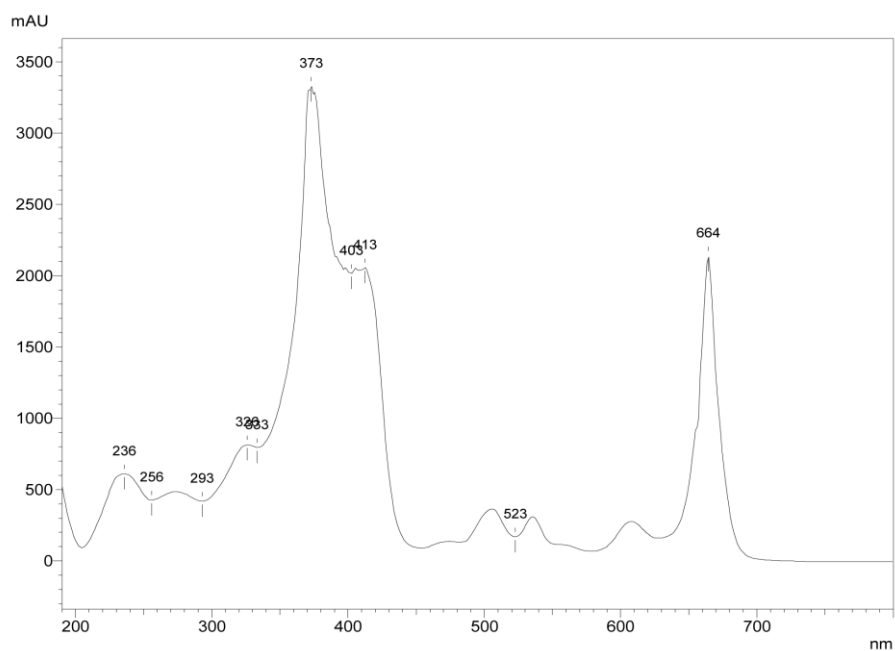
Figure 5.4.2.2 UV-Visible spectrum of HU-2
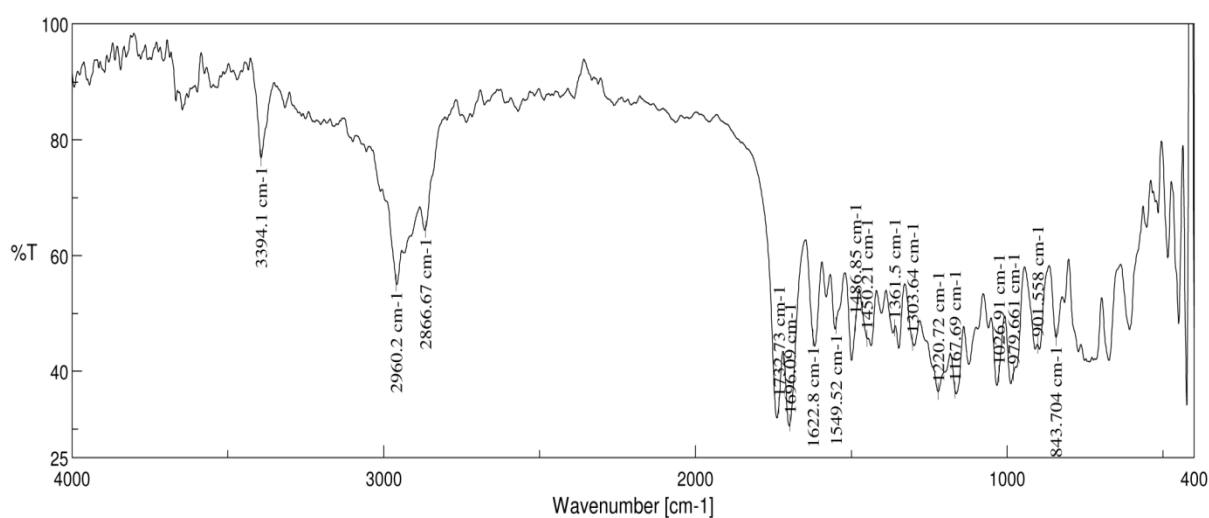
Figure 5.4.2.3 FT-IR spectrum of HU-2

The carbon NMR spectrum (Figure 5.4.2.5) measured using CDCl$_3$ at 125 MHz showed thirty six signals constituting three carbonyls, two ester methyl, five methyl, four methylene, eight methoane, three olefinic and eleven quarternary carbons. Both the proton and carbon NMR confirmed **HU-2** as a tetrapyrrollic pigment of porphyrin A type, possessing an isocyclic ring and β keto ester. The definitive presence of isocyclic ring was

identified from the ^{1}H NMR spectrum (Figure 5.4.2.6), which showed the typical methine proton singlet (δ_H 6.25 ppm, 1H) and carboxy methyl ester singlet (δ_H 3.88 ppm, 3H) signals. Compound HU- 2 was identified to have a large π system of macrocycle producing induced current and hence the peripheral protons were found to be deshielded i.e. signals for protons at α, β, and δ appeared at δ_H 9.35, 9.50 and 8.55 ppm, respectively. A thorough literature search based on the obtained spectral data resulted with the identification of **HU-2** as pheophorbide A methyl ester (**2**) (Rho et al., 2003). Table 5.4.2 describes the identity of the observed and reported ^{13}C NMR spectral data.
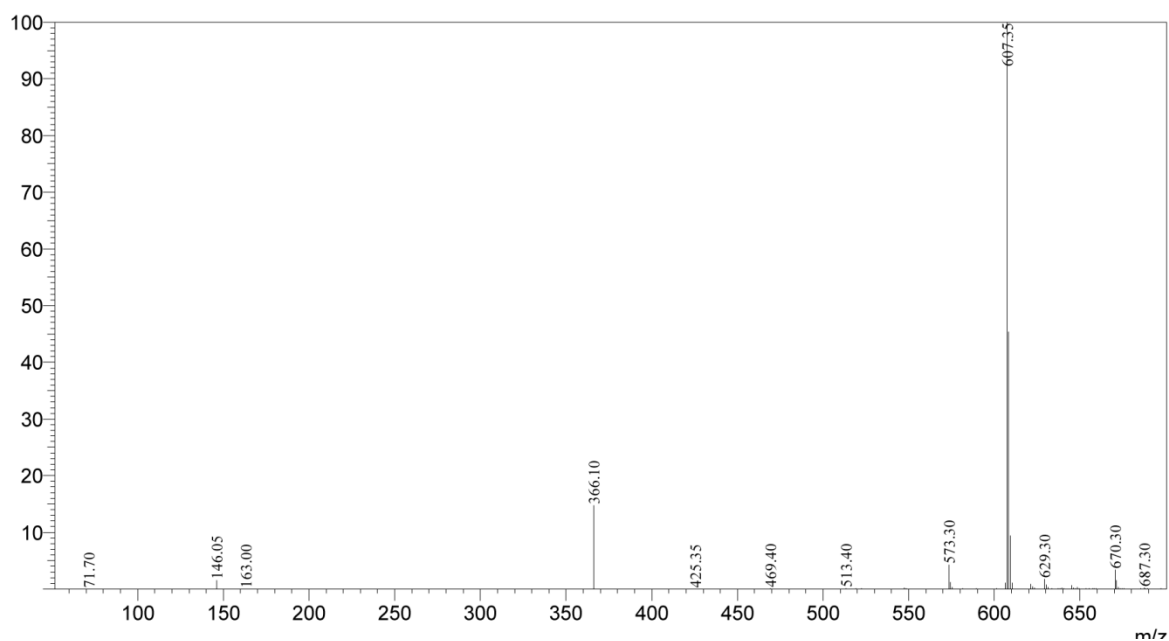
Figure 5.4.2.4 ESI-Mass spectrum of HU-2

YF1676/HU-20, in CDCl3, 13C, 125 MHz, ti 1150, 2013/6/5

11.20
12.07
12.09
17.38
19.43
23.05
29.85
31.04
50.10
51.11
51.64
52.83
64.71
76.75
77.00
77.26
93.10
97.54
104.42
105.20
122.77
128.96
129.05
129.07
131.85
136.19
136.27
136.51
137.94
142.05
145.22
149.66
150.99
155.66
161.19
169.57
172.17
173.33
189.60
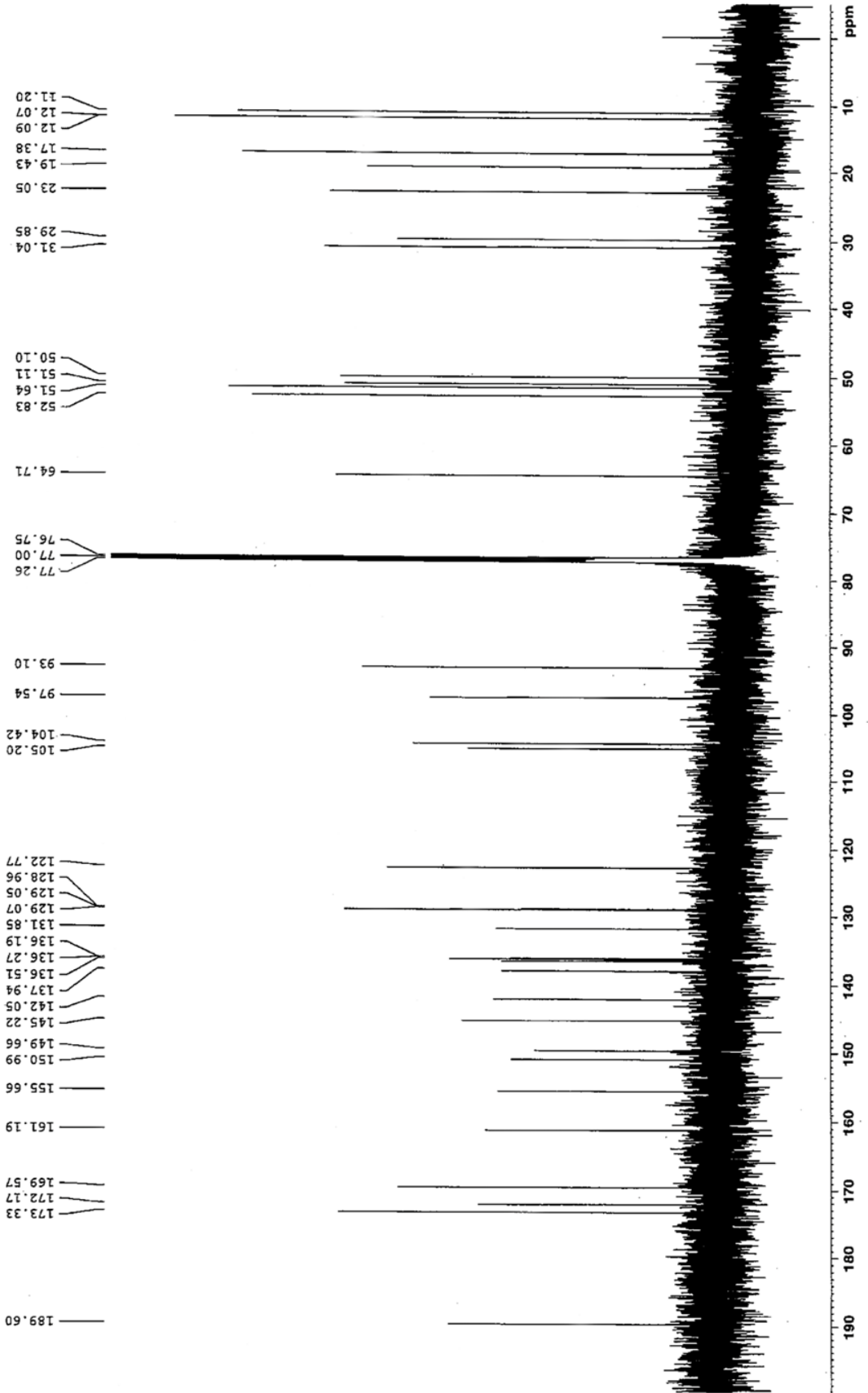
Figure 5.4.2.5 ^{13}C NMR spectrum of HU-2

67

YF1670/HU-20, in CDCl3, 1H, 500 MHz, tl 32, 2013/6/4

0.000
0.001
0.533
1.559
1.666
1.681
1.696
1.803
1.817
2.041
2.206
2.216
2.225
2.236
2.247
2.255
2.265
2.277
2.295
2.304
2.313
2.323
2.333
2.341
2.483
2.497
2.501
2.515
2.527
2.532
2.545
2.609
2.621
2.628
2.635
2.641
2.648
3.203
3.388
3.571
3.630
3.645
3.661
3.677
3.876
4.194
4.199
4.206
4.211
4.216
4.446
4.450
4.461
4.465
6.154
6.177
6.250
6.287
6.289
7.252
7.934
7.958
7.970
7.993
8.552
9.349
9.491
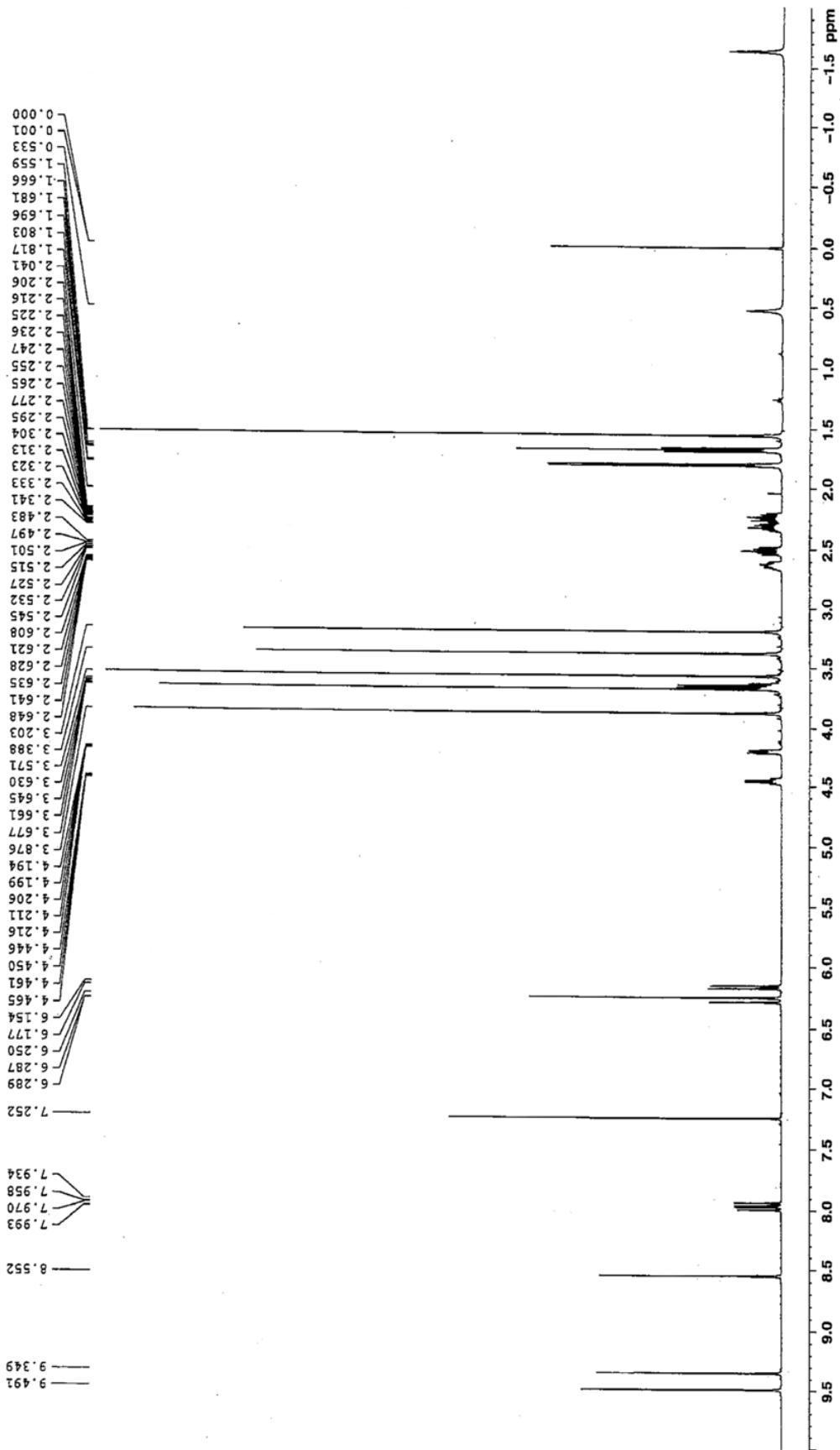
Figure 5.4.2.6 ^{1}H NMR spectrum of HU-2

68

Table 5.4.2 Comparison of ^{13}C NMR of HU-2 with reported values

C. Position	Reported value (δ_C)	Observed value (δ_C)
1	31.0	31.0
2	29.9	29.9
3	51.1	51.1
4	50.1	50.1
5	172.2	172.2
6	93.2	93.1
7	142.1	142.1
8	131.9	131.9
9	136.2	136.2
10	136.2	136.3
11	97.6	97.5
12	155.4	155.7
13	136.5	136.5
14	145.2	145.2
15	149.7	151.0
16	104.4	104.4
17	137.9	137.9
18	129.1	129.1
19	129.0	129.0
20	189.6	189.6
21	64.7	64.7
22	105.3	105.2
23	161.3	161.2
24	149.7	149.7
25	23.1	23.1
26	12.1	12.1
27	129.1	129.1
28	122.8	122.8
29	11.2	11.2
30	19.6	19.4
31	17.4	17.4
32	12.1	12.1
33	169.5	169.6
34	52.8	52.8
35	173.3	173.3
36	51.7	51.6
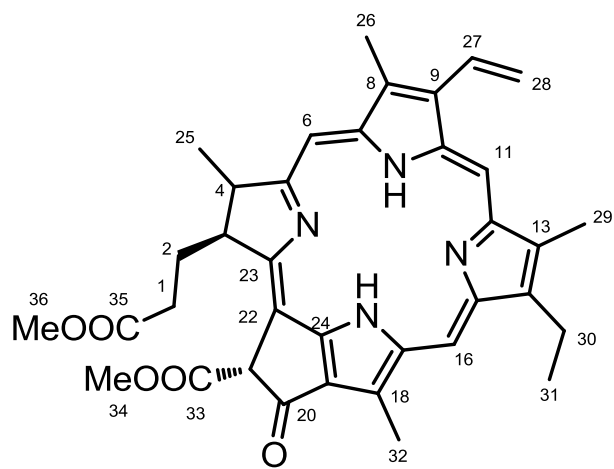
HU-2 (**2**)

5.4.3 Characterization of HU-3

HU-3 was isolated as yellow amorphous powder, showing m.p. of 172-175 ˚C. The homogeneity of the compound was determined by RP-HPLC using step gradient of MeCN in H_2O (Figure 5.4.3.1). The molecular formula was deduced as $C_{15}H_{16}O_4$, based on ESI-MS, ^{1}H- and ^{13}C NMR analysis. The ESI-MS spectrum showed [M-H]$^{-}$ peak at *m/z* 259.25 (Figure 5.4.3.2). The IR spectrum measured using DRA technique showed broad absorption bands for hydroxyl groups at 3300 cm^{-1}, strong carbonyl absorption at 1663 cm^{-1} and absorption bands for aromatic functionalities at 1590 and 1493 cm^{-1} (Figure 5.4.3.3). The UV-Visible absorption spectrum of **HU-3** exhibited absorption maxima at λ_{max} 280 and 319 nm, which is characteristic of 6,7,8-trisubstituted coumarin moiety (Figure 5.4.3.4).
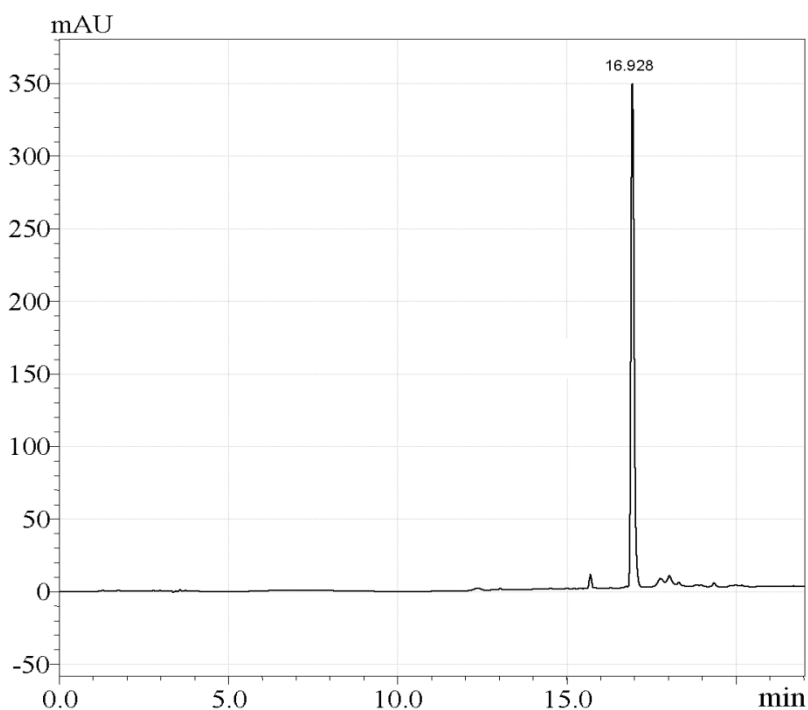
Figure 5.4.3.1 RP-HPLC chromatogram of HU-3 detected at λ_{max} 280 nm

HU-3 was corroborated as a 6,7,8-trisubstituted coumarin derivative from its ^{1}H NMR spectrum, which demonstrated signals indicative of H-3 and H-4 of coumarin nucleus as

mutually coupled doublets at δ_H 6.25 and 7.57ppm (J = 9.5 Hz) and a lone aromatic proton singlet at δ_H 6.72 ppm, might probably be due to 5-H proton (Figure 5.4.3.5).
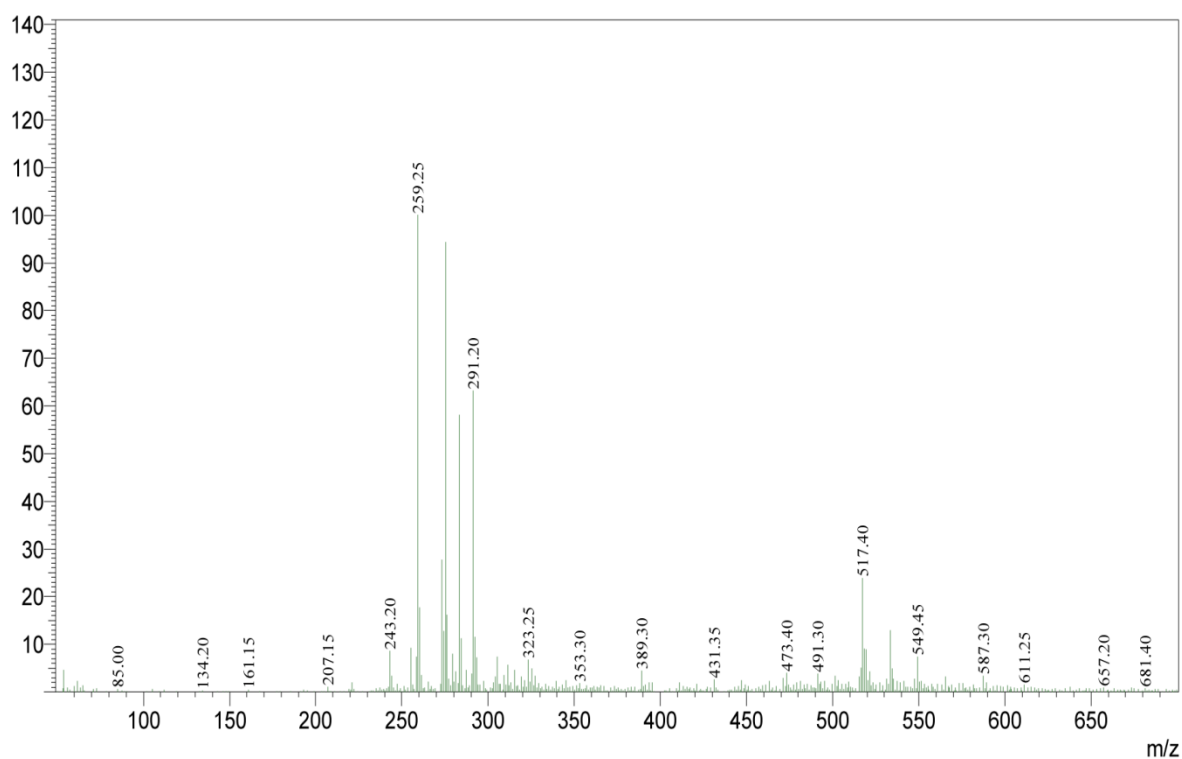
Figure 5.4.3.2 ESI-Mass spectrum of HU-3
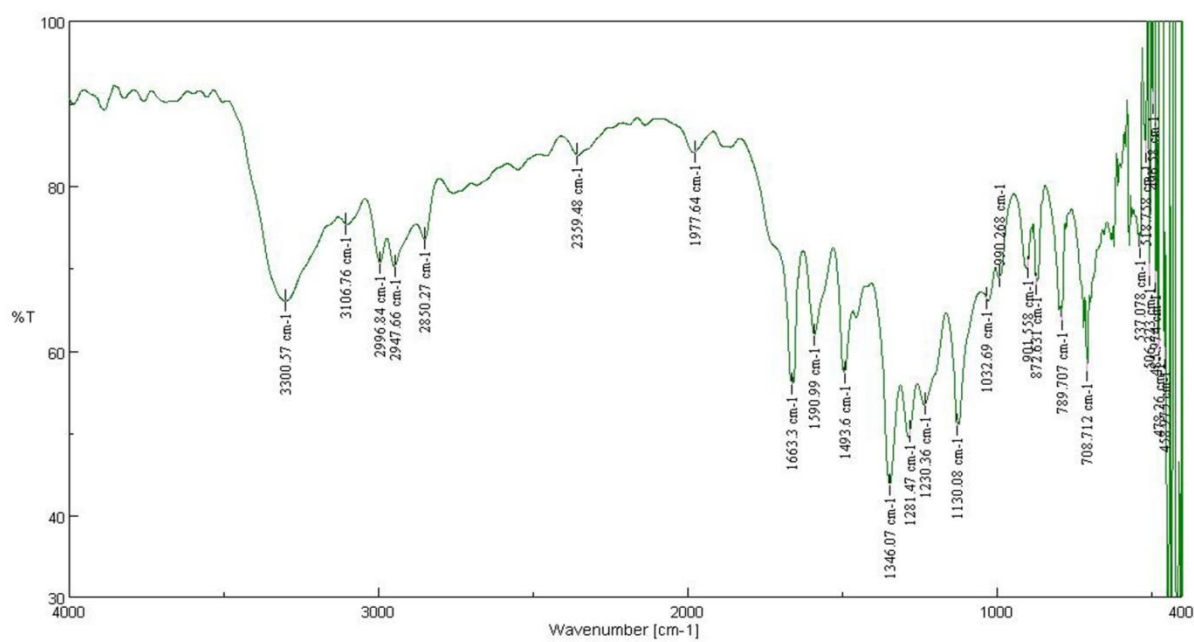
Figure 5.4.3.3 FT-IR spectrum of HU-3

The PMR spectrum further revealed the presence of an aromatic methoxyl group (δ_H 3.94 ppm) and a prenyl group (3-methyl-but-2-en-1-yl), determined from the existence of a doublet at δ_H 3.57 ppm, triplet at δ_H 5.29 ppm and two methyl singlets at δ_H 1.68 and 1.85 ppm. Further, the singlet at δ_H 6.20 ppm in the spectrum was considered to be due to a hydroxyl group, in accordance with IR spectral data (*vide supra*). The information gathered from the ^{1}H NMR spectrum gained support from the ^{13}C NMR data (Figure 5.4.3.6), which showed signals for chromone nucleus having three signals (δ_C 143.1, δ_C 148.4 and δ_C 116.2 ppm) deshielded, which might be due to substitution. In addition, the ^{13}C NMR spectrum confirmed the existence of an aromatic methoxyl group (δ_C 56.3 ppm) and a prenyl group (δ_C 18.0 and 25.8 (CH_3), 133.2 (C), 120.7 (CH) and 22.2 ppm (CH_2) in **HU-3**.
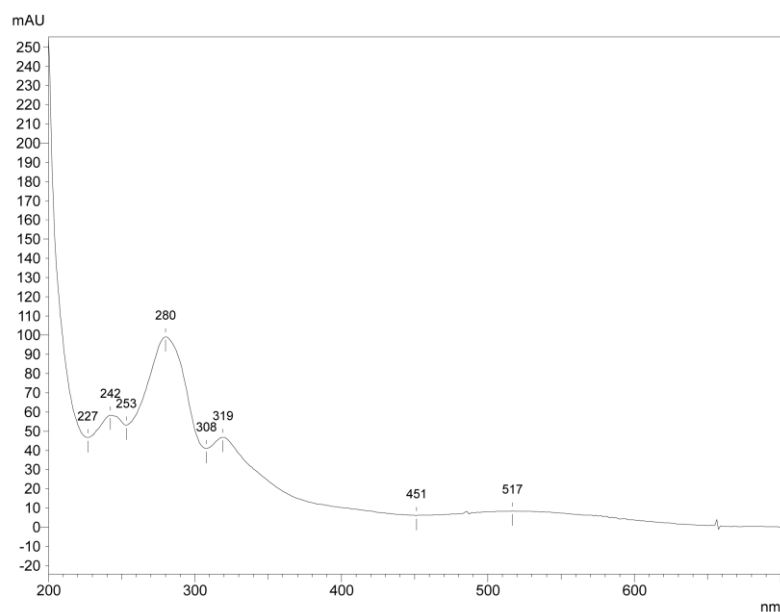
Figure 5.4.3.4 UV-Visible spectrum of HU-3

The exact point of attachment of identified substituents with the coumarin nucleus was apparent from the 2D NMR spectrum. The [1]H-^{13}C correlations observed under HMBC analysis (Figure 5.4.3.7) corroborated the attachment of methoxyl and prenyl groups at C-6

and C-8 positions, respectively. The methoxyl protons (δ_H 3.94 ppm) exhibited strong

correlation
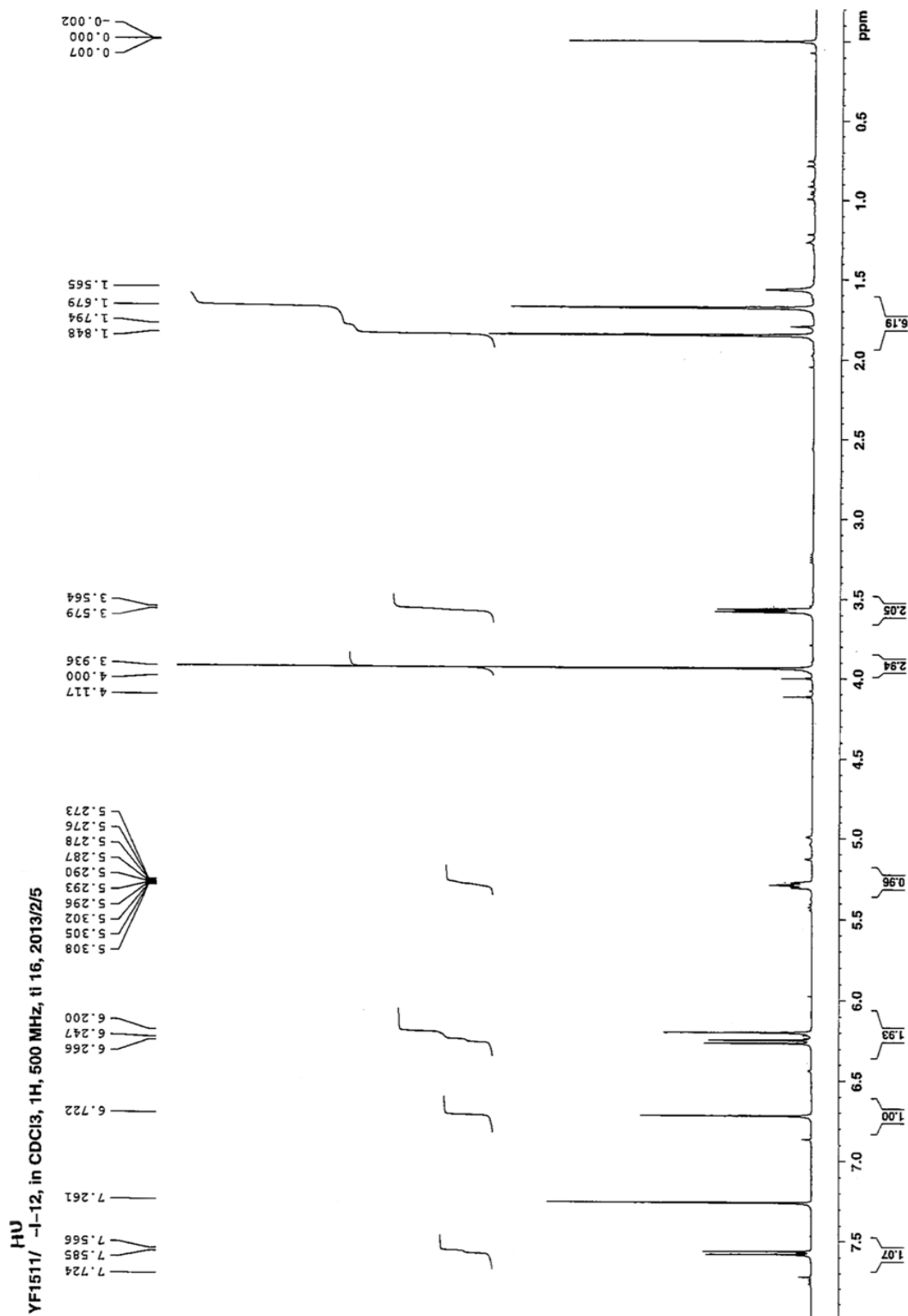
Figure 5.4.3.5 ^{1}H NMR spectrum of HU-3

YF1512/ I-12, in CDCl3, 13C, 125 MHz, ti 640, 2013/2/5

17.95
22.17
25.75
56.32
76.75
77.00
77.25
105.08
111.21
113.11
116.21
120.69
133.16
143.68
143.71
147.40
148.38
161.59

ppm
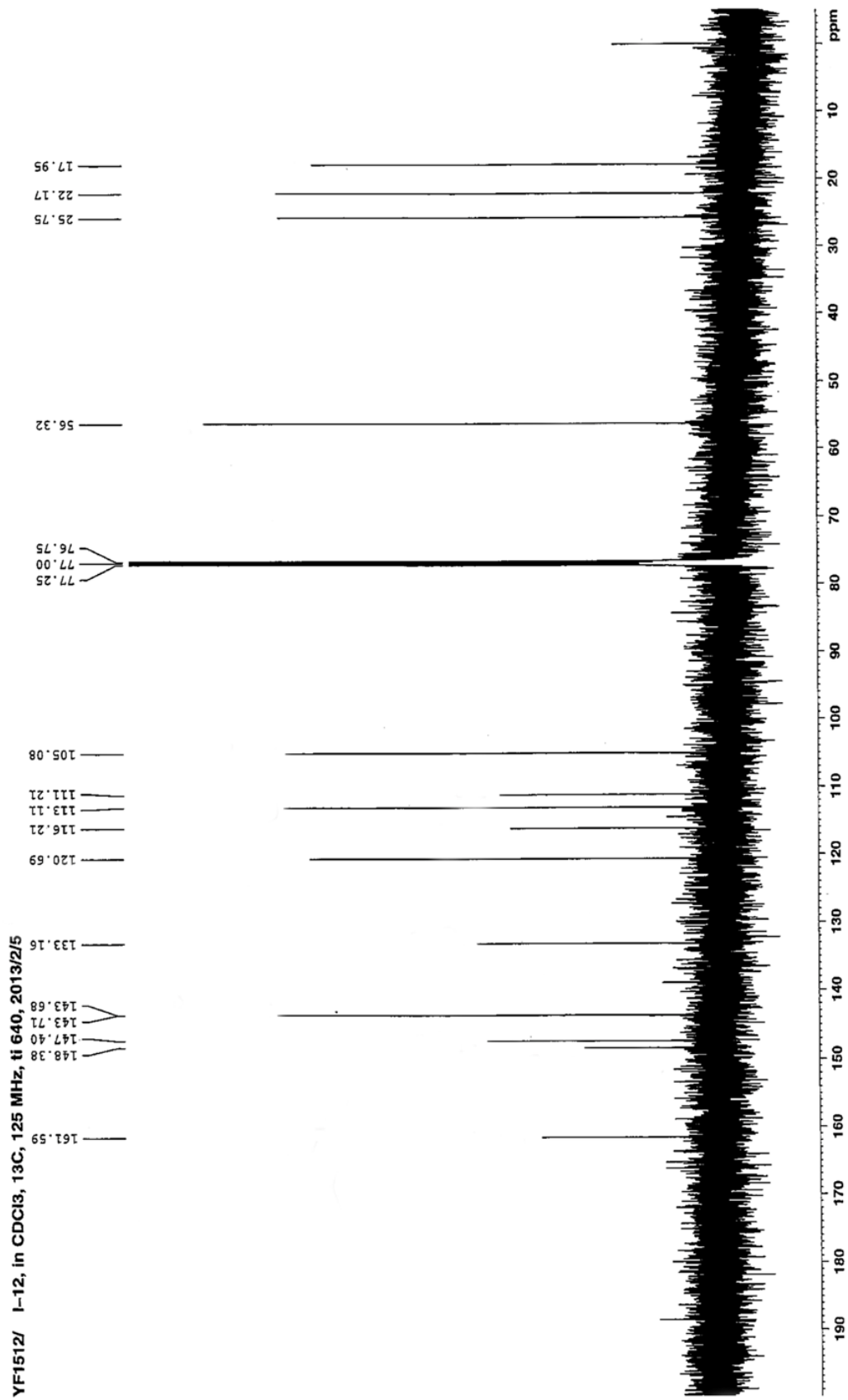
Figure 5.4.3.6 ^{13}C NMR spectrum of HU-3

75
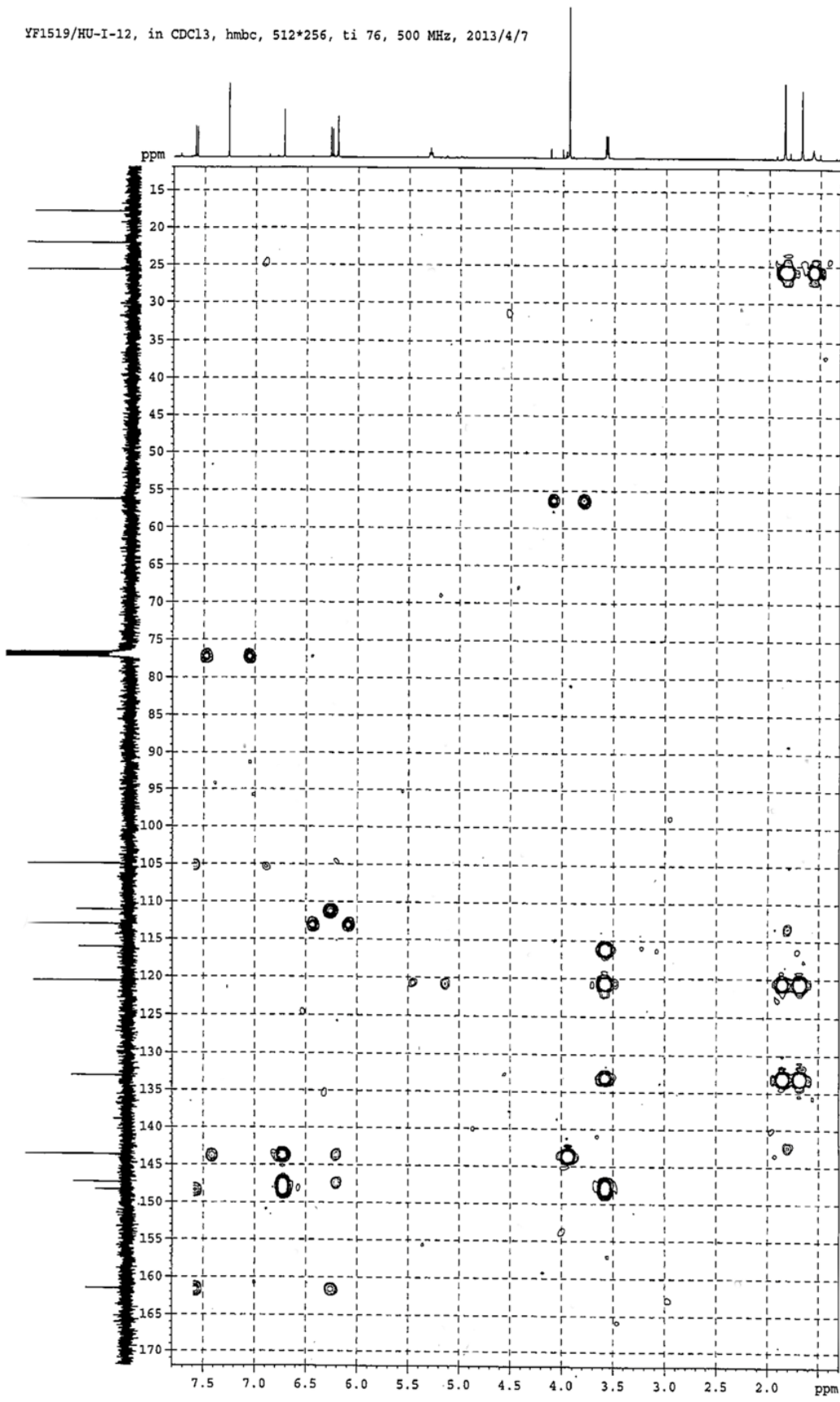
Figure 5.4.3.7 HMBC spectrum of HU-3

with C-6 (δ_C 143.7). The CH$_2$ protons (δ_H 3.57) of prenyl group showed strong correlation with C-8 (δ_C 116.2) and C-7 (δ_C 148.4) and the hydroxyl at δ_H 6.20 exhibited correlation with C-6 (δ_C 143.7) and C-7 (δ_C 148.4). Hence, the hydroxyl group should be flanked by methoxyl and prenyl groups. Based on the congregated spectral data, **HU-3** was unambiguously identified as 7-hydroxy-6-methoxy-8-(3-methylbut-2-enyl)-2H-chromen-2-one (**3**). The assignment of chemical shift values based on the correlations discerned in the HMBC spectrum, are presented in Table 5.4.3. A search of literature revealed that this compound has earlier been reported as cedrelopsin, isolated from *Cedrelopsis grevei*, Family: Rutaceae (Eshiett and Taylor 1968). This is the first report of isolation of a prenylated coumarin compound from a Rubiaceae plant.

Table 5.4.3 ^{13}C and ^{1}H NMR data of HU-3

C. position	δ_C (ppm)	δ_H (ppm)
2	161.6	-
3	113.1	6.25
4	143.7	7.57
5	105.1	6.72
6	143.7	-
7	147.4	-
8	116.2	-
9	148.4	-
10	111.2	-
1'	22.2	3.57
2'	120.7	5.29
3'	133.2	-
4'	25.8	1.85
5'	18.0	1.68
-OMe	56.3	3.94
-OH	-	6.20
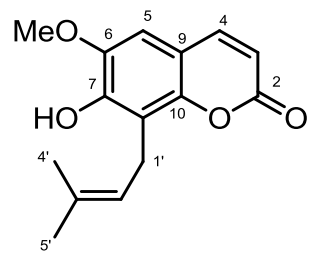
HU-3 (3)

5.4.4 Characterization of HU-4

HU-4 was obtained as white amorphous powder showing m.p. 275-278 °C. It was identified as single compound through TLC studies using different solvent system (C_6H_6:$CHCl_3$; 9:1; R_f 0.59) and the developed spot showed intense pink color change with Liberman Buchard reagent, suggesting it to be a triterpenoid compound. The negative mode ESI-MS analysis showed [M-H]⁻ peak at *m/z* 455.40 (Figure 5.4.4.1). The UV spectrum of **HU-4** displayed characteristic absorption bands (262 and 324 nm) for a typical triterpenoid nucleus (Figure 5.4.4.2). The data collected from the IR spectrum (Figure 5.4.4.3) showed the presence of hydroxyl (3436 cm⁻¹), carbonyl (1692 cm⁻¹) and olefinic (1457 cm⁻¹) groups.
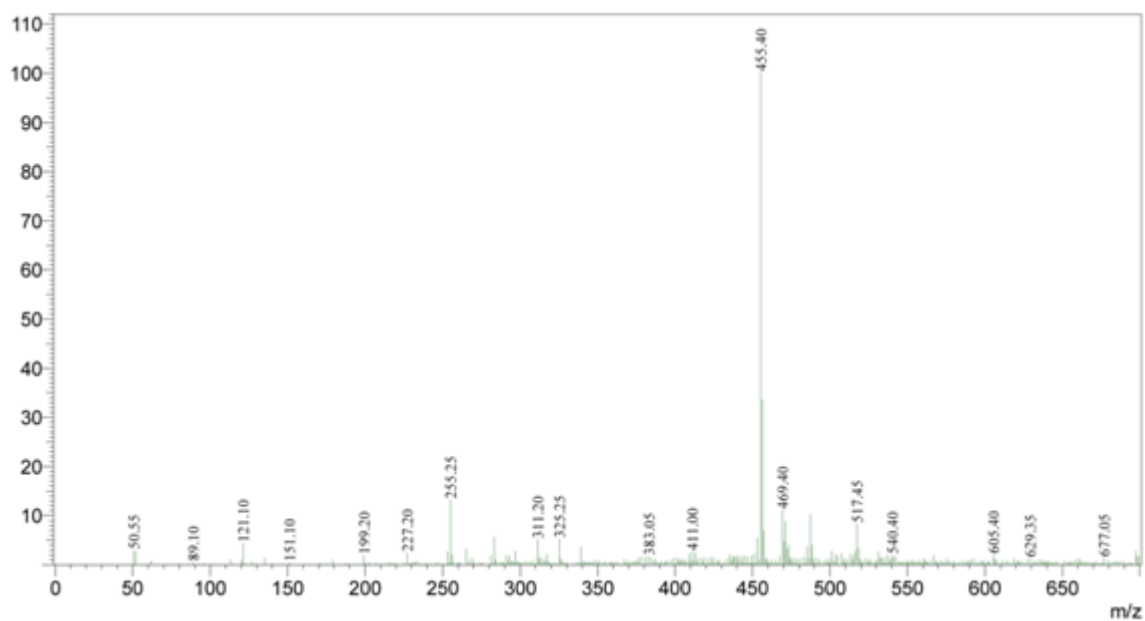
Figure 5.4.4.1 ESI-Mass spectrum of HU-4
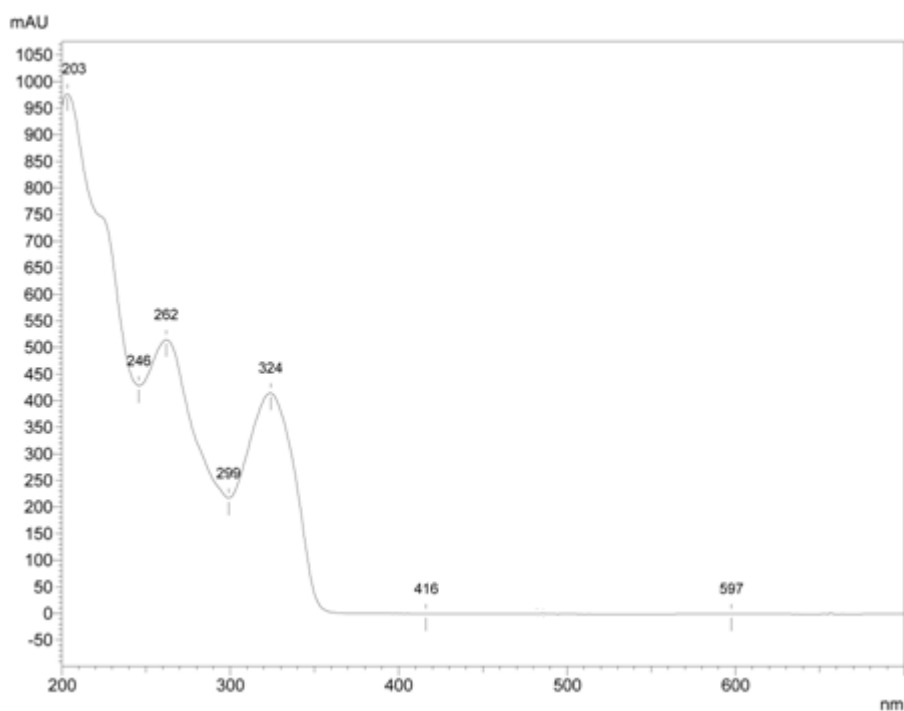
Figure 5.4.4.2 UV-Visible spectrum of HU-4
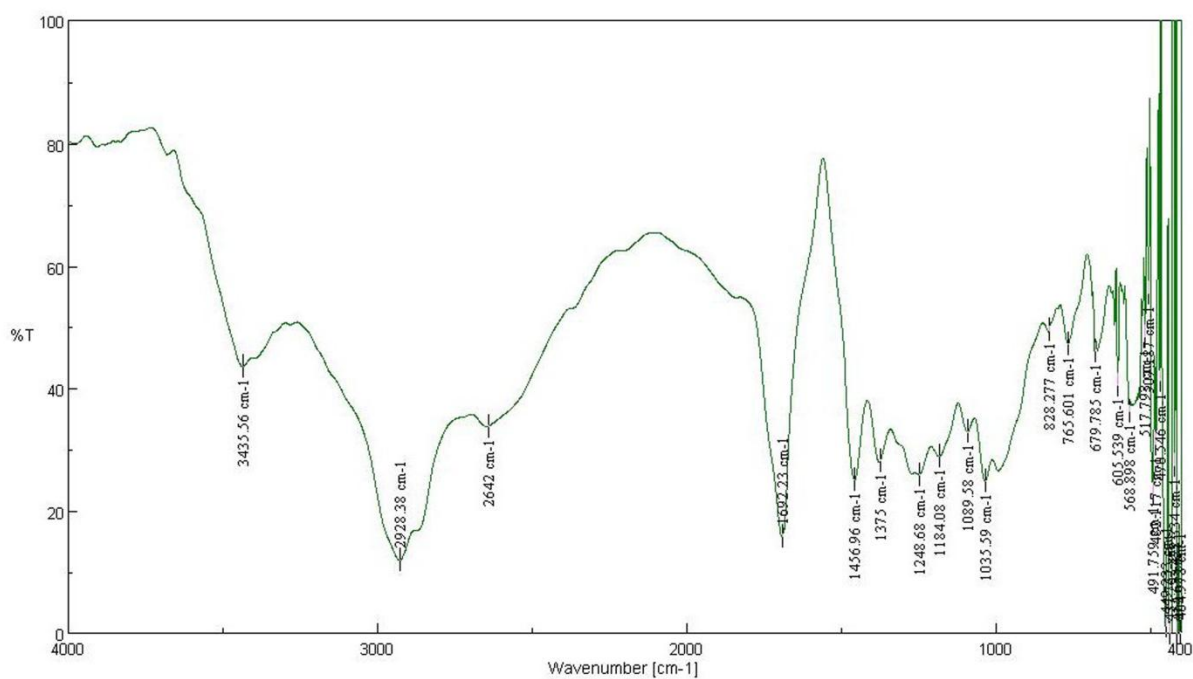
Figure 5.4.4.3 FT-IR spectrum of HU-4

The ^{1}H NMR spectrum (Figure 5.4.4.4) measured in a mixture of $CDCl_3$ and CD_3OD solvents exhibited the presence of carboxylic proton (δ_H 11.95 ppm, s) and olefenic proton

(δ_H 5.24 ppm, br s) signals. Further the chemical shift value at δ_H 3.38 ppm [(br s, 1H), -O**H**] and 3.20 ppm [(t, H-3), OH-C**H**-] indicated the presence of hydroxyl group. In addition, the chemical shift values in the up field region of the spectrum [2.02-1.54 (m), 1.49 (s, 3H), 1.45 (s, 3H), 1.27 (s, 3H), 1.03 ppm (s, 3H)] affirmed the presence of methylenic and methyl protons. Through extensive review on the triterpenoidal derivatives, the obtained PMR spectral data was found to be in good correlation with the reported data for the pentacyclic triterpenoid, ursolic acid. The doublet obtained at δ_H 2.19 ppm (d, IH, J = 11.5 Hz) differentiated the isolated compound from the congener, oleanolic acid and the presence of vicinal dimethyl group was confirmed by the upfield signals at δ_H 0.90 (d, 3H), δ_H 0.78 ppm (d, 3H).

The chemical shift values obtained in ^{13}C NMR (Figure 5.4.4.5) was found to be in well agreement with the proposed structure of ursolic acid (**4**). The highly downfield shift at δ_C 180.6 ppm can be attributed to carboxylic carbon, the signals at δ_C 138.1 and δ_C 125.4 ppm confirmed the presence of double bond and δ_C 78.8 ppm could be assigned to carbon bearing hydroxyl group.

Based on the above discussion, **HU-4** was confirmed as ursolic acid (**4**). The identity was further confirmed through co-TLC [R_f: 0.59 (9:1 C_6H_6:$CHCl_3$)] and mixed melting point studies (m.p. 276 ℃) with the authentic sample.

Figure 5.4.4.4 ¹H NMR spectrum of HU-4

YF1499/ I-05, in CDCl3, 1H, 500 MHz, ti 16, 2013/2/1

HU-4 + CD₃OD (stamsl)

82

YF1496/ I-09, in CDCl3, 13C, 125 MHz, ti 470, 2013/1/3
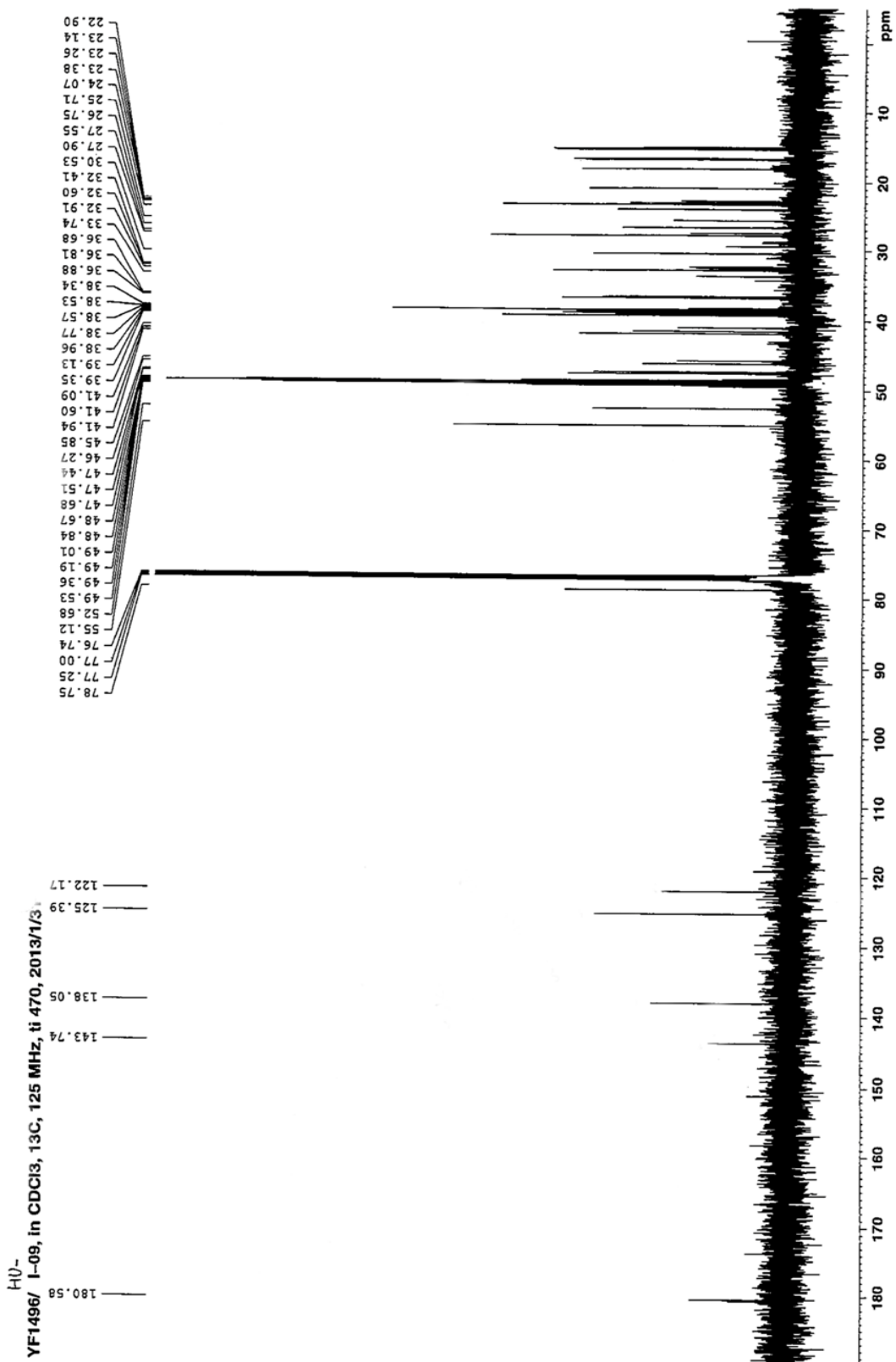
Figure 5.4.4.5 ^{13}C NMR spectrum of HU-4

83
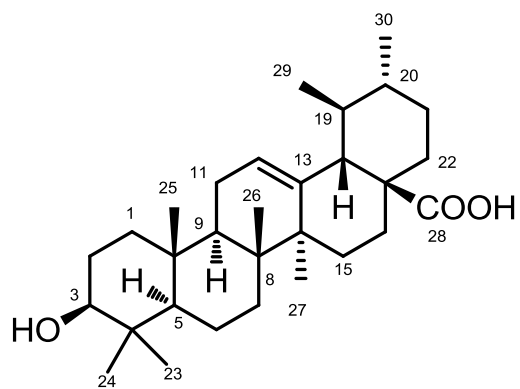
HU-4 (4)

5.4.5 Characterization of HU-5

HU-5 was obtained as yellow needles, showing m.p. of 227-230 ℃. The compound was found to be freely soluble in ethyl acetate, chloroform and methanol and insoluble in n-hexane. The isolated **HU-5** showed single spot in thin layered chromatogram (solvent system: n-hexane:EtOAc 7:3; R_f: 0.57) when developed using different solvents and heating the plate after spraying with 10% methanolic sulphuric acid. This was further confirmed by analytical RP-HPLC (Figure 5.4.5.1). An organic solution of **HU-5** showed pink color change when treated with 10% ammonia solution specifying the presence of anthraquinone nucleus. The UV spectrum of **HU-5** (Figure 5.4.5.2) showed π-π^* absorption bands at 241, 252, 278, 313 and 358 nm and n-π^* absorption band at 478 nm, which are characteristic of anthraquinones (Diaz 1990). The IR spectrum displayed absorption peaks substantiating our assumption of 9,10-anthracenedione derivative through the strong conjugated carbonyl stretching bands at 1663 and 1573 cm^{-1}. In addition, a hydroxyl stretching band at 3312 cm^{-1} was found to be present in the spectrum (Figure 5.4.5.3).
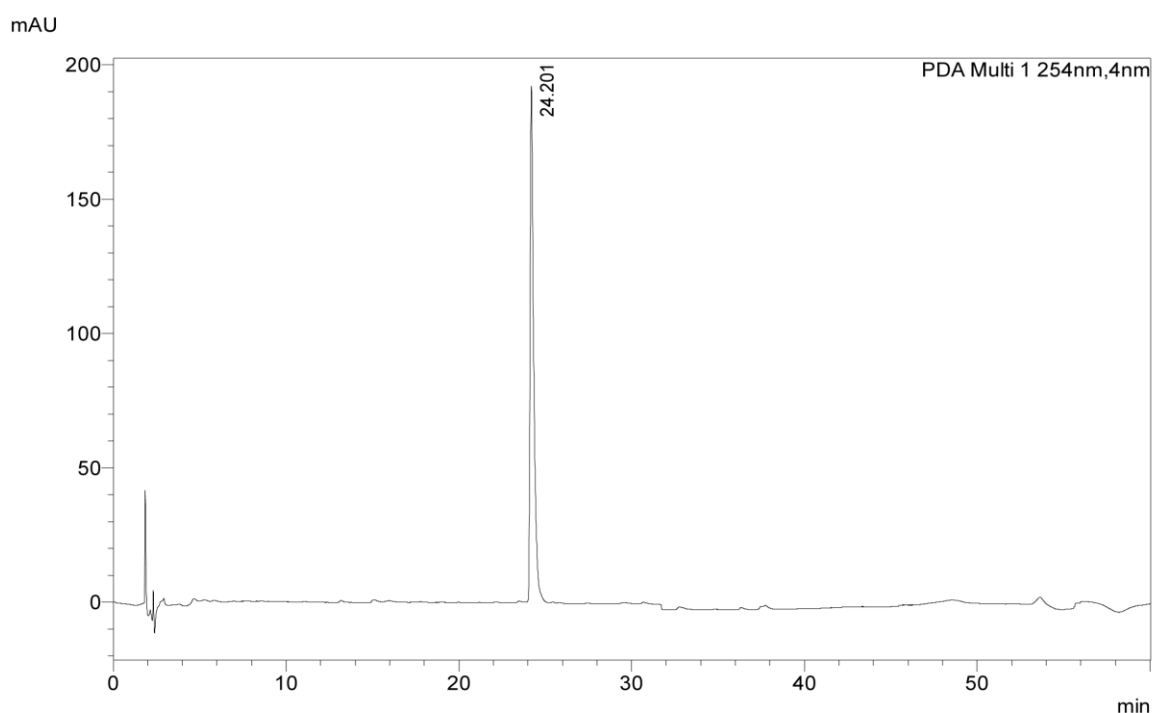
Figure 5.4.5.1 RP-HPLC chromatogram of HU-5 detected at λ_{max} 254 nm
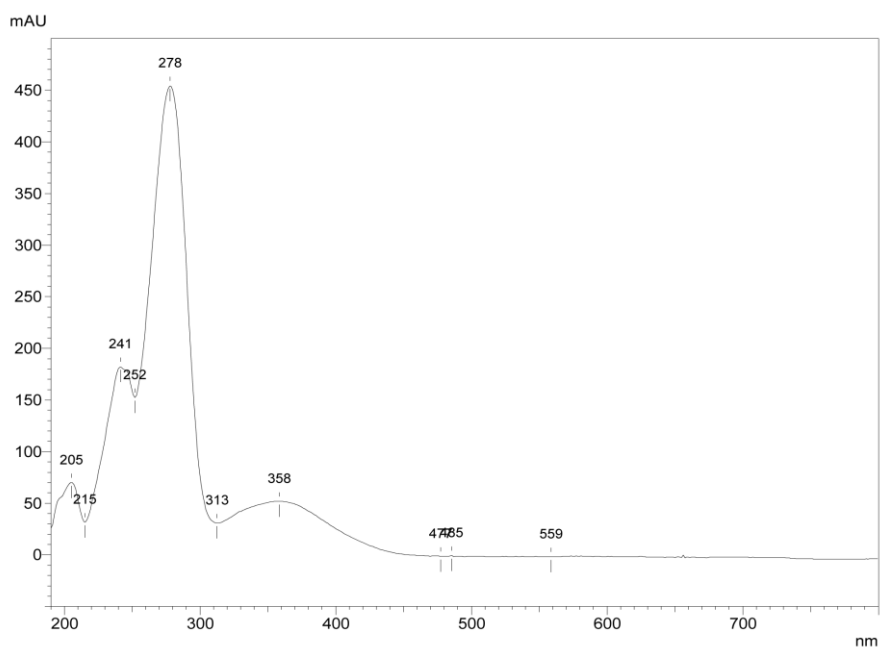
Figure 5.4.5.2 UV-Visible spectrum of HU-5
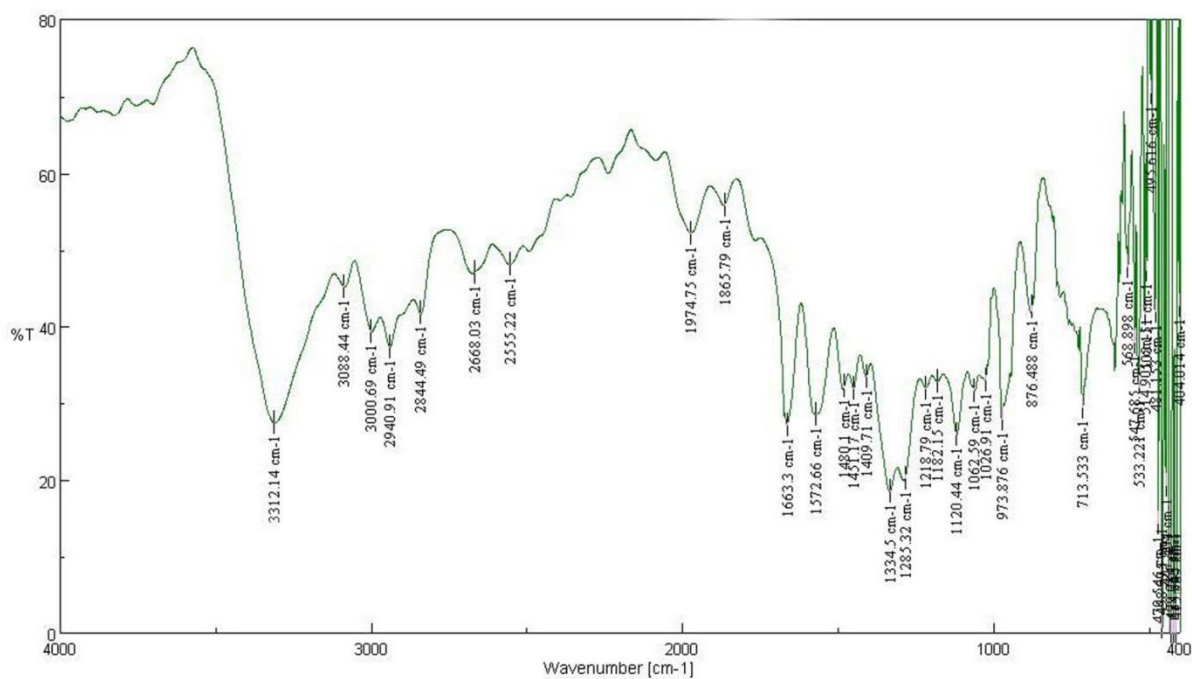
Figure 5.4.5.3 FT-IR spectrum of HU-5

The molecular formula was arrived as $C_{16}H_{12}O_5$ based on the molecular weight determined from the negative mode APCI-MS analysis, which showed [M-H]$^-$ peak at *m/z*

283.25 (Figure 5.4.5.4) and consistency with ^{1}H- and ^{13}C NMR spectral analysis.
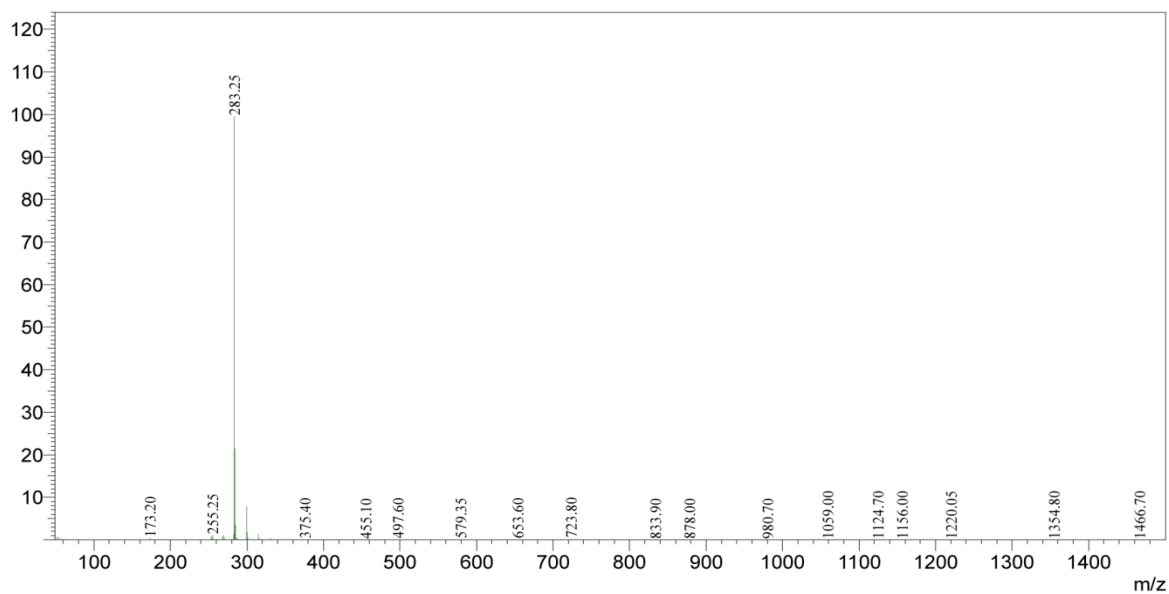
Figure 5.4.5.4 APCI-Mass spectrum of HU-5

The 500 MHz ^{1}H NMR spectrum (Figure 5.4.5.5) showed two sets of closely placed aromatic multiplets integrating for two protons each at δ_H 8.23-8.27 and 7.76-7.78 ppm.
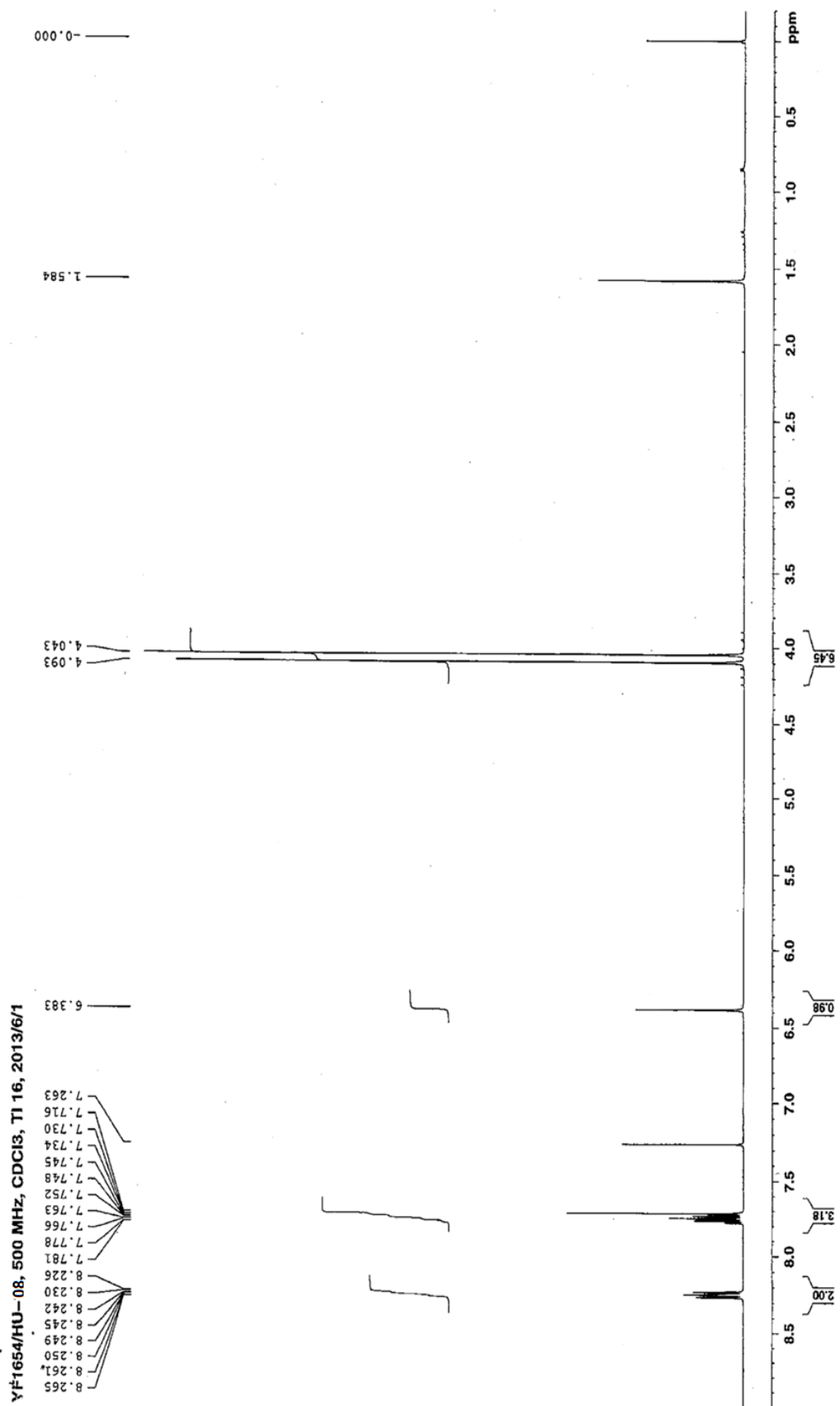
Figure 5.4.5.5 ^{1}H NMR spectrum of HU-5

YF1654/HU–08, 500 MHz, CDCl3, TI 16, 2013/6/1

-0.000

1.584

4.043
4.093

6.383

7.263
7.716
7.730
7.734
7.745
7.748
7.752
7.763
7.766
7.778
7.781
8.226
8.230
8.242
8.245
8.249
8.250
8.261
8.265

88
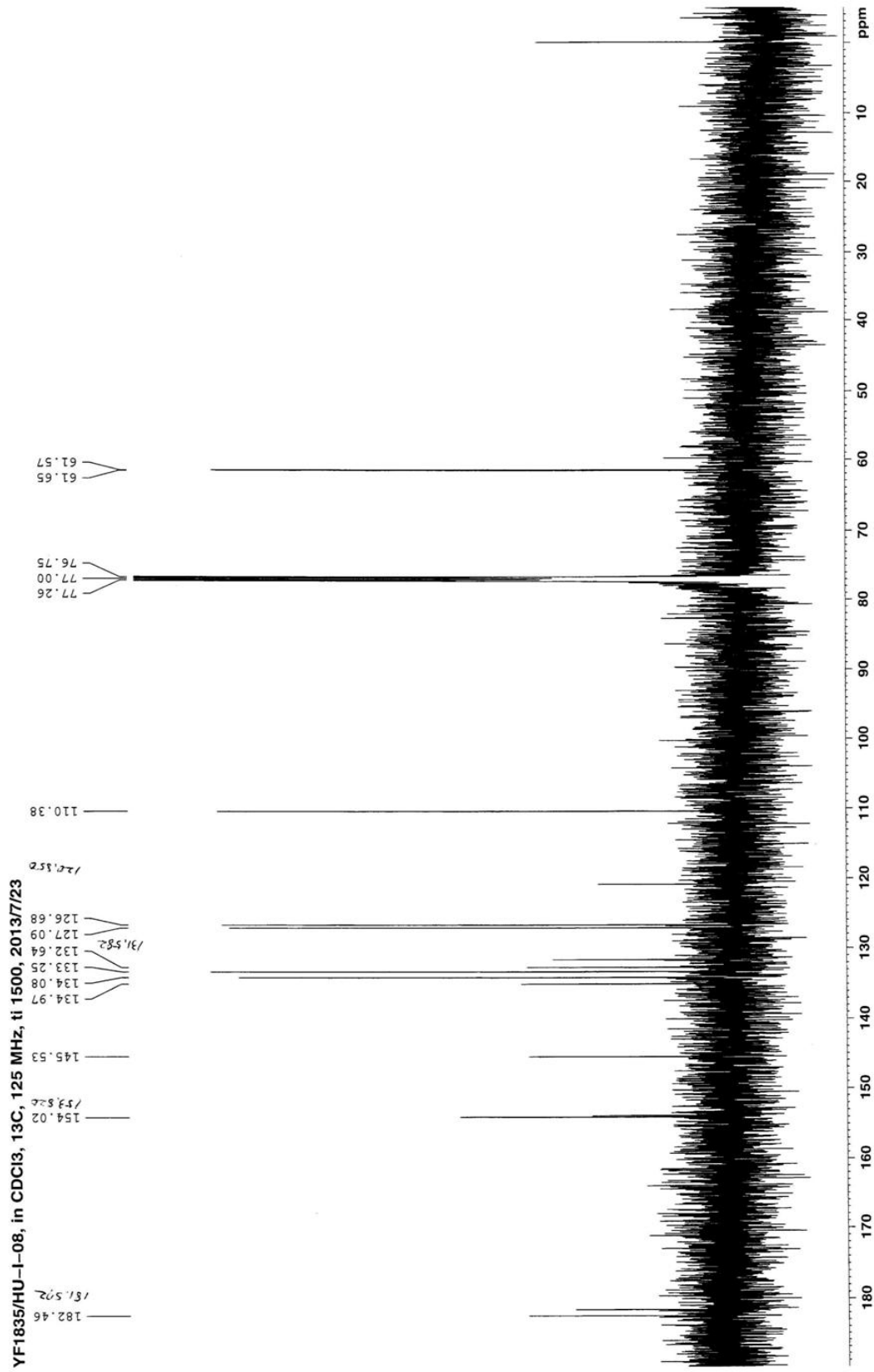
Figure 5.4.5.6 ^{13}C NMR spectrum of HU-5

YF1835/HU-I-08, in CDCl3, 13C, 125 MHz, ti 1500, 2013/7/23

61.57
61.65

76.75
77.00
77.26

110.38

126.85
126.68
127.09
131.585
132.64
133.25
134.08
134.97

145.53

153.826
154.02

181.595
182.46

Additionally, presence of an isolated singlet at δ_H 7.72 ppm in the downfield region of the spectrum exemplified **HU-5** to be 1,2,3-trisubstituted 9,10-anthracenedione derivative. Two of the substituents were straightforwardly identified as methoxyl groups from the singlets appeared at δ_H 4.04 and 4.09 ppm. The third substituent could possibly be a non-chelated hydroxyl group ascertained from the one proton broad singlet appeared at δ_H 6.38 ppm, which was also in accordance with IR spectral data.

The ^{13}C NMR spectrum of **HU-5** (Figure 5.4.5.6) revealed sixteen different carbon signals sorted into seven quarternary carbons (δ_C 154.0, 153.8, 145.5, 135.0, 134.1, 131.6, and 120.9 ppm), five aromatic methines (δ_C 133.3, 132.6, 127.1, 126.7 and 110.4 ppm), two carbonyls (δ_C 182.5 and 181.6 ppm) and two methoxyls (δ_C 61.7 and 61.6 ppm). The exact point of attachment of methoxyls (C-1 and C-2) and hydroxyl (C-3) substituents were ascertained based on the comparison of NMR values with those of reported values of anthragallol-1,2-dimethyl ether (Long et al., 2010). Thus, **HU-5** was identified as 1,2-dimethoxy-3-hydroxy-9,10-anthacenedione (**5**).
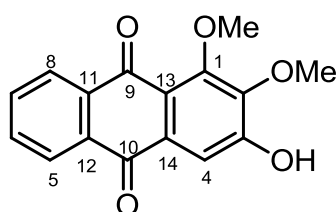
HU-5 (5)

5.4.6 Characterization of HU-6

HU-6 was isolated as a yellow amorphous powder and was found to have m.p. of 215-217 ˚C. **HU-6** demonstrated free solubility in ethyl acetate, chloroform and methanol. The purity of **HU-6** was verified by TLC (solvent system: n-hexane:EtOAc 7:3; R_f: 0.28) studies followed by analytical RP-HPLC (Figure 5.4.6.1).
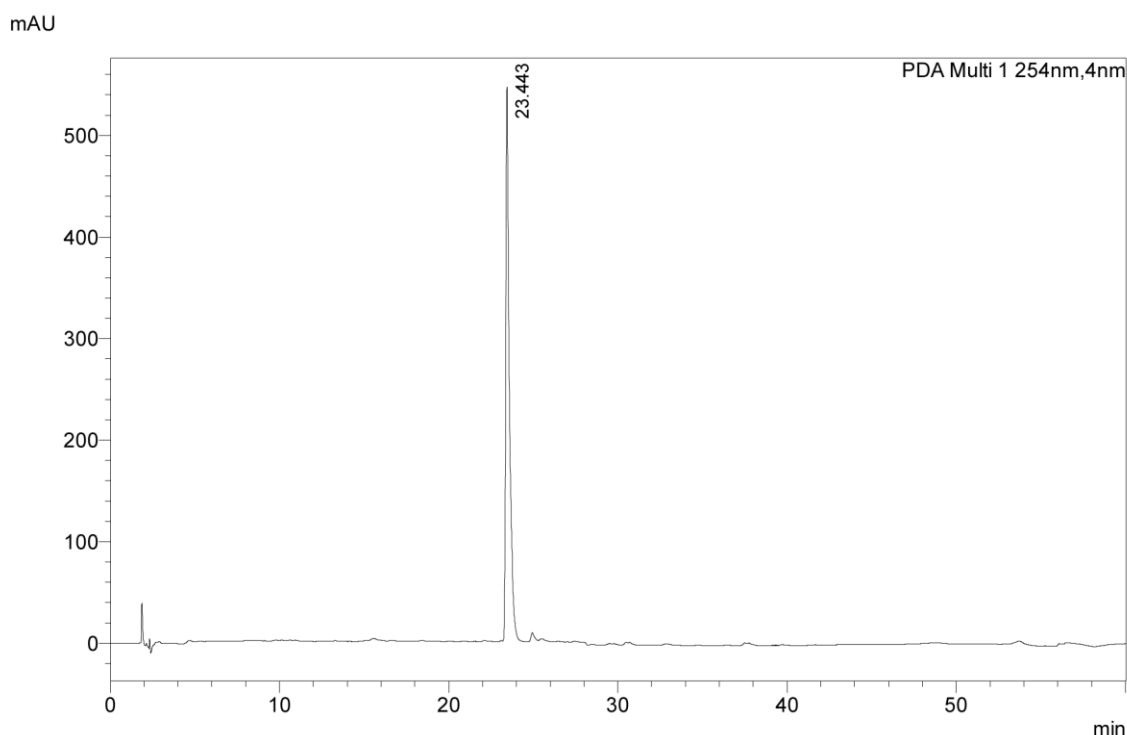
Figure 5.4.6.1 RP-HPLC chromatogram of HU-6 detected at λ_{max} 254 nm

HU-6 inferred positive result (pink color) for anthraquinone derivatives while testing with 5% ammonia solution. In addition, the observed UV absorption bands (240, 253, 279 and 365 nm) (Figure 5.4.6.2) and IR absorption bands (3300, 1670, 1590, 1560 cm^{-1}) (Figure 5.4.6.3) characteristic of 9,10-anthracenedione derivative established the similarity between **HU-6** and **HU-5**. The molecular weight of **HU-6** was found to be 284 based on the negative APCI-MS analysis which showed [M-H]$^-$ peak at *m/z* 283.25 (Figure 5.4.6.4), which was identical to **HU-5**. The ^{1}H (500 MHz) and ^{13}C NMR (125 MHz) spectra further reflected the

91

close resemblance and thereby the isomeric nature of **HU-6** and **HU-5**. The precise spectral interpretation corroborated them to be regioisomers.
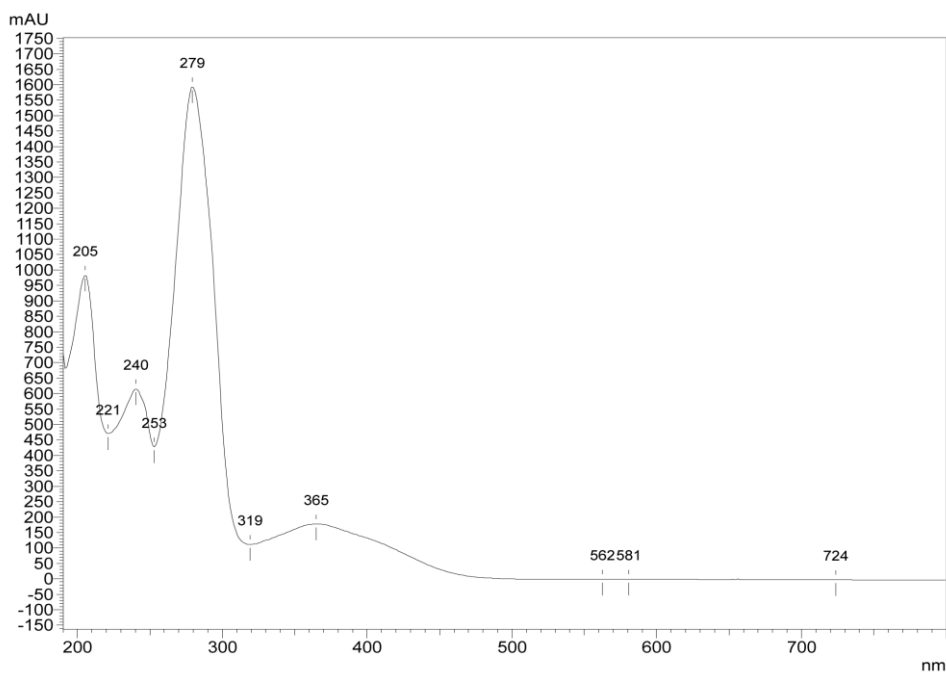
Figure 5.4.6.2 UV-Visible spectrum of HU-6
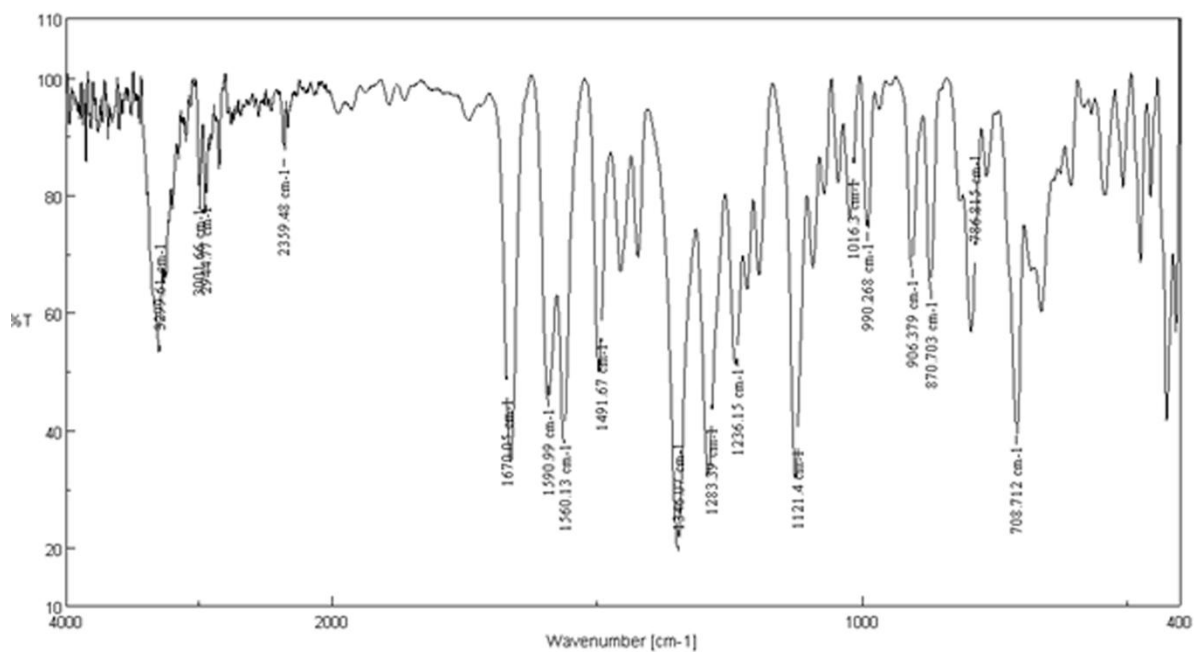
Figure 5.4.6.3 FT-IR spectrum of HU-6
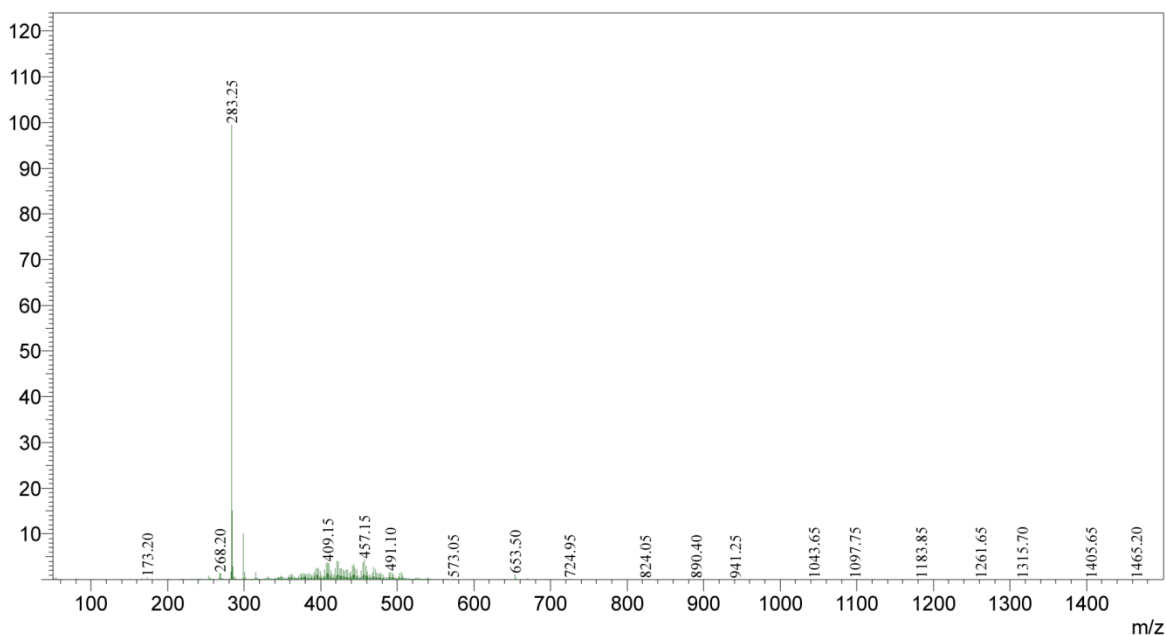
Figure 5.4.6.4 APCI-Mass spectrum of HU-6

The analysis of PMR spectrum of **HU-6** (Figure 5.4.6.5) revealed the presence of 1,2,3-trioxygenated anthraquinone moiety from the appearance of signals at δ_H 8.18-8.30 (m, 2H), 7.71-7.79 (m, 2H), 7.62 (s, 1H), 3.07 (s, 1H), 4.04 (s, OCH$_3$) and 4.0 (s, OCH$_3$). The data presented so far were found to be in complete consistent with the structure given for **HU-5** with a positional modification, which was evident in the ^{13}C NMR spectrum (Figure 5.4.6.6). The shift in the δ_C values of -OCH$_3$ groups and carbons of ring C suggested **HU-6** as regioisomeric anthragallol.

Further the difference in the R_t on RP-HPLC, the R_f value and the melting point allowed us to consider that **HU-6** as 1,3-dimethoxy-2-hydroxy-9,10-anthracenedione. The possibility of 1-hydroxy-2,3-dimethoxy anthraquinone was ruled out from the absence of chelated hydroxyl signal in the downfield region of ^{1}H NMR spectrum. **HU-6** was found to show no depression in the observed spectral data when compared to the reported data of anthragallol-1,3-dimethyl ether (Fraga et al., 2009). Finally the structure of **HU-6** was determined as 1,3-dimethoxy-2-hydroxy-9,10-anthacenedione (**6**).

93
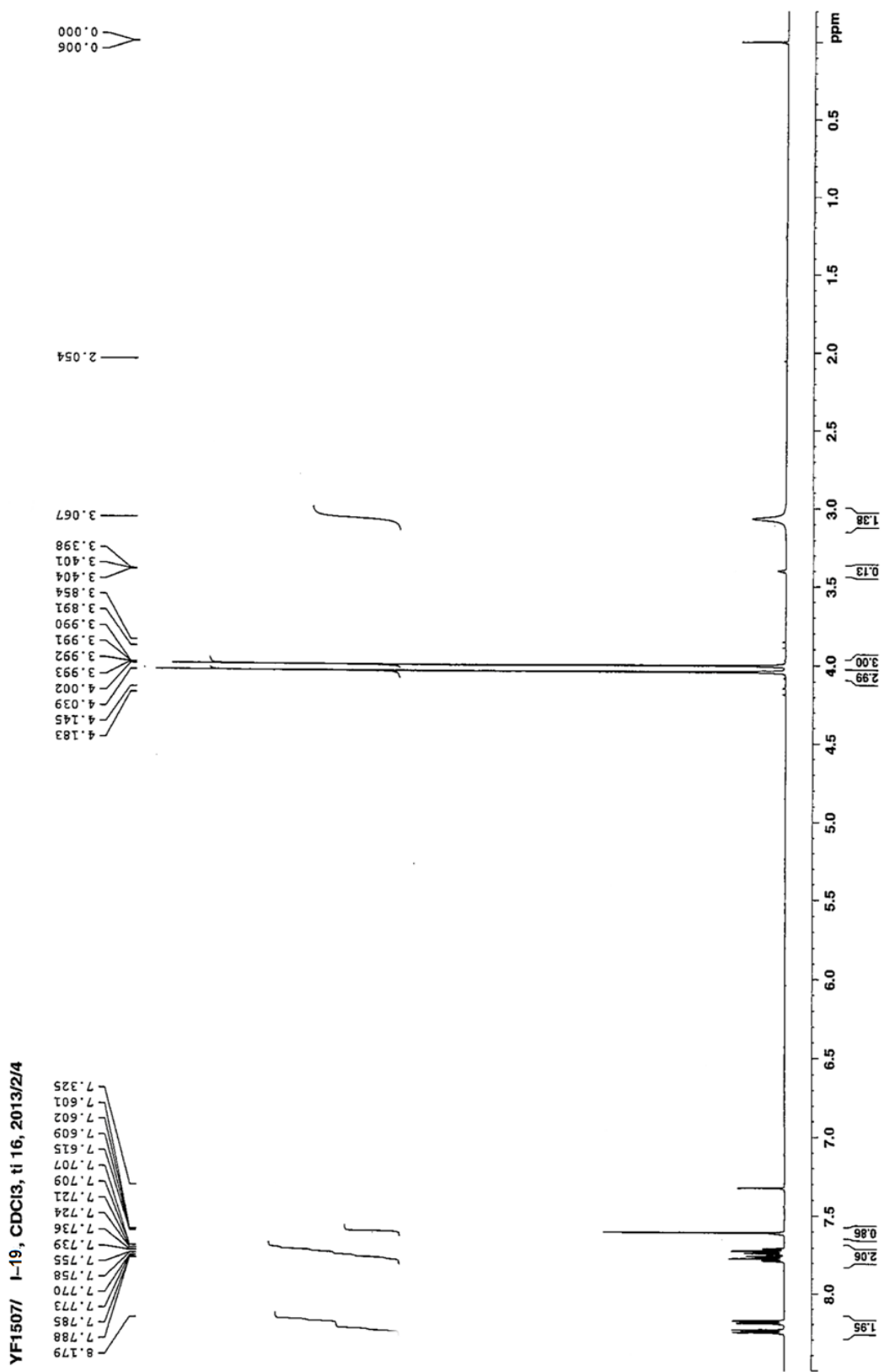
Figure 5.4.6.5 ¹H NMR spectrum of HU-6

YF1655/HU-19, in CDCl3, 13C, 125 MHz, ti 340, 2013/6/1

56.63
61.81
76.75
77.00
77.26
106.28
120.81
126.67
127.02
127.68
132.71
133.34
133.94
134.65
144.90
147.38
151.54
181.74
182.46
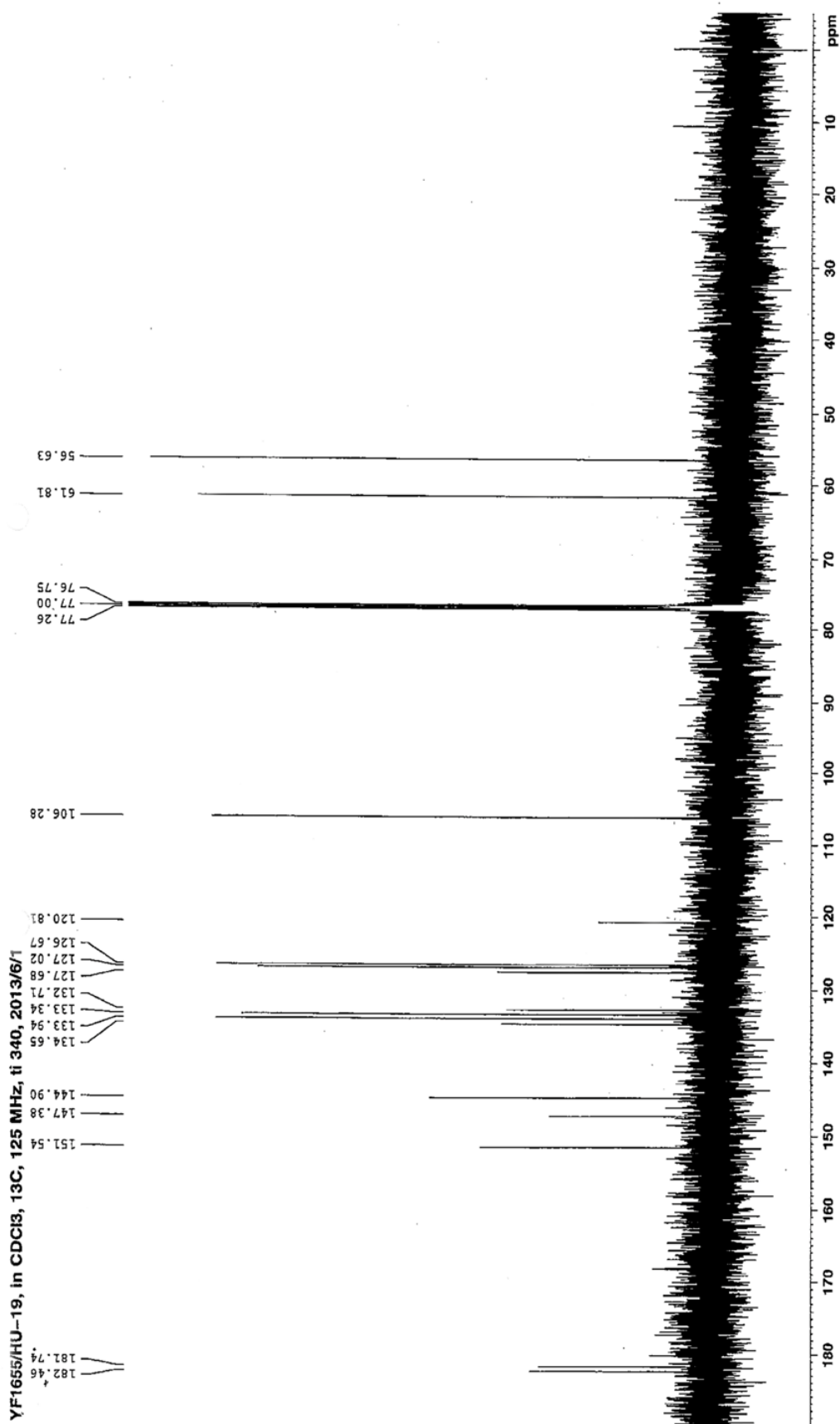
Figure 5.4.6.6 ^{13}C NMR spectrum of HU-6

95
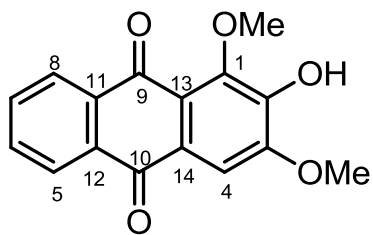
HU-6 (**6**)

5.4.7 Characterization of HU-7

HU-7, obtained as yellow amorphous powder was found to be soluble in ethyl acetate, chloroform and methanol. It was just insoluble in n-hexane, showing $[\alpha]_D^{25}$ -15.6 (c = 0.20, CH$_3$OH). The purity of the **HU-7** was determined by TLC studies. The TLC plates developed in different solvent system, showed single spot when exposed to iodine vapours and charring with 10% methanolic sulphuric acid as well. The homogeneity of **HU-7** was also verified by analytical RP-HPLC, which showed single chromatogram (R_t 16.92 min) using ODS column and H$_2$O/MeCN as mobile phase (Figure 5.4.7.1).
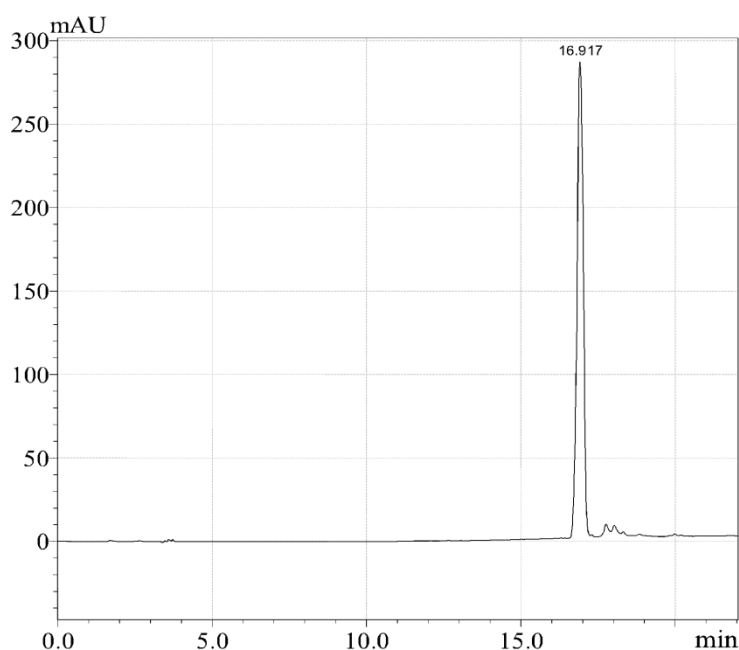
Figure 5.4.7.1 RP-HPLC chromatogram of HU-7 detected at λ_{max} 280 nm

The molecular formula was deduced as C$_{14}$H$_{12}$O$_4$, based on the ESI-mass spectrometrically derived [M+H]$^+$ peak at *m/z* 245.05 (Figure 5.4.7.2) and collective proton and carbon NMR spectral data. The UV-Visible spectrum of **HU-7** showed distinguishable absorption maxima at λ_{max} 230, 272 (sh) and 347 nm, which are characteristic of a 6,7,8-trisubstituted coumarin nucleus (Figure 5.4.7.3).
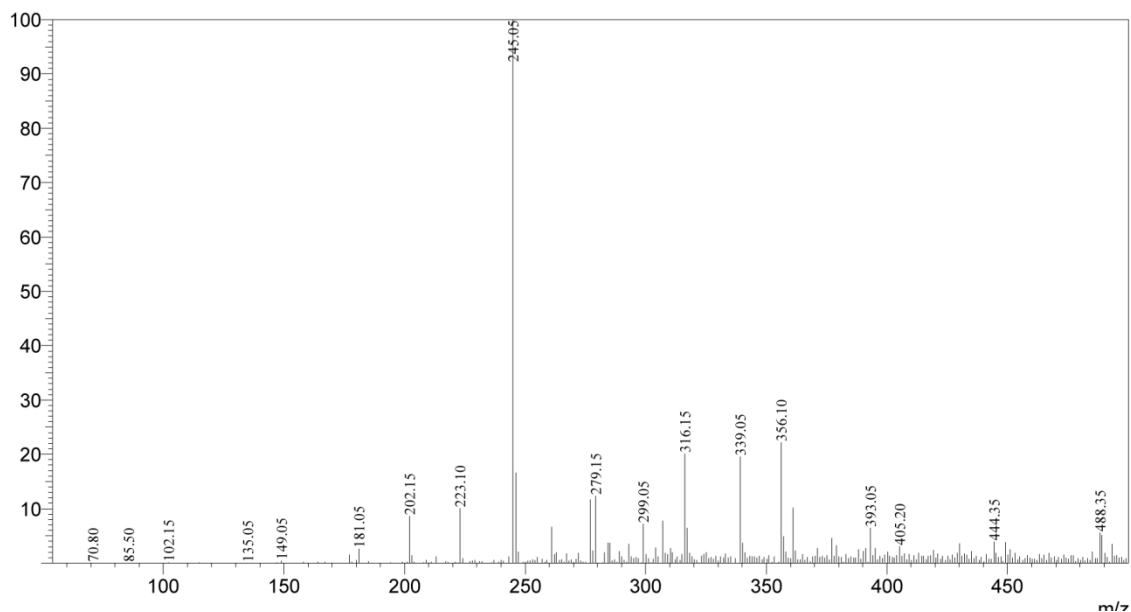
Figure 5.4.7.2 ESI-Mass spectrum of HU-7
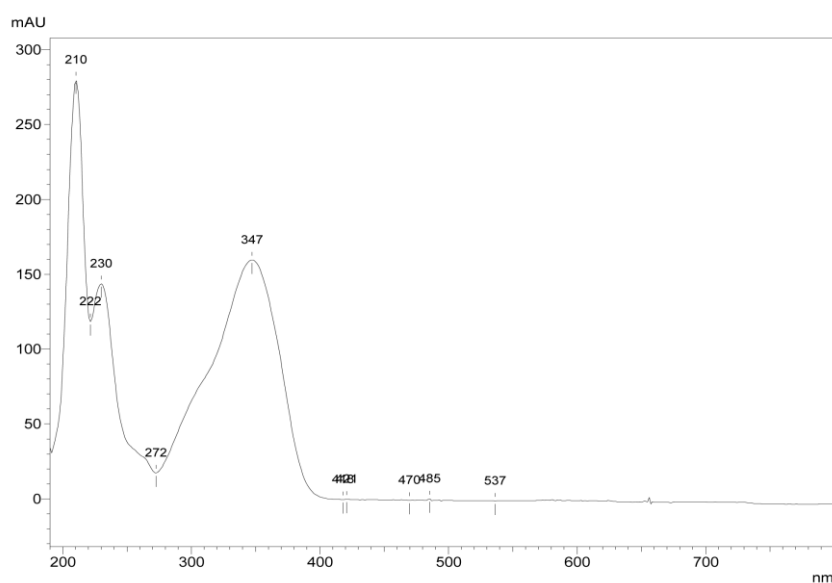
Figure 5.4.7.3 UV-Visible spectrum of HU-7

The coumarin core of **HU-7** was forthrightly recognized from the ^{1}H NMR spectrum, which was measured at 500 MHz by dissolving in CD$_3$OD (Figure 5.4.7.4). The PMR spectrum exhibited two mutually coupled doublets at δ_H 6.18 and 7.78 ppm with coupling constant value of 9.5 Hz, characteristic of an α,β-unsaturated δ-lactone group of a coumarin ring. A lone singlet in the downfield region of the spectrum at δ_H 6.87 pm, ascertained the

trisubstitution in ring A of coumarin. The spectrum further explained the presence of non-equivalent methylene protons adjacent to an oxymethine chiral centre, which was evident from the signals at δ_H 3.56 (dd, J = 15.9, 7.8 Hz, 1H), 3.17 (dd, J = 15.9, 7.8 Hz, 1H) and 5.45 ppm (t, J = 18.7 Hz, 1H). Also, the presence of terminal olefenic proton signals at δ_H 5.14 (d, J =1.5 Hz), 4.96 ppm (d, J = 1.5 Hz) and a vinylic methyl proton signal at δ_H 1.78 ppm was recognized on careful interpretation. The signals discerned in the PMR spectrum clearly corroborated the presence of an isoprenyl group attached to the coumarin nucleus through furan bridge. Further proof for this interpretation came from double bond equivalence (DBE) for **HU-7**, which was calculated to be 9. The terminal olefine and the coumarin nucleus constituted eight degrees of unsaturation and the remaining one could be well accommodated as a ring involving oxygen and thus the presence of furanocoumarin nucleus in the structure of **HU-7** was confirmed.

The ^{13}C NMR spectrum measured at 125 MHz demonstrated signals pertaining to furanocoumarin moiety (Figure 5.4.7.5). In all, the CMR spectrum of **HU-7** presented fourteen carbon signals sorted as one -CH$_3$ (δ_C 17.0 ppm), one -CH$_2$- (δ_C 32.8 ppm), one terminal =CH$_2$ (δ_C 113.0 ppm), α and β carbons of unsaturated carbonyl system (δ_C 114.5 and 146.3 ppm), one aromatic >CH- (δ_C 112.6 ppm), one oxymethine (δ_C 89.4 ppm), six quarternary carbons (δ_C 153.6, 146.3, 144.9, 140.5, 115.5 and 114.6 ppm) and a carbonyl carbon (δ_C 163.7 ppm), based on DEPT 135 spectral analysis (Figure 5.4.7.6) substantiating the determination of **HU-7** as furanocoumarin derivative. The third substituent was assumed as hydroxyl from the highly deshielded quarternary carbon signal at δ_C 144.9 ppm, apart from the signals of C-6a (δ_C 153.6 ppm) and C-9b (δ_C 146.3 ppm) of furanocoumarin nucleus.
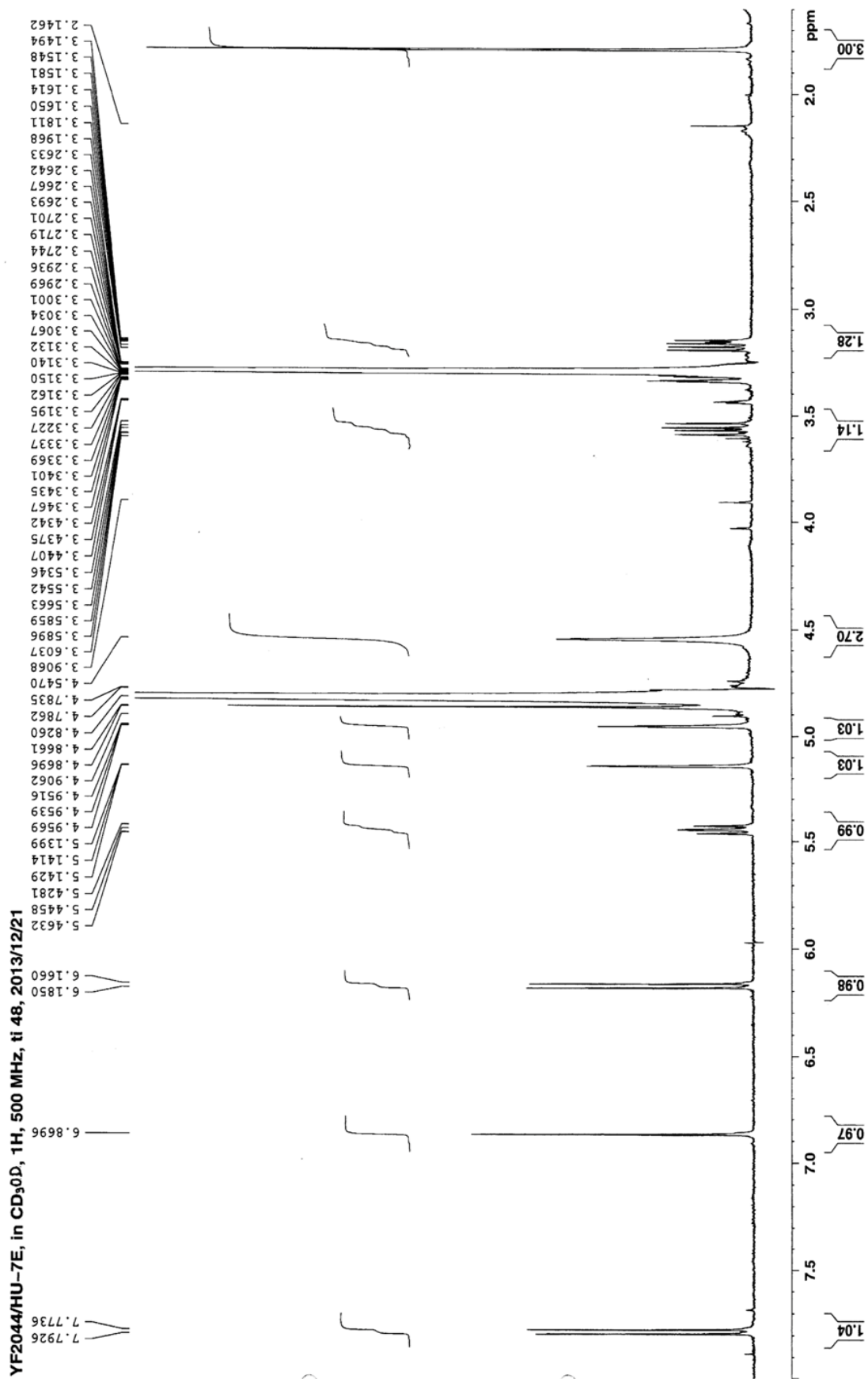
Figure 5.4.7.4 ^{1}H NMR spectrum of HU-7

YF2044/HU-7E, in CD₃OD, 1H, 500 MHz, ti 48, 2013/12/21

2.1462
3.1494
3.1548
3.1581
3.1614
3.1650
3.1811
3.1968
3.2633
3.2642
3.2667
3.2693
3.2701
3.2719
3.2744
3.2936
3.2969
3.3001
3.3034
3.3067
3.3132
3.3140
3.3150
3.3162
3.3195
3.3227
3.3337
3.3369
3.3401
3.3435
3.3467
3.3472
3.4375
3.4407
3.5346
3.5542
3.5663
3.5859
3.5896
3.6037
3.9068
4.5470
4.7835
4.7862
4.8260
4.8661
4.8696
4.9062
4.9516
4.9539
4.9569
5.1399
5.1414
5.1429
5.4281
5.4458
5.4632
6.1660
6.1850
6.8696
7.7736
7.7926

100

YF25077/7E, in CD3OD, 13C, 125 MHz, ti 7000, 2015/2/22

17.04
32.81
48.49
48.66
48.83
49.00
49.17
49.28
49.34
49.45
49.51
89.43
112.57
113.02
114.52
114.56
115.52
140.46
144.91
146.28
153.61
163.72

Figure 5.4.7.5 ^{13}C NMR spectrum of HU-7

YP2508/7-E, in CD3OD, dept135, 125 MHz, ti 10040, 2015/2/22
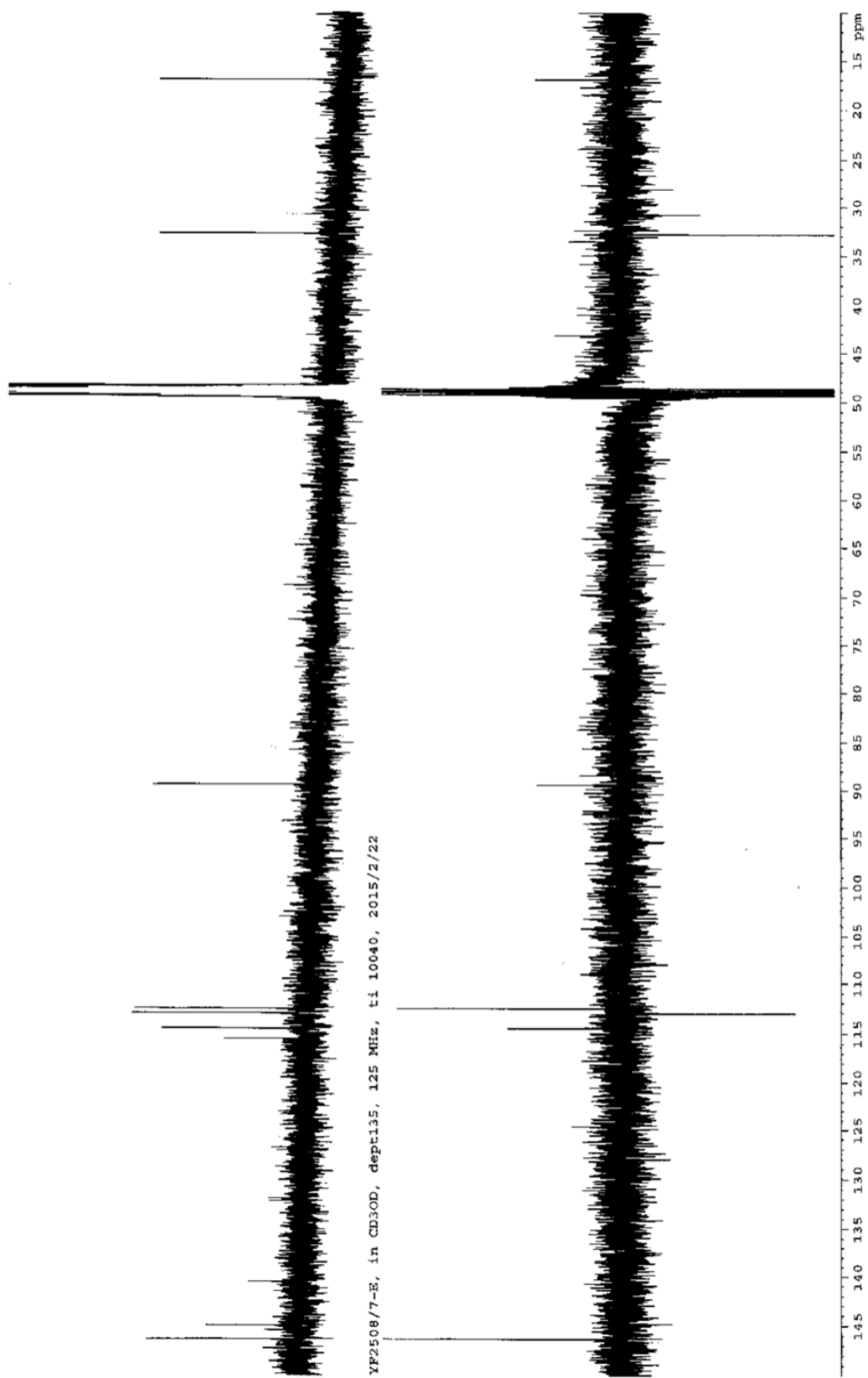
Figure 5.4.7.6 DEPT135 spectrum of HU-7

On the basis of the spectral data discussed so far, it was inferred that the molecule **HU-7** could possess any one of the possible angular or linear structures having 6-oxygenated 8,9-dihydrofurocoumarin (**A** and **B**) or 9-oxygenated 6,7-dihydrofurocoumarin (**C** and **D**) as drawn in the following figure.
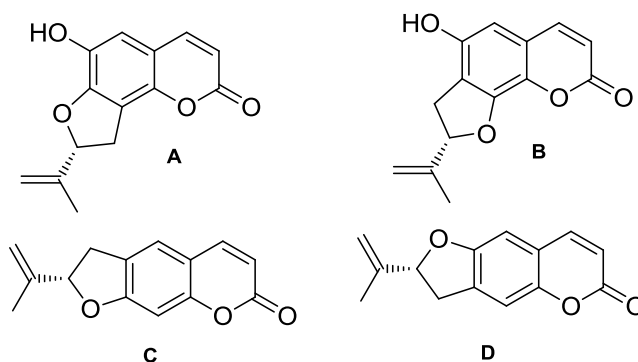
A search of literature on oxygenated furanocoumarins disclosed the identity of spectral data of **HU-7** with a 6-oxygenated 8,9-dihydrofurocoumarin, Hedyotiscone B, which was previously reported from *Hedyotis biflora* (Chen et al., 2006). Thus, the structure of **HU-7** was elucidated as **7**. To the best of our knowledge this is the second report of isolation of this compound from a natural source.
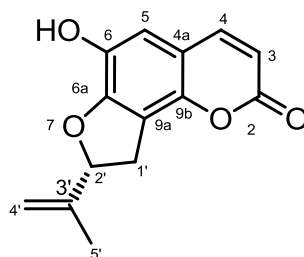
HU-7 (7)

5.5 Isolation and characterization of chemical constituents of HUM-B

Repeated normal and reverse phase chromatography of **HUM-B** culminated five compounds. The isolation procedure is briefly presented in scheme II. The structure of the isolated compounds was elucidated using various spectroscopic techniques including ^{1}H NMR, ^{13}C NMR and mass spectroscopy.

Scheme II

HUM-B (105.0 g)

Diaion HP-20; H_2O → MeOH

H_2O eluate
(Fr. 1-12)

i. Concentrated; ii. MeOH soluble fraction
ii. CC; SiO_2; $CHCl_3$ → MeOH

CHCl$_3$: MeOH
eluate (90:10)

CHCl$_3$: MeOH
eluate (80:20)

i. FC; SiO_2; EtOAc → MeOH
ii. λ_{max}: 214 & 254 nm

i. FC; SiO_2; CHCl$_3$-MeOH
ii. p-TLC; CHCl$_3$:MeOH (80:20)

HU 12

EtOAc: MeOH
elutes (92:8)

EtOAc: MeOH
elutes (85:15)

p-HPLC; C_{18}; H_2O → MeOH;

p-HPLC; C_{18}; H_2O → MeCN

HU 11

R_t 25 min
HU-8

R_t 30 min
HU-9

R_t 33 min
HU-10
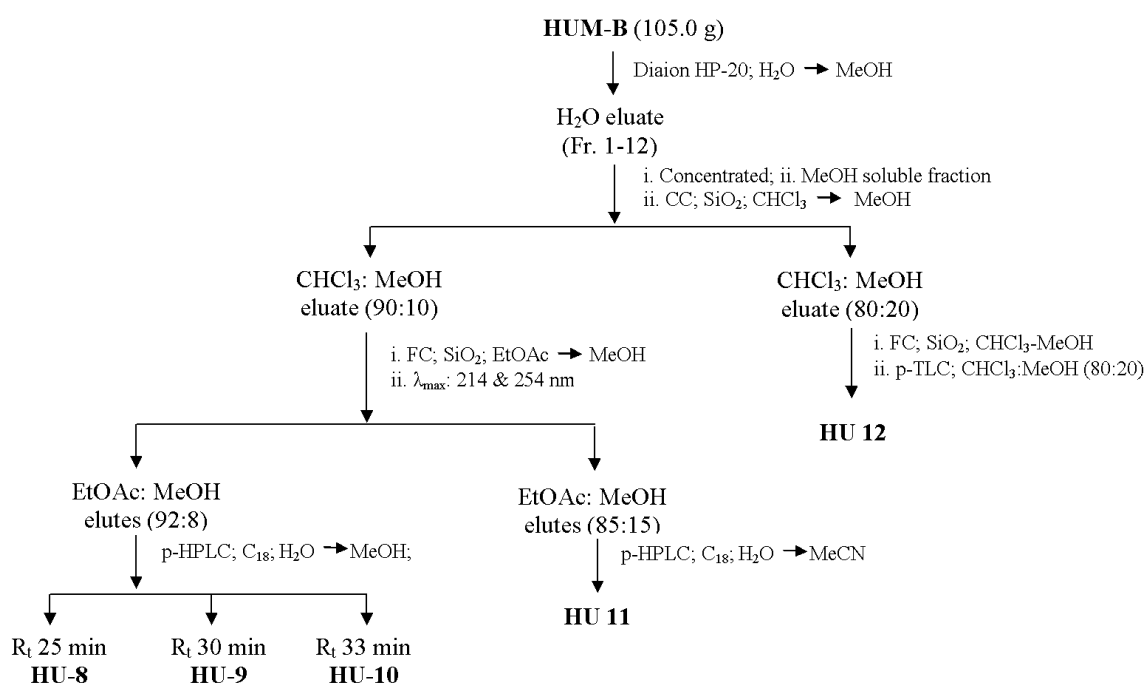
5.5.1 Characterization of HU-8

HU-8 was isolated in the form of white amorphous powder showing m.p. of 129-132 °C and $[\alpha]_D^{25}$ +7.46° (c = 0.85, CH$_3$OH). **HU-8** showed single spot under TLC studies carried out using different solvent system and spray reagents [solvent system: CHCl$_3$: MeOH, 7:3; (R_f 0.28)]. The purity of the compound was further studied using analytical RP-HPLC (Figure 5.5.1.1). The spot developed in TLC exhibited a dark purple color changing to black when sprayed with 10% methanolic sulphuric acid and heated at 105 °C. In addition, the TLC spots showed pink color change when sprayed and heated with anisaldehyde-sulphuric acid reagent, indicating the terpenoid glycosidic nature of **HU-8**. Further, spraying the TLC plates with 1% concentrated hydrochloric solution of paradimethyl amino benzadehyde displayed intense purple color spots confirming **HU-8** to be an iridoid glycoside.
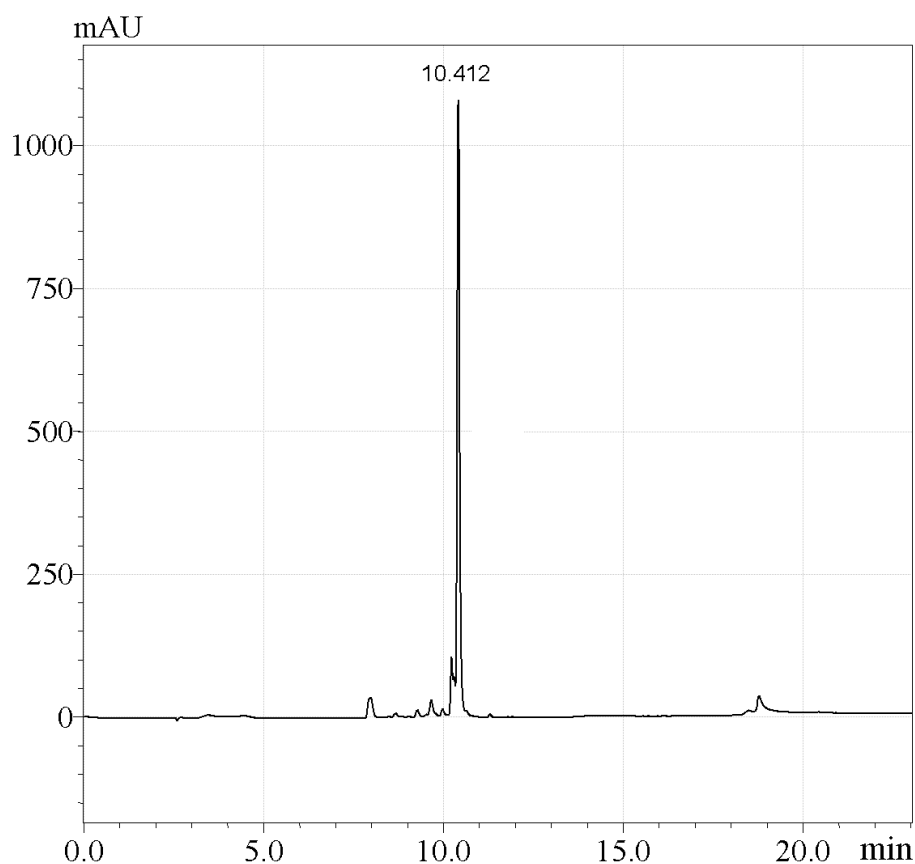
Figure 5.5.1.1 RP-HPLC chromatogram of HU-8 detected at λ_{max} 240 nm

The UV spectrophotometric analysis of **HU-8** (Figure 5.5.1.2) exhibited wavelength absorption maxima at 238 nm, a characteristic band for α, β-unsaturated carbonyl chromophore suggesting the presence of acid or ester group at C-4 of iridoid nucleus (Liang et al., 2011). The molecular weight of **HU-8** was derived as 432 from negative mode ESI-MS analysis, which showed [M-H]⁻ peak at *m/z* 431.20 (Figure 5.5.1.3). The 500 MHz proton NMR (Figure 5.5.1.4) measured by dissolving **HU-8** in CD_3OD revealed the presence of one proton doublet at $δ_H$ 5.05 ppm, characteristic of H-1 of an iridoid glycoside and two olefinic protons signals at $δ_H$ 7.63 ppm (s, 1H) and 6.01 (br s, 1H), one hydroxymethine proton signal at $δ_H$ 3.86 ppm (dd, *J* = 1.8, 12.1 Hz) and an oxymethylene proton signal at $δ_H$ 4.93 (m, 1H) and 4.85 ppm (m, 1H). The spectrum further showed two methine proton signals at $δ_H$ 3.01 (m, 1H) and 2.62 ppm (m, 1H) and one acetyl proton at $δ_H$ 2.08 ppm (s, 3H).
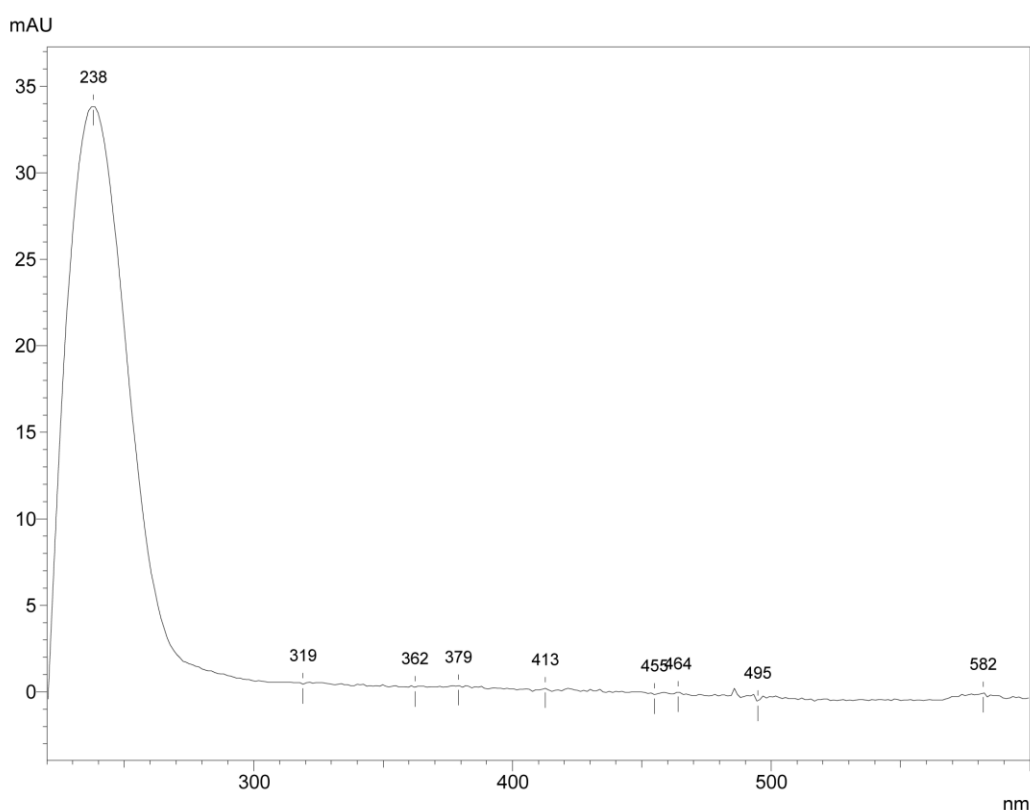
Figure 5.5.1.2 UV-Visible spectrum of HU-8
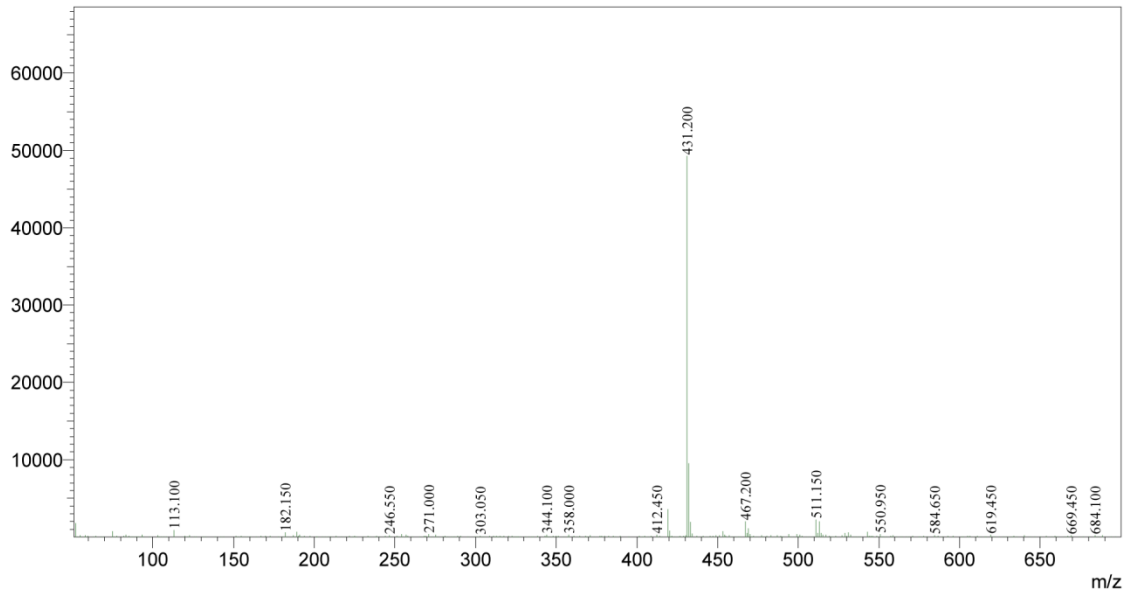
Figure 5.5.1.3 ESI-Mass spectrum of HU-8
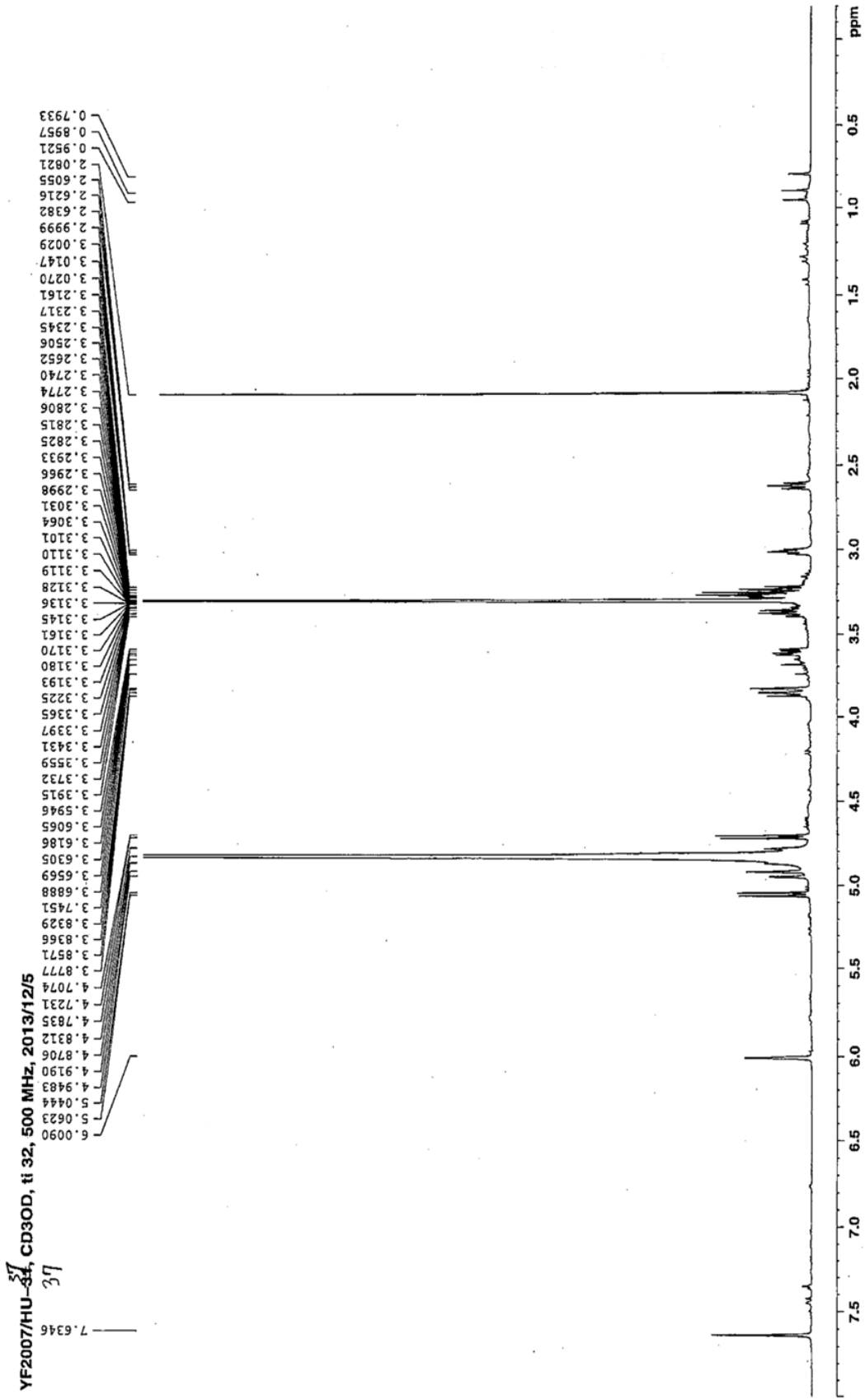
Figure 5.5.1.4 ^{1}H NMR spectrum of HU-8

YF2007/HU-8, CD3OD, ti 32, 500 MHz, 2013/12/5

37

7.6346

6.0090
5.0623
5.0444
4.9483
4.9190
4.8706
4.8312
4.7835
4.7231
4.7074
3.8777
3.8571
3.8366
3.8329
3.7451
3.6888
3.6569
3.6505
3.6386
3.6065
3.5946
3.5915
3.5732
3.5559
3.5431
3.5397
3.5365
3.5225
3.5193
3.5180
3.5170
3.5161
3.5345
3.5336
3.5328
3.5319
3.5110
3.5101
3.5064
3.5031
3.4998
3.4966
3.4933
3.4825
3.4815
3.4806
3.4274
3.4740
3.2652
3.2506
3.2345
3.2317
3.2161
3.2070
3.0147
3.0029
2.9999
2.6382
2.6216
2.6055
2.0821
0.9521
0.8957
0.7933

108

The PMR spectral interpretation culminated with the confirmation of presence of cyclo pentan-[c]-pyran monoterpenoid nucleus substituted with an acetoxy methyl group, a hydroxyl and a glucose moiety. The signals for anomeric proton, oxymethine and oxymethylene protons of glucose were found to be discerned at δ_H 4.72 (d, J = 8.95 Hz, β-anomeric H), 3.23-3.29 (m, 4H), 3.59 ppm (m, 2H) in the PMR spectrum.

The carbon NMR spectrum measured at 125 MHz further corroborated the presence of iridoid nucleus having an O-glycosidic linkage with glucose (δ_C 100.6, 75.0, 78.6, 71.6, 77.9 and 63.0 ppm) and substituted with an acetoxy methyl ester (δ_C 63.8, 170.4 and 20.7 ppm) and a carboxyl (δ_C 172.6 ppm) group (Figure 5.5.1.5). With this information, a thorough literature search was carried out on reported iridoid glycosides. The observed spectral values were found to be in well agreement with the reported values of asperulosidic acid (Table 5.5.1) (Kamiya et al., 2002). Thus **HU-8** was identified as asperulosidic acid (**8**), whose occurrence in *O. umbellata* is newly reported through the present investigation.

Table 5.5.1 Comparison of ^{13}C NMR of HU-8 with reported values

C. position	Reported value (δ_C)	Observed value (δ_C)
1	101.2	101.2
3	155.2	155.2
4	108.4	108.7
5	42.3	42.6
6	75.3	75.4
7	131.8	131.9
8	145.7	146.0
9	46.2	46.3
10	63.7	63.8
11	172.5	170.2
1'	100.5	100.5
2'	74.8	74.8
3'	78.2	78.2
4'	71.4	71.4
5'	77.7	77.9
6'	62.8	62.8
CH$_3$<u>C</u>O	172.4	172.6
<u>C</u>H$_3$CO	20.8	20.7

YF2008/HU-37, in CD3OD, 13C, 125 MHz, ti 800, 2013/12/5

20.73

42.55
46.30
48.49
48.66
48.83
49.00
49.17
49.28
49.34
49.45
49.51
49.63
63.00
63.81
71.60
74.95
75.43
77.91
78.57
100.59
101.24
108.66
131.93
145.96
155.16
170.36
172.55
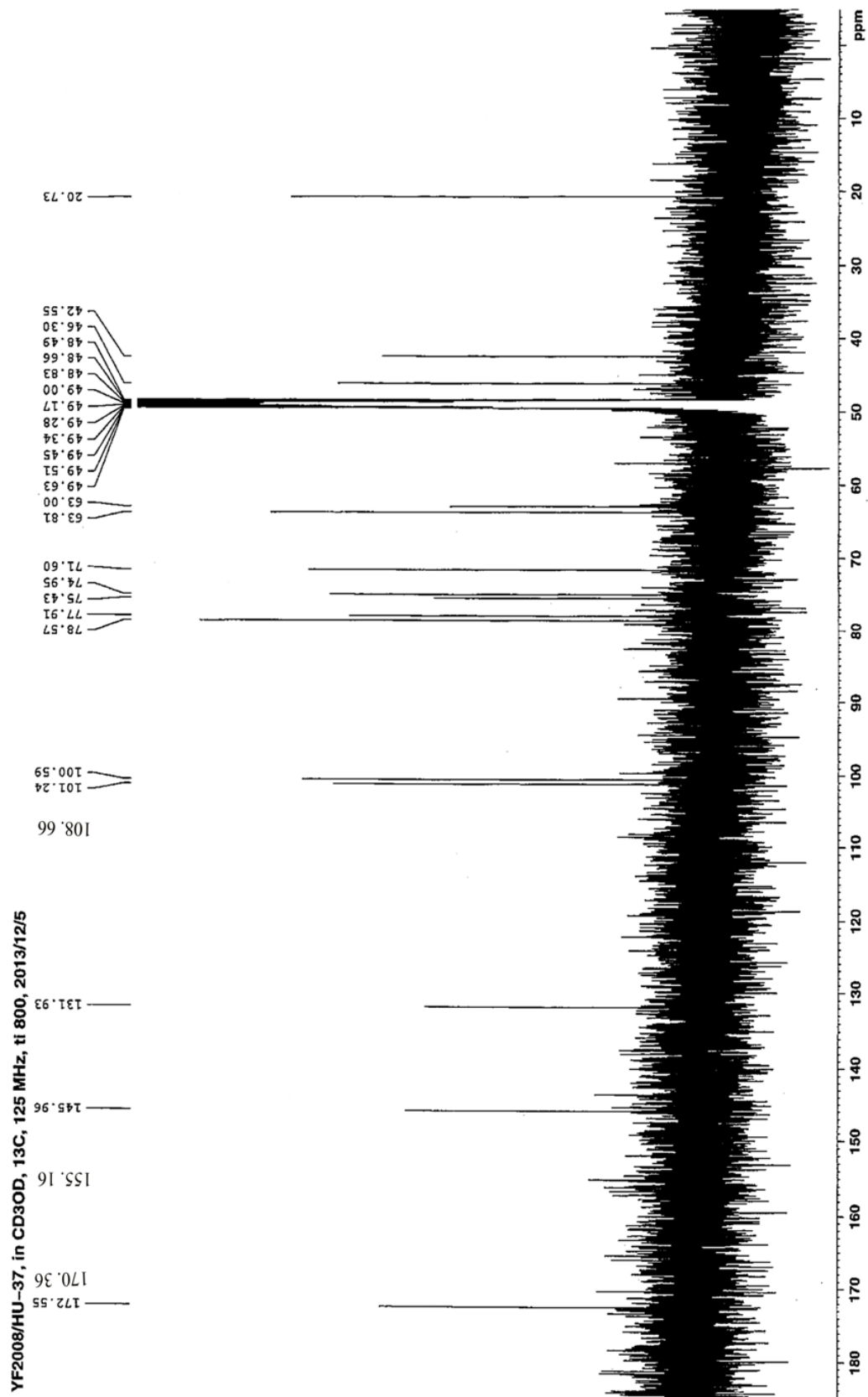
Figure 5.5.1.5 ^{13}C NMR spectrum of HU-8

111
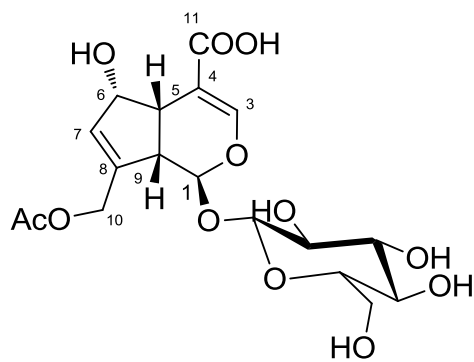
HU-8 (8)

5.5.2 Characterization of HU-9

HU-9 was obtained as white amorphous solid having m.p. of 116-119 ˚C. The compound's homogeneity was analyzed by TLC [solvent system: CHCl$_3$: MeOH, 7:3; (R$_f$ 0.65)] and analytical RP-HPLC (Figure 5.5.2.1) studies. **HU-9** was also identified as an iridoid glycoside based on its positive reaction with anisaldehyde-sulphuric acid reagent and 1% concentrated hydrochloric acid solution of 4-(dimethylamino) benzadehyde. The UV absorption spectrum (Figure 5.5.2.2) measured by dissolving **HU-9** in methanol exhibited characteristic absorption pattern of a α, β-unsaturated carbonyl chromophoric system.
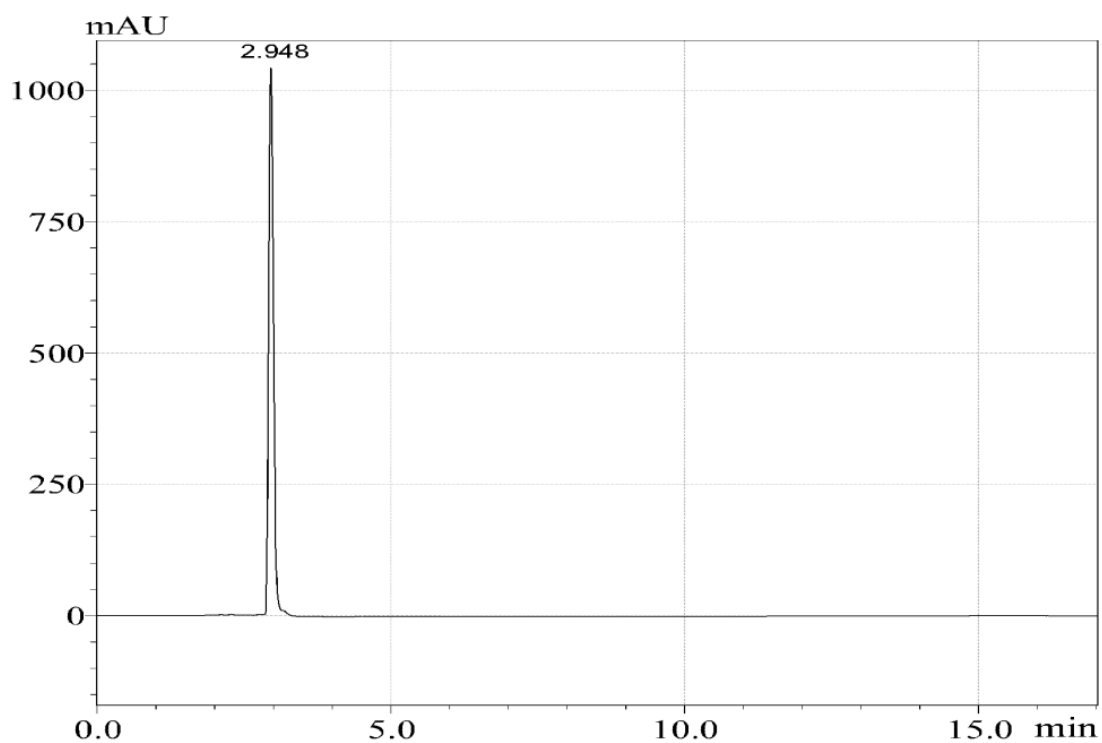
Figure 5.5.2.1 RP-HPLC chromatogram of HU-9 detected at λ_{max} 240 nm
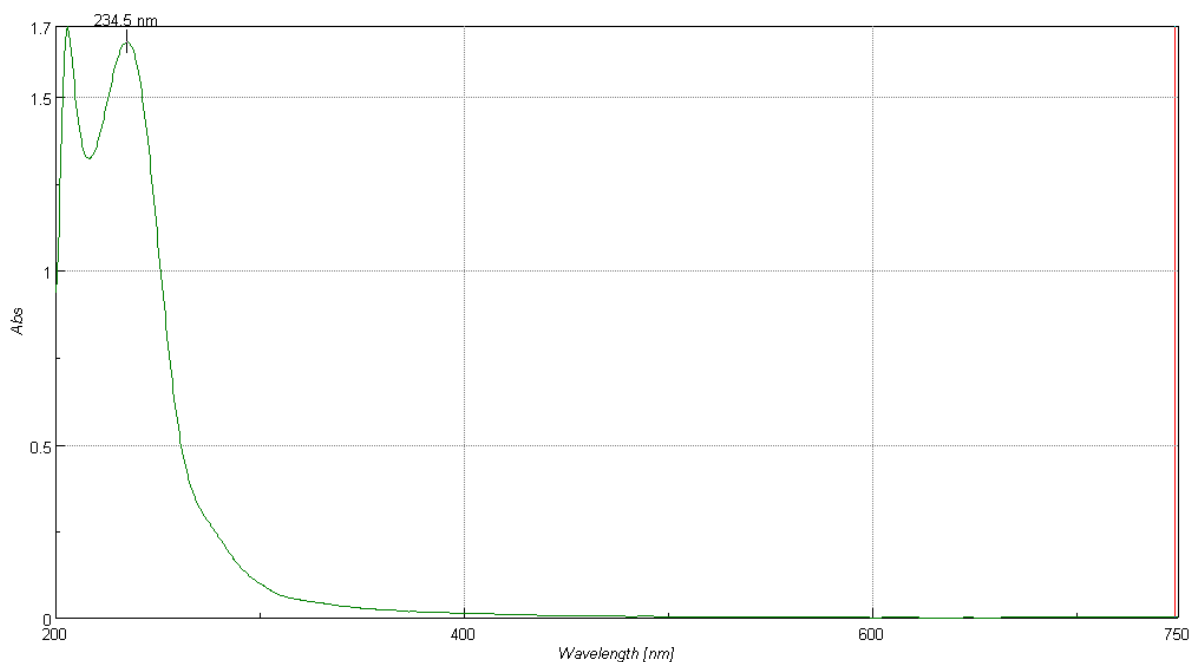
Figure 5.5.2.2 UV-Visible spectrum of HU-9

A careful interpretation of the ^{1}H NMR spectrum of **HU-9** measured at 500 MHz by dissolving in CD$_3$OD, displayed a close resemblance with the NMR spectrum of **HU-8** and expressing characteristic signals for iridoid glucoside (Figure 5.5.2.3). A careful analysis and comparison of ^{1}H NMR spectra of **HU-8** and **HU-9** unveiled the absence of acetyl protons (δ_H 2.08 ppm). Also, the difference in the chemical shift value of H-3 (δ_H 7.28 ppm), H-5 (δ_H 3.15-3.20 ppm), H-6 (δ_H 5.56 ppm) and H-7 (δ_H 5.94 ppm) protons of **HU-8** and **HU-9** revealed the structural difference between them. Similar difference was found to be reflected on comparing the ^{13}C NMR spectra of **HU-8** and **HU-9**. The CMR spectrum of **HU-9** was found to show one keto carbonyl (δ_C 171.5 ppm) signal, upshielded C-3 (δ_C 148.9 ppm), C-4 (δ_C 105.1 ppm), C-5 (δ_C 36.1 ppm) and C-10 (δ_C 58.7 ppm) signals. However, a deshielding effect was observed on C-6 (δ_C 85.3 ppm) and C-7 (δ_C 124.3 ppm) carbons (Figure 5.5.2.4).
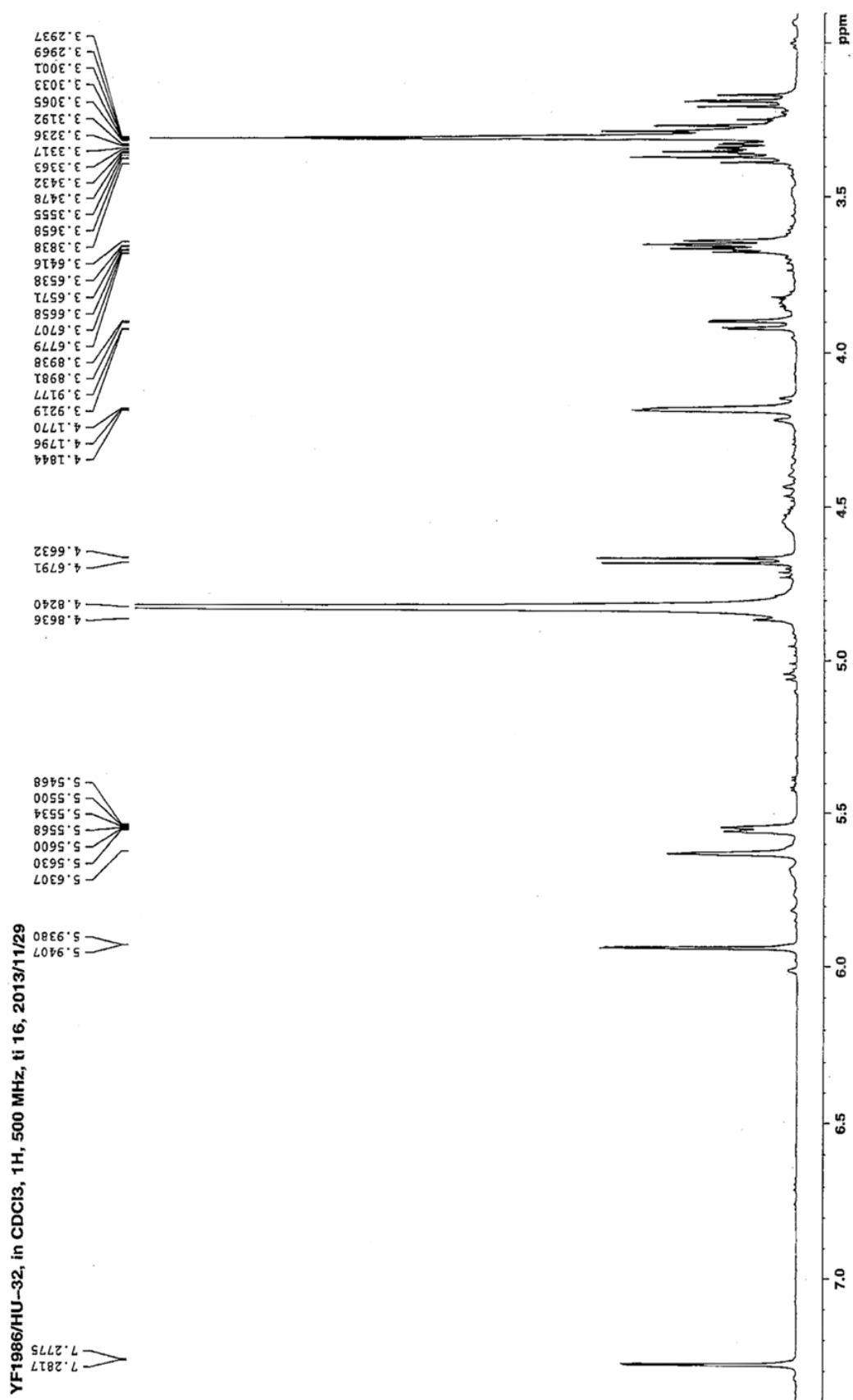
Figure 5.5.2.3 ^{1}H NMR spectrum of HU-9

YF1986/HU–32, in CDCl3, 1H, 500 MHz, ti 16, 2013/11/29

3.2937
3.2969
3.3001
3.3033
3.3065
3.3192
3.3236
3.3317
3.3363
3.3432
3.3478
3.3555
3.3658
3.6383
3.6416
3.6538
3.6571
3.6658
3.6707
3.6779
3.8938
3.8981
3.9177
3.9219
4.1770
4.1796
4.1844

4.6632
4.6791

4.8240
4.8636

5.5468
5.5500
5.5534
5.5568
5.5600
5.5630
5.6307

5.9380
5.9407

7.2775
7.2817

115

YF1988/HU-32, in CD3OD, 13C, 125 MHz, ti 350, 2013/12/2

36.06
43.60
47.09
47.26
47.43
47.60
47.77
47.94
48.06
48.11
58.69
61.39
70.19
73.27
76.50
77.02
85.25
91.92
98.51
105.06
124.32
148.44
148.85
171.46

ppm

Figure 5.5.2.4 ^{13}C NMR spectrum of HU-9

The ESI-MS analysis of **HU-9** displayed [M-H]⁻ ion peak at *m/z* 371.20 (Figure 5.5.2.5), showing molecular weight as 372. The difference in the molecular weight between H-9 and **HU-8** was identified as 60 amu. This 60 amu could be accommodated with the absence of acetyl group (43) in **HU-9** as proved from the NMR data. The difference in the δ_C values of C-3, C-4, C-5 and C-6 between **HU-9** and **HU-8**, absence of COOH signal in **HU-9** and a deficiency of 17 amu in addition to 43 amu of acetyl group, corroborated **HU-9** to be a cyclo-condensed and deacetylated product of **HU-8**, which is highly possible in the biosynthesis of terpenoidal lactone. Table 5.5.2 presents the assignment of ¹H NMR data with the predicted structure.

Table 5.5.2 ¹H NMR data of HU-9

S. No.	δ_H (ppm)	Splitting pattern	Coupling constant (*J*, Hz)	Position
1	7.28	d	2.1	H-3
2	5.94	d	1.4	H-7
3	5.63	s	-	H-1
4	5.56	m	-	H-6
5	4.67	d	7.95	H-1'
6	4.18	t	2.4	H-10
7	3.89-3.92	dd	2.1, 2.2	C-6'b
8	3.64-3.67	m	-	C-6'a
9	3.31-3.38	m	-	H-2'-5'
10	3.15-3.20	m	-	H-9 and H-5
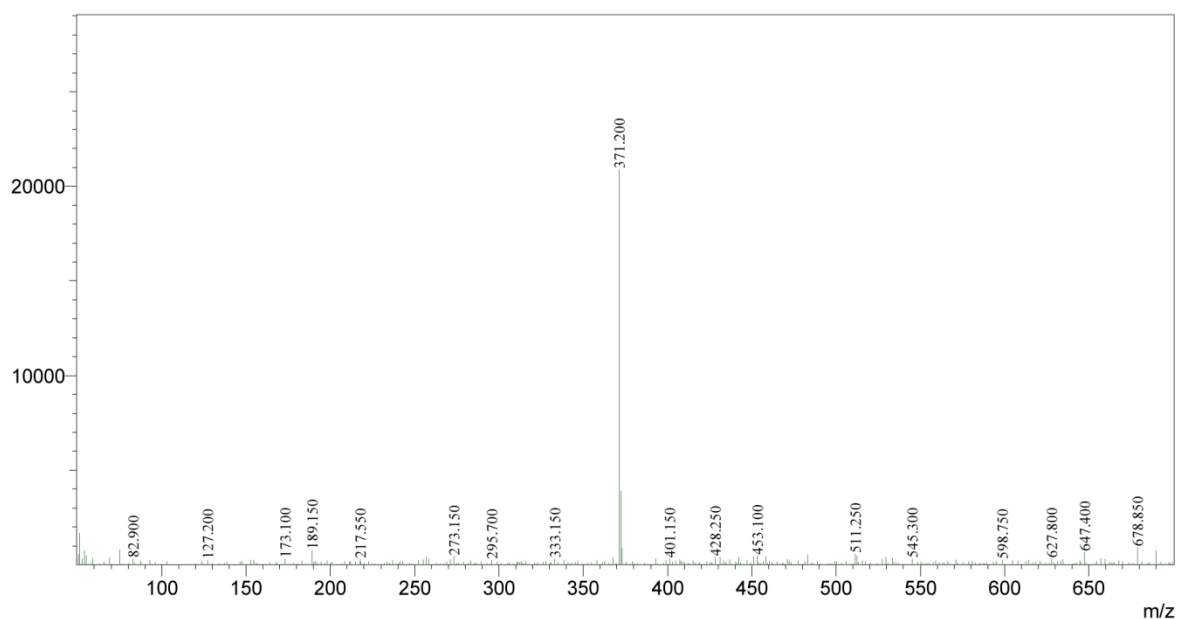
Figure 5.5.2.5 ESI-Mass spectrum of HU-9

On the basis of the above presented data and discussion, the structure of **HU-9** was determined as **9**. Further, a search of literature was carried out on reported deacetylated products of asperulosidic acid and the experimental data was found to be matching with deacetyl asperuloside (**9**) and thus **HU-9** was characterized. This is the first report of isolation of **HU-9** from *O. umbellata.*
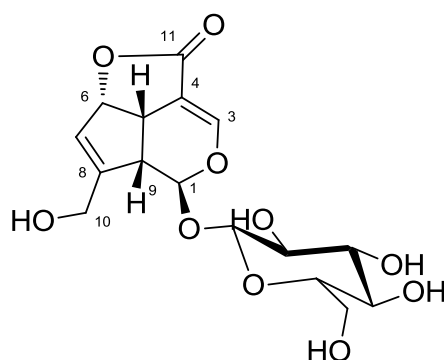

HU-9 (9)

5.5.3 Characterization of HU-10

HU-10 was obtained as white amorphous solid having m.p. of 130 - 133 ˚C. The homogeneity of the compound was analyzed through TLC [solvent system: CHCl$_3$: MeOH, 7:3; (R$_f$ 0.76)] and RP-HPLC (Figure 5.5.3.1).
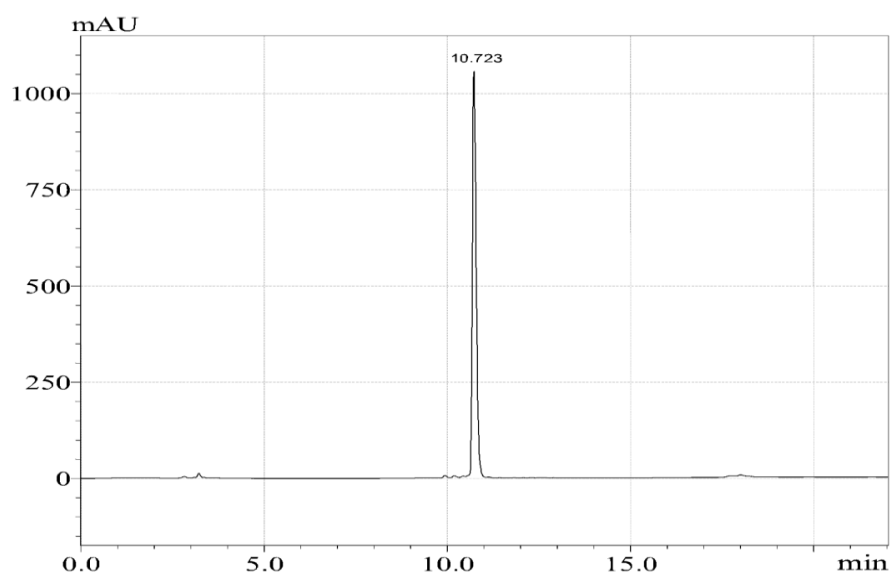
Figure 5.5.3.1 RP-HPLC chromatogram of HU-10 detected at λ_{max} 240 nm

Iridoidal glycoside nature of **HU-10** was observed through the positive reactions with anisaldehyde-sulphuric acid reagent and 1% concentrated hydrochloric acid solution of para dimethylamino benzadehyde. The UV absorption spectrum of **HU-10** (Figure 5.5.3.2) exhibited strong absorption band at λ_{max} 240 nm, characteristic of α, β-unsaturated carbonyl chromophoric system indicating the presence of carbonyl substitution at 4th position.
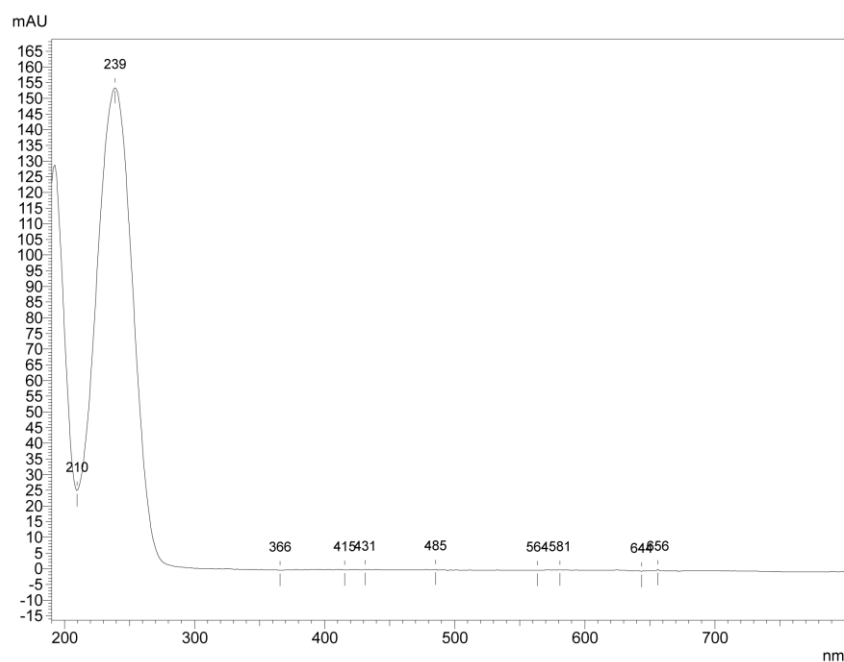
Figure 5.5.3.2 UV-Visible spectrum of HU-10

The molecular weight was identified as 404, based on the ESI-mass spectrometrically derived [M-H]$^-$ peak at 403.200 and [M+Na]$^+$ peak at 427.10 under negative and positive mode, respectively (Figure 5.5.3.3a and 5.5.3.3b).

The 125 MHz ^{13}C NMR spectrum displayed eighteen signals constituting a carbonyl carbon (δ_C 170.3 ppm), two olefinic cabons (δ_C 153.9 and 130.1 ppm), two quarternary carbons (δ_C 147.5 and 110.8 ppm), one dioxymethine carbon (δ_C 98.3 ppm), one hydroxymethine carbon (δ_C 82.3 ppm), one hydroxymethylene carbon (δ_C 61.0 ppm), two methine carbons (δ_C 47.1 and 45.6 ppm) and one ester methyl carbon (δ_C 52.1 ppm) along with an anomeric carbon (δ_C 100.3 ppm), oxymethine (δ_C 78.4, 77.9, 74.8 and 71.5 ppm) and oxymethylene (δ_C 62.7 ppm) signals (Figure 5.5.3.4). The discerned signals in the ^{13}C NMR spectrum showed a typical iridoidal glucoside moiety showing close similarity with the previously isolated iridoid glucoside, **HU-8** (**8**).

120
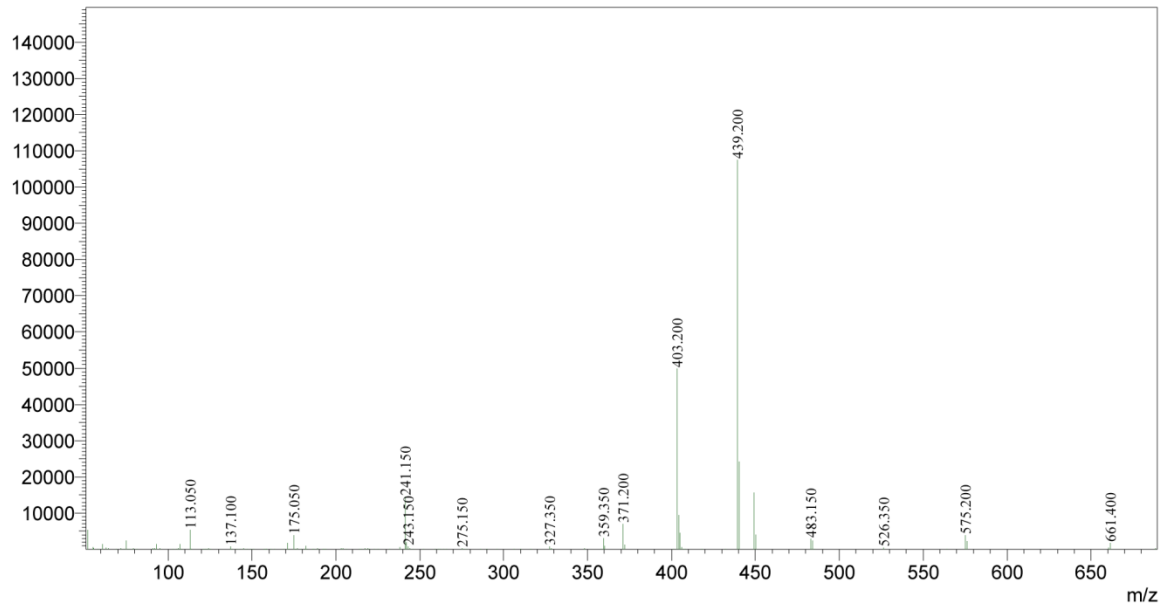
Figure 5.5.3.3a ESI-Mass spectrum of HU-10 in negative polarity

Figure 5.5.3.3b ESI-Mass spectrum of HU-10 in positive polarity

121
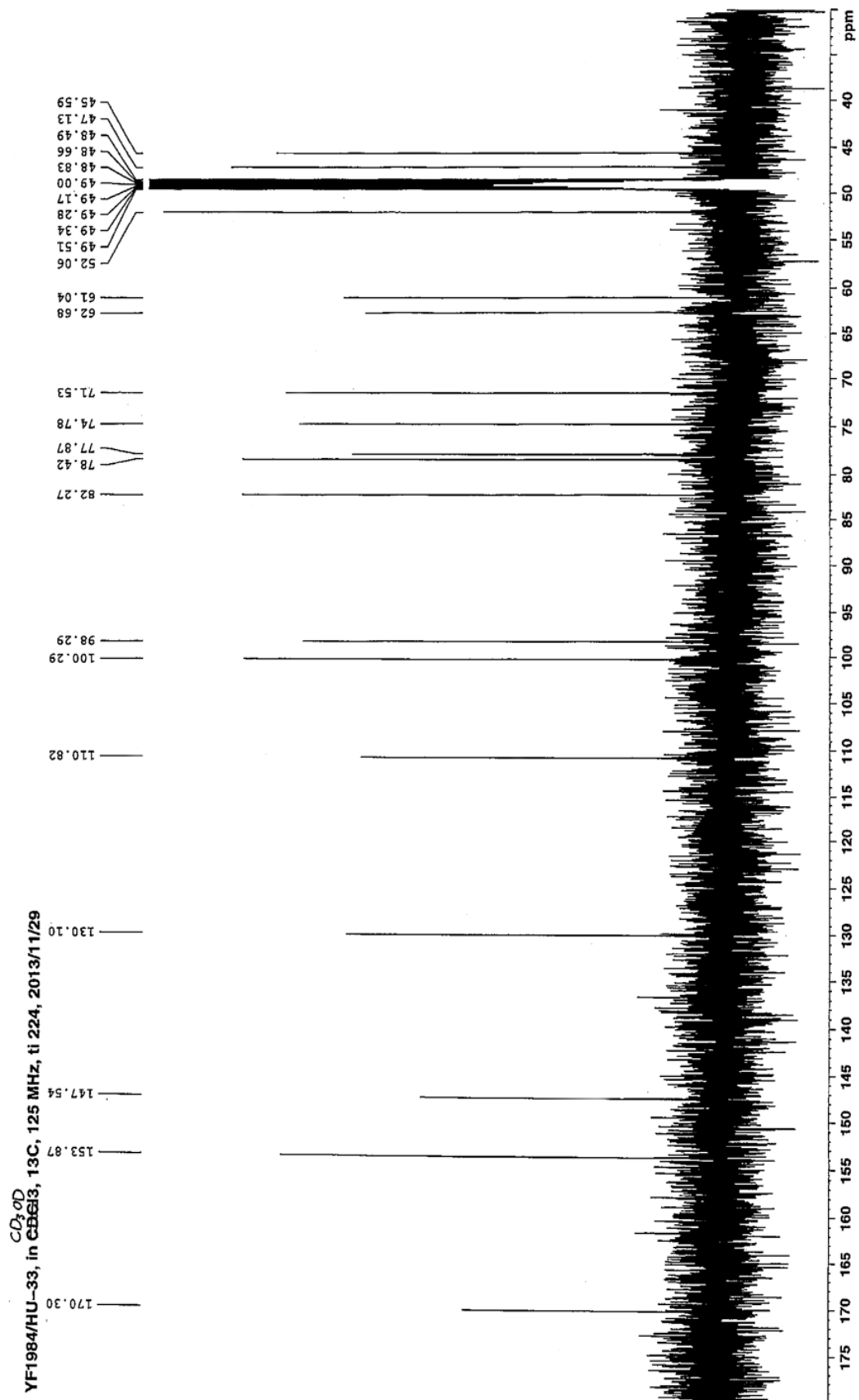
Figure 5.5.3.4 ^{13}C NMR spectrum of HU-10

YF1984/HU-33, in CDCl3, 13C, 125 MHz, ti 224, 2013/11/29

CD₃OD

45.59
47.13
48.49
48.66
48.83
49.00
49.17
49.28
49.34
49.51
52.06

61.04
62.68

71.53

74.78

77.87
78.42

82.27

98.29
100.29

110.82

130.10

147.54

153.87

170.30

On careful comparison of CMR spectra of **HU-8** and **HU-10**, absence of acetyl group and carboxyl group was identified. However, signals for ester methyl and alcoholic carbon were found to be present in **HU-10**. This assumption suggested, **HU-10** to be a deacetylated and methyl esterified product of **HU-8**. Additionally, the difference in the 28 amu (C=O) between **HU-8** (MW 432) and **HU-10** (MW 404) confirmed the predicted structure of **10a**.
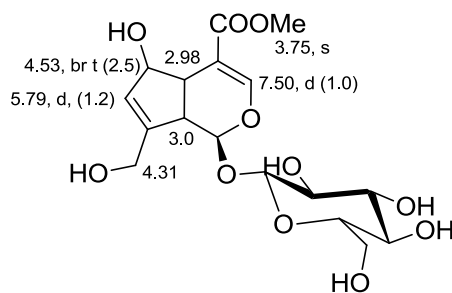
10a

The 500 MHz ^{1}H NMR spectrum (Figure 5.5.3.5) of **HU-10** displayed similar chemical shift values as that of **HU-8** with additional signal for –COOCH$_3$ (δ_H 3.75, s). The observed δ_H values with their splitting pattern and *J* values are depicted around the structure 10a and presented in Table 5.5.3. The exact point of attachment of -COOMe, -OH, -CH$_2$OH and glucose at C-4, C-6, C-8 and C-1 respectively was ascertained from 2D correlation spectroscopy, which unambiguously confirmed the structure of **HU-10** as **10a**. The Key ^{1}H-^{1}H correlations observed in the ^{1}H-^{1}H COSY (Figure 5.5.3.6) spectral analysis is presented in Figure 5.5.3.7. An identical compound was found in the literature, named as feretoside, previously isolated from *O. diffusa*. Comparison of the spectral data with the earlier reports revealed the configurations shown in **10**. To the best of investigator's knowledge the isolation of feretoside (**10**) is reported for the first time from *O. umbellata*.

Table 5.5.3 ^{1}H NMR data of HU-10

S. No.	δ_H (ppm)	Splitting pattern	Coupling constant (J, Hz)	Position
1	7.50	d	1.0	H-3
2	5.79	d	1.2	H-7
3	5.18	d	6.3	H-1
4	4.65	d	2.2	H-1'
5	4.53	br t	2.5, 4.4	H-6
6	4.31	d	15.3	H-10b
7	4.16	d	15.3	H-10a
8	3.84	dd	-	H-6'b
9	3.61	dd	-	H-6'a
10	3.75	s	-	-COOC<u>H</u>$_3$
11	3.18-3.36	m	-	H-2'-H5'
12	3.00	dd	6.5	H-9
13	2.98	dd	7.7, 4.6	H-5
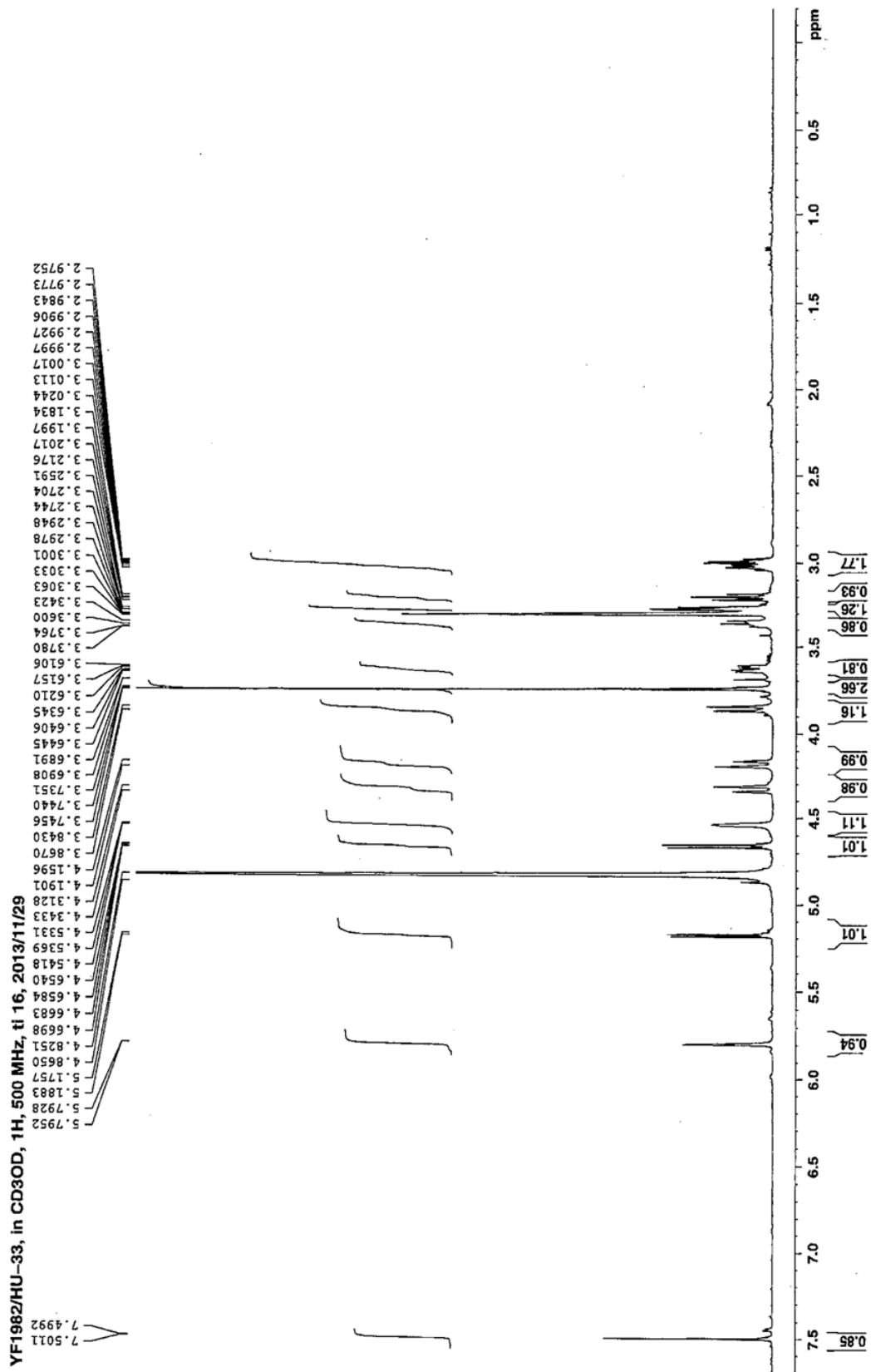
Figure 5.5.3.5 ¹H NMR spectrum of HU-10
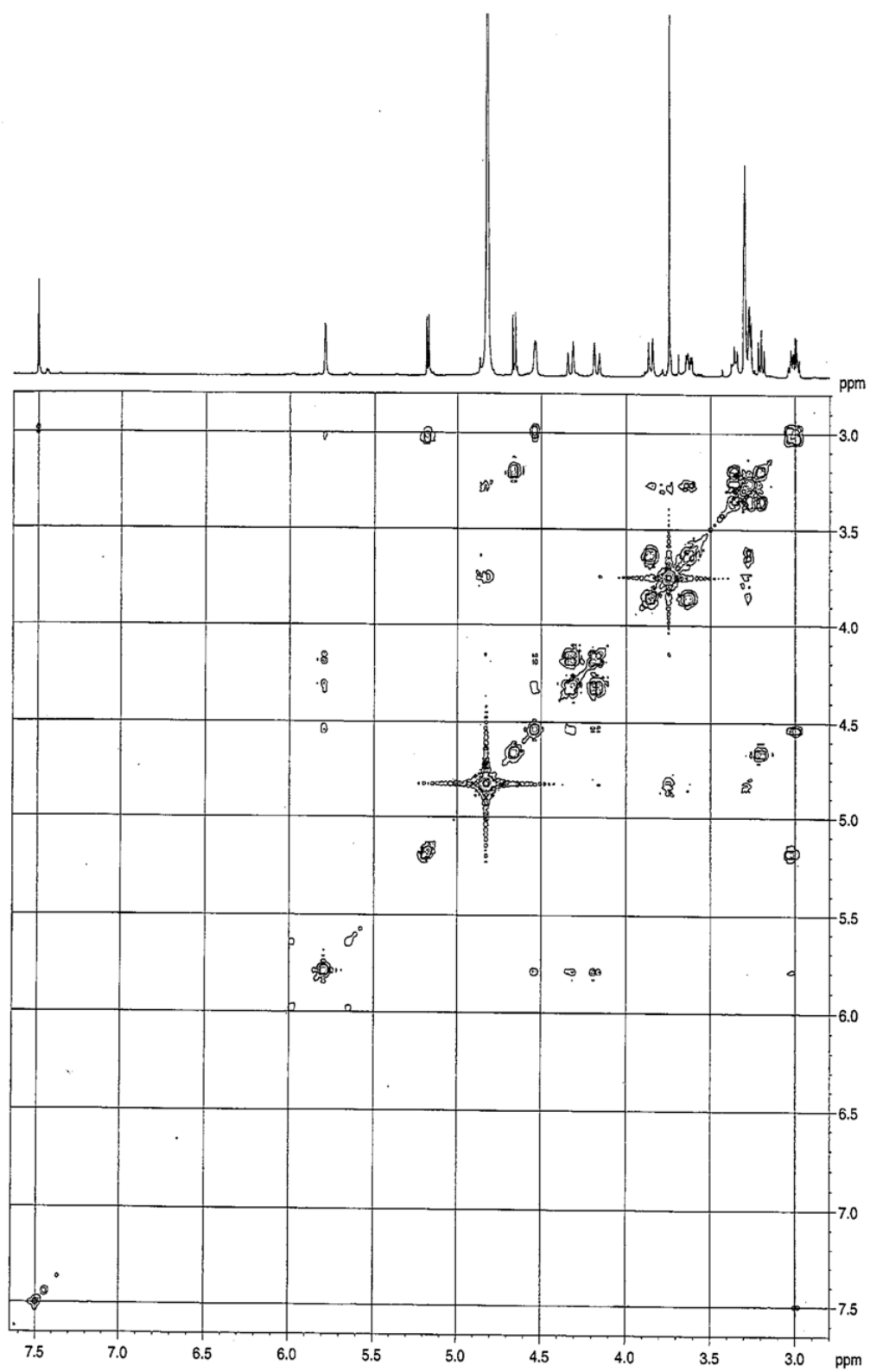
Figure 5.5.3.6 ^{1}H-^{1}H COSY spectrum of HU-10
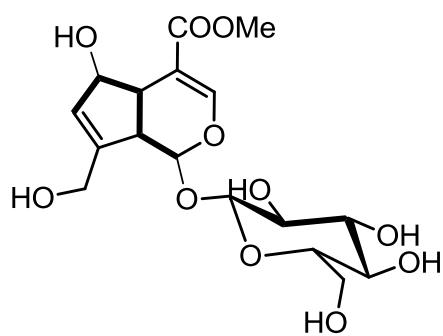
Figure 5.5.3.7 Key ^{1}H-^{1}H correlations for **HU-10** (▬)
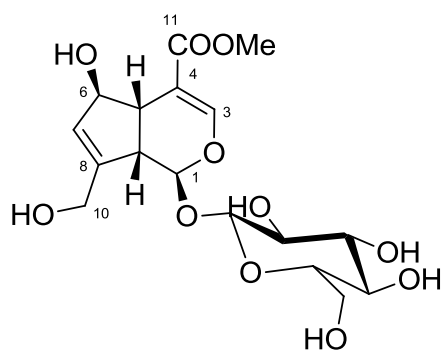
HU-10 (**10**)

5.5.4 Characterization of HU-11

HU-11 isolated as white amorphous solid was found to show m.p. of 142-144 ˚C. The singularity of the compound was verified through TLC studies [solvent system: CHCl$_3$: MeOH, 8:2; (R$_f$ 0.20)] and RP-HPLC (Figure 5.5.4.1) analysis. **HU-11** was answering positive for terpenoidal glycoside test reagents like anisaldehyde-sulphuric acid reagent and 1% concentrated hydrochloric acid solution of para dimethylamino benzadehyde. The UV spectrophotometric analysis of **HU-11** exhibited strong absorption band at λ_{max} 240 nm, characteristic of α, β-unsaturated carbonyl chromophoric system indicating the presence of carbonyl substitution at 4th position of iridoid glycoside (Figure 5.5.4.2). The molecular weight was identified as 390 based on the ESI-mass spectrometrically derived [M-H]$^-$ peak at 389.20 under negative mode analysis (Figure 5.5.4.3).
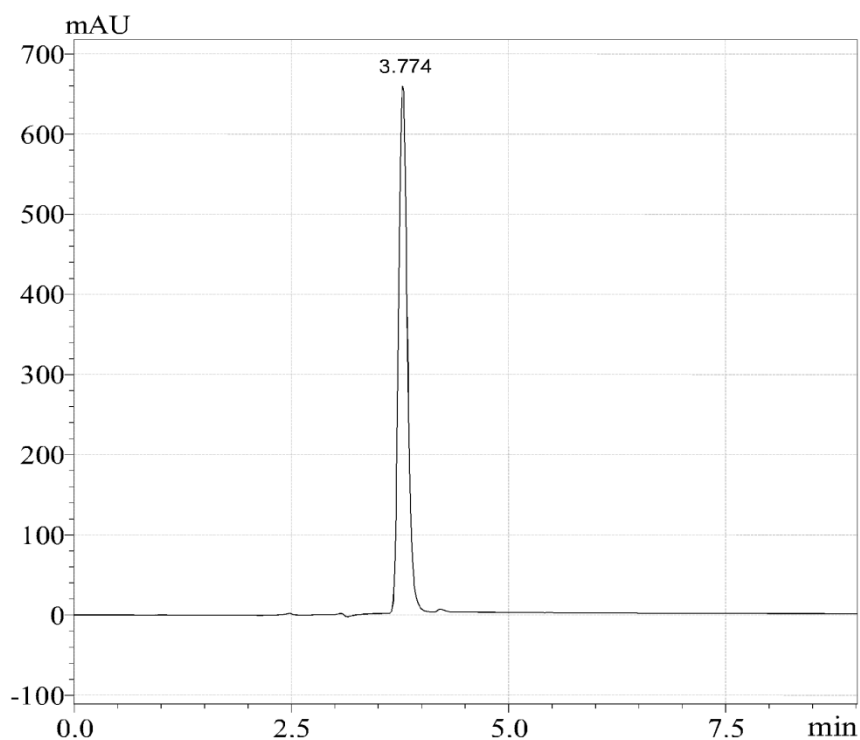
Figure 5.5.4.1 RP-HPLC chromatogram of HU-11 detected at λ_{max} 240 nm

128
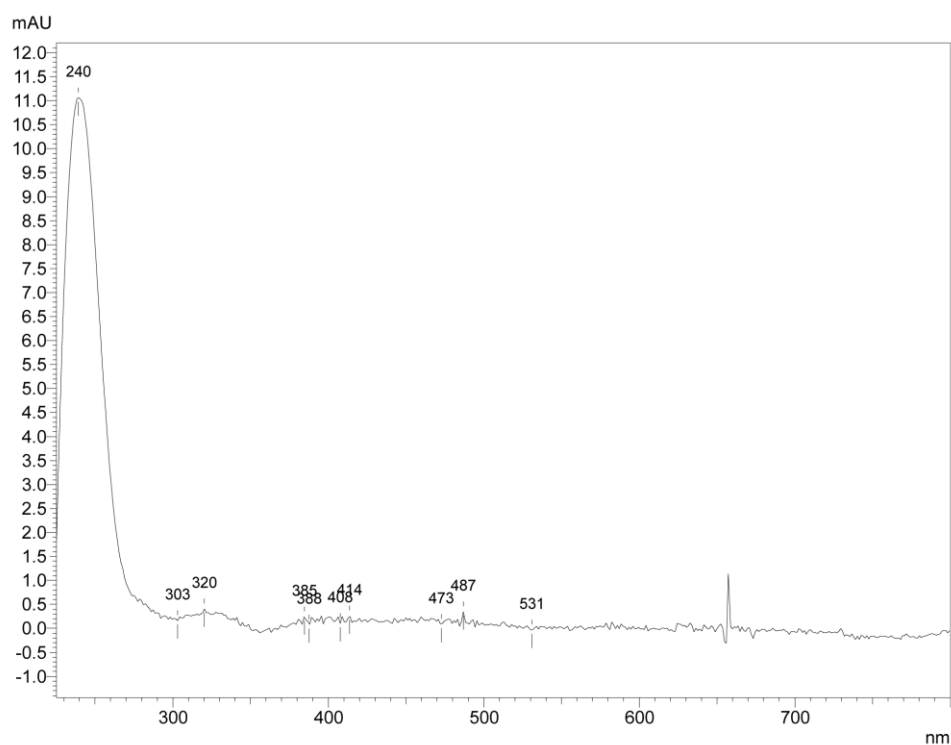
Figure 5.5.4.2 UV-Visible spectrum of HU-11
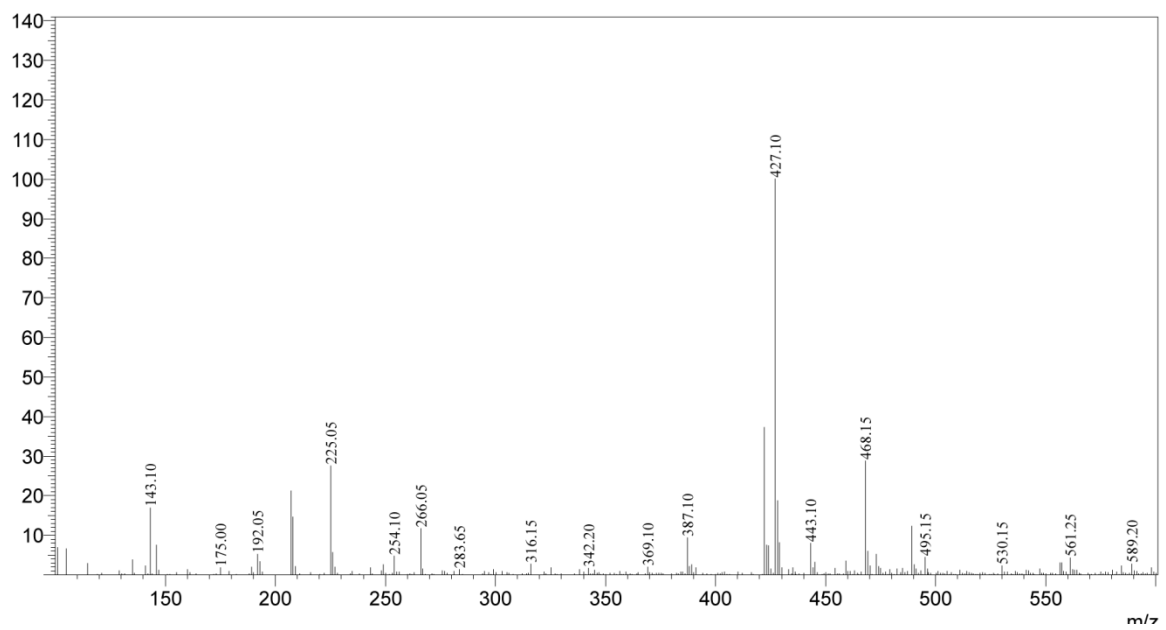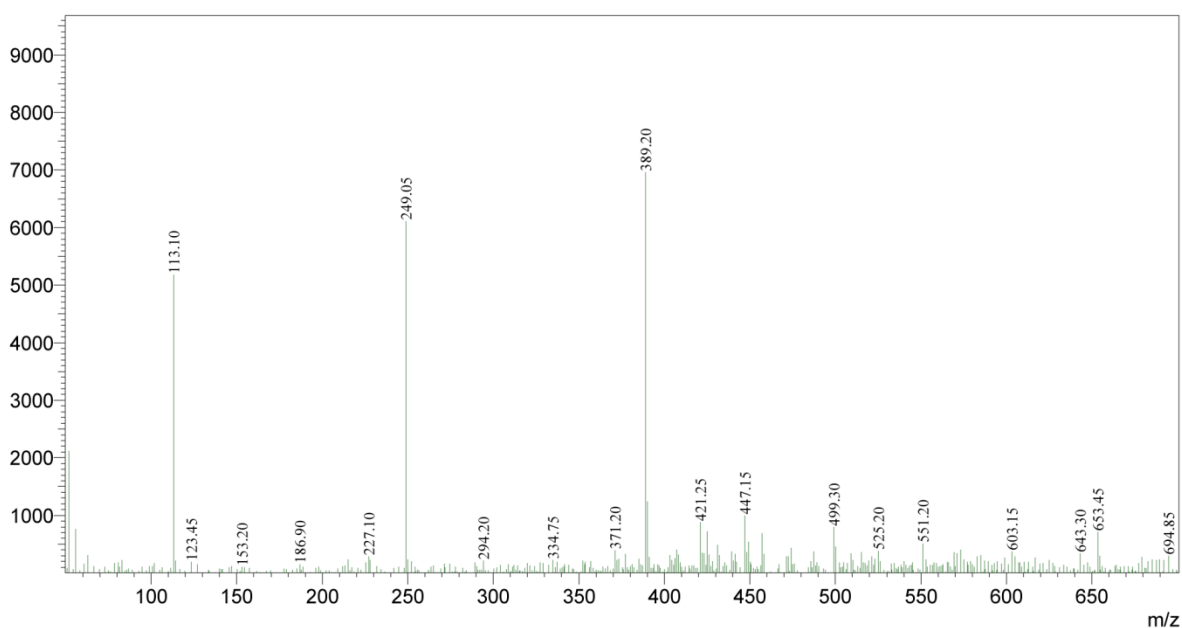

Figure 5.5.4.3 ESI-Mass spectrum of HU-11

The 500 MHz ^{1}H NMR spectrum (Figure 5.5.4.4) of **HU-11**, clearly presented signals which were characteristic of irodoid glucoside nucleus. The downfield region of the spectrum

129

was very much identical to that of previously discussed compound **HU-10** i.e. feretoside (**10**). The comparative PMR data of **HU-10** and **HU-11** is presented in Table 5.5.4. The only major difference in the NMR signals discerned in the spectra of **HU-10** and **HU-11** was the absence of ester methyl signal in **HU-11**. This assumption further gained support from the mass spectral data, which showed a difference of 14 amu confirming the presence of –COOH in place of –COOMe. Thus, **HU-11** should possibly be the hydrolysed product of (**10**). Natural occurrence of such molecule has been reported as scandoside, which was previously isolated from *O. diffusa*. Finally, the structure of **HU-11** was confirmed as **11**, based on the comparison of spectral data with those of reported data of scandoside (Kamiya et al., 2002). The occurrence of **HU-11** in *O. umbellata* is reported for the first time through this investigation.

Table 5.5.4 Comparison of ^{1}H NMR data of HU-10 and HU-11

S. No.	HU-10 δ_H (ppm), (J Hz)	HU-11 δ_H (ppm), (J Hz)	Position
1	7.50, d (1.0)	7.44, s	H-3
2	5.79, d (1.2)	5.82, s	H-7
3	5.18, d, (6.3)	5.0, d (7.7)	H-1
4	4.65, d (2.2)	4.69, d (7.9)	H-1'
5	4.53, br t (2.5)	4.56, br s	H-6
6	4.31, d (15.3)	4.34, d (15.5)	H-10b
7	4.16, d (15.3)	4.16, d (15.2)	H-10a
8	3.84, dd	3.83, m	H-6'b
9	3.61, dd	3.61, m	H-6'a
10	3.75, s	-	-COOC$\underline{H}_3$
11	3.18-3.36, m	3.19-3.39, m	H-2'-H5'
12	3.00, dd (6.5)	2.92, m	H-9
13	2.98, dd (7.7, 4.6)	2.88, m	H-5
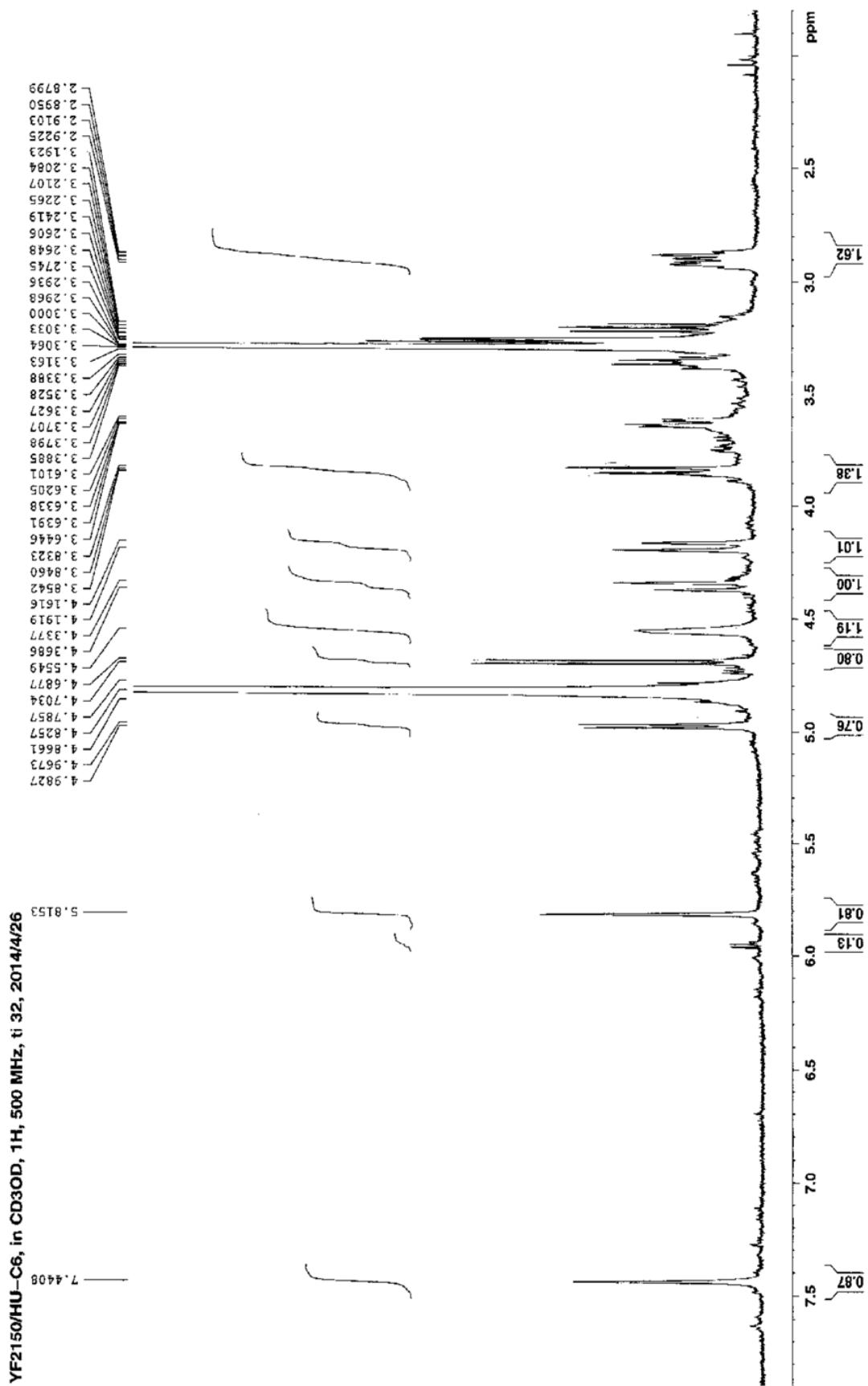
Figure 5.5.4.4 ^{1}H NMR spectrum of HU-11

YF2150/HU–C6, in CD3OD, 1H, 500 MHz, ti 32, 2014/4/26

2.8799
2.8950
2.9103
2.9225
3.1923
3.2084
3.2107
3.2265
3.2419
3.2606
3.2648
3.2745
3.2936
3.2968
3.3000
3.3033
3.3064
3.3163
3.3388
3.3528
3.3627
3.3707
3.3798
3.3885
3.6101
3.6205
3.6338
3.6391
3.6446
3.8323
3.8460
3.8542
4.1616
4.1919
4.3377
4.3686
4.5549
4.6877
4.7034
4.7857
4.8257
4.8661
4.9673
4.9827

5.8153

7.4408

131
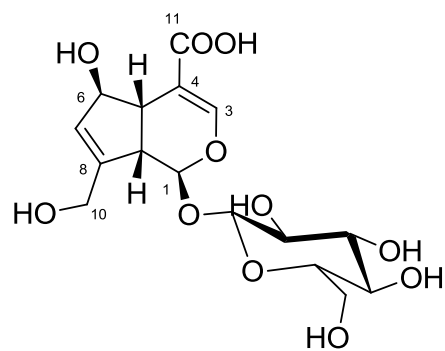
HU-11 (11)

5.5.5 Characterization of HU-12

HU-12 was isolated as amorphous solid showing m.p. of 131 - 134 ˚C. The purity of the sample was assessed through RP-HPLC analysis using gradient elution of MeOH in H_2O. **HU-12**, eluated at R_t 2.97 min detected to be single peak under PDA analysis (Figure 5.5.5.1). The UV spectroscopic analysis revealed **HU-12** to be an iridoid glycoside having α, β-unsaturated carbonyl chromophore displaying strong absorption maxima at λ_{max} 235.5 nm (Figure 5.5.5.2). **HU-12** showed [M-H]⁻ peak at *m/z* value 403.15 (Figure 5.5.5.3a) and [M+Na]⁺ at *m/z* 427.19 (Figure 5.5.5.3b) under negative and positive mode of ESI-mass spectroscopic analysis respectively. Both the ESI-mass spectrum was found to be overlapping with that of previously discussed compound **HU-10** (**10**).
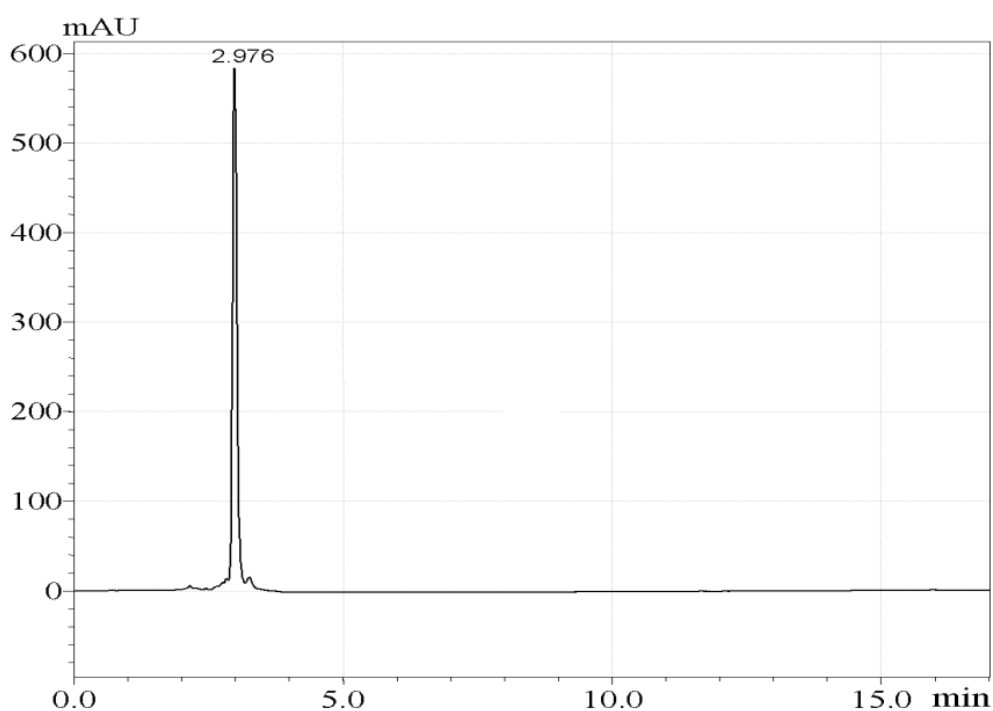
Figure 5.5.5.1 RP-HPLC chromatogram of HU-12 detected at λ_{max} 240 nm

133
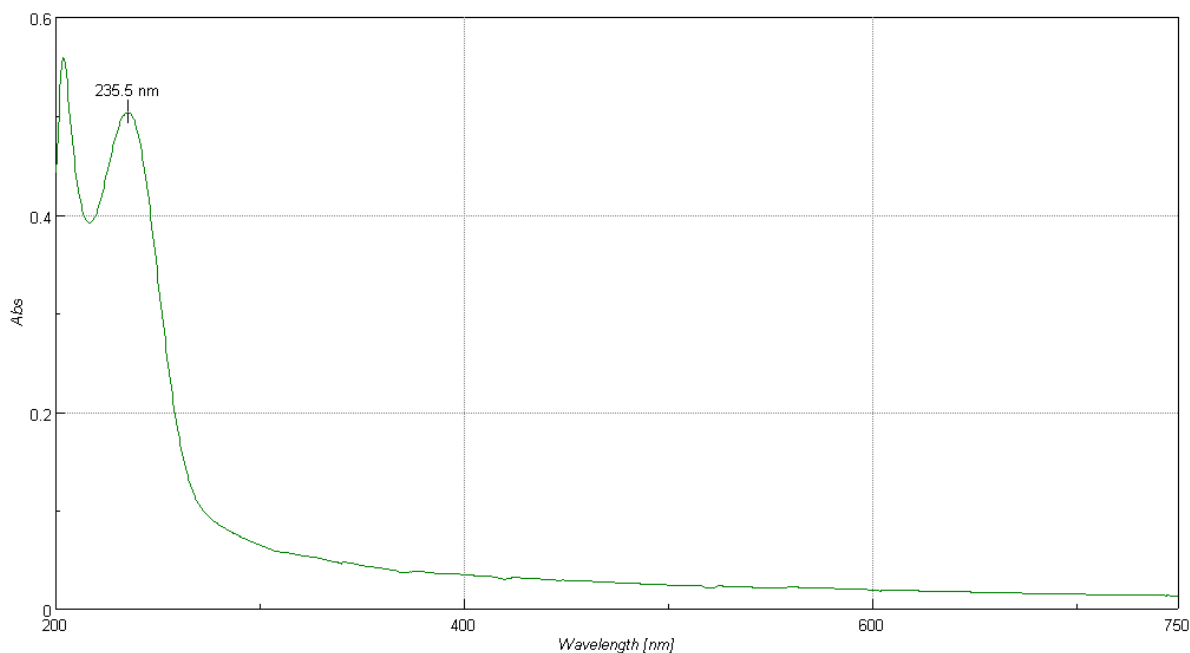
Figure 5.5.5.2 UV-Visible spectrum of HU-12
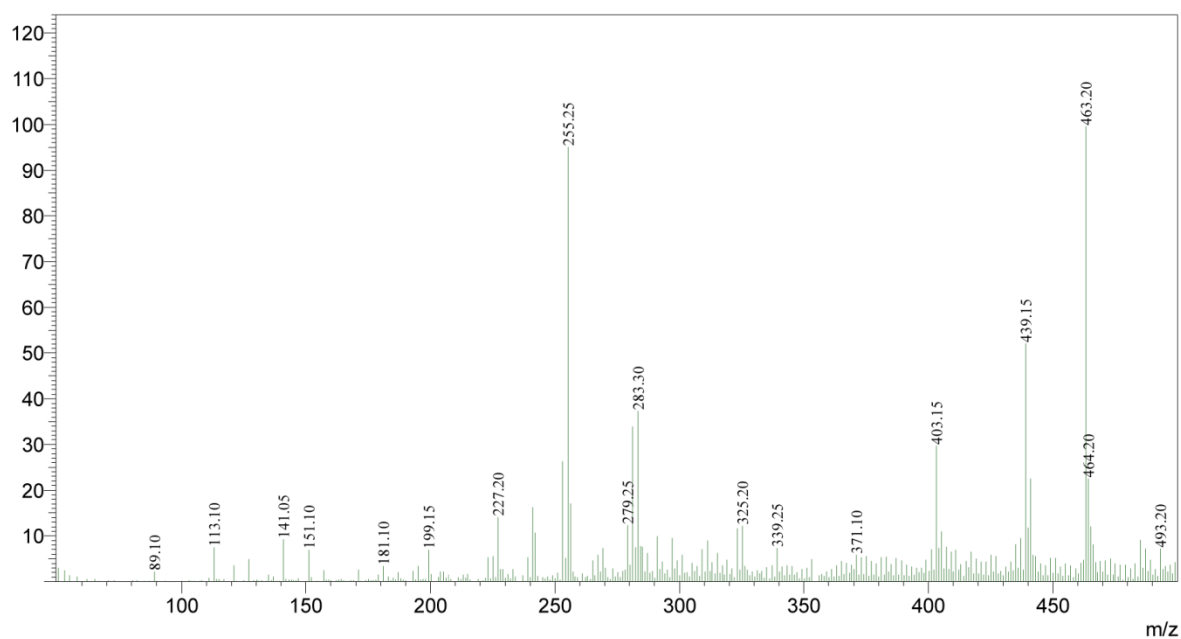
Figure 5.5.5.3a ESI-Mass spectrum of HU-12 in negative polarity

The proton NMR of **HU-12** was measured at 500 MHz by dissolving the sample in CD$_3$OD and the signals existed in the spectrum were analyzed (Figure 5.5.5.4). The total number of signals discerned in the PMR spectrum of **HU-12** was found to be same as that of

HU-10 and surprisingly the chemical shift values were also found to be similar with minor difference. The very close resemblance of ^{1}H NMR spectrum of **HU-12** and **HU-10** ruled out the possibility of their regioisomeric relationship.
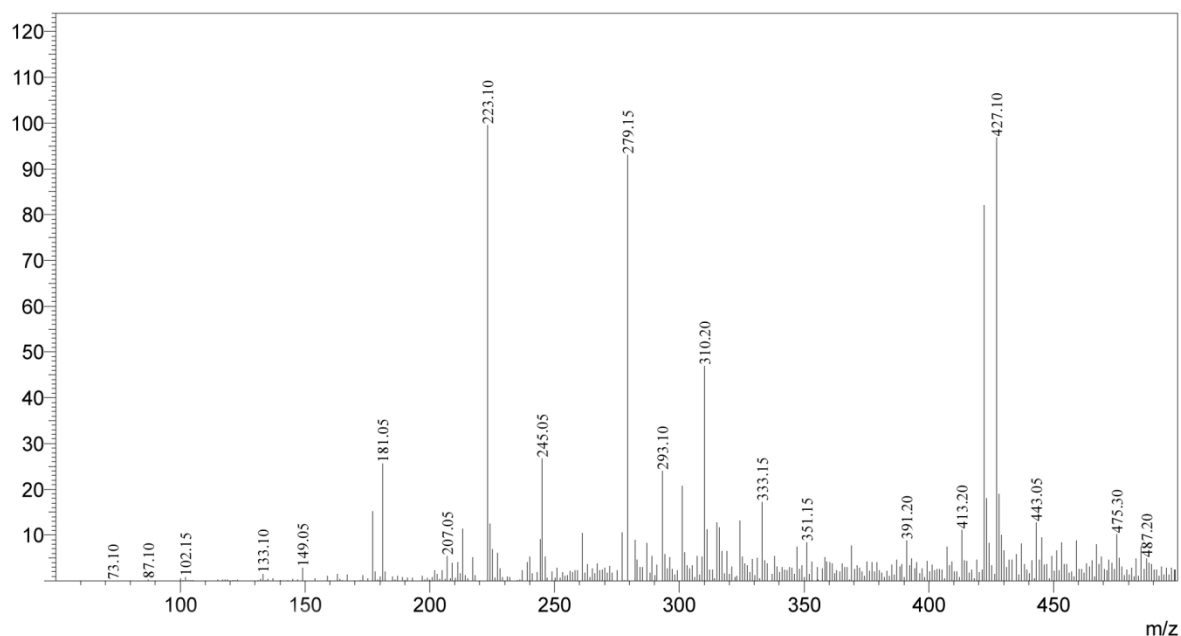
Figure 5.5.5.3b ESI-Mass spectrum of HU-12 in positive polarity

However, they must be stereoisomers, which were clarified from the very keen interpretation of δ_H value, splitting pattern and coupling constants of protons of four chiral centers. The variation in the δ_H value of H-5, H-6, and H-7 suggested the stereochemical difference in the attachment of hydroxyl group at C-6. Also, search for literature revealed the identity of **HU-12** with that of deacetyl asperulosidic acid methyl ester (Kamiya et al., 2002), also called as 6-α-hydroxy geniposide (**12**). This is the first report of isolation of **HU-12** from *O. umbellata.*

YF2394–Shigemi/HU–58, in CD3OD, 1H, 500 MHz, ri 32, 2014/9/3

1.2798
1.3001
1.3138
1.3175
1.8088
2.5596
3.0140
3.2159
3.2287
3.2318
3.3345
3.3482
3.2501
3.2609
3.2637
3.2772
3.2911
3.2936
3.2967
3.3000
3.3033
3.3066
3.3140
3.3231
3.3628
3.3807
3.5197
3.5432
3.5608
3.5704
3.5962
3.6080
3.6205
3.6328
3.6565
3.7261
3.7352
3.7458
3.7826
3.8323
3.8531
4.1871
4.2185
4.4301
4.4329
4.4613
4.4641
4.7018
4.7176
4.7863
4.8256
4.8650
5.0441
5.0620
6.0123
7.6444
7.6466

Figure 5.5.5.4 ^{1}H NMR spectrum of HU-12

136

HU-12 (12)

5.6 Cytotoxic studies of HUM, HUM-E and HUM-B

The mother extract (**HUM**) and its fractions **HUM-E** and **HUM-B** were subjected for cytotoxic effect against a panel of cell lines, lung cancer (A549), breast cancer (MDA-MB-231) and colorectal cancer (HT-29) using MTT method. **HUM-E** showed dose dependent and more pronounced effect against HT-29, A549 and MDA-MB-231 with IC_{50} values of 25.7, 67.7 and 69.3 μg/mL respectively after 72 hours (Figure 5.6.1).   On contrary, **HUM** and **HUM-B** were less active against MDA-MB-231 (7 % and 18.4 % growth inhibition respectively at 200 μg/mL) and not cytotoxic against HT-29 and A549 cells.
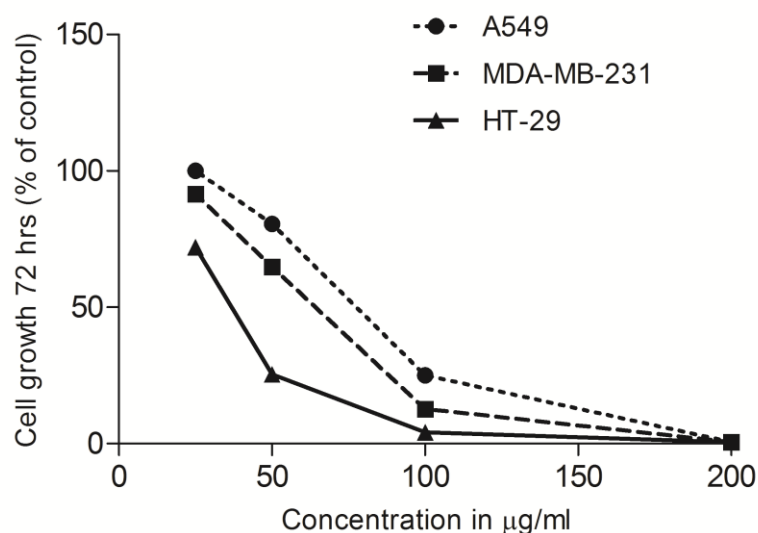
Figure 5.6.1 Dose dependent cytotoxic effect of HUM-E on human mammalian cells

5.7 Cytotoxic studies of isolated compounds

Compounds **HU-2** to **HU-6** and **HU-8** to **HU-10** were screened for in-vitro cytotoxic potential against same set of cancer cell lines and the results compared with standard drug 5-Fluorouracil are presented in Table 5.6.2. Compounds **HU-1**, **HU-7**, **HU-11** and **HU-12** were not subjected for cytotoxic effect as they were obtained only in trace quantity. The purity of selected compounds was verified using RP-HPLC-PDA analysis before the assay.

138

Table 5.6.2 Cytotoxic effect of isolated compounds on human mammalian cells

Compounds	A549	MDA-MB-231	HT-29
HU-2	3.6 ± 0.8^a	3.6 ± 0.9^a	1.7 ± 0.3^a
HU-3	3.7 ± 0.4^a	$> 100^b$	$> 100^b$
HU-4	7.2 ± 0.5^a	4.0 ± 0.2^a	4.9 ± 0.2^a
HU-5	5.9 ± 0.3^a	8.8 ± 0.7^a	$> 100^b$
HU-6	5.1 ± 0.1^a	9.1 ± 0.5^a	$> 100^b$
HU-8	$> 100^b$	$> 100^b$	6.1 ± 0.9^a
HU-9	$> 100^b$	$> 100^b$	$> 100^b$
HU-10	$> 100^b$	$> 100^b$	$> 100^b$
5-Fluorouracil	0.3 ± 0.1^a	0.5 ± 0.1^a	0.4 ± 0.2^a

[*] Results are mean $\pm$ SEM of three experiments; [a] Values are in μg/mL; [b] Values are in μM

Results showed significant and selective inhibition of growth of cancer cells lines. Compound **HU-3** i.e. cedrelopsin effectively inhibited the growth of A549 cells with IC_{50} value of 3.7 μg/mL, but it was found to be weakly effective against MDA-MB-231 and HT-29 cells. Similarly, two positional isomers **HU-5** (1,2-dimethoxy, 3-hydroxy anthraquinone) and **HU-6** (1,3-dimethoxy, 2-hydroxy anthraquinone) were found to be inhibiting A549 and MDA-MB-231 cells with IC_{50} values ranging between 5.1-9.1 μg/mL. The changes in the position of attachment of functional groups in **HU-5** and **HU-6** did not make any significant impact on their cytotoxic activity.

Compound **HU-2** i.e. pheophorbide A methyl ester exhibited the most strong cytotoxicity against all three cell lines with IC_{50} values of 3.6 (A549), 3.6 (MDA-MB-231) and 1.7 μg/mL (HT-29). These results were in corroboration with the findings of Cheng et al.,

(2001) where the EC_{50} of pheophorbide A methyl ester was found to be 0.83 μg/mL against lung cancer cells. A broad dose levels (62.5, 125 and 250 μg/mL) study carried out by Sowemimo et al. (2012) against HT-29 cells proved their cytotoxic effect; however IC_{50} value was not identified and reported. Our study results validated this report and had clearly revealed the IC_{50} of **HU-2** against HT-29 as 1.7 μg/mL.

HU-4 (ursolic acid) was found to be second most active compound followed by **HU-2**, and exhibited inhibition against growth of all three cell lines with the IC_{50} values ranging between 4.0-7.2 μg/mL. Thus by performing MTT assay on major isolated compounds of **HUM-E**, the cytotoxic effect of **HUM-E** against A549, MDA-MB-231 and HT-29 cell lines was chemically validated. However the effect of isolated compounds was much higher than the crude fraction (**HUM-E**), which indicated the possibility of presence of other compounds in **HUM-E** that hinder the inhibition effect.

Of the isolated compounds of **HUM-B**, only **HU-8** (asperulosidic acid) exhibited significant growth inhibition of HT-29 cells (IC_{50}: 6.1 μg/mL). However it was very weakly inhibiting MDA-MB-231 and A549 cells. This observation was in accordance with the findings of Zhang et al., (2010) where the compound, **HU-8** was found to be inactive on A549 cells at 4.0 μg/mL. Similarly, **HU-9** (deacetyl asperuloside) and **HU-10** (feretoside) have exhibited no inhibition of the growth of tested cell lines up to 37.2 and 40.4 μg/mL respectively. The LC-PDA-ESI-MS analysis of **HUM-B** revealed that **HU-10** is contributing for more than 50% to the total area of **HUM-B**. Hence the inactive nature of **HUM-B** on these three cell lines might be due to the presence of **HU-10**. Interestingly none of the compounds were found to be toxic on human normal cells (HEK 293) except **HU-8**.

A team led by Isiguro (Isiguro et al., 1986) found that feretoside (**HU-10**) was inactive on leukaemia P388 cell lines. Conversely, the aglycone part of it was found to be

very effective in inhibiting the growth of leukaemia P388 and Meth A cells in a dose dependent manner at concentrations of 10^{-7}-10^{-4} g/mL. In-vivo experiment performed on mice bearing Meth A, Sarcoma 180 cells demonstrated that the average life span was increased by 81.8 and 94.4% respectively and this was higher than 5-Fluorouracil. A mean survival day of mice bearing Ehrlich Ascites Carcinoma was also increased by twofold than 5-Fluorouracil. Hence it was suggested that the aglycones part of **HU-8**, **HU-9** and **HU-10** might emerge as promising cytotoxic molecules.

5.8 Interpretation of LC-PDA-ESI-Mass spectrum of HUM-E

The LC-PDA-ESI-MS fingerprint (Figure 5.3.1) revealed the presence of 18 major compounds in **HUM-E** (Table 5.8). The peak no. 6 was identified as hedyotiscone-B (**7**) based on the observed [M+H]$^+$ peak at *m/z* 245.05 (Figure 5.8.1). Similarly, peak no. 8, 9 and 10 were identified as 1,3-dimethoxy-2-hydroxy anthraquinone (**6**), 1,2-dimethoxy-3-hydroxy anthraquinone (**5**) and cedrelopsin (**3**) as they exhibited [M-H]$^-$ peak at *m/z* 283.10, 283.10 and 259.15 (Figure 5.8.2 to 5.8.4) which were corresponding to the molecular weight of **HU-6** (284.07), **HU-5** (284.07) and **HU-3** (260.10) respectively. As compound **HU-6** and **HU-5** are structural isomers they were further confirmed by comparing the retention time of characterized molecules. The peak no. 16 was identified as ursolic acid (**4**) as it formed a water adduct at *m/z* 473.35 in the negative mode (Figure 5.8.5). The peak no. 17 and 18 were found to be oledicoumarin (**1**) and pheophorbide A methyl ester (**2**) from the exhibited [M+H]$^+$ peak at *m/z* 513.40 (Figure 5.8.6) and 607.30 (Figure 5.8.7), respectively. The peak no. 5, 11 and 15 (Figure 5.8.8 to 5.8.10) were tentatively identified as 1,2-dimethoxy anthraquinone, 1,2-dimethoxy-3-hydroxy anthraquinone monoacetate and 1,2,3-trimethoxy anthraquinone, respectively from the previous reports of these compounds from *O. umbellata* (Purushothaman et al., 1968; Ramamoorthy et al., 2009).

141

Table 5.8 Identification of major compounds present in HUM-E by LC-PDA-ESI-MS

Peak No.	R_t (min)	$[M+H]^+$	$[M-H]^-$	$[M+H_2O]^-$	Mol. Formula	UV-Visible absorption (λ_{max})	Name of the compound
1	9.725	-	353.10	-	-	254/321/385/423/582	Unknown
2	10.799	249.05	-	-	-	221/260/292/385/582	Unknown
3	13.904	-	229.05	-	-	323/237/424/582/625	Unknown
4	16.081	335.15	-	-	-	273/240/424/582/624	Unknown
5	19.332	-	-	285.10	$C_{16}H_{12}O_4$	272/242/409/582/	1,2-dimethoxy anthraquinone*
6	21.122	245.05	-	-	$C_{14}H_{12}O_4$	227/280/424/582	Hedyotiscone B (7)
7	22.187	-	329.30	-	-	256/328/423/582/	Unknown
8	23.382	-	283.10	-	$C_{16}H_{12}O_5$	280/242/368/582	1,3-dimethoxy-2-hydroxy-9,10-anthracenedione (6)
9	24.122	-	283.10	-	$C_{16}H_{12}O_5$	278/245/354/582	1,2-dimethoxy-3-hydroxy-9,10-anthracenedione (5)
10	26.042	-	259.15	-	$C_{15}H_{16}O_4$	344/241/582/424/459	Cedrelopsin (3)
11	27.202	-	341.20	-	$C_{18}H_{14}O_7$	279/245/321/405/582	1,2-dimethoxy-3-hydroxy anthraquinone-monoacetate*
12	32.525	-	293.25	-	-	239/625/409/655/494	Unknown
13	34.928	-	295.25	-	-	238/485/655/412/625	Unknown
14	36.516	-	293.25	-	-	277/485/421/386/574	Unknown
15	44.455	-	297.30	-	$C_{17}H_{14}O_5$	268/279/410/664/494	1,2,3-trimethoxy anthraquinone*
16	46.308	-	-	473.35	$C_{30}H_{48}O_3$	409/664/272/506/536	Ursolic acid (4)
17	47.360	513.40	-	-	$C_{30}H_{24}O_8$	409/266/655/494/538	Oledicoumarin (1)
18	50.834	607.30	-	-	$C_{36}H_{38}N_4O_5$	254/409/655/485/532	Pheophorbide a methyl ester (2)

*Tentatively identified

142
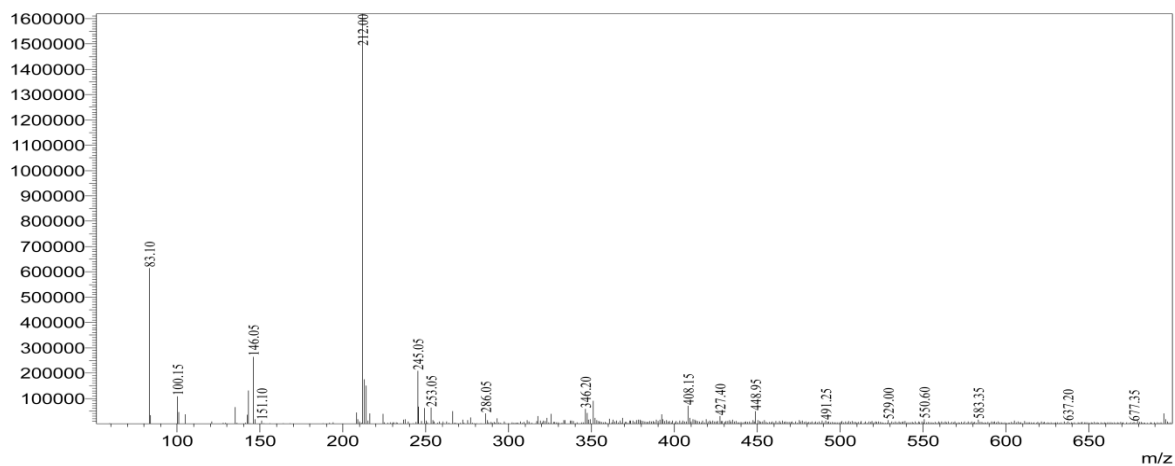
Figure 5.8.1 ESI-Mass spectrum of peak no.6
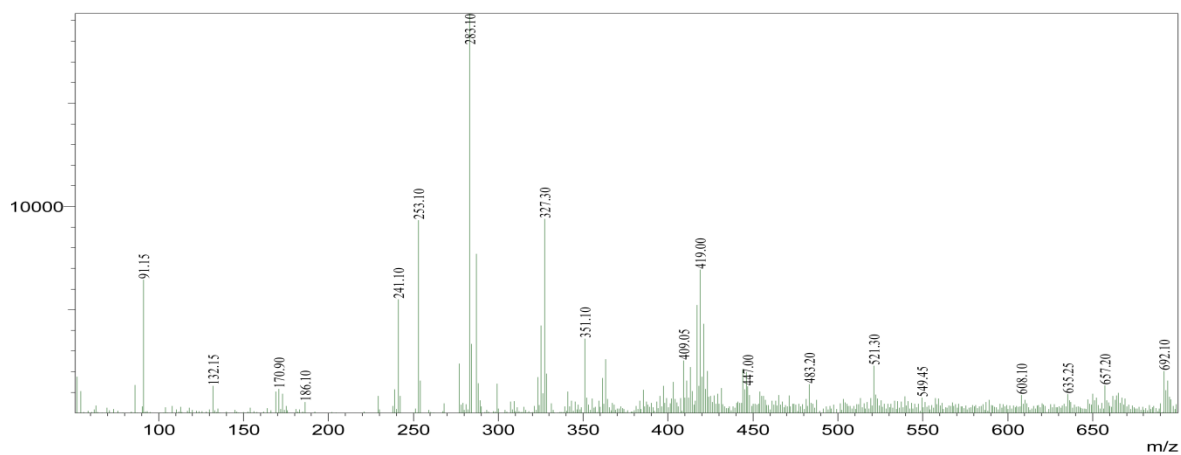
Figure 5.8.2 ESI-Mass spectrum of peak no.8
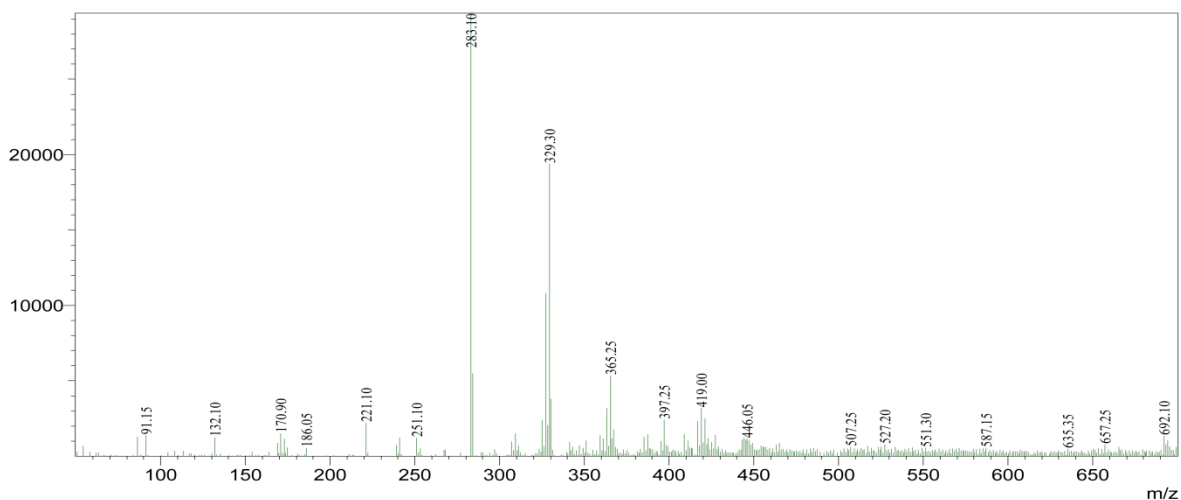
Figure 5.8.3 ESI-Mass spectrum of peak no.9
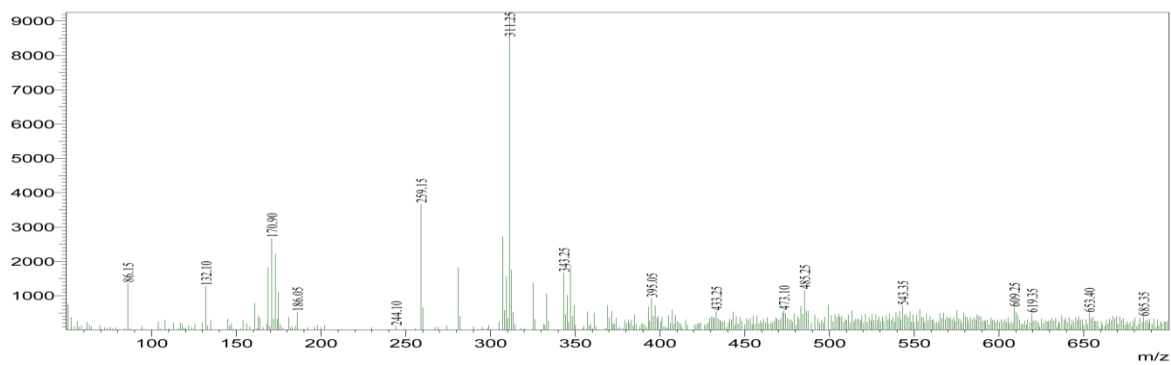
Figure 5.8.4 ESI-Mass spectrum of peak no.10
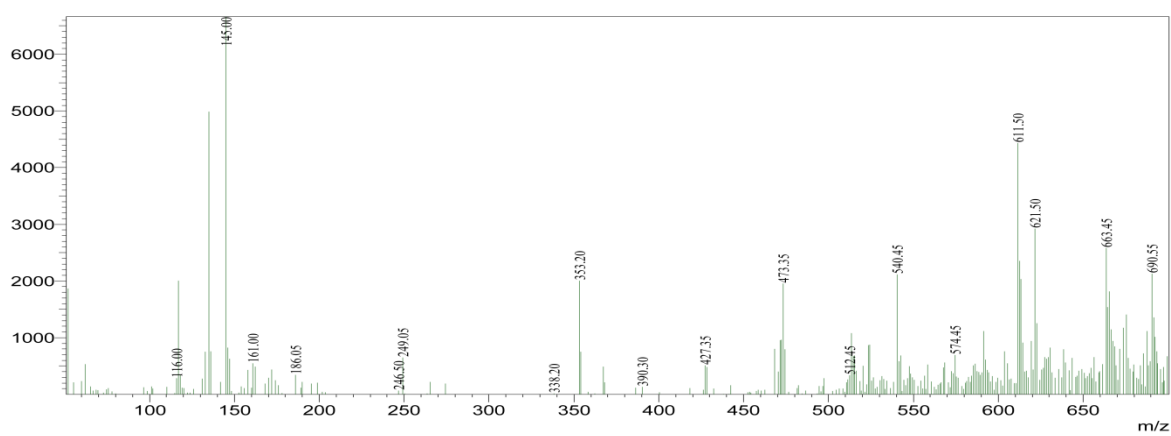
Figure 5.8.5 ESI-Mass spectrum of peak no.16
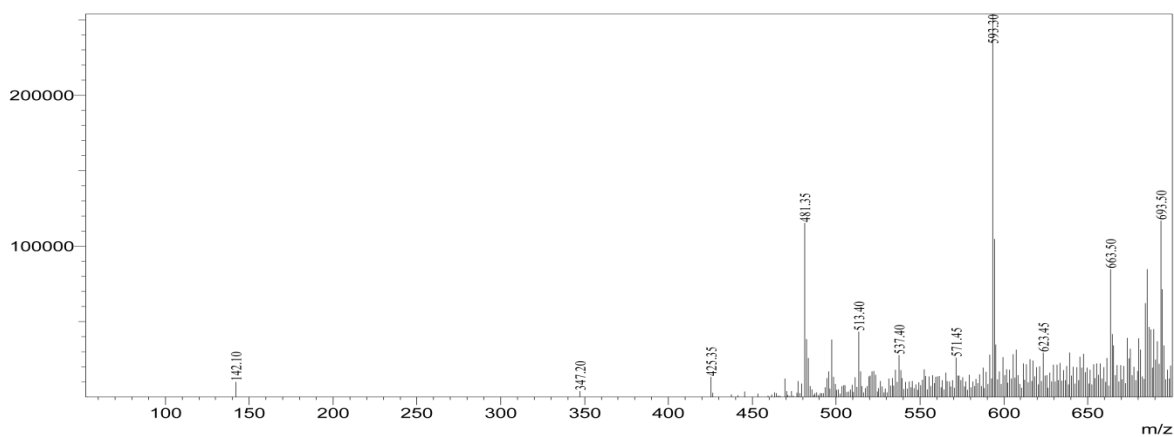
Figure 5.8.6 ESI-Mass spectrum of peak no.17
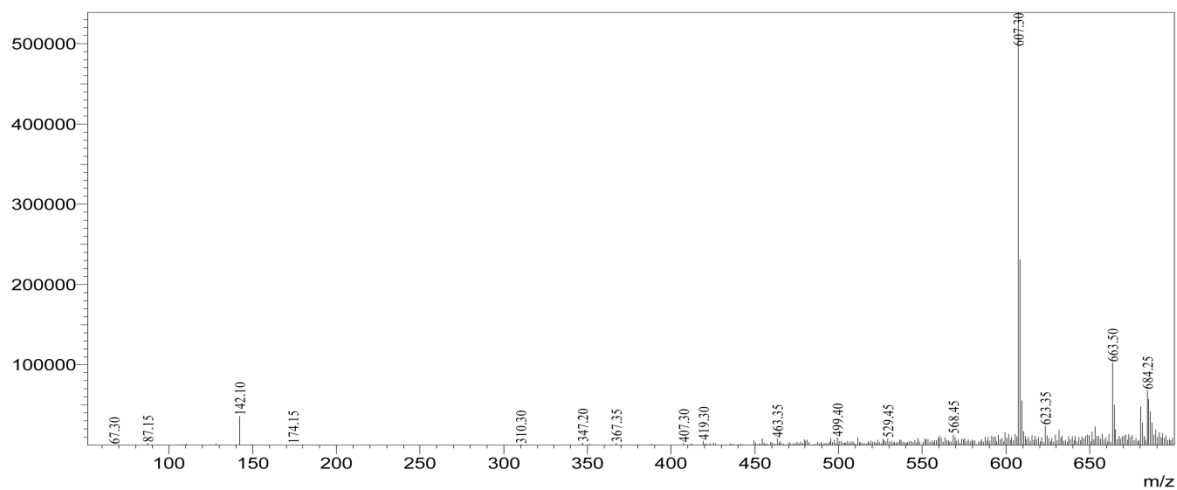
Figure 5.8.7 ESI-Mass spectrum of peak no.18
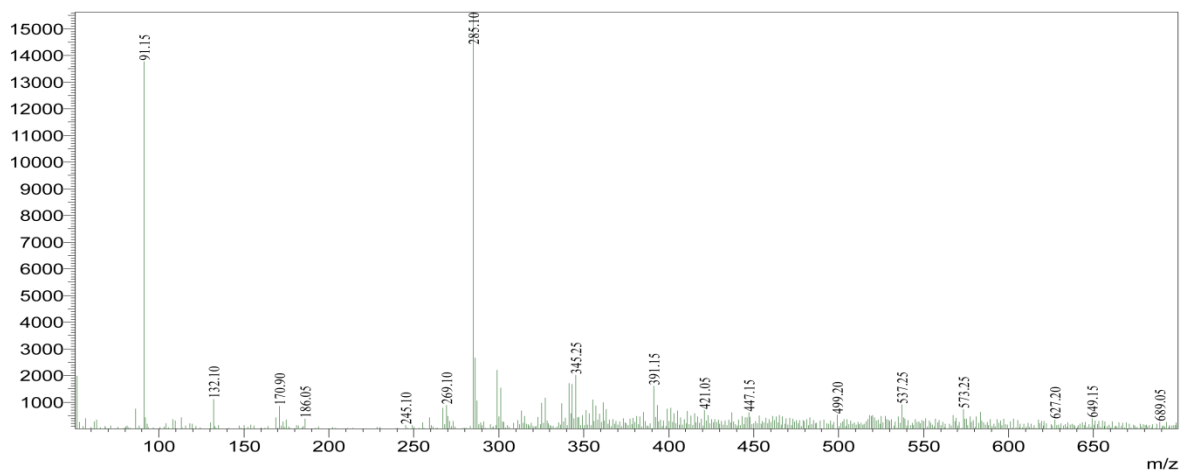
Figure 5.8.8 ESI-Mass spectrum of peak no.5
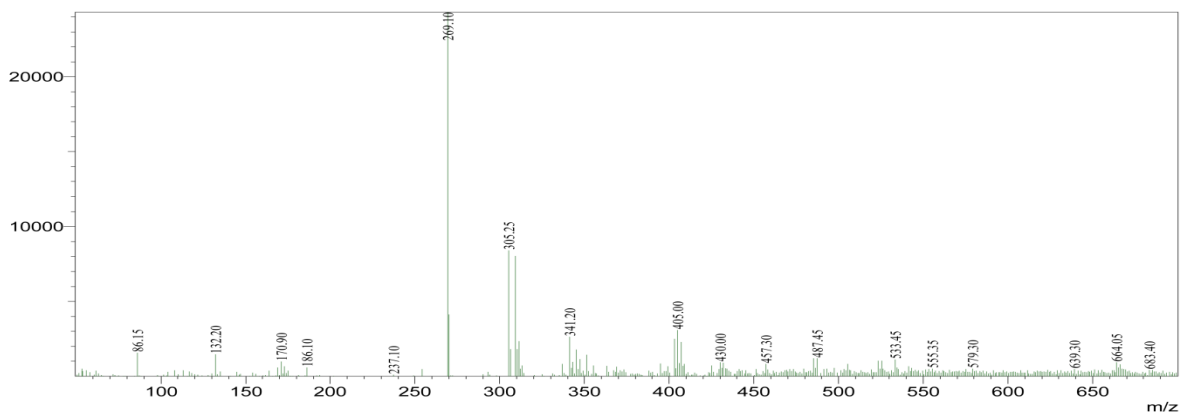
Figure 5.8.9 ESI-Mass spectrum of peak no.11

145
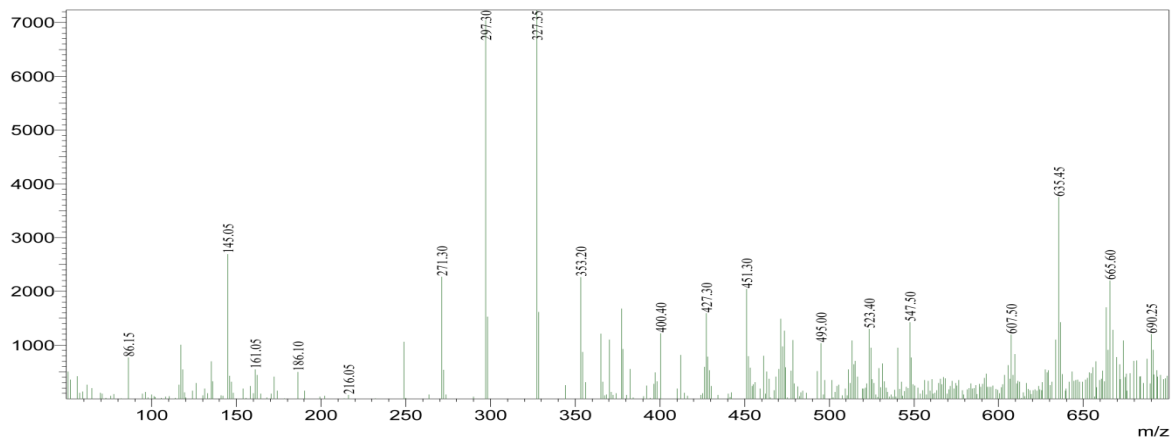
Figure 5.8.10 ESI-Mass spectrum of peak no.15

5.9 Interpretation of LC-PDA-ESI-Mass spectrum of HUM-B

From the LC-ESI-MS fingerprint of **HUM-B**, around 9 major compounds were identified (Table 5.9). The peak 7 and 8 (Figure 5.3.2) were present predominantly and together contributing 71.3% (53.4% and 17.9% respectively) to the total area. The peak no. 7 showed *m/z* at 427.10 in positive mode (Figure 5.9.1) by forming sodium adduct, which corresponded to the molecular formula $C_{17}H_{24}O_{11}$ (calc. 404.37) of **HU-10**. Similarly, peak no. 8 showed $[M+Na]^+$ and $[M-H]^-$ at *m/z* 455.10 (Figure 5.9.2a) and 431.20 (Figure 5.9.2b), respectively. This was corresponding to the molecular formula $C_{18}H_{24}O_{12}$ (calc. 432.13) of **HU-8**. In addition, both the peaks exhibited similar type of UV absorption pattern that suggested the presence of iridoid derivatives (238 and 236 nm respectively). Hence, based on the above observations it was corroborated that peak no. 7 should be feretoside (**10**) and peak no. 8 should be asperulosidic acid (**8**).

The peak no. 1 showed $[M+Na]^+$ and $[M-H]^-$ peaks at *m/z* 413.10 (Figure 5.9.3a) and 389.20 (Figure 5.9.3b), respectively. This was corresponding to molecular formula $C_{16}H_{22}O_{11}$ (calc. 390.34) and identified as scandoside (**11**). The peak no. 5 displayed $[M+Na]^+$ peak at *m/z* 427.10 (Figure 5.9.4). Further comparison with retention time of one of the characterized compounds helped to identify it as 6α-hydroxygeniposide (**12**). The peak no. 9 has shown $[M+H]^+$ and $[M+H_2O]^-$ at *m/z* 373.15 (Figure 5.9.5a) and 389.20 (Figure 5.9.5b), respectively corresponding to the molecular formula $C_{16}H_{20}O_{10}$ (calc. 372.11) suggested it as deacetylasperuloside (**9**). Thus, out of the 9 compounds displayed in the **HUM-B** fingerprint, five compounds were isolated and characterized.

Table 5.9 Identification of major compounds present in HUM-B by LC-PDA-ESI-MS

Peak No.	R_t (min)	$[M+H]^+$	$[M+Na]^+$	$[M-H]^-$	$[M+H_2O]^-$	Mol. Formula	UV-Visible absorption (λ_{max})	Name of the compound
1	2.510	-	413.10	389.20	-	$C_{16}H_{22}O_{11}$	656/424/487/582	Scandoside (**11**)
2	7.031	-	-	371.15	-	-	256/426/674	Unknown
3	9.414	-	-	375.15	-	-	253/289/656/485	Unknown
4	10.672	-	397.10	373.20	-	-	656/485/568	Unknown
5	12.586	-	427.10	-	-	$C_{17}H_{24}O_{11}$	231/656/485/441	6α-hydroxygeniposide (**12**)
6	15.783	-	-	341.15	-	-	288/485/574/421/533	Unknown
7	18.461	-	427.10	-	-	$C_{17}H_{24}O_{11}$	238/656/485/421	Feretoside (**10**)
8	22.307	-	455.10	431.20	-	$C_{18}H_{24}O_{12}$	236/656/485/574/441	Asperulosidic acid (**8**)
9	26.926	373.15	-	-	389.20	$C_{16}H_{20}O_{10}$	222/301/656/485/574	Deacetylasperuloside (**9**)
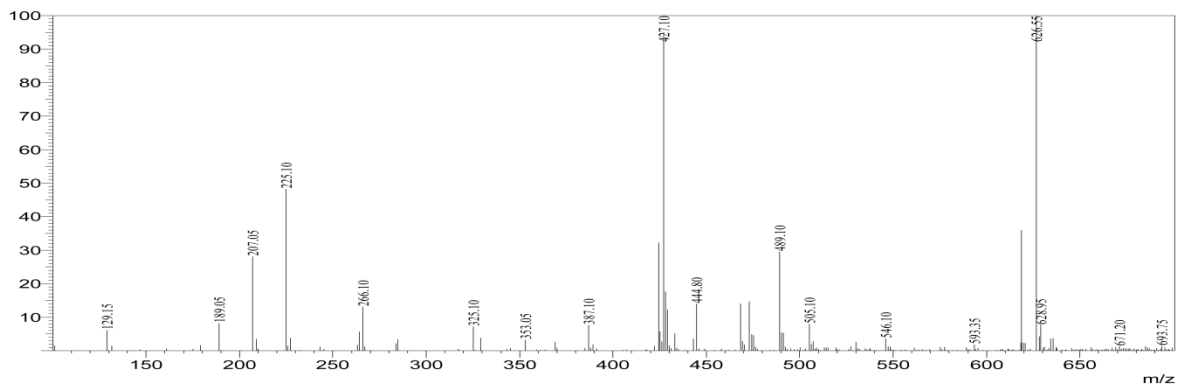
Figure 5.9.1 ESI-Mass spectrum of peak no.7
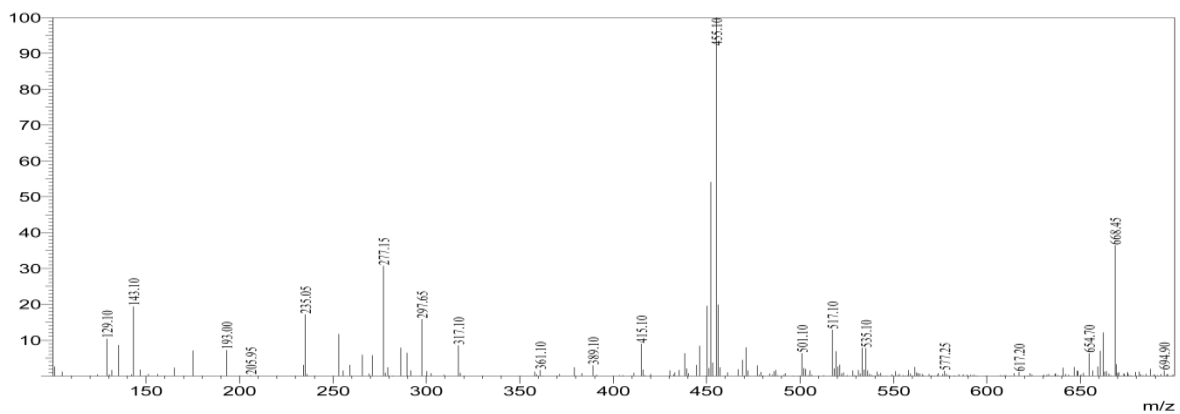
Figure 5.9.2a ESI-Mass spectrum of peak no.8 in positive polarity
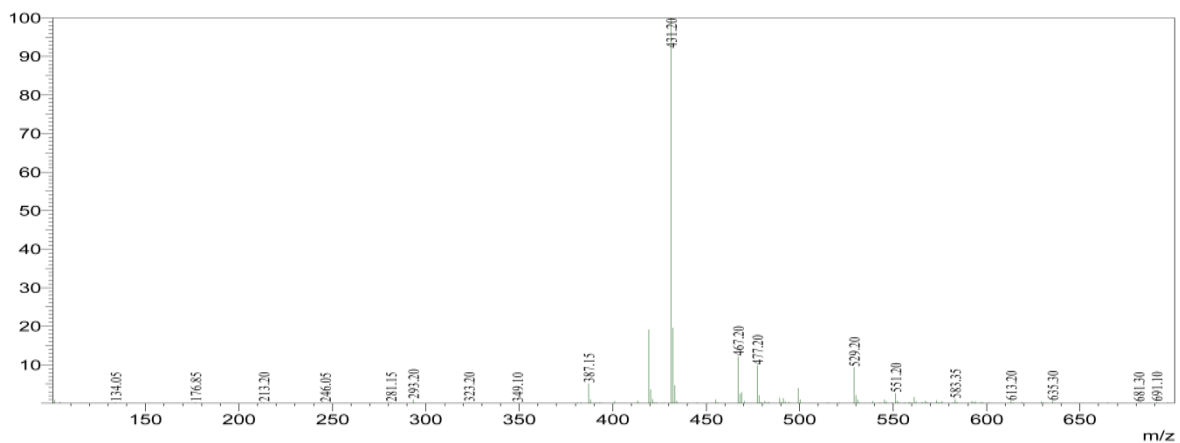
Figure 5.9.2b ESI-Mass spectrum of peak no.8 in negative polarity

149
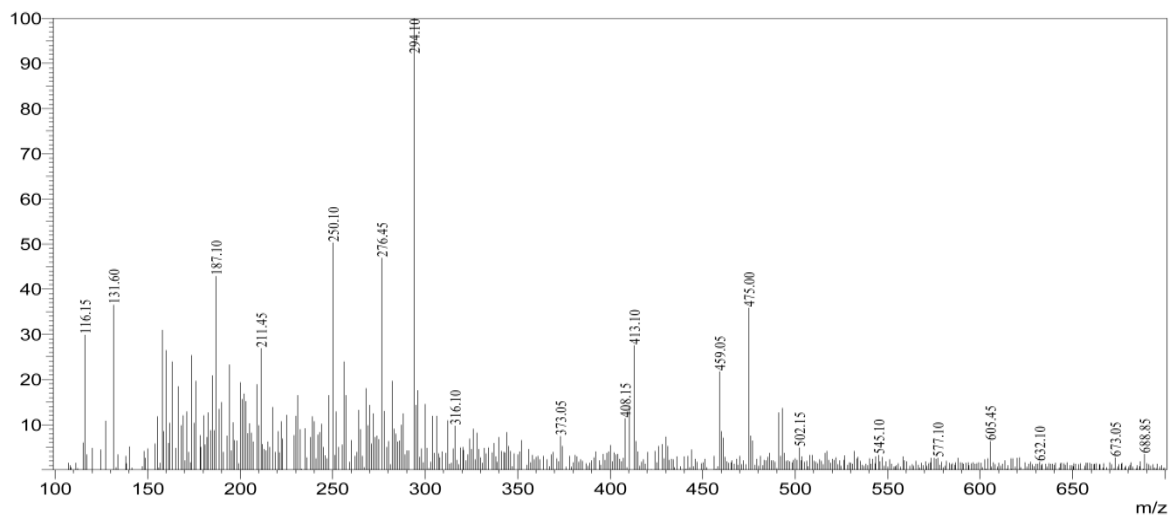
Figure 5.9.3a ESI-Mass spectrum of peak no.1 in positive polarity
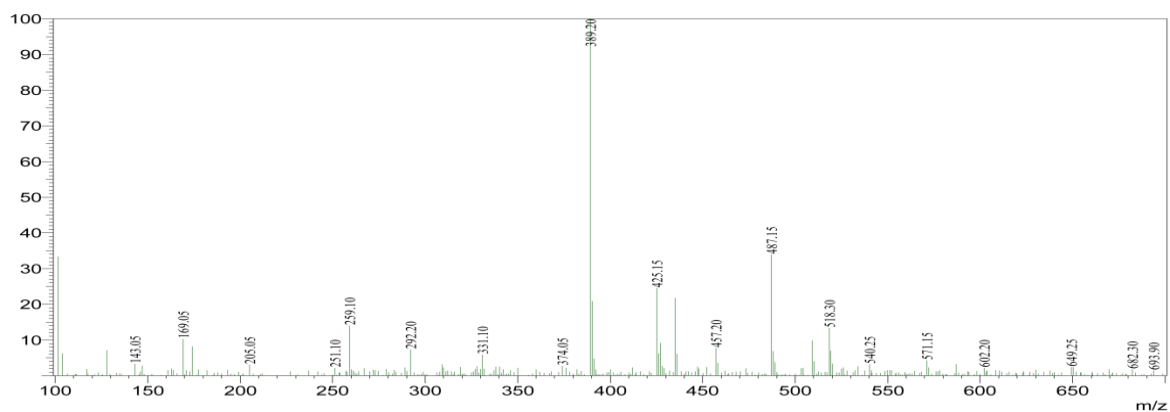
Figure 5.9.3b ESI-Mass spectrum of peak no.1 in negative polarity
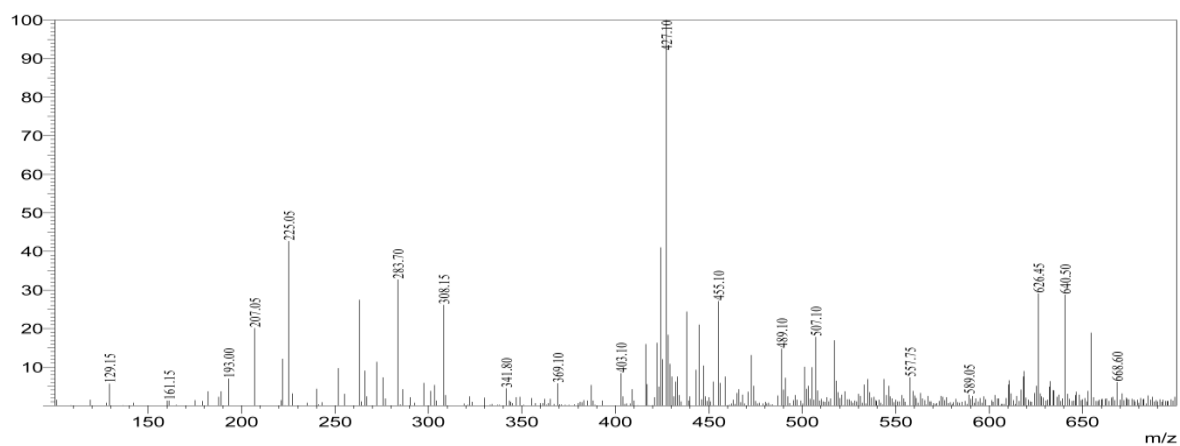
Figure 5.9.4 ESI-Mass spectrum of peak no.5

150
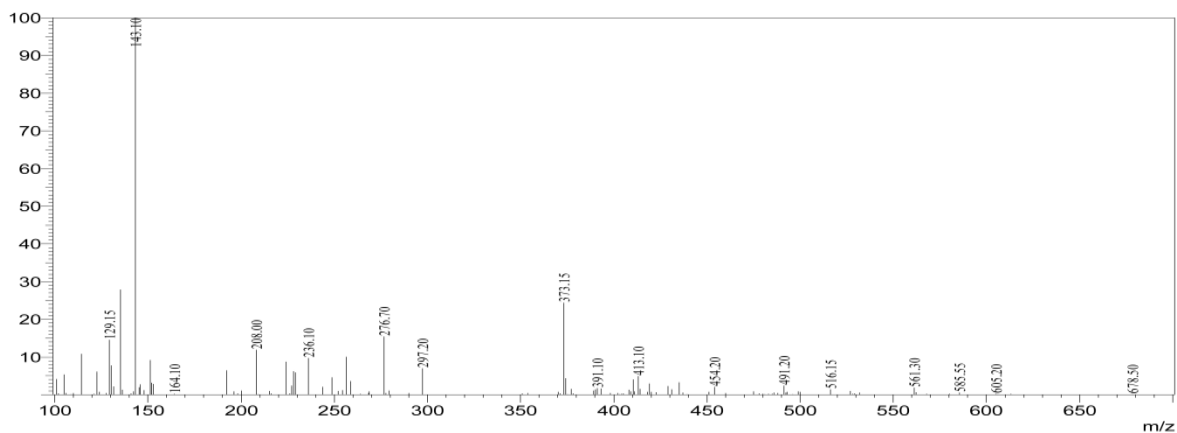
Figure 5.9.5a ESI-Mass spectrum of peak no.9 in positive polarity
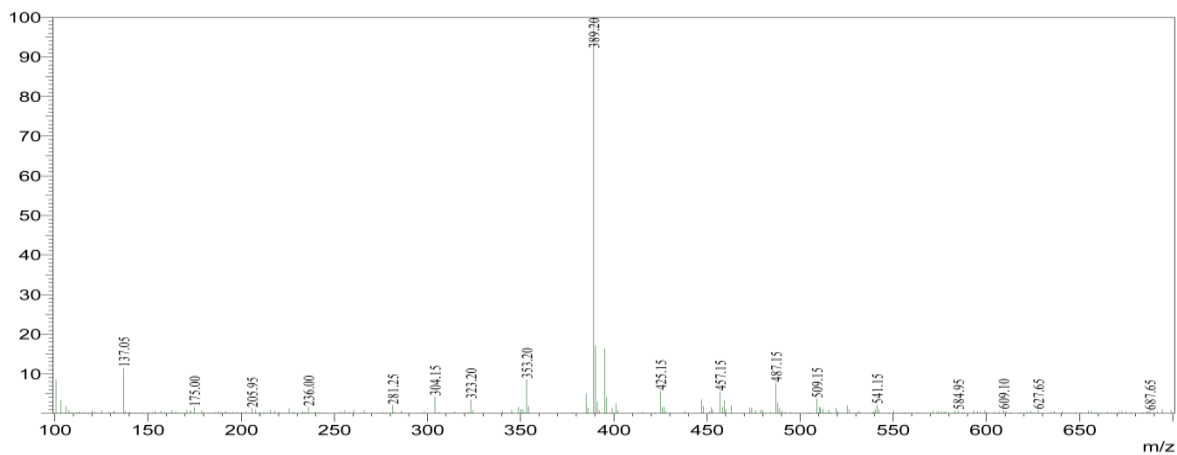
Figure 5.9.5b ESI-Mass spectrum of peak no.9 in negative polarity

151

PART II

Safflower, NARI-NH-01 released in 2001 was the first non-spiny hybrid in the world, which yields red colored florets. NARI-06 is high oil yielding spineless variety, producing dark red colored florets. These two non-spiny cultivars analyzed for total sugar, proteins, amino acids, and minerals like K, Ca, Mg, Fe, Na, Mn, Zn, Cu, etc., are reported to be highly nutritive. Sagaramutyalu (APRR3) is a rust resistance spiny safflower variety, yielding yellow colored florets. TSF-1 is a wilt resistance spiny variety yielding red florets which are difficult to collect from fields. These four major cultivars cultivated throughout India are commercially exported and sold as herbal tea by small scale industries. Although little preliminary studies related to nutritive value of safflower were found in the literature, there is no systematic report on the quantitative determinations pertaining to physico-chemical properties and flavonoid content (NARI 2014). Hence an extensive analytical investigations was carried out and the results are presented in sequel.

5.10 Quantitative pharmacognostic studies as per WHO guidelines

Whole safflower petals of all four varieties can be classified as coarse powder as they pass through No. 2000 sieve. A relative report on different physicochemical parameters analyzed on safflower petals are presented in Table 5.10. Total ash describes the amount of remaining after ignition. This includes physiological (derived from plant tissue itself) and non-physiological ash (residue of extraneous matter, e.g. soil and sand) adhering to the plant surface. Acid insoluble ash helps to detect the presence of heavy metals in earthy matter in drugs since the calcium oxide, carbonate and silicates obtained by incineration are soluble (Folashade et al., 2012). Among all, the total ash and water soluble ash was found to be high in APRR3 (171.45 mg/kg and 103.42 mg/kg). Similarly, NARI-06 has yielded high amount of acid insoluble ash than other varieties (9.53 mg/kg). However all these values were under

152

acceptable limit (not more than 18%) set by WHO. The extractive value was assessed by two cold maceration and hot extraction to identify the suitable method to extract the maximum bioactive compounds from the given material. The results suggested that cold maceration was suitable for spiny varieties (APRR3 and TSF-1) whereas non-spiny petals (NARI-NH-01 and NARI-06) afforded highest yield by hot extraction technique. Presence of excess of moisture in the HMs will favor the growth of microbes and hydrolyse the bioactive molecules. Results suggested that the content of moisture in all four varieties were within the limit (not more than 13%).

The presence of mucilage, pectin and hemicelluloses can be recognized through swelling index. Swelling index is the volume in ml taken up by the swelling of 1 g of plant material under specified conditions. It was noted that NARI-NH-01 was considerably more (2.83 mL/g) than other varieties. Estimation of tannins is a part of quality control as they produce astringent effect in living system by converting animal hides into water insoluble substances. Tannins are susceptible to oxidation and polymerization in solution; as a consequence of this they lose their therapeutic effect. Hence it is mandate to determine the level of tannins in the plant products to ensure its astringent effect. In this study no sizeable difference was shown between spiny and non-spiny varieties towards the presence of tannins. A maximum of 26.25% was found to be present in TSF-1 followed by APRR3 (19.99 %). Many medicinal plants that contain saponins cause persistent foam when an aqueous decoction is shaken. But it was observed that there were no stable foams formed in all four varieties. Hence the concentration of saponins in safflower decoction would be much less or even might be absent. This observation was further supported by testing hemolytic activity, a specific test for saponins which cause changes in erythrocyte membrane when mixed with blood suspension, making haemoglobin to diffuse into surrounding medium. The hemolytic activity of a preparation containing saponins was determined by comparing with that of a

153

reference material, saponin R, which has a hemolytic activity of 1000 units/g (Table 5.10). The results indicated, that safflower decoction until the concentration of 10 mg/mL did not show any haemolysis. This concentration is almost 3 times higher than what is being consumed by human in the form of safflower tea.

Bitterness value was determined by comparing the threshold bitter concentration of aqueous extract of safflower petals with that of a dilute solution of quinine hydrochloride R. The bitterness value is expressed in unit equivalent to the bitterness of a solution containing 1g of quinine hydrochloride R in 2000 mL and it was found to be 1257 units/g. Medicinal plants exhibiting strong bitter taste are therapeutically used as appetizing agent and no general limit has been prescribed by WHO for bitterness value. Spiny petals (APRR3 2200 units/g) were found to be bitterer than non-spiny variety. On the other hand, more volatile matter was found to be present in non-spiny variety, a maximum of 16% by NARI-06. The amount of volatile oil shown by the same sample was found to be higher (1.4 mL/g) compared to others.

Table 5.10 Results of pharmacognostical evaluation of safflower petals of different varieties

S. No.	Parameter	APRR3	TSF-1	NARI-NH-01	NARI-06
1	Total ash	171.45 mg/g	88.8 mg/g	63.22 mg/g	107.23 mg/g
2	Acid insoluble ash	7.995 mg/g	4.995 mg/g	3.33 mg/g	9.53 mg/g
3	Water soluble ash	103.42 mg/g	55.49 mg/g	39.99 mg/g	84.3 mg/g
4	Extractives (cold maceration)	116.25 mg/g	96.875 mg/g	91.25 mg/g	65.3 mg/g
5	Extractives (Hot extraction)	83.75 mg/g	92.5 mg/g	99.38 mg/g	72.39 mg/g
6	Loss on drying	57.48 mg/g	74.16 mg/g	77.5 mg/g	25 mg/g
7	Swelling index	1.1 mL/g	0.93 mL/g	2.83 mL/g	1.0 mL/g
8	Foaming index	<100	<100	<100	<100
9	Haemolytic activity	-	-	-	-
10	Tannins	19.99 %	26.25 %	20%	25%
11	Bitterness value	2200 units/g	1467 units/g	1257 units/g	1467 units/g
12	Volatile oil	0.6 mL/g	1.0 mL/g	0.4 mL/g	1.4 mL/g
13	Volatile matter	4 %	6 %	12 %	16 %

 ̄ No haemolysis occurred at the maximum prescribed dose level.

155

5.11 Microscopic analysis of *C. tinctorius*

Microscopic examination is the fundamental and foremost important test to identify the correct plant material. Although it often does not provide substantial data, still it is a better way to authenticate the material by comparing with reference standard. The microanalysis of corolla and style of spiny (APRR3) and non-spiny (NARI-06) safflower flowers were found to be indistinguishable. In cross sectional view, the corolla tube appeared circular with five slightly thick ridges. The ridges represented the union of five petal lobes. The cells were slightly rectangular or squarish with thick walls and were 10 μm thick. The ridges of the corolla tube were slightly thicker and consisted of three or four cells (Figure 5.11.1a and 5.11.1b).

In the median position of the petal and in between two ridges, prominent forked ribbon like outgrowths were seen. The outgrowths were uniseriate and fork into two lobes from the middle part. The cells were transversely rectangular and thick walled. They were 110-150 μm long and 40 μm thick (Figure 5.11.2a and 5.11.2b). In the cross sectional view, the style exhibited thick walled, compact parenchymatous ground tissue and two xylem strands arranged radially and alternating with each other (Figure 5.11.3a and 5.11.3b). The surface of the style had prominent dense spikes or short projecting outgrowths. The upper part of the style was thick and cylindrical having dense spines all over. The spines were unicellular, unbranched, pointed at the tip and were 50 μm long (Figure 5.11.4a and 5.11.4b).
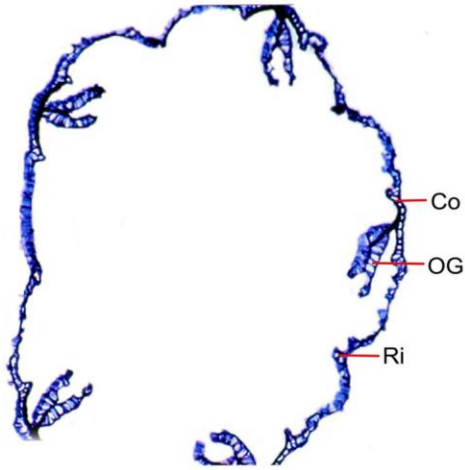
Figure 5.11.1a T. S. of corolla tube (NARI-NH-01) 10X
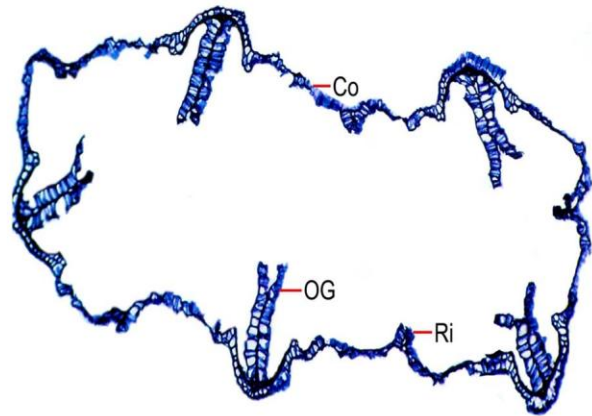
Figure 5.11.1b T. S. of corolla tube (APRR3) 10X
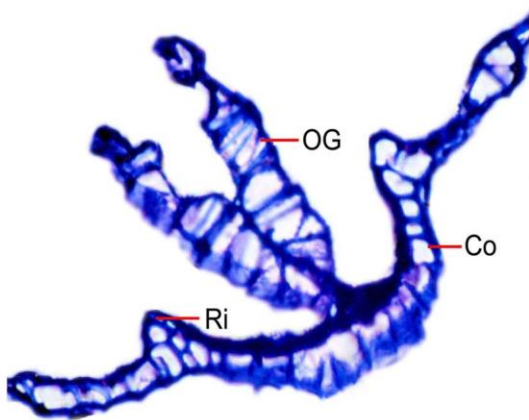
Figure 5.11.2a A part of corolla tube with outer growths (NARI-NH-01) 40X
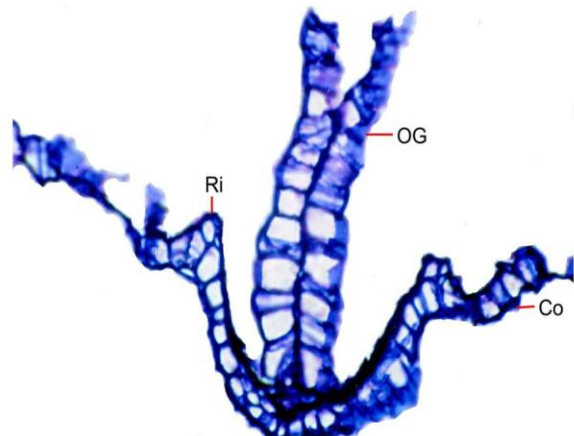
Figure 5.11.2b A part of corolla tube with outer growths (APRR3) 40X

(Co: Corollatube; OG: Outer growths; Ri: Ridge)
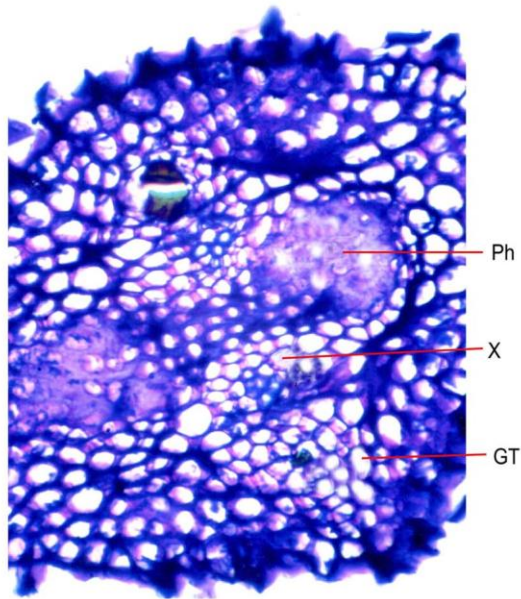
Figure 5.11.3a T. S. basal part of the style (NARI-NH-01) 16X
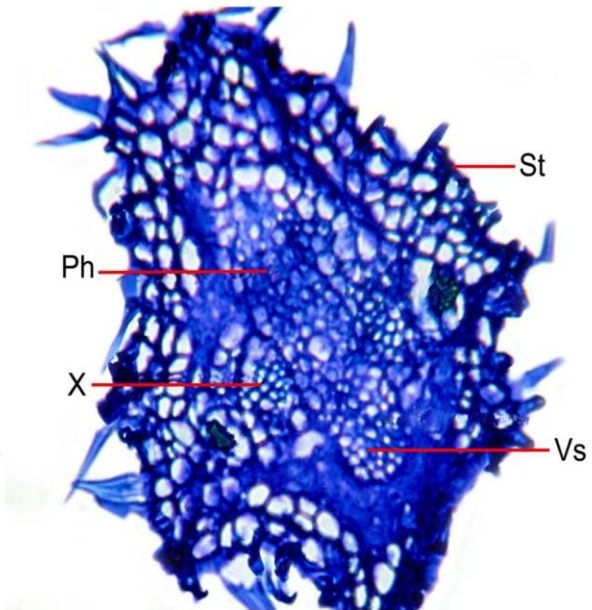
Figure 5.11.3b T. S. Basal part of the style APRR3) 16X
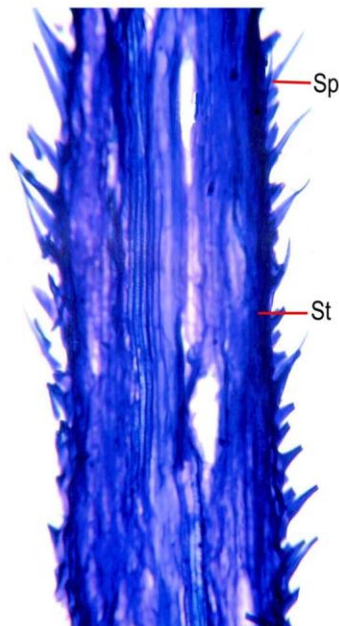
Figure 5.11.4a L. S. of style (NARI-NH-01) 16X
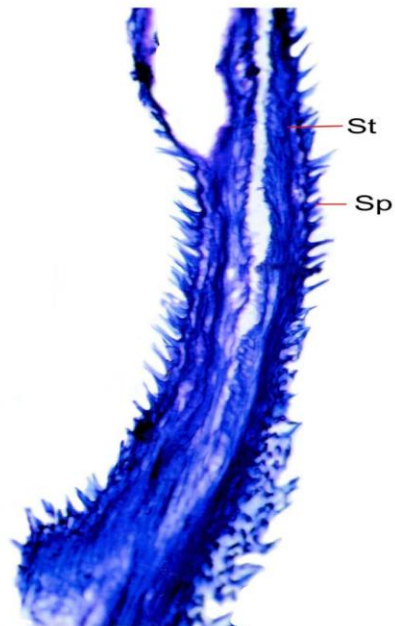
Figure 5.11.4b L. S. of style (APRR3) 10X

(Ph: Phloem; X: Xylem; GT: Ground tissue; Sp: Spine; St: Style; Vs: Vascular strand)

5.12 Determination of heavy metals using AAS

Heavy metals of non-anthrogenic origin are always associated with soils that rose from parent rocks and pedogenesis (Ghiyasi et al., 2010). Similarly, the anthropogenic

158

activity has resulted in the increase of several heavy metals in certain ecosystems (Street 2012). As the environment sets contaminated heavily with heavy metals, their residue reaches and are assimilated by plants (Sarma et al., 2012). Contamination of medicinal plant based products by heavy metals occurs by following ways: contamination during cultivation, inadvertent cross contamination and/or the purposeful introduction of heavy metals for alleged medicinal purposes (Denholm, 2010). The presence of high level of certain heavy metals causes hepatic, renal failure and intensive gastro-intestinal haemorrhage (Steenkamp et al., 2002; Woods et al., 1990). Certain heavy metals in trace quantity are essential for healthy life. But metals like lead, arsenic, cadmium and mercury causes serious side effects even if it is present in trace amount (Maobe et al., 2012). Accumulation of chromium in biological system may result in skin rash, liver, lung and kidney failure (Khan et al., 2008). Excess of chromium lead causes both acute and chronic adverse effects on vascular and immune system, kidney and liver (Jabeen et al., 2010). Exposure to high concentration of mercury can damage the kidney, brain and developing foetus (Vaikosen and Alade 2011). Lead is a non-essential heavy metal that causes lead poisoning which is characterised by anaemia, headache, convulsions and chronic nephritis, central nervous system disorder and brain damage (Khan et al., 2008). Hence the determination of heavy metals in safflower petals extract is essential to ensure the safety of consumers.

Estimation of heavy metals using AAS disclosed the presence of arsenic and lead below the detectable level in all four varieties (Table 5.12). Trace amount of mercury was found in all samples, however it was observed to be within the limit of 0.02 mg/day according to NSF International Drafts Standard (2011). While APRR3 and NARI-NH-01 were detected with no chromium, TSF-1 and NARI-06 showed 0.67 and 0.95 mg of chromium/100g of extract. With respect to cadmium, although APRR3 (0.3 mg/kg) complied the acceptable limit of WHO standard, other varieties did not comply the limit. As per WHO,

the maximum permissible limit for cadmium is 0.3 mg/kg of dried plant material (Asgarpanah and Kazemivash 2013). Hence, consumption of safflower decoction of TSF-1, NARI-NH-01 and NARI-06 could cause cadmium toxicity leading to reproductive hazards, cancer, heart disease, zinc-deficiency, etc., (Linder 1985).

Table 5.12 Amount of heavy metals (mg/100 g) present in different varieties of safflower petals

S. No.	Metals	APRR3	TSF-1	NARI-NH-01	NARI-06	Acceptable limit
1	Arsenic	Bdl	Bdl	Bdl	Bdl	0.01 mg/day[*]
2	Cadmium	0.030	0.150	0.220	0.100	0.03 mg/100 g[**]
3	Chromium	Bdl	0.670	Bdl	0.950	0.02 mg/day[*]
4	Lead	Bdl	Bdl	Bdl	Bdl	10 mg/ kg[**]
5	Mercury	0.000015	0.00011	0.000048	0.0000022	0.02 mg/day[*]

[*] as per NSF International Drafts Standard; [**] as per WHO; Bdl: Below the detection limit.

5.13 Determination of pesticide residues

Pesticides are widely employed to improve the quality and yield of agricultural products (Torres et al., 1996). Beside its unquestionable effects as herbicides, insecticides and fungicides, their deposition on plants can produce deleterious effect on human and environment. Pesticide residues are currently considered as one of the most dangerous environmental contaminants as they are stable, mobile and produce long term effects on living organisms. Pesticides could assimilate by plants and their metabolites might be amassed. Hence it is essential to study the various pesticides residue to protect the consumers from undesirable effects (Fenik et al., 2011). Gas chromatographic analysis was performed to detect the presence of 38 pesticides which are commonly employed during various stages of

cultivation process. These include organo-chlorines, organo-phosphates and synthetic pyrethroids (Figure 5.13.1 to 5.13.3 and Table 5.13.1 to 5.13.3). Results displayed no significant ECD, PFPD detectable pesticide residues in the tested sample.
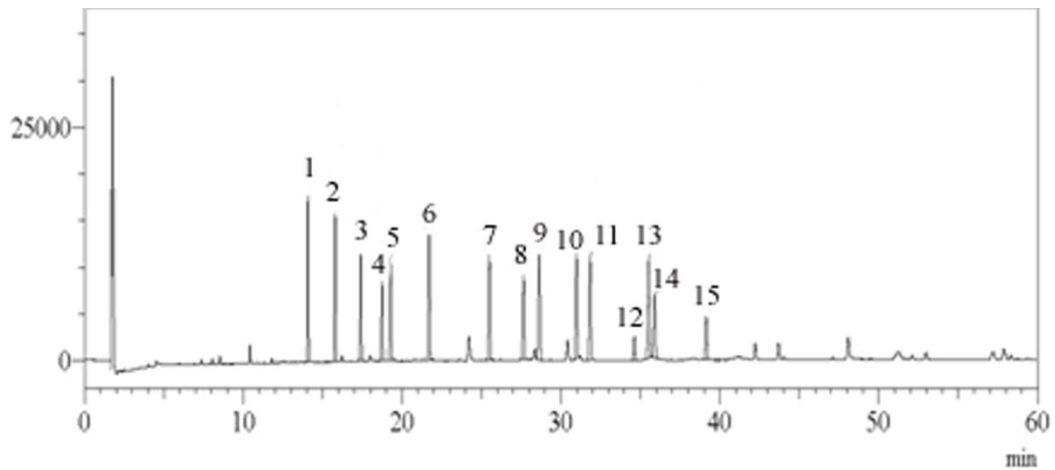
Figure 5.13.1 GC-ECD chromatogram of standard organochlorine pesticides mixture

Table 5.13.1 GC analytical data of standard organochlorine pesticides mixture

Peak No.	Pesticide	R_t (min)	Area
1	alpha-HCH	14.08	68475
2	gamma-HCH	15.78	68144
3	beta-HCH	17.39	57339
4	delta-HCH	18.73	44813
5	Heptachlor	19.26	69814
6	Dicofol	21.70	85488
7	Heptachlor-exo- epoxide	25.48	80110
8	2,4'-DDE	27.64	64296
9	alpha-Endosulfan	28.63	87237
10	4,4'-DDE	30.97	80633
11	2,4'-DDD	31.83	81024
12	2,4'-DDT	34.61	19373
13	beta-Endosulfan	35.50	80478
14	4,4'-DDT	35.90	54019
15	Endosulfan sulfate	39.13	37240
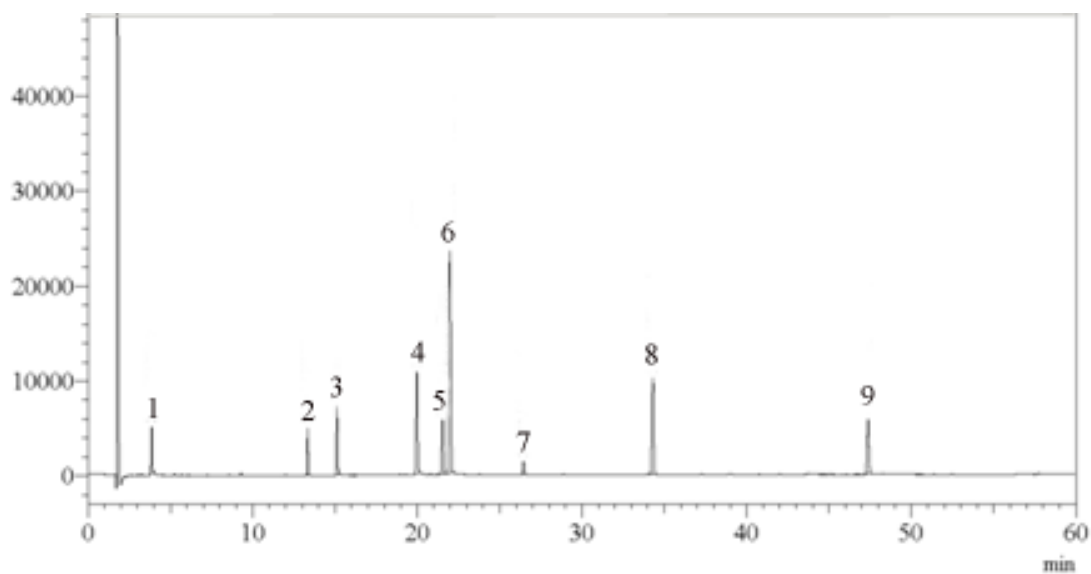
Figure 5.13.2 GC-PFPD chromatogram of standard organophosphate pesticides mixture

Table 5.13.2 GC analytical data of standard organophosphate pesticides mixture

Peak No.	Pesticide	R_t (min)	Area
1	Dichlorvos	3.86	18255
2	Phorate	13.34	20464
3	Dimethoate	15.12	32784
4	Parathion-methyl	19.97	65889
5	Malathion	21.53	35884
6	Chlorpyrifos	21.98	158878
7	Quinalphos	26.45	9576
8	Ethion	34.29	77587
9	Phosalone	47.36	45686
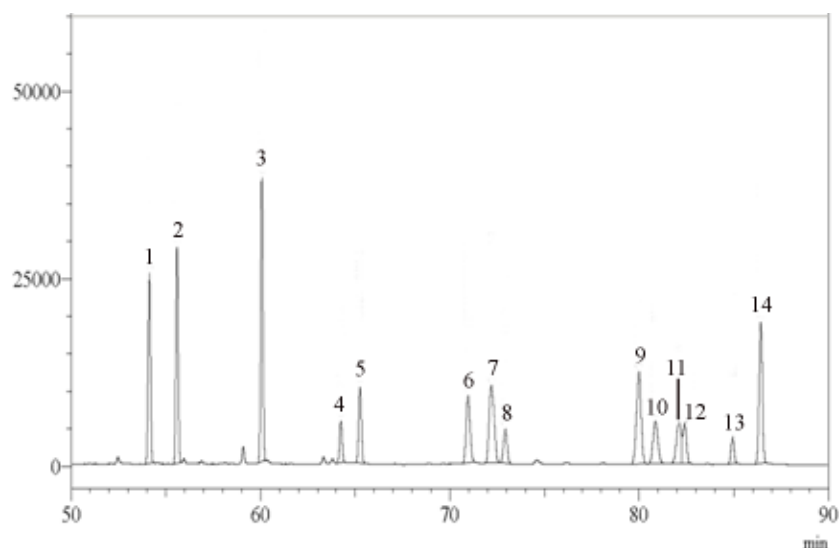
Figure 5.13.3 GC-ECD chromatogram of standard synthetic pyrethroids pesticide mixture

Table 5.13.3 GC analytical data of standard synthetic pyrethroids pesticide mixture

Peak No.	Pesticide	R_t (min)	Area
1	Bifenthrin	54.14	225417
2	Fenpropathrin	55.59	243211
3	lambda-Cyhalothrin	60.06	309051
4	Permethrin 1	64.23	52256
5	Permethrin 2	65.25	103589
6	Cypermethrin 1	70.96	129677
7	Cypermethrin 2	72.20	193865
8	Cypermethrin 3	72.94	60281
9	Fenvalerate 1	79.99	208048
10	Fluvalinate 1	80.85	101278
11	Fluvalinate 2	82.11	94954
12	Fenvalerate 2	82.40	75400
13	Deltamethrin 1	84.94	40029
14	Deltamethrin 1	86.42	227417

5.14 Quantification of flavonoids by HPTLC

Several analytical methods correlating chemical constituents with bio-activity of various species belonging to same genus are available in the literature for measuring the quality of herbal materials. Recently, Santana et al., (2014) had correlated total phenolic and flavonoid contents of Brazilian honeys with colour and antioxidant capacity. HPLC fingerprint analysis of *Flos carthami* from China for the presence of yellow pigment safflor A had been reported in literature, however analytical study using HPTLC for flavonoids are not explored (Zhang et al., 2005). *C. tinctorius* flowers have been reported as good antioxidants (Kruawan and Kangsadalampai 2006). The free radical scavenging property could be accounted by estimating the amount of flavonoids present in the sample. Presence of three bioactive flavonoids, rutin, quercetin and kaempferol was identified through co-TLC studies between aqueous extracts of different safflower petals and authentic samples. Estimation of flavonoids using HPTLC has been identified as a reliable method as it can provide chromatographic fingerprint which can be visualized and stored as electronic images (Mariswamy et al., 2011).

HPTLC analytical conditions such as, mobile phase composition, wavelength of detection, scan speed and scan mode were optimized. Mobile phase consisting of toluene: ethyl acetate: methanol: formic acid (3: 1: 1: 0.1 v/v/v/v) offered the best separations with well resolved zones. Chamber saturation for 20 min with the mobile phase facilitated the best chromatographic behaviour. Densitometric measurement was carried out simultaneously for all standards at 350 nm. Baseline separation was obtained between all three standard compounds and the R^2 value of rutin, quercetin and kaempferol was found to be 0.9985, 0.9997 and 0.9995 respectively. The linear regression equation of three standard compounds were found to be y = -221.540+5.211*x, y = -933.336+13.765*x and y = -1105.408+13.316*x, where y is the spot area and x in ng/spot. Based on the identity of

retention factor (R_f) of samples with that of standards, rutin (0.04 ± 0.03), quercetin (0.48 ± 0.03) and kaempferol (0.58 ± 0.02), identification of flavonoids was done. Results of HPTLC analysis are presented in Figure 5.14.1 to 5.14.4 and Table 5.14.
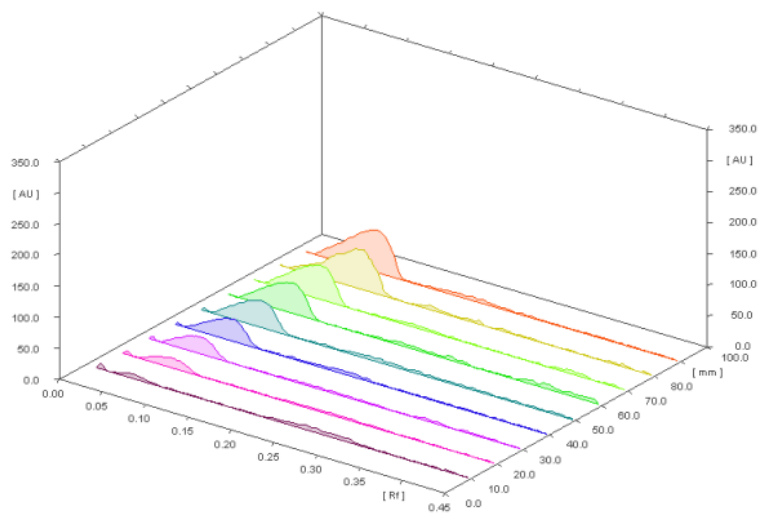
Figure 5.14.1 Standard HPTLC chromatogram of rutin
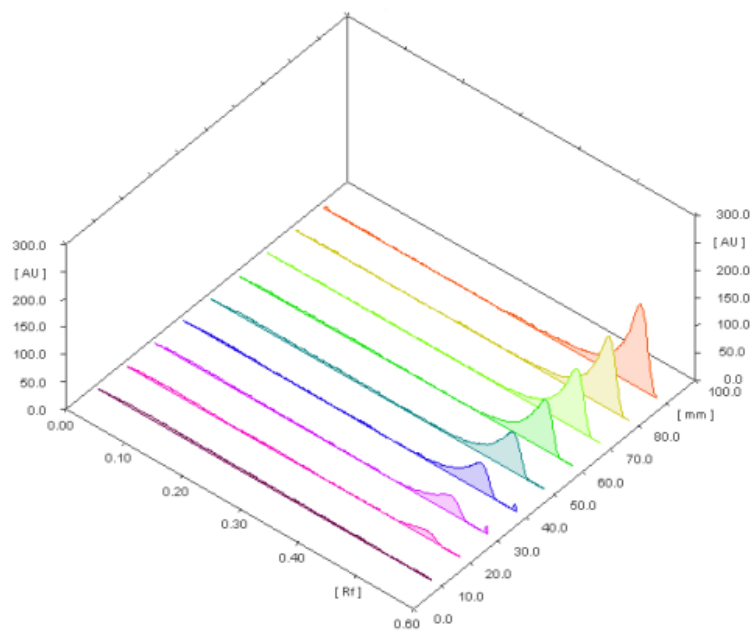
Figure 5.14.2 Standard HPTLC chromatogram of quercetin
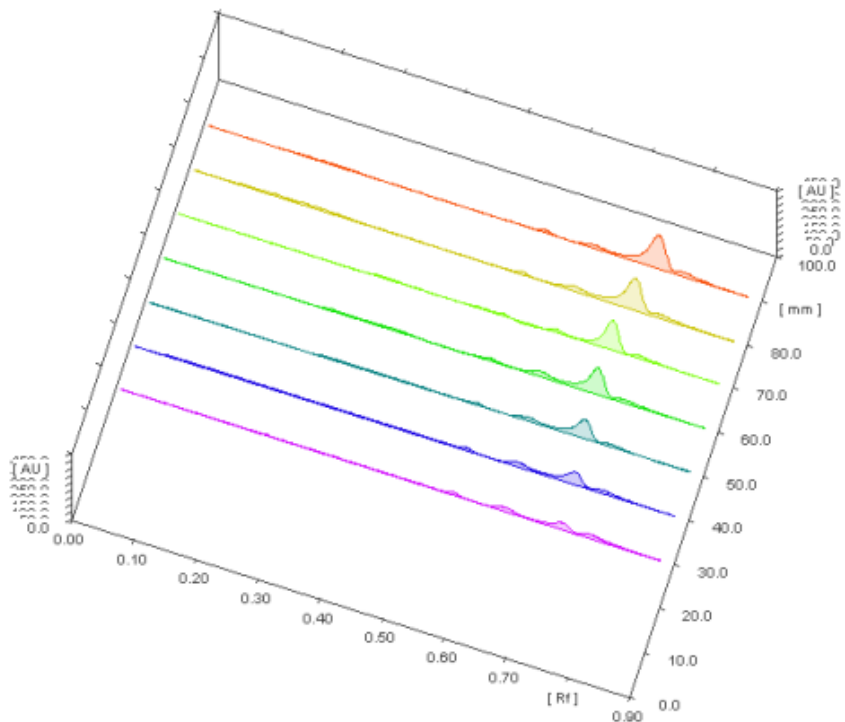
Figure 5.14.3 Standard HPTLC chromatogram of kaempferol
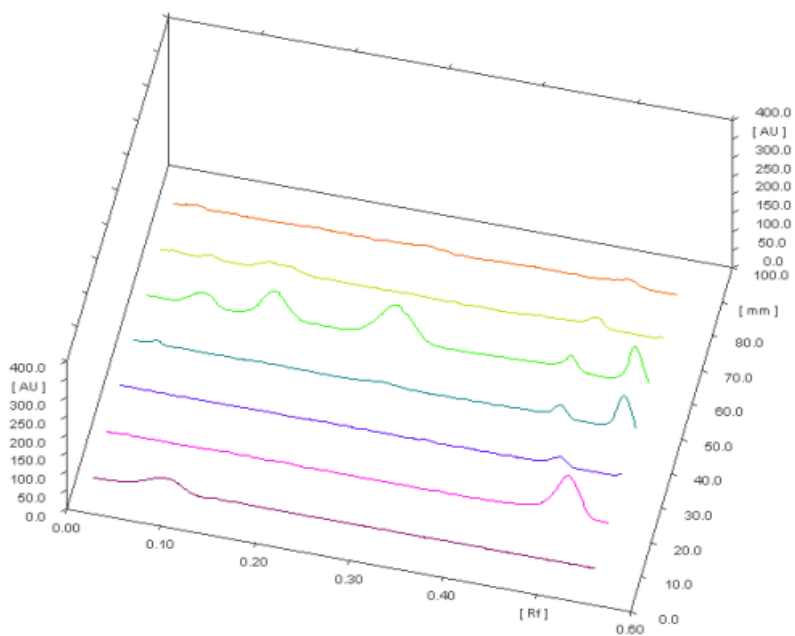
Figure 5.14.4 Overlay chromatogram of standards and samples

167
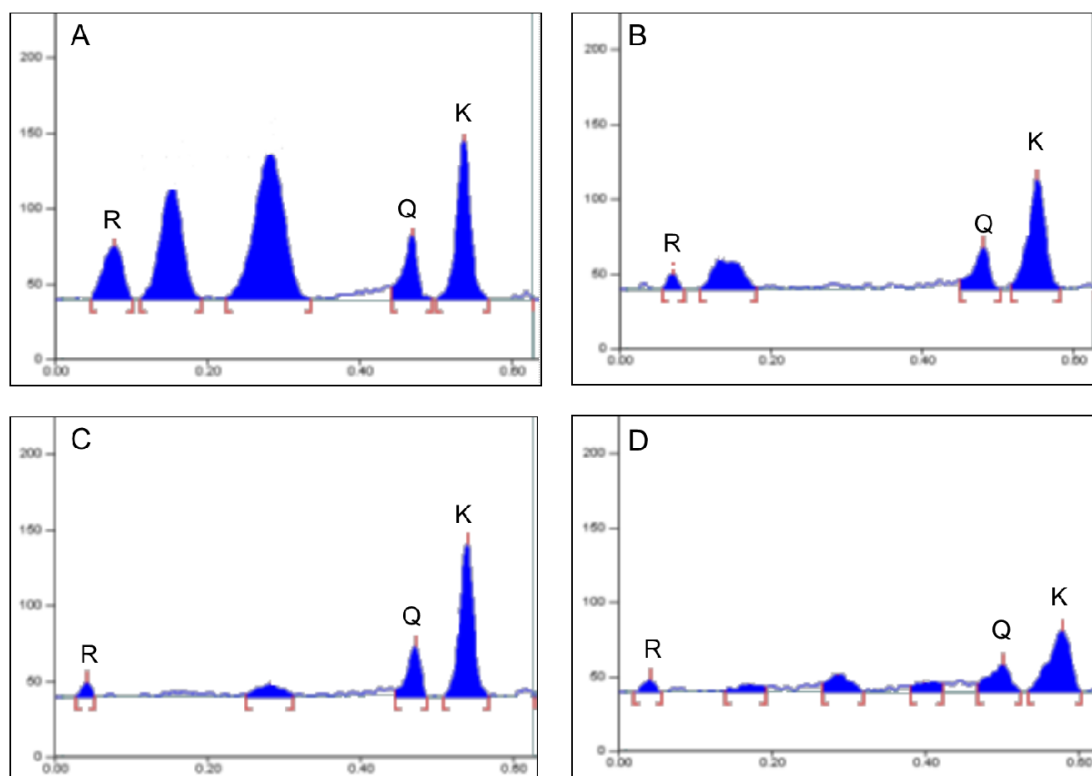
Figure 5.14.5 HPTLC chromatogram of safflower decoction of four varieties (A: APRR-3; B: TSF-1; C: NARI-NH-01; D: NARI-06. R: Rutin; Q: Quercetin; K: Kaempferol)

Table 5.14 Amount (ng/g) of rutin, quercetin and kaempferol in safflower decoction

Compounds	APRR3	TSF-1	NARI-NH-01	NARI-06
Rutin	189.7	87.85	72.97	77.24
Quercetin	116.6	115.70	112.36	101.60
Kaempferol	185.07	169.69	177.20	107.80

The amount of rutin present in APRR3, TSF-1, NARI-NH-01 and NARI-06 was found to be 189.7, 87.85, 72.97 and 77.24 ng/g of extract, respectively (Table 5.14).

Significant variation was not observed among the four varieties with respect to quercetin content. While 185.07 ng/g of kaempferol was found in spiny APRR3 variety, this was comparatively less in TSF-1 (169.69 ng/g). The spineless NARI-NH-01 and NARI-06 possessed 177.20 and 107.80 ng of kaempferol/g of aqueous extract, respectively. Kaempferol was found to be predominantly present in all varieties except APRR3, which has rutin as major flavonoid. In a nutshell, the study revealed the presence of higher amount of bioactive flavonoids in spiny safflower petals of sagaramutyalu (APRR3) variety.

Chapter 6
Summary and Conclusion

6. SUMMARY AND CONCLUSION

PART I

Over 20 species of *Oldenlandia* are in clinical use to treat various diseases. *O. diffusa* and *O. corymbosa* are the active ingredients in many Chinese Traditional Medicines, such as Peh-hue-juwa-chi-cao, Jiedu Yanggan Gao powder, Xiao Wei Yan powder and Feibao syrup which are used in the treatment of cancer (Lajis and Ahmad 2006). Search of such medicinally important species referred in Indian System of Medicine which is widely distributed in India lead to the selection of *O. umbellata* plant to analyze the possibility of its use as a substitute for *O. diffusa*. The identification characters of *O. umbellata* were established based on the microscopical studies of leaves and stems. The leaf was dorsiventral with planoconvex prominent midrib and thick lamina. The adaxial epidermis was thick, cells were vertically oblong and thin walled. The cuticle was fairly prominent. The abaxial epidermal layer was thin and cells were narrow and cylindrical. The stem was circular in cross section, comprising thick epidermal cells (50 μm), thin walled compact parenchyma cells in cortex zone, vascular strands and circular, homogeneous thin walled pith cells. The vessels were up to 20 μm in diameter.

Chemical investigations on *O. umbellata* involved methanolic extraction of aerial parts (**HUM**) followed by fractionation using diethyl ether (**HUM-E**) and n-butanol (**HUM-B**). Finger printing of **HUM-E** and **HUM-B** by HPLC-PDA-ESI-MS analysis explored the presence of eighteen and nine major constituents, respectively.

Chromatographic separation of **HUM-E** and subsequent purification using silica gel, Diaion resin (HP-20) and preparative RP-HPLC (Luna C$_{18}$, 250 $\times$ 21.20 mm, 5μm) afforded seven compounds, which were designated as **HU-1** to **HU-7**. Fraction **HUM-B** was subjected

170

for reverse phase chromatography over Diaion resin (HP-20) followed by repeated chromatography which yielded five compounds coded as, **HU-8** to **HU-12**. The homogeneity of the isolated compounds was determined by RP-HPLC analysis. The structure of isolated compounds was identified based on their physio-chemical, UV-Visible, FT-IR, 1D-, 2D NMR and Mass spectral analysis. Based on the extensive spectral studies, **HU-1** was characterized to be a novel symmetrical coumarin dimer, trivially named as Oledicoumarin (**1**). Compounds **HU-2** to **HU-7** were identified as pheophorbide A methyl ester (**2**), cedrelopsin (**3**), ursolic acid (**4**), 1,2-dimethoxy-3-hydroxy-9,10-anthracenedione (**5**), 1,3-dimethoxy-2-hydroxy-9,10-anthracenedione (**6**) and hedyotiscone B (**7**), respectively. To the best of our knowledge, compounds **HU-2** (**2**) and **HU-3** (**3**) are reported for the first time from Rubiaceae family. Also, this is the second report of isolation of **HU-7** (**7**) from natural source.

Compounds **HU-8** to **HU-12** isolated from the polar fraction **HUM-B** were determined as asperulosidic acid (**8**), deacetyl-asperuloside (**9**), feretoside (**10**), scandoside (**11**) and 6α-hydroxygeniposide (**12**), respectively based on careful spectral analysis. Existence of these compounds in *O. umbellata* is reported for the first time.

The cytotoxic effect of mother extracts (**HUM**, **HUM-E** and **HUM-B**) and isolated compounds were studied on three tumor cell lines (A549, MDA-MB-231 and HT-29) using MTT assay. Compounds **HU-1**, **HU-7**, **HU-11** and **HU-12** were not tested for cytotoxic effect as they were obtained in trace quantity. Of the tested extracts, only **HUM-E** showed significant cytotoxicity with IC_{50} values of 25.7, 67.7 and 69.3 μg/mL, against HT-29, A549 and MDA-MB-231, respectively. Amongst the isolated compounds, **HU-2**, **HU-3**, **HU-4**, **HU-5** and **HU-6** showed significant inhibition against A549 cells with IC_{50} values between 3.6-7.2 μg/mL. In addition, compounds **HU-2**, **HU-4**, **HU-5** and **HU-6** showed marked inhibitory effect against MDA-MB-231 cells (IC_{50} 3.6-9.1 μg/mL). Further, compounds **HU-**

2, **HU-4** and **HU-8** demonstrated promising growth inhibitions against HT-29 cells with IC_{50} values of 1.7-6.1 μg/mL. Interestingly none of the compounds were found to be toxic on human normal cells (HEK 293) except **HU-8**.

For the first time the extract of *O. umbellata* and its fractions were explored for its cytotoxic effect. Bio-active ether fraction culminated the isolation of seven compounds. The promising activity of **HUM-E** against HT-29 and MDA-MB-231 could be due to the presence of **HU-2** (IC_{50} 1.7 μg/mL) and **HU-4** (IC_{50} 4.9 μg/mL). Similarly, compounds **HU-2**, **HU-3** and **HU-4** could be rationalized for the growth inhibition effect of **HUM-E** against A549 cells. However, the isolated single entities were found to be much effective than the mother fraction **HUM-E**. This suggested that **HUM-E** can be enriched with these bioactive molecules and standardized to be developed as a 'botanical'. The crude extract **HUM** and its polar fraction, **HUM-B** did not show any inhibition on HT-29 and A549 cells. However, very less inhibition was found on MDA-MB-231 (7% and 18.4% respectively) cells at 200 μg/mL. Surprisingly, compound **HU-8** exhibited significant inhibition on HT-29 cells (IC_{50}: 6.1 μg/mL) although the mother fraction, **HUM-B** was found to be inactive. Further, LC-MS finger print analysis unveiled the fact that the inactive compound **HU-10** was found to be present predominantly (53.42%) in **HUM-B**, thereby responsible for its non-cytotoxicity.

The results of chemical investigation and cytotoxic studies proved similarity between *O. umbellata* and the well established species, *O. diffusa*. Thus the study validated the possibility of usage of *O. umbellata* as a substitute for *O. diffusa*.

PART II

Four varieties of safflower petals, two each of spiny (APRR3 and TSF-1) and non-spiny (NARI-NH-01 and NARI-06) were collected and subjected for systematic quantitative pharmacognostic studies as per WHO guidelines. All four varieties were found to comply

with the WHO standard limits pertaining to ash values and moisture content. The extractive values suggested that cold maceration is suitable for spiny varieties whereas non-spiny varieties afforded highest yield in hot extraction method. Tannin content was found to be comparatively more in TSF-1 (26.25%) than other varieties which ensured the astringent effect of safflower petals. Foaming test and haemolytic activity suggested that the content of saponins was very less or might be absent. Higher bitterness value of APRR3 suggested that the spiny varieties could promote digestion better than non-spiny varieties. The microscopical characters of corolla and style of spiny and non-spiny safflower petals were found to be indistinguishable.

Presence of heavy metals like arsenic, cadmium, chromium, lead and mercury were determined by atomic absorption spectroscopic method. Results indicated that only APRR3 was safe for consumption as the tested heavy metals were within the prescribed limit. The consumption of other varieties could cause cadmium toxicity leading to reproductive hazards, cancer, heart disease, zinc-deficiency (Linder 1985). Similarly, presence of common pesticides in the safflower petals was analyzed by gas chromatography. A total of 15 organochlorines, 9 organophosphates and 14 synthetic pyrethroids were tested. Interestingly none were detected in any of the varieties.

It was identified from the thorough literature survey that, most of the clinically used formulations were prepared from water extract of safflower petals. Also, it was reported that the water soluble flavonoids were responsible for the broad spectrum of biological properties like antioxidant effect. Hence, an attempt was made to quantify three water soluble flavonoids namely rutin, quercetin and kaempferol by HPTLC. Results demonstrated higher quantity of all three flavonoids in APRR3 than other varieties. Based on the extensive quality control and quantification studies, the spiny safflower petals of APRR3 variety was found to be safe for consumption and more effective than other three varieties.

Future Scope of Work

FUTURE SCOPE OF WORK

Part I

- Isolation and characterization of other constituents present in the cytotoxic **HUM-E** fraction, as evidenced by LC-MS analysis can be attempted.

- The selective inhibition of A549 cells by **HU-3** need to be studied extensively to understand the mechanism of action. Anticancer studies on other coumarin derivatives, **HU-1** and **HU-7** can also be carried out in future.

- Lead optimization of **HU-2** may provide potent new therapeutic agents against lung, breast and colon cancer.

- Testing of aglycones of isolated iridoid glycosides may yield some useful leads.

- The isolated active compounds can be explored for their effect on other cancer cell lines too. In-vivo anticancer studies of **HU-2** and **HU-3** can also be initiated.

PART II

- In-vivo toxicity studies of decoction of APRR3 safflower petals can be performed to ensure its safety.

- Defined extract of APRR3 safflower petals can be formulated to develop it as a botanical product.

References

REFERENCES

Ahmed, K. M.; Marzouk, M. S.; el-Khrisy, E. A.; Wahab, S. A.; el-Din S. S. A new flavone diglycoside from *Carthamus tinctorius* seeds. *Pharmazie* **2000**, *55*, 621-622.

Akihisa, T.; Nozaki, A.; Inoue, Y.; Yasukawa, K.; Kasahara, Y.; Motohashi, S.; Kumaki, K.; Tokutake, N.; Takido, M.; Tamura, T. Alkane diols from flower petals of *Carthamus tinctorius*. *Phytochemistry* **1997**, *45*, 725-728.

Akihisa, T.; Yasukawa, K.; Oinuma, H.; Kasahara, Y.; Yamanouchi, S.; Takido, M.; Kumaki K.; Tamura, T. Triterpene alcohols from the flowers of compositae and their anti-inflammatory effects. *Phytochemistry* **1996**, *43*, 1255-1260.

Asgarpanah, J.; Kazemivash, N. Phytochemistry, pharmacology and medicinal properties of *Carthamus tinctorius* L. *Chinese Journal of Integrative Medicine* **2013,** *19*, 153-159.

Audomkasok, S.; Singpha, W.; Chachiyo, S.; Somsak, V. Antihemolytic activities of green tea, safflower and mulberry extracts during *Plasmodium berghei* infection in mice. *Journal of Pathogens* [Online early access]. DOI: 10.1155/2014/203154.

Blumenthal, M. Herb industry sees mergers, acquisitions, and entry by pharmaceuticals giants in 1998. *HerbalGram* **1999**, *45*, 67-68.

Brevoort, P. The U.S. botanical market. An overview. *HerbalGram* **1995**, *36*, 49-59.

Butler, M. S.; Robertson, A. A. B.; Cooper, M. A. Natural product and natural product derived drugs in clinical trials. *Natural Product Reports* **2014**, *31*, 1612-1661.

Chen, J.; Tu, P.; Jiang, Y. HPLC fingerprint-oriented preparative separation of major flavonoids from safflower extract by preparative pressurized liquid chromatography. *Journal of Chinese Pharmaceutical Sciences* **2014**, *23*, 490-495.

Chen, L.; Xiang, Y.; Kong, L.; Zhang, X.; Sun, B.; Wei, X.; Liu, H. Hydroxysafflor yellow A protects against cerebral ischemia-reperfusion injury by anti-apoptotic effect through PI3K/Akt/GSK3β pathway in rat. *Neurochemical Research* **2013a**, *38*, 2268-2275.

Chen, Y.; S.; Lee, S. M.; Lin, C. C.; Liu, C. Y.; Wu, M. C.; Shi, W. L. Kinetic study on the tyrosinase and melanin formation inhibitory activities of carthamus yellow isolated from *Carthamus tinctorius* L. *Journal of Bioscience and Bioengineering* **2013b**, *115*, 242-245.

Chen, S. H.; Su, J. Y.; Wu, M. J. Hedyotis pinifolia Wall.ex G. Don (Rubiaceae), a new record to the flora of Taiwan. *Taiwania* **2010**, *55*, 86-89.

Chen, Y. H.; Chang, F. R.; Wu, C. C.; Yen, M. H.; Liaw, C. C.; Huang, H. C.; Kuo, Y. H.; Wu, Y. C. New cytotoxic 6-oxygenated 8,9-dihydrofurocoumarins, hedyotiscone A-C, from *Hedyotis biflora*. *Planta Medica* **2006**, *72*, 75-78.

Cong, H.; Cong, A. Chinese medicinal decoction for treating postmenopausal osteoporosis. *Faming Zhuanli Shenqing* **2014**, CN 104225159 A 20141224.

Cragg, G. M.; Kingston, D. G. I.; Newman, D. J. Anticancer agents from natural products: Boca Raton, FL, 2005; pp 5-176.

Cragg, G. M.; Newman, D. J. Naturals products: a continuing source of novel drug leads. *Biochimica et Biophysica Acta* **2013**, *1830*, 3670-3695.

Cragg, G. M.; Newman, D. J. Plants as a source of anticancer agents. *Journal of Ethnopharmacology* **2005**, *100*, 72-79.

Dajue, L.; Mundel, H. H. Safflower. Carthamus tinctorius L: In Promoting the conservation and use of underutilized and neglected crops; Rome, Italy, 1996; pp 8-83.

De, S.; Dey, A.; Sudhakar Babu, A. M. S.; Aneela, S. In-vitro anthelmintic activity of aqueous and methanolic extracts of *Oldenlandia umbellata*. *International Journal of Pharmacy and Pharmaceutical Sciences* **2014**, *6*, 94-95.

Denholm, J. Complementary medicine and heavy metal toxicity in Australia. *WebmedCentral* **2010**, *1*, 1-6.

Diaz, A. N. Absorption and emission spectroscopy and photochemistry of 1,10-anthraquinone derivatives: a review. *Journal of Photochemistry and Photobiology A: Chemistry* **1990**, *53*, 141-167.

Droge, W. Free radicals in the physiological control of cell function. Physiological Reviews. **2002**, *82*, 47-95.

Esau, K. Plant Anatomy: New York, 1964; pp 767.

Eshiett, I. T.; Taylor, D. A. H. The isolation and structure elucidation of some derivatives of dimethyl-allyl-coumarin, chromone, quinoline and phenol from *Fagara* species and from *Cedrelopsis grevei*. *Journal of the Chemical Society C: Organic* **1968**, 481-484.

Fan, L.; Zhao, H. Y.; Xu, M.; Zhou, L.; Guo, H.; Han, J.; Wang, B. R.; Guo, D. A. Quality evaluation and quantitative determination of 10 major active components in *Carthamus tinctorius* L. by high-performance liquid chromatography coupled with diode array detector. *Journal of Chromatography A* **2009**, *1216*, 2063-2070.

Fenik, J.; Tankiewicz, M.; Biziuk, M. Properties and determination of pesticides in fruits and vegetables. *Trends in Analytical Chemistry* **2011**, *30*, 814-826.

Folashade, K. O.; Omoregie, E. H.; Ochogu, A. P. Standardization of herbal medicines-A review. *International Journal of Biodiversity and Conservation* **2012**, *4*, 101-112.

Fraga, B. M.; Quintana, N.; Diaz, C. E. Anthraquinones from natural and transformed roots of *Plocama pendula*. *Chemistry & Biodiversity* **2009**, *6*, 182-192.

Ghiyasi, S.; Karbassi, A.; Moattar, F.; Modabberi, S.; Sadough, M. B. Origin and concentrations of heavy metals in agricultural land around aluminium industrial complex. *Journal of Food, Agriculture & Environment* **2010**, *8*, 1237-1240.

Gold, L. S.; Slone, T. H.; Annes, B. N.; Manley, N. B. Pesticide residue on food and cancer risk: A critical analysis: In Handbook of Pesticide Technology; San diego, CA, 2001; pp 799-843.

Guimiao, W.; Yilli, L. Clinical application of safflower (*Carthamus tinctorius*). *Zhejiang Traditional Chinese Medical Science J* **1985**, *1*, 42-43.

Guo, M.; Zhang, G.; Zhang, W.; Zhang, H.; Su, Z. Determination of safflor yellow A by RP-HPLC and resources quality comparison in *Carthamus tinctorius*. *Zhongguo Zhongyao Zazhi* **2006**, *31*, 1234-1236.

Han, S.; Huang, J.; Cui, R.; Zhang, T. Screening anti-allergic components from *Carthamus tinctorius* using RBL-2H3 cell membrane chromatography combined with high-performance liquid chromatography and tandem mass spectrometry. *Journal of separation science* [Online early access] DOI: 10.1002/jssc.201401275.

Hang, C.; Dunyi, Z.; Jinglian, X.; Shuzhen, C,; Shuying, H. Yi Qi Hua Yu prescription was used for treatment on chronic gastritis of 106 cases. *Journal of Combination of Traditional Chinese and Western Medicine* **1985**, *5*, 267-268.

He, J.; Yang, Y. N.; Jiang, J. S.; Feng, Z. M.; Zhang, P. C. Saffloflavonesides A and B, two rearranged derivatives of flavonoid C-glycosides with a furan-tetrahydrofuran ring from *Carthamus tinctorius*. *Organic Letters* **2014a**, *16*, 5714-5717.

He, J.; Chen, Z.; Yang, Y. N.; Jiang, J. S.; Feng, Z. M.; Zhang, P. C. Chemical constituents from aqueous extract of *Carthamus tinctorius*. *Zhongguo Yaoxue Zazhi* (Beijing, China) **2014b**, *49*, 455-458.

Hema, V.; Venkidesh, R.; Maheswari, E. Antitussive activity of *Oldenlandia umbellata*. *International Journal of Chemical Sciences* **2007**, *5*, 2480-2484.

Honghai, Y. Treatment of bone arthritis with Shenjindan (muscle stretching powder) of 126 cases. *Shandong Traditional Chinese Medical Science Journal*. **1985**, *1*, 21-25.

Huang, J. L.; Fu, S. T.; Jiang, Y. Y.; Cao, Y. B.; Guo, M. L.; Wang, Y.; Xu, Z. Protective effects of Nicotiflorin on reducing memory dysfunction, energy metabolism failure and oxidative stress in multi-infarct dementia model rats. *Pharmacology Biochemistry Behavior* **2007**, *86*, 741-748.

Isiguro, K.; Yamaki, M.; Takagi. S.; Ikeda, Y.; Kawakami, K.; Ito, K.; Nose, T. Studies on iridoid-related compounds. IV. Antitumor activity of iridoid aglycones. Chemical and Pharmaceutical Bulletin (Tokyo) **1986**, *34*, 2375-2379.

Jabeen, S.; Shah, M. T.; Khan, S.; Hayat, M. Q. Determination of major and trace elements in ten important folk therapeutic plants of Haripur basin, Pakistan. *Journal of Medicinal Plants Research* **2010**, *4*, 559-566.

Jiang, J. S.; Chen, Z.; Yang, Y. N.; Feng, Z. M.; Zhang, P. C. Two new glycosides from the florets of *Carthamus tinctorius*. *Journal of Asian Natural Products Research* **2013**, *15*, 427-432.

Jiang, J. S.; He, J.; Feng, Z. M.; Zhang, P. C. Two new quinochalcones from the florets of *Carthamus tinctorius*. *Organic Letters* **2010**, *12*, 1196-1199.

Jiang, T. F.; Lv, Z. H.; Wang, Y. H. Separation and determination of chalcones from *Carthamus tinctorius* L. and its medicinal preparation by capillary zone electrophoresis. *Journal of Separation Science* **2005**, *28*, 1244-1247.

Jiang, Z. S.; Wang, L. N.; Weng, W. Determination of the hydroxysafflor yellow A contents of safflower extract and aceglutamide injection by HPLC. *Zhongguo Xiandai Zhongyao* **2011**, *13*, 26-28.

Jianxin, L. The treatment on joint wrench of 458 cases by Chinese medicine ointment for external application. *Journal of PLA Medicine* **1989**, *14*, 228.

Jin, Y.; Xiao, Y. S.; Zhang, F. F.; Xue, X. Y.; Xu, Q.; Liang, X. M. Systematic screening and characterization of flavonoids glycosides in *Carthamus tinctorius* L. by liquid chromatography/UV diode-array detection/electrospray ionization tandem mass spectrometry. *Journal of Pharmaceutical and Biomedical Analysis* **2008**, *46*, 418-430.

Johansen, D. A. Plant Microtechnique; New York, 1940; pp 523.

Joseph, J. M.; Sowndhararajan, K.; Manian, S. Protective effects of methanolic extract of *Hedyotis puberula* (G. Don) R. Br. ex. Arn. against experimentally induced gastric ulcers in rat. *Journal of Ethnopharmacology* **2010**, *131*, 216-219.

Kamiya, K.; Fujita, Y.; Saiki, Y.; Hanani, E.; Mansur, U.; Satake, T. Studies on the constituents of Indonesian *borreria latifolia*. *Heterocycles* **2002**, *56*, 537-544.

Khan, S. A.; Khan, L.; Hussain, I.; Marwat, K. B.; Ashtray, N. Profile of heavy metals in selected medicinal plants. *Pakistan Journal of Weed Science Research* **2008**, *14*, 101-110.

Konishi, M.; Hano, Y.; Takayama, M.; Nomura, T.; Hamzah, A. S.; Ahmad, R. B.; Jasmani, H. Triterpenoid saponins from *Hedyotis nudicaulis*. *Phytochemistry* **1998**, *48*, 525-528.

Koyama, N.; Kuribayashi, K.; Seki, T.; Kobayashi, K.; Furuhata, Y.; Suzuki, K.; Arisaka, H.; Nakano, T.; Amino, Y.; Ishii, K. Serotonin derivatives, major safflower (*Carthamus tinctorius* L.) seed antioxidants, inhibit low density lipoprotein (LDL) oxidation and atherosclerosis in Apolipoprotein E-deficient mice. *Journal of Agricultural and Food Chemistry* **2006**, *54*, 4970-4976.

Kruawan, K.; Kangsadalampai, K. Antioxidant activity, phenolic compound contents and antimutagenic activity of some water extract of herbs. *Thai Journal of Pharmaceutical Science* **2006**, *30*, 28-35.

Kurkin, V. A.; Kharisova, A. V. Flavonoids of *Carthamus tinctorius* flowers. *Chemistry of Natural Compounds* **2014**, *50*, 446-448.

Lajis, N. H. J.; Ahmad, R. Phytochemical studies and pharmacological activities of plants in genus *Hedyotis*/*Oldenlandia*: In Studies in natural products chemistry; Rahman, A. U., Ed.; **2006**, *33*, 1057-1090.

Lee, J. Y.; Chang, E. J.; Kim, H. J.; Park, J. H.; Choi, S. W. Antioxidative flavonoids from leaves of *Carthamus tinctorius*. *Archives of Pharmacol Research* **2002**, *25*, 313-319.

Lehotay, S. J. Determination of pesticide residues in foods by acetonitrile extraction and partitioning with magnesium sulphate: Collaborative study. *Journal of AOAC International* **2007**, *90*, 485-520.

Li, Q.; Song, T.; Wang, G.; Liu, Y. Determination of Puerarin and HSYA in extracts of *Radix Puerariae*, *Fructus crataegi* and *Carthamus tinctorius* by HPLC. *Shizhen Guoyi Guoyao* **2008**, *19*, 1860-1861.

Li, W. C.; Wang, X. Y.; Lin, P. C.; Hu, N.; Zhang, Q. L.; Suo, Y. R.; Ding, C. X. Preparative separation and purification of four cis-trans isomers of coumaroylspermidine analogs from safflower by high-speed counter current chromatography. *J Chromatogr B* **2013**, *938*, 75-79.

Li, X. F.; Hu, X. R.; Dai, Z.; Zhang, Y.; Liang, H.; Lin, R. C. Study on chemical constituents of *Carthamus tinctorius*. *Zhong Yao Cai* **2012**, *35*, 1616-1619.

Li, Y.; Piao, D.; Zhang, H.; Kim, T.; Lee, S. H.; Chang, H. W.; Woo, M. H.; Son, J. K. Quality evaluation of *Carthami Flos* by HPLC-UV. *Archives of Pharmacol Research* [Online early access]. 2014a, DOI: 10.1007/s12272-014-0402-9.

Li, Y. Y.; Wu, Y.; Guan, Y.; Wang, Z.; Zhang, L. Hydroxysafflor yellow A induces apoptosis in MCF-7 cells by blocking NFκB/p65 pathway and disrupting mitochondrial transmembrane potential. *RSC Advances* **2014b**, *4*, 47576-47586.

Lianen, W. Yi Qi Huo Xue prescription used for treatment of gastritis. *Journal of Jiangsu Traditional Chinese Medical Science* **1992**, *13*, 35-37.

Liang, X. M.; Jin, Yu.; Feng, J. T.; Ke, Y. X. Identification and structure elucidation of compounds from herbal medicines: In Traditional herbal medicine research methods:

Identification, analysis, bioassay and pharmaceutical and clinical studies; Liu, W. J. H., Ed.; Hoboken, NJ, USA, 2011; pp 139-223.

Liao, H.; Banbury, L.; Liang, H.; Wang, X.; Lu, X.; Hu, L.; Wu, J. Effect of honghua (*Flos Carthami*) on nitric oxide production in RAW 264.7 cells and alpha-glucosidase activity. *Journal of Traditional Chinese Medicine* **2014**, *34*, 362-368.

Lin, C. C.; Ng, L. T.; Yang, J. J.; Hsu, Y. F. Anti-inflammatory and hepatoprotective activity of Peh-Hue-Juwa-Chi-Cao in male rats. *The American Journal of Chinese Medicine* **2002**, *30*, 225-234.

Lin, J.; Chen, Y.; Wei, L.; Chen, X.; Xu, W.; Hong, Z.; Sferra, T. J.; Peng, J. *Hedyotis diffusa* Willd extract induces apoptosis via activation of the mitochondrion-dependent pathway in human colon carcinoma cells. *International Journal of Oncology* **2010**, *37*, 1331-1338.

Linder, M. Nutritional Biochemistry and Metabolism; New York, 1985; pp 70.

Liu, E. H.; Zhou, T.; Li, G. B.; Li, J.; Huang, X. N.; Pan, F.; Gao, N. Characterization and identification of iridoid glucosides, flavonoids and anthraquinones in *Hedyotis diffusa* by high-performance liquid chromatography/electrospray ionization tandem mass spectrometry. *Journal of Separation Science* **2012**, *35*, 263-272.

Liu, H.; Huang, Z.; Luo, Z. Determination of 6-hydroxylkaempferol-3-O-glycoside in *Carthamus tinctorius* by HPLC. *Zhongcaoyao* **2001**, *32*, 707-708.

Liu, J.; Zhang, J.; Wang, F. A new flavanone glucoside from the flowers of *Carthamus tinctorius* and assignment of absolute configuration. *Chemistry of Natural Compounds* **2014**, *50*, 427-429.

Liu, S. Y.; Li, W. L.; Qu, H. B.; Zhao, B. C.; Zhao, T. On-line detection of Salvia miltiorrhiza and *Carthamus tinctorius* injection based on near-infrared spectroscopy. *Zhongguo Zhongyao Zazhi* **2013**, *38*, 1657-1662.

Liu, Y. L.; Liu, Y. J.; Liu, Y.; Li, X. S.; Liu, S. H.; Pan, Y. G.; Zhang, J.; Liu, Q.; Hao, Y. Y. Hydroxy safflower yellow A ameliorates lipopolysaccharide-induced acute lung injury in mice via modulating toll-like receptor 4 signalling pathways. *International Immunopharmacology* **2014a**, *23*, 649-657.

Liu, Y.; Tian, X.; Cui, M.; Zhao, S. Safflower yellow inhibits agiotensin II induced adventitial fibroblast proliferation and migration. *Journal of Pharmaceutical Sciences* (Tokyo, Japan) **2014b**, *126*, 107-114.

Liu, Y.; Yang, J.; Liu, Q. Studies on chemical constituents from the flowers of *Carthamus tinctorius* L. *Zhong Yao Cai* **2005**, *28*, 288-289.

Long, Z. H.; Wen, Z. Q.; Qi, Z. X.; Cai, Y. W.; Tao, W. Y. Chemical constituents from the roots of *Morinda officinalis*. *Chinese Journal of Natural Medicine* **2010**, *8*, 192-195.

Luo, D. A. Chinese medicinal granule for the treatment of rheumatic arthritis and its preparation method. *Faming Zhuanli Shenqing* **2004**, CN 104248681 A 20141231.

Ma, G. N.; Yu, F. L.; Wang, S.; Li, Z. P.; Xie, X. Y.; Mei, X. G. A novel oral preparation of hydroxysafflor yellow A base on a chitosancomplex: A strategy to enhance the oral bioavailability. *AAPS PharmSciTech* [Online early access] DOI: 10.1208/s12249-014-0255-z.

Malaya, G.; Mazumder, U. K.; Thamilselvan, V.; Manikandan, L.; Senthilkumar, G. P.; Suresh, R.; Kakotti, B. K. Potential hepatoprotective effect and antioxidant role of methanol extract of *Oldenlandia umbellata* in carbon tetrachloride induced

hepatotoxicity in wistar rats. *Iranian Journal of Pharmacology and Therapeutics* **2007**, *6*, 5-9.

Maobe, M. A. G.; Gatebe, E.; Gitu, L.; Rotich, H. Profile of heavy metals in selected medicinal plants used for the treatment of diabetes, malaria and pneumonia in Kisii region, Southwest Kenya. *Global Journal of Pharmacology* **2012**, *6*, 245-251.

Mariswamy, Y.; Gnaraj, W. E.; Antonisamy, J. M. Chromatographic fingerprint analysis on flavonoids constituents of the medicinally important plant *Aerva lanata* L. by HPTLC technique. *Asian Pacific Journal of Tropical Biomedicine* **2011**, *1*, S8-S12.

Meselhy, M. R.; Kadota, S.; Momose, Y.; Hatakeyama, N.; Kusai, A.; Hattori, M.; Namba, T. Two new quinochalcone yellow pigments from *Carthamus tinctorius* and Ca^{2+} antagonistic activity of tinctormine. *Chemical and Pharmaceutical Bulletin* **1993**, *41*, 1796-1802.

Meselhy, M. R.; Kadota, S.; Momose, Y.; Hattori, M.; Namba, T. Tinctormine, a novel Ca^{2+} antagonist *N*-containing quinochalcone *C*-glycoside from *Carthamus tinctorius* L. *Chemical and Pharmaceutical Bulletin* **1992**, *40*, 3355-3357.

NARI Home Page. http://nariphaltan.org/safflower.pdf (accessed Sep 10, 2014).

National Medicinal Plants Board, Home Page. http://www.nmpb.nic.in/ (accessed Feb 5, 2014).

Newman, D. J.; Cragg, G. M.; Snader, K. M. Natural products as source of new drugs over the period 1981-2002. *Journal of Natural Products* **2003**, *66*, 1022-1037.

Niu, Y.; Meng, Q. X. Chemical and preclinical studies on *Hedyotis diffusa* with anticancer potential. *Journal of Asian Natural Products Research* **2013**, *15*, 550-565.

NSF International standard for dietary supplements-NSF/ANSI 173-2010; Michigan, USA, 2011; pp. 37.

Obara, H.; Onodera, J. I. Structure of carthamin. *Chemistry Letters* **1979**, *8*, 201-204.

O'Brien, T. P.; Feder, N.; Mc Cully, M. E. Polychromatic staining of plant cell walls by toluidine blue O. *Protoplasma* **1964**, *59*, 364-373.

Olaleye, O.; Li, S. S.; Liu, H. T.; Chai, X.; Wang, Y. F.; Gao, X. M. Studies on chemical constituents and DPPH free radical scavenging activity of Carthamus tinctorius L. *Tianran Chanwu Yanjiu Yu Kaifa* **2014**, *26*, 60-63.

Onodera, J. I.; Obara, H.; Hirose, R.; Matsuba, S.; Sato, N.; Sato, S.; Suzuki, M. The structure of safflomin C, a constituent of safflower. *Chemistry Letters* **1989**, *18*, 1571-1574.

Onodera, J. I.; Obara, H.; Osone, M.; Maruyama, Y.; Sato, S. The structure of safflomin-A, A component of safflower yellow. *Chemistry Letters* **1981**, *3*, 433-436.

Padhy, I. P.; Endale, A. Evaluation of anti-inflammatory and antipyretic activity of *Oldenlandia umbellata* Linn. roots. *International Journal of Pharmacy and Health Care Research* **2014**, *02*, 12-4.

Park, J. B. Serotomide and safflomide modulate forskolin stimulated cAMP formation via 5-HT1 receptor. *Phytomedicine* **2008**, *15*, 1093-1098.

Peng, J. N.; Feng, X. Z.; Zheng, Q. T.; Liang, X. T. A β-carboline alkaloid from *Hedyotis chrysotricha*. *Phytochemistry* **1997**, *46*, 1119-1121.

Perkin, A. G.; Hummel, J. J. The colouring and other principles contained in chay root. *Journal of the Chemical Society Transcations* **1893**, *63*, 1160-1184.

Phuong, N. M.; Sung, T. V.; Schmidt, J.; Porzel, A.; Adam, G. Capitelline - A new indole alkaloid from *Hedyotis capitellata*. *Natural Product Letters* **1998**, *11*, 93-100.

Purushothaman, K. K.; Saradambal, S.; Narayanaswami, V. Isolation and identification of some anthraquinones derivatives from *Oldenlandia umbellata*. *Leather Science* (Madras) **1968**, *15*, 49-51.

Qingliang, S.; Nengquan, C.; Daoxi, S.; Yunguang, B. Experimental studies on the antithrombus effect of E-Hong injection liquor. *Chinese Traditional Medicine Bulletin* **1988**, *13*, 46-47.

Ramamoorthy, S. M.; Gaurav, D.; Rajesh, K. F.; Nawaz, V.; Vijayakumar, C.; Rajasekaran, *Natural Product Research* **2009**, *23*, 1210.

Rekha, S.; Srinivasan, V.; Vasanth, S.; Gopal, R. H. The in-vitro antibacterial activity of *Hedyotis umbellata*. *Indian Journal of Pharmaceutical Sciences* **2006**, *68*, 236-238.

Rho, M. C.; Chung, M. Y.; Song, H. Y.; Kwon, O. E.; Lee, S. W.; Baek, J. A.; Jeune, K. H.; Kim, K.; Lee, H. S.; Kim, Y. K. Pheophorbide A-methyl ester, Acyl-CoA: Cholesterol acyltransferase inhibitor from *Diospyros kaki*. *Archives of Pharmacal Research* **2003**, *26*, 716-718.

Sai, W. A report on the treatment of chronic suppurative osteomyelitis of 520 cases. *Tianjin Traditional Chinese Medical Science* **1992**, *2*, 6-7.

Santana, L. D.; Ferreira, A. B. B.; Lorensen, M. C. A.; Berbara, R. L. L.; Castro, R. N. Correlation of total phenolic and flavonoid contents of Brazilian honeys with colour and antioxidant capacity. *International Journal of Food Properties* **2014**, *17*, 65-76.

Sarma, H.; Deka, S.; Deka, H.; Saikia, R. R. Accumulation of heavy metals in selected medicinal plants. *Reviews of Environmental Contamination and Toxicology* **2012**, *214*, 63-86.

Sass, J. E. Elements of botanical microtechnique; New York, 1940; pp 222.

Shang, M.; Fangxing, L.; Shangrui, W.; Shuping, D.; Shengguang, Y.; Changlian, X.; Zongli, L. The curative effect of Wei-You for treatment on atrophic gastritis of 910 cases. *Journal of Traditional Chinese Medicine* **1989**, *30*, 32-33.

Shao, J. F.; Wang, Y. B.; Chen, Q.; Liu, Z. Q.; Liu, Q.; Cai, W. G.; Wu, W. A daily variation in essential oil composition of flower of different accessions from *Carthamus tinctorius* L. in Sichuan province of China. *Journal of Medicinal Plants Research* **2011**, *5*, 3042-3051.

Shengyun, W. Sanhua atomizing agent used for treatment of 100 cases of acute throat diseases. *Journal of Heilongjiang Traditional Chinese Medicine* **1985**, *6*, 23-24.

Shulin, L. Treated of goitre with goitre-resolved therapy. Sichuan Traditional Chinese Medical Science **1992**, *10*, 47.

Shuqun, H.; Guangyi, Z.; Wenjun, Z. Inhibition effects of safflower on the activity of Ca2$^+$/CaM-Pk II in the model of cerebral ischemia. *Journal of Xuzhou Medical College* **1995**, *15*, 349-351.

Sivaprakasam, S. S. K.; Karunakaran, K.; Subburaya, U.; Kuppusamy, S.; Subashini T. S. A review on phytochemical and pharmacological profile of *Hedyotis corymbosa* Linn. *International Journal of Pharmaceutical Sciences Review and Research* **2014**, *26*, 320.

Song, Y.; Long, L.; Zhang, N.; Liu, Y. Inhibitory effects of hydroxysafflor yellow A on PDGF-BB-induced proliferation and migration of vascular smooth muscle cells via mediating Akt signalling. *Molecular Medicine Reports* **2014**, *10*, 1555-1560.

Sowemimo, A.; Venter, M. V. D.; Baatjies, L.; Koekemoer, T.; Adesanya, S.; Lin, W. Cytotoxic compounds from the leaves of *Combretum paniculatum* Vent. *African Journal of Biotechnology* **2012**, *11*, 4631-4635.

Steenkamp, V.; Stewart, M. J.; Curowska, E.; Zuckerman, M. A severe case of multiple metal poisoning in a child treated with a traditional medicine. *Forensic Science International* **2002**, *128*, 123-126.

Stewart, B. W.; Wild, C. P. World Cancer Report 2014: Geneva, 2014.

Street, R. A. Heavy metals in medicinal plant products-An African perspective. *South African Journal of Botany* **2012**, *82*, 67-74.

Sun, Y.; Guo, T.; Sui, Y.; Li, F. M. Determination of adenosine, rutin and quercetin in *Carthamus tinctorius* by HPCE. *Acta Pharmaceutica Sinica* **2003**, *38*, 283-285.

Takii, T.; Kawashima, S.; Chiba, T.; Hayashi, H.; Hayashi, M.; Hirmura, H.; Inukai, Y.; Shibata, Y.; Nagatsu A.; Sakakibara, J.; Oomoto, Y.; Hirose, K.; Onozaki, K. Multiple mechanisms involved in the inhibition of proinflammatory cytokine production from human monocytes by *N*-(*p*-coumaroyl) serotonin and its derivatives. *International Immunopharmacology* **2003**, *3*, 273-277.

Tao, C.; Taylor, C. M. Hedyotis Linnaeus. *Flora of China* **2011**, *19*, 147-174.

Torres, C. M.; Pico, Y.; Manes, J. Determination of pesticide residues in fruit and vegetables. *Journal of Chromatography A* **1996**, *754*, 301-331.

Toyoda, K.; Yaoita, Y.; Kikuchi, M. Three new dimeric benzofuran derivatives from the roots of *Ligularia stenocephala* Matsum. et Koidz. *Chemical and Pharmaceutical Bulletin* **2005**, *53*, 1555-1558.

Tuyen, P. N. K.; Duy, l. H.; Phung, N. K. P. Four flavonoids from *Hedyotis nigricans*. *Tap Chi Hoa Hoc* **2010**, *48*, 546-550.

Vaikosen, E. N.; Alade, G. O. Evaluation of pharmacognostical parameters and heavy metals in some locally manufactured herbal drugs. *Journal Chemical and Pharmaceutical Research* **2011**, *3*, 88-97.

Wang, J.; Sheng, J.; Xie, E.; Zhou, G. HPLC determination of p-coumaric acid in *Carthamus tinctorius* L. of various sources. *Yaowu Fenxi Zazhi* **2011**, *31*, 938-940.

Wang, Y.; Tang, C.; Zhang, H. Hepatoprotective effects of kaempferol 3-O-rutinoside and kaempferol 3-O-glucoside from *Carthamus tinctorius* L. on CCl_4-induced oxidative liver injury in mice. *Journal of Food and Drug Analysis* [Online early access] DOI: 10.1016/j.jfda.2014.10.002.

Weiss, E. A. Castor, Sesame and Safflower; New York, 1971; pp 529-744.

Weiss, E. A. Safflower: In Oilseed crops; London, UK, 1983; pp 216-281.

Wengxuan, Q.; Yunxia, Z.; Daowu, W.; Yanying, Z.; Jianying Y. Effects of safflower yellow pigment on the blood fat and liver function of rabbits. *Journal of Lanzhou College of Medical Science* **1987**, *3*, 57-60.

Wenyu, Z. Tian Ying's prescription was used for treatment on sterility of 77 cases. *Journal Traditional Chinese Medicine* **1986**, *27*, 31-32.

WHO. Quality control methods for medicinal plant materials; Geneva, 1998; pp 8.

Wikstrom, N.; Neupane, S.; Karehed, J.; Motley, T. J.; Bremer, B. Phylogeny of *Hedyotis* L. (Rubiaceae: Spermacoceae): Redefining a complex Asian-Pacific assemblage. *Taxon* **2013**, *62*, 357-374.

Woods, R.; Mills, P. B.; Knobel, G. J.; Hurlow, W. E.; Stokol, J. M. Acute dichromate poisoning after use of traditional purgatives. A report of 7 cases. *South African Medical Journal* **1990**, *77*, 640-642.

Yadava, R. N.; Chakravarti, N. Anti-inflammatory activity of a new triterpenoid saponin from *Carthamus tinctorius* linn. *Journal of Enzyme Inhibition and Medicinal Chemistry* **2008**, *23*, 543-548.

Yaling, L. The application of Chinese herbal medicine in inducing labor for women in later gestation. *Beijing Medical Science* **1985**, *7*, 44.

Yang, L. J.; Wang, L. M.; Yao, M.; Wu, S. H.; Wang, Y. Y. The effectiveness and safety of edaravone combined with safflower yellow injections for the treatment of acute cerebral infarction: a meta-analysis. *Zhongguo Linchuang Yanjiu* **2013**, *26*, 313-316.

Yao, M.; Ren, A.; Dong, Z. RP-HPLC determination of safflomin A and safflower yellow A in *Carthamus tinctorius* L. *Yaowu Fenxi Zazhi* **2010**, *30*, 263-265.

Ye, S. Y.; Gao, W. Y.; Guo, Q.; Yang, B. M.; Du, X. Determination of hydroxysafflor yellow A in Xiaoyuzhitong Qiwuji by HPLC. *Jiefangjun Yaoxue Xuebao* **2007**, *23*, 448-450.

Yin, H. B.; He, Z. S.; Ye, Y. Cartorimine, a new cycloheptenone oxide derivative from *Carthamus tinctorius*. *Journal of Natural Products* **2000**, *63*, 1164-1165.

Yoganarasimhan, S. N. Medicinal Plants of India; Bangalore, India, 2000; pp 262.

Yongna, P. Pharmacological action and clinical application of safflower. *Shizhen Traditional Chinese Medicine* **2005**, *16*, 144-146.

Yongyong, Z.; Jiabo, L. Chemical constituents in herb of *Hedyotis diffusa*. *Zhongyaocai* **2008**, *31*, 522-534.

Youan, D. Observation on the recent curative effect of the traditional Chinese medicine invigorating blood circulation and reducing stasis. *Journal of Combination of Traditional Chinese and Western Medicine* **1988**, *8*, 683.

Yu, H.; Xu, L. X. Separation and determination of flavonoids in the flowers of *Carthamus tinctorius* by RP-HPLC. *Acta Pharmaceutica Sinica* **1997**, *32*, 120-122.

Yue, S.; Tang, Y.; Li, S.; Duan, J. A. Chemical and biological properties of quinochalcone *C*-glycoside from the florets of *Carthamus tinctorius*. *Molecules* **2013**, *18*, 15220-15254.

Yue, S.; Tang, Y.; Xu, C.; Li, S.; Zhu, Y.; Duan, J. A. Two new quinochalcone C-glycosides from the florets of *Carthamus tinctorius*. *International Journal of Molecular Sciences* **2014a**, *15*, 16760-16771.

Yue, S. J.; Tang, Y. P.; Wang, L. Y.; Tang, H.; Li, S. J.; Liu, P.; Su, S. L.; Duan, J. A. Separation and evaluation of antioxidant constituents from *Carthamus tinctorius*. *Zhongguo Zhong Yao Za Zhi* **2014b**, *39*, 3295-3300.

Yue, W.; Luqiu, W. A clinical observation on the effect of rheumatic prescription for treatment of rheumatoid arthritis of 50 cases. *Journal of Jiangsu Traditional Chinese Medicine* **1990**, *11*, 1-3.

Yukun. The treatment of thorax rheumatism of 800 cases with milkvetchpeach-safflower, etc. decoction. *Liaoning Traditional Chinese Medical Science Journal* **1988**, *12*, 19-20.

Zaihe, S. The treatment of erythema tuberosum with blood circulation-invigorated and dampness-benefited decoction. *Zhejian Traditional Chinese Medicine Journal* **1989**, *24*, 112.

Zargari, A. Medicinal Plants; Iran, 1988; pp 619.

Zhang, H. L.; Nagatsu, A.; Watanabe, T.; Sakakibara, J.; Okuyama, H. Antioxidative compounds isolated from safflower (*Carthamus tinctorius* L.) oil cake. Chemical and Pharmaceutical Bulletin **1997**, *45*, 1910-1914.

Zhang, H. L.; Nishiyama, K. Safflower colors. *Foods and Food Ingredients Journal of Japan* **2014**, *219*, 291-296.

Zhang, J.; Ke, Y.; Liu, H. M.; Yang, X. Fingerprint analysis of *Flos Carthami* and safflower yellow pigments by high performance liquid chromatography. *Analytical Letters* **2005**, *38*, 981-995.

Zhang, J. A Traditional Chinese Medicine for the treatment of chronic pulmonary heart disease. *Faming Zhuanli Shenqing* **2014**, CN 104189242 A 20141210.

Zhang, Y.; Gan, M.; Li, S.; Wang, S.; Zhu, C.; Yang, Y.; H. U. J.; Chen, N.; Shi, J. Chemical constituents of stems and branches of *Adina polycephala*. *Zhongguo Zhongyao Zazhi* **2010**, *35*, 1261-1271.

Zhangquan, Q. Treatment of wrist muscle tenosynovitis by washing method with decoction. *Sichuan Traditional Chinese Medical Science* **1985**, *3*, 46.

Zhao, G.; Qin, G. W.; Gai, Y.; Guo, L. H. Structural identification of a New Tri-p-coumaroylspermidine with serotonin transporter inhibition from safflower. *Chemical and Pharmaceutical Bulletin* **2010**, *58*, 950-952.

Zhengliang, H.; Qiming, G.; Zhumei C. Studies on pharmacology of the yellow pigment of safflower (*Carthamus tinctorius* L.). *Traditional Chinese Medicine* **1984**, *15*, 12-14.

Zhou, F. R.; Zhao, M. B.; Tu, P. F. Simultaneous determination of four nucleosides in *Carthamus tinctorius* L. and safflower injection using high performance liquid chromatography. *Journal of Chinese Pharmaceutical Science (Chin)* **2009**, *18*, 326-330.

Zhou, Y. Z.; Qiao, L.; Chen, H.; Li, R. F.; Hua, H. M.; Pei, Y. H. New aromatic glucosides from *Carthamus tinctorius*. *Journal of Asian Natural Product Research* **2008a**, *10*, 817-821.

Zhou, Y. Z.; Chen, H.; Qiao, L.; Xu, N.; Cao, J. Q.; Pei, Y. H. Two new compounds from *Carthamus tinctorius*. *Journal of Asian Natural Product Research* **2008b**, *10*, 429-433.

Zhou, Y. Z.; Ma, H. Y.; Chen, H. New acetylenic glucoside from *Carthamus tinctorius*. *Chemical and Pharmaceutical Bulletin* **2006**, *54*, 1455-1456.

Zhu, H.; Wang, Z.; Ma, C.; Tian, J.; Fu, F.; Li, C.; Guo, D.; Roeder, E.; Liu, K. Neuroprotective effects of hydroxysafflor yellow A. in-vivo and in-vitro studies. *Planta Medica* **2003**, *69*, 429-433.

Zuolin, Z. The curative effects of Tao-Hong-Si-Wu decoction for treatment on cerebral embolism of 32 cases. *Correspondence of Traditional Chinese Medicine* **1992**, *11*, 44-45.

Zuozuo, C.; Jianquo, L.; Yunfeng, G.; Youcai, Y.; Zuoying, Z.; Dingfeng, S. Effects of safflower yellow III on Myocardial Ischemia of Canine. *Chinese Pharmacological Bulletin* **2000**, *16*, 590-591.

List of Publications and Presentations

From thesis

1. Senthi Mahibalan, Poorna Chandra Rao, Rukaiyya Khan, Ameer Basha, Ramakrishna BS, Hironori Masubuti, Yoshinori Fujimoto, Ahil Sajeli Begum. Cytotoxic constituents of *Oldenlandia umbellata* and isolation of a new symmetrical coumarin dimer. Med Chem Res. (Under review)

2. Sajeli Begum Ahil, Senthi Mahibalan, Shaik Ameer Basha, Ramesh Babu and Katragadda Suresh Babu. Comparative Pharmacognostic evaluation and HPTLC analysis of petals of spiny and non-spiny safflower cultivars. International Journal of Food Properties. DOI: 10.1080/10942912.2014.988722

3. S. Mahibalan, A. Sajeli Begum, Ravi Sojitra, S. Ameer Basha, Sameer K. Chandavenkata and C. Sudhakar. Physico-Chemical Characterization of Spineless Safflower Petals and HPLC-Based Process Optimization for Extracting Rutin. Journal of the Indian Chemical Society 2014, 91, 2179-2187.

4. S. Mahibalan, A. Sajeli Begum, S. Ameer Basha and C. V. Sameer Kumar. Quality control studies on non-spiny hybrid safflower petals as per World Health Organisation (WHO) requirement. Journal of Oilseeds Research 2012, 29, 452-455.

Other publications

1. Rukaiyya Sirajuddin Khan, Mahibalan Senthi, Poorna Chandra Rao, Ameer Basha, Mallika Alvala, Dinesh Tummuri, Hironori Masubuti, Yoshinori Fujimoto, Ahil Sajeli Begum. Cytotoxic constituents of *Abutilon indicum* leaves against U-87 MG human glioblastoma cells. Natural Product Research. DOI: 10.1080/14786419.2014.976643

2. S. Mahiblan, Ruben Sharma, Aditya Vyas, S. Ameer Basha and A. Sajeli Begum. Assessment of extraction techniques for total phenolics and flavonoids from *Annona muricata* seeds. Journal of the Indian Chemical Society 2013, 90, 2199-2205.

3. G. Raghavendra, S. Ameer Basha, M. V. Nagesh Kumar, K. Dharma Reddy, Sajeli Begum S. Mahibalan, C. V. Sameer Kumar and M.Suresh. Effect of safflower petal extracts on spore germination of sorghum grain mold fungi. Journal of Oilseeds Research, 2012, 29, 329-332.

Papers presented in conference

From thesis

1. S. Mahibalan, G. Kumaresan, A. Sajeli Begum. In-vitro Anticancer Assay of *Hedyotis Umbellata* On AGC-Gastric Cell Line and Identification of Major Constituents. Presented in International Conference on Bioactive Phytochemicals and Therapeutics (ICBPT-2013), held at Chidambaram from April 05-07, 2013, p. 29-30. (Oral presentation)

2. S Mahibalan, P V C Rao, Rukaiyya S Khan and A Sajeli Begum. Newer cytotoxic leads from *Hedyotis umbellata* against lung and breast cancer. Presented in 66th IPC, held at Hyderabad from January 23-25, 2015.

3. A.S. Begum, S. Mahibalan, P.C. Rao, S.R. Khan, Y. Fujimoto, B.S. Ramakrishna Reddy. Cancer cell proliferation effect of iridoid glucosides isolated from *Hedyotis umbellata* L. Presented in 15th Tetrahedron Symposium-Asia Edition, held at Singapore from October 28-31, 2014.

4. Ruben Sharma, Aditya Vyas, Ramya, Mahibalan S, Sajeli Begum A, Ameer Basha S. Quality Control Studies on Spiny Safflower Petals as per World Health Organisation (WHO) Requirement. Presented in 2nd National Symposium on Current Trends in

Pharmaceutical Sciences (CTPS-2012), held at Hyderabad on 17th November 2012, A110772, p. MISC10.

5. S. Mahibalan, A. Sajeli Begum, S. Ameer Basha and C. V. Sameer Kumar. Quality control studies on non-spiny hybrid safflower petals as per World Health Organisation (WHO) requirement. Presented in 8th International Safflower Conference, held at Hyderabad from January 19-23, 2012, J. Oilseeds Res., (29, Spl. Issue), January 2012, p.452-455.

Other presentations

1. Rukaiyya S Khan, S. Mahibalan and A. Sajeli Begum. Isolation and identification of chemical constituents of *Abutilon indicum*. Presented in International Conference and Exhibition on Pharmacognosy, Phytochemistry & Natural Products, held at Hyderabad from October 21-23, 2013. doi.org/10.4172/2167-0501.S1.003.

2. S. Mahibalan, S. Maria, T. N. Rohan, Rukaiyya S Khan, A. Sajeli Begum. Dermal Wound Healing Potential of Alkaloid Enriched Ointment of *Evolvulus Alsinoides* in Albino Rats. Presented in Chemistry and Chemical Biology of Natural Products (CCBNP-2012), held at IICT-Hyderabad from August 2-4, 2012.

3. Rukaiyya S Khan, Mallika A, Mahibalan S, Sriram D and Sajeli Begum A. In-vitro anticancer activity of Abutilon indicum on human breast carcinoma cell line (MDA-MB-231). Presented in 4th International Conference on Drug Discovery & Therapy, held at Dubai, UAE from February 12-15, 2012. Current Medicinal Chemistry, Feb., 2012, p. 156-157 (PO-36).

4. G. Raghavendra, S. Ameer Basha, M. V. Nagesh Kumar, K. Dharma Reddy, Sajeli Begum S. Mahibalan, C. V. Sameer Kumar and M.Suresh. Effect of safflower petal extracts on spore germination of sorghum grain mold fungi. Presented in 8th International Safflower Conference, held at Hyderabad from January 19-23, 2012, J. Oilseeds Res., (29, Spl. Issue), January 2012, p. 329-332.

5. Mahibalan. S, Rukaiyya S. Khan, Patnaik. A. Sajeli Begum. A. Biological and chemical validation for the traditional use of Physalis peruviana leaves in the treatment of rheumatism. Presented in XLIV Annual Conference of Indian Pharmacological Society, held at Manipal from December 19-21, 2011. Indian Journal of Pharmacology, 43, Suppl. 1, Dec. 2011, p. S42-43.

6. Rukaiyya S. Khan, S. Mallika, S. Mahibalan, D. Sriram, A. Sajeli Begum. In-vitro anticancer activity of Abutilon indicum leaves on U87MG-A brain tumor cell line. Presented in XLIV Annual Conference of Indian Pharmacological Society, held at Manipal from December 19-21, 2011. Indian Journal of Pharmacology, 43, Suppl. 1, Dec. 2011, p. S110.

7. Mahibalan S, Mallika A, Rukaiyya S. Khan, Sriram D, Sajeli Begum A. In-vitro anticancer activity of safflower petals on Osteosarcoma (U87MG) cell line. Presented in A Symposium on Current Trends in Pharmaceutical Sciences (CTPS-2011), held at Hyderabad, on November 12th 2011, p. 53-54.

Biography

BRIEF BIOGRAPHY OF THE CANDIDATE

S Mahibalan obtained his B. Pharm (2005) and M. Pharm degree (2008) from The Tamilnadu Dr. M.G.R. Medical University, Chennai. Soon after he joined as a lecturer in Balaji Institute of Pharmacy, Warangal and worked for 2 years. In 2010, he then moved to Karpagam College of Pharmacy and served as lecturer until March 2011. In April 2011, he joined as a Project Fellow under UGC-Major Research in the Department of Pharmacy, BITS-Pilani Hyderabad Campus and later in the same year he started his Ph. D thesis work under Prof. AS Begum in the same department. He worked on various projects and published 7 papers in peer reviewed journals and presented 12 posters in various national and international conferences. Mr. Mahibalan received a travel grant from UGC-New Delhi to present a poster at Manipal University, Manipal. He received "Young Investigator Award" at ICBPT-2013 held at Annamalai University, Chidambaram. He is also a recipient of "Senior Research Fellowship" from CSIR-New Delhi and he is a life member of Association of Pharmaceutical Teachers of India (APTI), Bangalore.

BRIEF BIOGRAPHY OF THE SUPERVISOR

Dr. Ahil Sajeli Begum is currently an Associate Professor in Department of Pharmacy, Birla Institute of Technology and Science, Pilani-Hyderabad Campus. She received her B. Pharm degree (1999) from The Tamilnadu Dr. M.G.R. Medical University, Chennai and M. Pharm degree (2001) in Pharmaceutical Chemistry from Institute of Technology-Banaras Hindu University (IT-BHU), Varanasi. She was awarded with Ph. D degree (2005) by BHU for her thesis work on "Chemical Investigation of Solanaceous Plants". Prof. AS Begum is a recipient of the Deutscher Akademischer Austausch Dienst (DAAD) fellowship (2004) to pursue research at Eberhard Karls Univesrity, Tubingen, Germany. Soon after completing her Ph.D. program, she joined in Department of Pharmaceutics at IT-BHU, Varanasi as an Assistant Professor and then moved to BITS-Pilani Hyderabad in mid 2010. She has 10 years of experience in teaching and research. She has successfully completed two projects funded by University Grants Commission (UGC) -New Delhi and Council of Scientific and Industrial Research-New Delhi. She has 26 publications to her credit and authored a book chapter in "Progress in the Chemistry of Organic Natural Products" published by Springer Wien New York. Prof. AS Begum is a life time member of various scientific forums like Association of Pharmaceutical Teachers of India (APTI), Indian Pharmacy Graduates Association (IPGA) and Indian Chemical Society. She is presently supervising four students for their doctoral thesis work.